

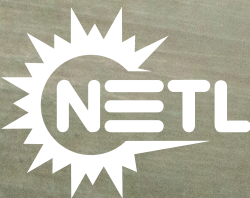
DOE/NETL  
CARBON  
CAPTURE  
PROGRAM

# CARBON DIOXIDE CAPTURE HANDBOOK

AUGUST 2015



U.S. DEPARTMENT OF  
**ENERGY**



Cover image: Goniometer, which measures contact angle and surface tension of liquids used in carbon capture, in the NETL Office of Research and Development's Nanoparticle Technology Laboratory, Morgantown, WV.

**DOE/NETL  
CARBON  
CAPTURE  
PROGRAM**

**CARBON DIOXIDE  
CAPTURE  
HANDBOOK**

AUGUST 2015

**NETL Contact:**

Lynn Brickett  
Technology Manager, Carbon Capture  
Strategic Center for Coal

**National Energy Technology Laboratory**  
[www.netl.doe.gov](http://www.netl.doe.gov)



U.S. DEPARTMENT OF  
**ENERGY**





this page intentionally left blank



## DISCLAIMER

This report was prepared as an account of work sponsored by an agency of the United States Government. Neither the United States Government nor any agency thereof, nor any of their employees, makes any warranty, express or implied, or assumes any legal liability or responsibility for the accuracy, completeness, or usefulness of any information, apparatus, product, or process disclosed, or represents that its use would not infringe privately owned rights. Reference herein to any specific commercial product, process, or service by trade name, trademark, manufacturer, or otherwise does not necessarily constitute or imply its endorsement, recommendation, or favoring by the United States Government or any agency thereof. The views and opinions of authors expressed herein do not necessarily state or reflect those of the United States Government or any agency thereof.

## TABLE OF CONTENTS

<b>PREFACE</b>	<b>10</b>
<b>CHAPTER 1: SOLVENT-BASED CO<sub>2</sub> CAPTURE</b>	<b>11</b>
1.1 HISTORY OF SOLVENT-BASED CO <sub>2</sub> CAPTURE	12
1.2 MASS-TRANSFER PRINCIPLES ASSOCIATED WITH SOLVENT-BASED CO <sub>2</sub> CAPTURE	13
1.3 SOLVENT-BASED CO <sub>2</sub> CAPTURE APPROACHES	15
1.3.1 AMINES	15
1.3.1.1 Primary, Secondary and Tertiary Amines	15
1.3.1.2 Relevance of Amine Structure to CO <sub>2</sub> Capture	17
1.3.1.3 MEA	18
1.3.1.4 Proprietary Amine Blends	18
1.3.1.5 Piperazine and Other Non-Proprietary Amines	23
1.3.2 NON-AQUEOUS SOLVENTS (NASS)	23
1.3.2.1 Hydrophobic Amines	23
1.3.2.2 CO <sub>2</sub> -Binding Organic Liquids	23
1.3.2.3 Aminosilicone Solvents	24
1.3.2.4 Functionalized-Ionic Liquids	25
1.3.2.5 Amine-Organic Solvent Mixtures	26
1.3.3 CARBONATE-BASED SOLVENTS	26
1.3.3.1 Ammonia-Based Processes	27
1.3.3.2 Enzyme-Catalyzed Processes	27
1.3.3.3 Amine-Promoted Carbonate	28
1.3.4 PHASE CHANGE SOLVENTS	28
1.3.5 PROCESS INNOVATIONS AND IMPROVEMENTS	29
1.3.5.1 Advanced Solvent Regeneration Technologies	29
1.3.5.2 Advanced Gas-Liquid Contactors	30
1.3.5.3 Advanced Heat Integration	30
1.3.6 KEY CHALLENGES FOR SOLVENT-BASED CO <sub>2</sub> CAPTURE	30
1.4 ADVANCES AND FUTURE WORK	31
1.4.1 SUMMARY OF ADVANCES	32
1.4.2 KEY PARAMETERS TO BE EVALUATED MOVING FORWARD	33
1.4.3 POTENTIAL FOCUS AREAS FOR FUTURE POST-COMBUSTION SOLVENT RD&D	34
<b>CHAPTER 2: SORBENT-BASED CO<sub>2</sub> CAPTURE</b>	<b>35</b>
2.1 ESTABLISHED APPLICATIONS OF SORBENT-BASED CO <sub>2</sub> CAPTURE	36
2.1.1 CHALLENGES ASSOCIATED WITH SORBENT-BASED CO <sub>2</sub> CAPTURE	37
2.1.2 ADVANTAGES OF SORBENT PROCESSES	37
2.2 PRINCIPLES ASSOCIATED WITH SORBENT-BASED CAPTURE	37
2.2.1 ADSORPTION	37
2.2.2 REGENERATION	38
2.2.2.1 Regeneration Heat Duty	38
2.2.3 TEMPERATURE SWING ADSORPTION	39
2.2.4 PRESSURE SWING ADSORPTION AND VACUUM SWING ADSORPTION	41
2.3 SORBENT-BASED CO <sub>2</sub> CAPTURE APPROACHES	43
2.3.1 LOW TEMPERATURE SORBENTS	46
2.3.1.1 Solid Amine-Based Adsorbents	46
2.3.1.2 Carbon-Based Adsorbents	48
2.3.1.3 Zeolite-Based Adsorbents	48
2.3.1.4 Metal-Organic Framework-Based Adsorbents	51
2.3.1.5 Alkali Metal Carbonate-Based Adsorbents	56
2.3.2 INTERMEDIATE TEMPERATURE SORBENTS	56
2.3.2.1 Layered Double Hydroxide-Based Sorbents	56
2.3.2.2 MGO Sorbents	57

2.3.3	HIGH TEMPERATURE SORBENTS	57
2.3.3.1	CAO-Based Sorbents	57
2.3.3.2	Alkali Ceramic-Based Sorbents	58
2.4	ADVANCES AND FUTURE WORK	58
2.4.1	SUMMARY OF ADVANCES	58
2.4.2	KEY PARAMETERS TO BE EVALUATED MOVING FORWARD	59
<b>CHAPTER 3: MEMBRANE-BASED CO<sub>2</sub> CAPTURE</b>		<b>61</b>
3.1	MEMBRANE-BASED GAS SEPARATIONS AND CO <sub>2</sub> CAPTURE	62
3.1.1	CONCEPT	62
3.1.2	HISTORY OF MEMBRANE-BASED GAS SEPARATIONS	62
3.1.3	ADVANTAGES OF MEMBRANE-BASED CO <sub>2</sub> CAPTURE PROCESSES	63
3.1.4	CHALLENGES ASSOCIATED WITH MEMBRANE-BASED CO <sub>2</sub> CAPTURE	63
3.1.5	TECHNICAL PRINCIPLES OF MEMBRANE-BASED CO <sub>2</sub> CAPTURE	64
3.1.5.1	<i>Nomenclature and Units of Measure</i>	64
3.1.5.2	<i>Membrane Separation Factor</i>	65
3.1.5.3	<i>Theory of Membrane-Based Gas Separation</i>	66
3.1.5.4	<i>Membrane Module Designs</i>	72
3.1.5.5	<i>Process Configurations for Membrane Separations</i>	74
3.1.6	COMMERCIAL MEMBRANE-BASED GAS SEPARATION	78
3.1.7	DEVELOPMENTAL TECHNOLOGY FOR PRE-COMBUSTION MEMBRANE-BASED SEPARATIONS	80
3.1.7.1	<i>Water Gas Shift Membrane Reactor</i>	80
3.1.7.2	<i>Types of Membranes</i>	81
3.2	DOE/NETL MEMBRANE-BASED CO <sub>2</sub> CAPTURE PORTFOLIO	82
3.3	ADVANCES AND FUTURE WORK	85
3.3.1	SUMMARY OF ADVANCES	85
3.3.2	KEY PARAMETERS TO BE EVALUATED MOVING FORWARD	86
<b>CHAPTER 4: CO<sub>2</sub> COMPRESSION</b>		<b>87</b>
4.1	CO <sub>2</sub> COMPRESSION	88
4.2	COMPRESSION WORK FUNDAMENTALS	88
4.2.1	COMPRESSION WORK	88
4.2.2	CONVENTIONAL CO <sub>2</sub> COMPRESSION	90
4.2.3	HIGH-PRESSURE RATIO COMPRESSION	92
4.2.4	ISOTHERMAL CO <sub>2</sub> COMPRESSION/COOLED-DIAPHRAGM CONCEPT	94
4.3	OPPORTUNITIES FOR PROCESS INTEGRATION	96
4.4	RESULTS AND DISCUSSION	97
4.5	CONCLUSIONS	104
4.6	RECOMMENDATIONS	105
4.7	APPENDIX	105
4.7.1	COMPRESSION WORK: THERMODYNAMICS	105
4.7.1.1	<i>Isentropic Compression</i>	108
4.7.1.2	<i>Polytropic Compression</i>	110
4.7.2	EOS-BASED NUMERICAL INTEGRATION APPROACH TO CALCULATE STAGE OUTLET TEMPERATURE AND COMPRESSION WORK	111
4.7.3	SCHULTZ POLYTROPIC PROCEDURE FOR CALCULATING OUTLET TEMPERATURE AND HEAD	111
4.7.4	IDEAL/REAL GAS POLYTROPIC COMPRESSION	111



## LIST OF FIGURES

Figure 1-1. Chart for Selecting CO <sub>2</sub> Removal Technologies Available Commercially.....	14
Figure 1-2. Schematic of CO <sub>2</sub> Absorption into a Liquid Solvent with Chemical Reaction.....	16
Figure 1-3. Schematic of Amine-Based CO <sub>2</sub> Capture Process.....	20
Figure 1-4. Progress in Reducing Parasitic Load of CO <sub>2</sub> Capture from Projects Funded by CCRP.....	34
Figure 1-5. Progress in Reducing Overall Energy Penalty Due to CO <sub>2</sub> Capture.....	35
Figure 2-1. Physisorption vs. Chemisorption.....	39
Figure 2-2. Two-Bed Temperature Swing Adsorption.....	41
Figure 2-3. Isotherm for Sorbents with Heat of Adsorption of -25kJ/kg and -60 kJ/kg.....	42
Figure 2-4. Sorption (top) and Desorption (bottom) Modes in Hollow Fiber Sorbents.....	43
Figure 2-5. Pressure Swing or Vacuum Swing Adsorption.....	44
Figure 2-6. Framework Structure of Low-Silica X Zeolite (cations not shown).....	51
Figure 2-7. MOF-5 Framework Designed and Synthesized by Li and Co-Researchers.....	54
Figure 2-8. 3D Structure of Crystalline MOF-5.....	54
Figure 2-9. Basic Structure of HKUST-1.....	55
Figure 2-10. Steam Stability Map for MOFs.....	57
Figure 2-11. Layered Double Hydroxide Structure.....	59
Figure 2-12. NETL Sorbent-Based Capture Projects Progression.....	61
Figure 3-1. Relative Permeabilities of Gases in Polydimethylsiloxane.....	64
Figure 3-2. Robeson Plot for H <sub>2</sub> /CO <sub>2</sub> Permselectivity in Polymers.....	73
Figure 3-3. Robeson Limits for H <sub>2</sub> Permselective Membranes.....	74
Figure 3-4. Common Membrane Module Designs.....	75
Figure 3-5. Spiral-Wound Module Flow Patterns.....	76
Figure 3-6. Two-Stage Membrane Circuitries: Serial Stripper Concept.....	77
Figure 3-7. Two-Stage Membrane Circuitries: Serial Enricher Concept.....	78
Figure 3-8. Two-Stage Membrane Circuitries: Enricher with Recycle.....	78
Figure 3-9. MTR Proposed Membrane Process to Capture and Sequester CO <sub>2</sub> in Flue Gas from a Coal-Fired Power Plant.....	79
Figure 3-10. MTR Hybrid Post-Combustion CO <sub>2</sub> Capture Process Cycles.....	80
Figure 3-11. Fuel Cell Energy Combined Electric Power and CO <sub>2</sub> Separation System Concept.....	80
Figure 3-12. Water Gas Shift Reactor Concept.....	83
Figure 3-13. NETL Post-Combustion Capture Projects Progression.....	88
Figure 4-1. Compressor Coverage Chart.....	90
Figure 4-2. Comparison of Isentropic, Isothermal, and Intercooled Polytropic Compression ( $\eta_p = 86\%$ ) Paths.....	93
Figure 4-3. Schematic of Two-Stage Compression of CO <sub>2</sub> Using Shock Wave Compression.....	94
Figure 4-4. p-H Diagram for Conventional and High-Pressure Ratio Compression ( $\eta_p = 86\%$ ).....	95
Figure 4-5. p-H Diagram for Semi-Isothermal Compression Cases Compared to Conventional Compression ( $\eta_p = 86\%$ ).....	97
Figure 4-6. T-Q Diagrams for the 231 psia (Case A, B) and 2,220 psia CO <sub>2</sub> Coolers (Case A) ( $\eta_p = 86\%$ , high-pressure ratio compression).....	100
Figure 4-7. Process Flow Diagram for Case A.....	101
Figure 4-8. Process Flow Diagram for Case B.....	101
Figure 4-9. T-Q Diagrams for HP Coolers in Case B.....	102
Figure 4-10. T-Q Diagrams for LP Coolers in Cases C and D.....	102
Figure 4-11. T-Q Diagrams for HP CO <sub>2</sub> Coolers (Case C and D) ( $\eta_p = 86\%$ , high-pressure ratio compression).....	103
Figure 4-12. Gross Steam Turbine Output and Compressor Load for High-Pressure Ratio Cases (A, B, C, D).....	104
Figure 4-13. Reduction of CO <sub>2</sub> Capture Cost and Cost of Electricity Upon the Integration of Advanced Compression Technologies.....	106
Figure 4-14. Schematic of a Compressor and the Control Volume.....	108
Figure 4-15. Workflow for Calculating Compressor Head and Power Requirements Using the Schultz Polytropic Analysis.....	114

## LIST OF TABLES

Table 1-1. CO <sub>2</sub> Capture Plants Built Prior to 1999 Using the Econamine Process .....	15
Table 1-2. Examples of Primary, Secondary, Tertiary, and Hindered Amines .....	17
Table 1-3. Key Challenges Addressed by Projects in Carbon Capture R&D Program Portfolio .....	33
Table 2-1. NETL CO <sub>2</sub> Capture Projects Portfolio .....	46
Table 2-2. Comparison of Sorbents for CO <sub>2</sub> Capture .....	47
Table 3-1. Molecular Parameters for Various Gases .....	70
Table 3-2. Process Profiles for Commercial Polymer Membrane Technologies .....	81
Table 3-3. NETL CO <sub>2</sub> Capture Projects Portfolio, Pre-Combustion Membrane Projects .....	84
Table 3-4. NETL CO <sub>2</sub> Capture Projects Portfolio, Post-Combustion Membrane Projects.....	86
Table 4-1. Inlet and Outlet Pressures for CO <sub>2</sub> Compression Using Conventional Centrifugal Compression with Intercooling in Between Stages .....	93
Table 4-2. Stage Outlet Temperature, Head, and Overall Compression Work .....	93
Table 4-3. Stage Outlet Temperature, Head, and Overall Compression Load for the Two-Stage Compression of CO <sub>2</sub> from 23.5–2,215 psia Using Prode and Schultz calculations .....	95
Table 4-4. Specific Work and Overall Compression Load for Compressing CO <sub>2</sub> from 23.5 to 2,215 psia Using Intercooler Temperature of 70 °F and 16 Compression Stages.....	96
Table 4-5. Specific Work and Overall Compression Load for Compressing CO <sub>2</sub> From 23.5 to 2,215 psia Using Intercooler Temperature of 50 °F and 16 Compression Stages16 .....	97
Table 4-6. Comparison of Results from the Excel Model for Case 12 to those from NETL Baseline.....	98
Table 4-7. BFW Exit Temperatures for the Feedwater Heaters for Case 12.....	99
Table 4-8. Results from Heat Integration Scenarios .....	101
Table 4-9. Comparison of Net Power and Efficiency for Conventional, High-Pressure Ratio Compression and Semi-Isothermal Compression .....	105
Table 4-10. Stage-Wise Exit Temperature and Head From Schultz Procedure for Conventional Compression .....	114
Table 4-11. Stage-Wise Exit Temperature and Head From Schultz Polytropic Analysis for High-Pressure Ratio Compression .....	115
Table 4-12. Parameters Used to Model Case 12 Steam Cycle.....	116

## PREFACE

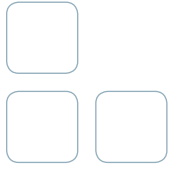
The U.S. Department of Energy's (DOE) Office of Fossil Energy (FE) has adopted a comprehensive, multi-pronged approach to the research and development (R&D) of advanced carbon dioxide (CO<sub>2</sub>) capture technologies for coal-based power plants. The National Energy Technology Laboratory (NETL) is implementing the Carbon Capture R&D program to develop a broad portfolio of the next generation of advanced CO<sub>2</sub> capture technologies.

Current DOE/NETL R&D efforts cover not only improvements to state-of-the-art, first-generation technologies, but also the development of second-generation and transformational advanced CO<sub>2</sub> capture technologies. While DOE/NETL activities have historically focused most heavily on coal power plants, many of the CO<sub>2</sub> capture-related R&D activities can also be applied to natural gas power plants as well as large industrial facilities such as refineries, steel plants, and cement plants. The success of this research will enable cost-effective implementation of advanced carbon capture and storage (CCS) technologies and ensure the United States will continue to have access to safe, reliable, and affordable energy from fossil fuels.

This Handbook focuses on advanced solvent, sorbent, and membrane technologies for CO<sub>2</sub> capture, as well as advanced CO<sub>2</sub> compression technologies. The significant advances that have been made with CO<sub>2</sub> capture and compression technologies are summarized with regard to thermodynamic, cost, and process characteristics. In addition, recommendations are provided regarding future carbon capture and compression R&D.

Additional information on DOE carbon capture R&D efforts is available at <http://www.netl.doe.gov/research/coal/carbon-capture>.





# CHAPTER 1:



# SOLVENT-BASED CO<sub>2</sub> CAPTURE

## 1.1 HISTORY OF SOLVENT-BASED CO<sub>2</sub> CAPTURE

The removal of CO<sub>2</sub> from industrial gas streams is not a new process. Gas absorption processes using chemical solvents to separate CO<sub>2</sub> from other gases have been in use since the 1930s in the natural gas industry. However, concentrations of CO<sub>2</sub> in natural gas are typically much higher than those found in gases resulting from the combustion process, which simplifies separation. The CO<sub>2</sub> partial pressures encountered in flue gas applications ( $\approx 2$  psia [ $\approx 13$ – $14$  kPa] CO<sub>2</sub> in feed flue gas,  $\approx 0.26$  psia [ $\approx 1.8$  kPa] in treated flue gas) necessitated the use of amine-based processes (see Figure 1-1).

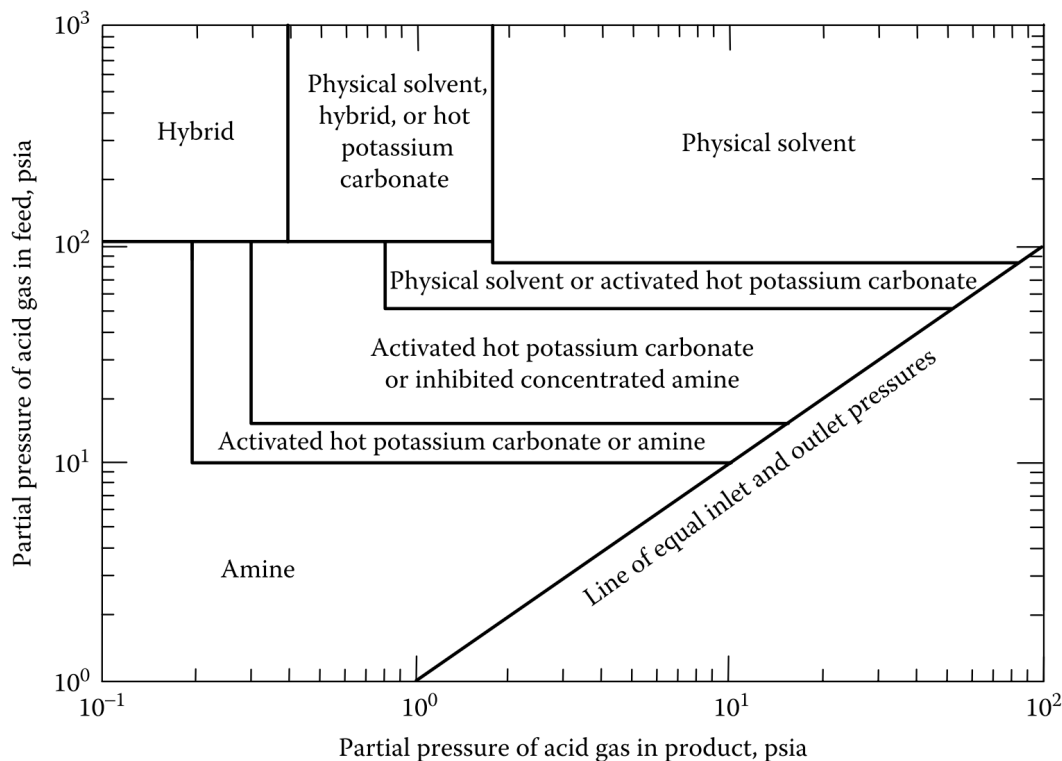


Figure 1-1. Chart for Selecting CO<sub>2</sub> Removal Technologies Available Commercially

Before the inception of the DOE/NETL Post-Combustion CO<sub>2</sub> Capture Program. Source: Kidnay and Parrish.<sup>1</sup> Note that the 'product' in the figure refers to treated flue gas.

The licensing history of the Econamine FG process provides a good example of past combustion-based applications of CO<sub>2</sub> removal technologies.<sup>2</sup> Prior to 1999, 25 facilities were built with CO<sub>2</sub> capture capacities ranging from 700 to 365,000 tonnes per year using this process (Table 1-1). The captured CO<sub>2</sub> from these facilities was used for enhanced oil recovery (EOR), urea production, and in the food and beverage industry. The capture capacities of these facilities reflect the fact that they were built to serve a specific commercial market for CO<sub>2</sub>. Other amine-based processes (e.g., ABB/Lummus) were implemented at similar capture capacities during this period. By comparison, a single 550 megawatt (MW) net output coal-fired power plant capturing 90% of the emitted CO<sub>2</sub> will need to separate approximately 5 million tonnes of CO<sub>2</sub> per year. Scaling up these existing processes represents a significant technical challenge.<sup>3</sup>

1 Kidnay, A. J. and Parrish, W. R. Gas treating in *Fundamentals of Natural Gas Processing* 91–132 (CRC Press, 2006).

2 Chapel et al. Recovery of CO<sub>2</sub> from flue gases: Commercial trends, *The Canadian Society of Chemical Engineers Annual Meeting*, Saskatoon, Saskatchewan, Canada. (4–6 October, 1999).

3 U.S. Department of Energy. 2010. *Coal-Fired Power Plants in the United States: Examination of the Costs of Retrofitting with CO<sub>2</sub> Capture Technology and the Potential for Improvements in Efficiency*, DOE/NETL-402/102309, Revised January 2010. [http://www.netl.doe.gov/energy-analyses/pubs/GIS\\_CCS\\_retrofit.pdf](http://www.netl.doe.gov/energy-analyses/pubs/GIS_CCS_retrofit.pdf).

Table 1-1. CO<sub>2</sub> Capture Plants Built Prior to 1999 Using the Econamine Process

OWNER	LOCATION	FUEL	CAPTURE RATE (TONS/Y)	CO <sub>2</sub> USE
Carbon Dioxide Technology	Lubbock, TX, USA	Natural Gas	365,000	EOR
Northeast Energy Associates	Bellingham, MA, USA	Natural Gas	117,000	Food Industry
Luzhou Natural Gas	Sechuan, China	Natural Gas	58,000	Urea Plant Feed
Sumitomo Chem/Nippon Oxygen	Chiba, Japan	Heavy Fuel Oil	58,000	Food Industry
Indo Gulf Fertilizer	Uttar Pradesh, India	Natural Gas	55,000	Urea Plant Feed
Prosint	Rio de Janeiro, Brazil	Natural Gas	33,000	Food Industry
N-Ren Southwest	Carlsbad, NM, USA	Natural Gas	33,000	EOR
Messer Greisheim do Brazil	Sao Paulo, Brazil	Natural Gas	29,000	Food Industry
Liquid Air Australia	Altona, Australia	Natural Gas	22,000	Food Industry
Liquid Air Australia	Botany, Australia	Natural Gas	22,000	Food Industry
Messer Greisheim do Brazil	Sao Paulo, Brazil	NR	18,000	Food Industry
San Miguel Corp.	San Fernando, Philippines	NR	16,000	Food Industry
European Drinks	Sudrigiu, Romania	NR	13,000	Food Industry
Cervezaria Bavaria	Barranquilla, Colombia	NR	9,000	Food Industry
Paca	Israel	NR	9,000	Food Industry
Industrial de Gaseoses	Quito, Ecuador	NR	2,200	Food Industry
Pepsi Cola	Manila, Philippines	NR	2,200	Food Industry
Pepsi Cola	Quezon City, Philippines	NR	2,200	Food Industry
Cosmos Bottling	San Fernando, Philippines	NR	2,200	Food Industry
Coca Cola	Cairo, Egypt	NR	2,200	Food Industry
Azucar Liquida	Santo Domingo, Dominican Republic	NR	2,200	Food Industry
Tokyo Electric Power	Yokosuka, Japan	Coal	1,800	Pilot Plant
Boundary Dam Power Plant	Saskatchewan, Canada	Coal	1,100	Pilot Plant
Kansei Electric Power	Osaka, Japan	Natural Gas	700	Pilot Plant
Sundance Generating	Alberta, Canada	Coal	700	Pilot Plant

NR – Not Reported

## 1.2 MASS-TRANSFER PRINCIPLES ASSOCIATED WITH SOLVENT-BASED CO<sub>2</sub> CAPTURE

The reactive absorption of CO<sub>2</sub> at the gas-liquid interface involves the diffusion of CO<sub>2</sub> from the bulk-gas phase to the interface, reaction at the interface and the diffusion of aqueous CO<sub>2</sub> species away from the interface into the bulk liquid.<sup>4</sup> The superscripts *i* and \* in the equations below refer to the concentration of CO<sub>2</sub> at the gas-reaction film interface and the bulk liquid respectively. The amount of CO<sub>2</sub> is represented by partial pressure or concentration in solution. If the reaction of CO<sub>2</sub> at the interface is irreversible and fast, the concentration in the bulk liquid is negligible, and the gas-film resistance controls the mass-transfer rate. For cases where the reaction of CO<sub>2</sub> at the gas-liquid interface is slow, CO<sub>2</sub> can diffuse into the bulk liquid before reacting with the solvent, and liquid-phase resistance controls the mass-transfer rate. For cases where the rate of reaction is intermediate, the reacting CO<sub>2</sub> species is not depleted in the liquid film and the overall mass-transfer rate is controlled by both gas-, and liquid-film resistances.

4 Tsai, R. E. Mass transfer area of structured packing, Masters Thesis. (2010). <http://repositories.lib.utexas.edu/handle/2152/ETD-UT-2010-05-1412>.



The flux of CO<sub>2</sub> is given by:

$$N = K_G(P_{CO_2} - P_{CO_2}^*) = k_G(P_{CO_2} - P_{CO_2}^i) = k'_g(P_{CO_2}^i - P_{CO_2}^*)$$

Equation 1-1

where  $K_G$  is the overall mass-transfer coefficient,  $P_{CO_2}$ ,  $P_{CO_2}^i$  and  $P_{CO_2}^*$  represent CO<sub>2</sub> partial pressures in the bulk gas, gas-liquid interface, and liquid respectively.

The mass-transfer rate can also be expressed in liquid-phase units as:

$$N = Ek_L^0([CO_2]^i - [CO_2]) = Ek_L^0/H_{CO_2}(P_{CO_2}^i - P_{CO_2}^*)$$

Equation 1-2

where  $E$  represents the enhancement of the liquid-film mass transfer rate due to the reaction,  $k_L^0$  represents the liquid-film mass-transfer coefficient (physical diffusion),  $H_{CO_2}$  is the Henry's law constant, and the superscripts refer to similar quantities as above, except that the concentration is measured in liquid-phase units.

The overall mass-transfer coefficient is depicted graphically in Figure 1-2 and can be expressed in terms of the gas- and liquid-film mass transfer coefficients as:

$$\frac{1}{K_G} = \frac{1}{k_g} + \frac{1}{k'_g} = \frac{1}{k_g} + \frac{H_{CO_2}}{Ek_L^0}$$

Equation 1-3

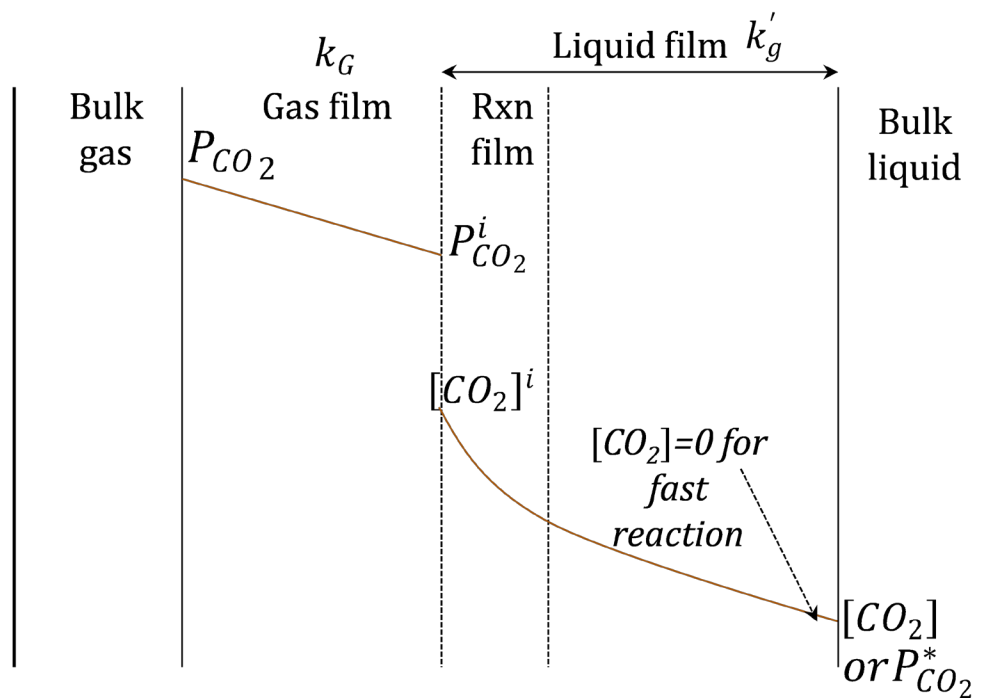


Figure 1-2. Schematic of CO<sub>2</sub> Absorption into a Liquid Solvent with Chemical Reaction

Source: Tsai, 2010.<sup>4</sup>

The enhancement factor  $E$  depends on the rate at which the amine reacts with CO<sub>2</sub> at the interface, and also depends on the diffusion

of CO<sub>2</sub> from the interface to the bulk liquid. Solvents which can react faster with CO<sub>2</sub> are beneficial for CO<sub>2</sub> capture because the mass-transfer coefficient is higher.<sup>5</sup> Similarly, solvents where CO<sub>2</sub> can diffuse more readily (i.e., less viscous solvents) also lead to higher E factors and higher mass transfer coefficients. For simple cases of CO<sub>2</sub> absorption by highly reactive solvents, the enhancement factor E (and thereby  $k'_g$ ) is directly proportional to the square root of the product of the rate constant and the diffusivity of CO<sub>2</sub> in the liquid.<sup>6</sup> Therefore, even if the intrinsic reaction kinetics of a particular solvent with CO<sub>2</sub> are very fast, if the diffusivity of CO<sub>2</sub> in the solvent is slow (e.g., due to high viscosity), the effect of the enhancement factor is limited.

### 1.3 SOLVENT-BASED CO<sub>2</sub> CAPTURE APPROACHES


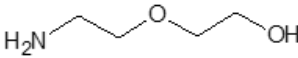
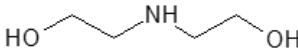
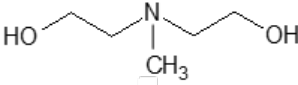
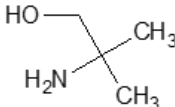
The Carbon Capture R&D program has examined a broad array of solvent-based capture approaches to address the technical challenges described above. These include the use of amines, non-aqueous solvents, carbonate-based solvents, phase-change solvents, and catalyzed processes. In addition, process innovations and improvements have contributed to overcoming the technical issues that serve as barriers to deployment of carbon capture technologies. All of these are described below.

#### 1.3.1 AMINES

##### 1.3.1.1 PRIMARY, SECONDARY AND TERTIARY AMINES

Amines are widely used to separate acid gases such as CO<sub>2</sub>, H<sub>2</sub>S and COS from a variety of gas streams. Typically, either a single amine, or a blend of two or more amines in aqueous solution reacts chemically with CO<sub>2</sub> in an acid-base reaction, forming a salt. The salts can be converted back into the acid and the base (amine) at high temperatures and reduced acid-gas partial pressures, regenerating the solvent and releasing CO<sub>2</sub>. Amines are characterized by the degree of substitution (up to 3 atoms) on the nitrogen atom. If an alkyl group substitutes for hydrogen, the amine is designated as a primary amine (e.g., MEA: HO-CH<sub>2</sub>-CH<sub>2</sub>-NH<sub>2</sub>, aminoethoxyethanol/diglycolamine [AEE/DGA]: H<sub>2</sub>N-CH<sub>2</sub>-CH<sub>2</sub>-O-CH<sub>2</sub>-CH<sub>2</sub>-OH). Secondary (e.g., diethanolamine [DEA]: HO-CH<sub>2</sub>-CH<sub>2</sub>-NH-CH<sub>2</sub>-CH<sub>2</sub>-OH) and tertiary amines (methyldiethanolamine [MDEA]: HO-CH<sub>2</sub>-CH<sub>2</sub>-N(CH<sub>3</sub>)-CH<sub>2</sub>-CH<sub>2</sub>-OH) have two and three groups substituting for hydrogen atoms respectively. Amines can be generally represented as R<sub>1</sub>R<sub>2</sub>R<sub>3</sub>N, where R<sub>i</sub> (i = 1, 2, 3) represent hydrogen atoms or organic groups. R<sub>2</sub> and R<sub>3</sub> are represented by hydrogen atoms in primary amines. Secondary amines have two organic moieties, and one hydrogen atom around the nitrogen atom, whereas tertiary amines have three organic moieties. Examples of primary, secondary, tertiary and hindered amines are shown in Table 1-2.

Table 1-2. Examples of Primary, Secondary, Tertiary, and Hindered Amines

PRIMARY	Monoethanolamine [MEA]	
	Diglycolamine [DGA]/ aminoethoxy ethanol [AEE]	
SECONDARY	Diethanolamine [DEA]	
TERTIARY	Methyldiethanolamine [MDEA]	
HINDERED	2-Amino-2-methyl-1-propanol (AMP)	

CO<sub>2</sub> can react with amines in two different ways: carbamate formation and bicarbonate formation.<sup>7</sup>

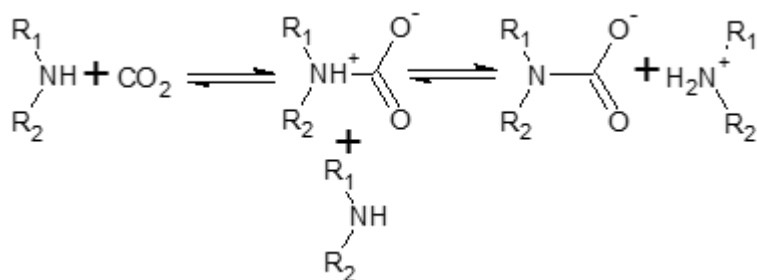
5 More CO<sub>2</sub> can be absorbed from the flue gas flow by a given flow rate of solvent if the mass-transfer coefficient is higher.

6 For example, see Bishnoi, S. and Rochelle, G.T. Absorption of carbon dioxide into aqueous piperazine: reaction kinetics, mass transfer and solubility. *Chemical Engineering Science* **55**, 5531–5543 (2000).

7 Wagner, R., Judd, B., Fundamentals—Gas sweetening, Presented at the 2006 Laurance Reid Gas Conditioning Conference, February 26–March 1, 2006, Norman, Oklahoma, USA.

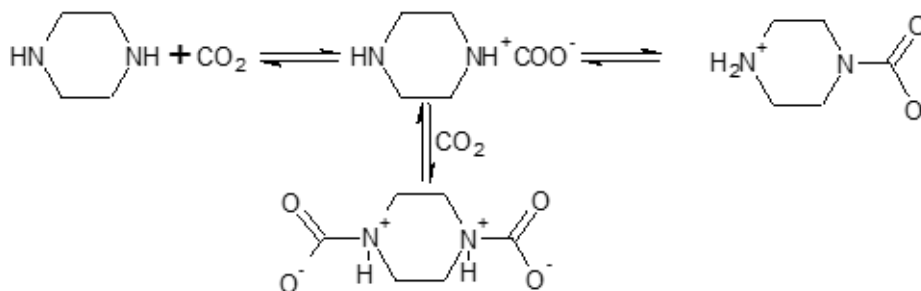
**Carbamate Formation**

CO<sub>2</sub> can react with a primary/secondary amine molecule (R<sub>1</sub>R<sub>2</sub>NH) forming a zwitterion which is further deprotonated by a base (amine) to form carbamate (R<sub>1</sub>R<sub>2</sub>NCOO<sup>-</sup>) and a cation (R<sub>1</sub>R<sub>2</sub>NH<sub>2</sub><sup>+</sup>). The overall reaction consumes 2 moles of amine per mole of CO<sub>2</sub>.



**Equation 1-4**  
Carbamate Formation

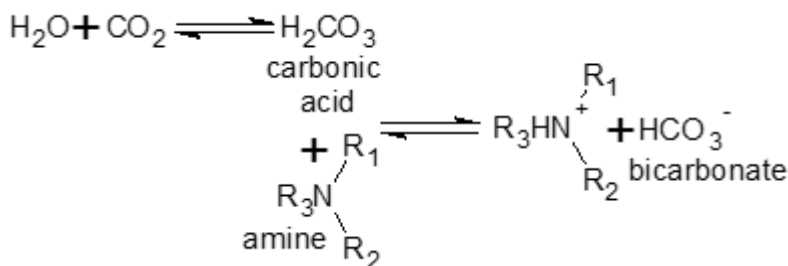
For polyamines that have multiple amine groups, the proton may be donated to the second amine group within the same molecule, resulting in higher molar-CO<sub>2</sub> capacity (e.g., piperazine [PZ]):



**Equation 1-5**

**Bicarbonate Formation**

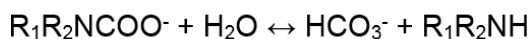
CO<sub>2</sub> can be slowly hydrated, forming carbonic acid, which forms a bicarbonate ion and an alkylammonium cation by reacting with an amine:



**Equation 1-6**  
Bicarbonate Formation from Tertiary Amines

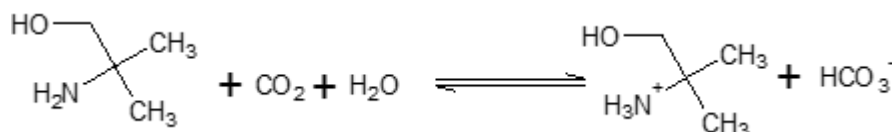
The formation of bicarbonate may occur with any amine (primary, secondary, tertiary) but is slow because the dissociation of carbonic acid to bicarbonate is slow.

The formation of carbamate requires the amine to have labile hydrogen atom(s), and thus is limited to primary and secondary amines. The rate of carbamate formation is considerably faster than the rate of bicarbonate formation. Carbamate formation with primary and secondary amines has a stoichiometry of 1:2 (the capture of 1 mole of CO<sub>2</sub> requires 2 moles of amine). In some cases, however, the carbamate formed can also be partially hydrolyzed to form bicarbonate, regenerating the amine, and increasing the CO<sub>2</sub> loading to values above 0.5.



Equation 1-7

A sterically-hindered amine is defined as a primary amine where the amino group is attached to a tertiary carbon atom (e.g., 2-amino-2-methyl-1-propanol [AMP]), or a secondary amine where the amino group is attached to a secondary or tertiary carbon atom.<sup>8,9</sup> Several proprietary amine technologies for CO<sub>2</sub> capture incorporate hindered amines. The presence of bulky organic groups around the amine destabilizes the carbamate, forming the bicarbonate (Equation 1-7), resulting in increased CO<sub>2</sub> capacity and lowering the heat of absorption while maintaining a relatively high-rate of CO<sub>2</sub> absorption compared to tertiary amines. Equation 1-8 represents the reaction of AMP with CO<sub>2</sub> forming the bicarbonate:



Equation 1-8

### 1.3.1.2 RELEVANCE OF AMINE STRUCTURE TO CO<sub>2</sub> CAPTURE

The primary characteristics of a solvent that make it a feasible candidate for post-combustion flue gas CO<sub>2</sub> capture are:

- **Fast reaction with CO<sub>2</sub>:** The cost of CO<sub>2</sub> capture is dictated to a large extent by the size of the absorber needed to separate a given quantity of CO<sub>2</sub> from the incoming flue gas. CO<sub>2</sub> can be separated from the flue gas using a smaller absorber volume if the solvent can absorb CO<sub>2</sub> at a faster rate, which lowers the capture costs. As noted in section 1.3, faster solvent kinetics results in better mass-transfer performance provided other factors are not limiting CO<sub>2</sub> transfer across the gas-liquid interface.
- **Large net-CO<sub>2</sub> carrying capacity:** The quantity of solvent needed to separate CO<sub>2</sub> from the flue gas determines the regeneration load, auxiliary unit costs, and energy requirements. Solvents need to have a high-net CO<sub>2</sub> carrying capacity.
- **Low-enthalpy of reaction with CO<sub>2</sub>:** Because the amine chemically reacts with CO<sub>2</sub>, energy is required to break the amine-CO<sub>2</sub> bond to desorb CO<sub>2</sub>. Primary amines and secondary amines forming carbamates have higher enthalpy of reaction with CO<sub>2</sub> compared to tertiary amines which form carbonates.
- **Low energy lost to heat and vaporize water:** Typically amines are used in concentrations varying from 30–50 w/w% in aqueous solutions. Because of its high latent heat of vaporization, water evaporation increases the steam requirements, parasitic load, and the energy penalty. Both CO<sub>2</sub> carrying capacity and the energy lost to evaporate water can be increased by reducing the water content in solution; however this increases the solution viscosity and may increase the corrosion rates. Solvent processes are typically operated with the highest feasible concentration of amine where viscosity, corrosion, carbamate precipitation, and column temperature bulge issues are minimal or well controlled.

In addition to these desirable characteristics, other favorable features for solvents include low CO<sub>2</sub> equilibrium backpressures at absorption conditions, easily reversible reactions at regeneration temperatures, low volatility, and resistance to oxidative and thermal degradation.

Primary and secondary amines typically have higher rates of reaction with CO<sub>2</sub> compared to tertiary amines. Among various primary amines, MEA has the highest reaction rate, and blends of MEA and other tertiary or hindered amines are typically used to exploit this feature while maintaining relatively-low reboiler loads. Primary/secondary (mono)amines with a 1:2 stoichiometry have lower CO<sub>2</sub> carrying capacity compared to tertiary amines which bind 1:1 with CO<sub>2</sub>. Further, polyamines such as piperazine have a higher carrying capacity because they have two amine groups per molecule. Tertiary amines have higher CO<sub>2</sub> capacities but the reaction kinetics with CO<sub>2</sub> are significantly slower than primary and secondary amines. Because the CO<sub>2</sub> carrying capacity is expressed in wt% CO<sub>2</sub> in the solvent, or the quantity of solvent circulated to capture a unit quantity of CO<sub>2</sub>, the molecular weight and density of the solvent also play a role in determining its volumetric or weight-based CO<sub>2</sub> carrying capacity.

From a health and environmental safety perspective, MEA is highly biodegradable, and has no direct adverse effects on human

8 Kohl, A. L. and Nielsen, R., *Alkanolamines for hydrogen sulfide and carbon dioxide removal*, in *Gas Purification* (Gulf Professional Publishing, 1997).

9 Sartori, G. and Savage, D. W. Sterically hindered amines for carbon dioxide removal from gases. *Ind. Eng. Chem. Fund.* **22**, 239–249 (1983).

health, animals, and vegetation. Other amine solvents such as AMP, MDEA and PZ are toxic and are not easily biodegraded compared with MEA.<sup>10</sup> The reaction of amines with  $\text{NO}_x$  in the flue gas leads to the formation of nitrosamines, which are carcinogenic. The reactivity with  $\text{NO}_x$  varies with the amine structure.

### 1.3.1.3 MEA

MEA scrubbing is the oldest of the amine-based CO<sub>2</sub> capture technologies. A schematic representation of the process is presented in Figure 1-3.

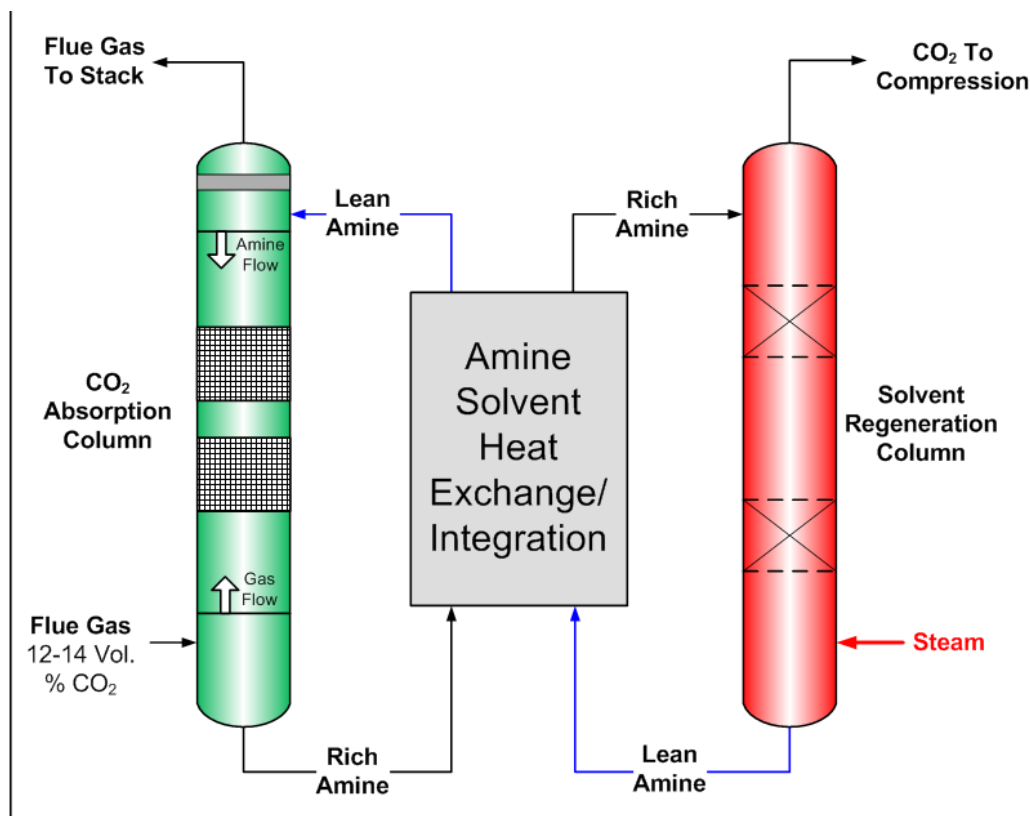


Figure 1-3. Schematic of Amine-Based Post-Combustion CO<sub>2</sub> Capture Process

After conventional air pollutant cleanup ( $\text{SO}_x$ ,  $\text{NO}_x$ , PM), the combustion flue gas enters an absorber reactor and flows counter-currently to a CO<sub>2</sub>-lean solvent where CO<sub>2</sub> is absorbed into, and reacts with, the MEA to form water-soluble compounds. The treated flue gas (mostly N<sub>2</sub>) is discharged to the atmosphere and the CO<sub>2</sub>-rich solution is pumped to a stripper reactor for regeneration. In the stripper, the CO<sub>2</sub>-rich solution is heated in order to break down the salt and regenerate the MEA solvent. A reboiler, supplied with steam extracted from the turbine cycle, provides the heat for regeneration of the MEA solvent in the stripper. Consequently, CO<sub>2</sub> is released, producing a concentrated stream which exits the stripper and is then cooled and dehumidified in preparation for compression, transport, and storage. From the stripper, the CO<sub>2</sub>-lean solution is cooled and returned to the absorber for reuse.

Usable MEA solution concentrations are typically limited by viscosity and corrosion. Therefore, current systems use only between 20% and 30% MEA, with the remaining being water. Although the water present in the solution helps control the solvent temperature during absorption, which is an exothermic reaction, the water also requires significant amounts of sensible heating and stripping energy upon CO<sub>2</sub> regeneration. Not every MEA system is the same and various vendors offer different designs. In general, depending on the amount of heat integration, anywhere from 1,550 to more than 3,000 British thermal units (Btu) per pound of CO<sub>2</sub> (3.6–7 GJ/T CO<sub>2</sub>) in the form of low-pressure steam (approximately 45 psia [3.1 bar]) is required to regenerate the solvent to produce a concentrated CO<sub>2</sub> stream at a pressure of approximately 25 psia (1.7 bar).

### 1.3.1.4 PROPRIETARY AMINE BLENDS

10 Shao, R., Stangeland, A., Amines used in CO<sub>2</sub> capture—Health and environmental impacts, The Bellona Foundation, September 2009. [http://bellona.org/ccs/uploads/media/fil\\_Bellona\\_report\\_September\\_2009\\_-\\_Amines\\_used\\_in\\_CO2\\_capture.pdf](http://bellona.org/ccs/uploads/media/fil_Bellona_report_September_2009_-_Amines_used_in_CO2_capture.pdf).

Because of its roots in refinery-gas processing and natural gas processing, many proprietary solvents have been developed to treat acid gases containing H<sub>2</sub>S and CO<sub>2</sub>, mostly focused on removing acid gases to very low levels meeting natural gas pipeline specifications. Historically, these solvent formulations have not been optimized exclusively for CO<sub>2</sub> capture alone, and further progress is feasible. Proprietary-amine blends might be comprised of sterically-hindered amines and patented amine blends. Activators (rate enhancers), and chemicals which retard oxidative/thermal degradation of amines are also considered proprietary additives. The reactions involved in the promotion or activation of an amine are complex. Astarita et al. note that several promoters are Lewis bases—molecules with lone pairs of electrons.<sup>11</sup> Further, they also note that the difference between the various explanations for amine promotion, e.g., “shuttle mechanism,”<sup>12</sup> and “homogeneous catalysis” simply lies in difference in the rate of the reaction of the CO<sub>2</sub>-amine intermediate with a second base (OH<sup>-</sup> in the case of carbonate solutions).<sup>10</sup> By modeling the CO<sub>2</sub> mass transfer in promoted amines in falling thin films, Puxty and Rowland suggested the basicity of the ‘promoted’ amine to be a primary factor controlling synergistic amine interactions.<sup>13</sup> For example, although AMP and PZ have similar acid strengths (pK<sub>a</sub> values 9.29 and 9.46 at 313 K), because AMP is present at a higher concentration (≈2.49 M vs. 0.94 M for one case presented in the article), it acts as a pH buffer maintaining high pH, allowing more free-PZ to react with CO<sub>2</sub>, thereby enhancing mass transfer within the gas-liquid reaction film compared to both PZ and AMP considered separately. Similarly, for PZ-MDEA mixtures, MDEA acts as a buffer, taking up the protons released due to the PZ-carbamate formation. However, it is a weaker base than AMP (pK<sub>a</sub> of 8.22 vs. 9.29 at 313 K), and as a result accepts a lower fraction of the protons released upon PZ-carbamate formation.<sup>12</sup>

### MDEA-Based Mixed Amine Blends

Amine mixtures of MDEA and DEA, MEA or piperazine are used to enhance CO<sub>2</sub> removal compared to pure MDEA. The added primary/secondary amine typically does not exceed 20% of the total amine on a molar basis. Total amine concentrations in liquid can approach 55 w/w%.<sup>14</sup> The use of PZ as an additive to MDEA was patented by BASF in 1982 (patent expired in 2002).<sup>15</sup> BASF’s aMDEA<sup>®</sup> solvent has been used where very low residual CO<sub>2</sub> levels in the treated gas were desired. Unpromoted MDEA is suitable for bulk-CO<sub>2</sub> removal (at intermediate-to-high pressures), but is unsuited for deep-CO<sub>2</sub> removal at intermediate pressures, or bulk-CO<sub>2</sub> removal at low pressures. Flue-gas CO<sub>2</sub> capture (90%) does not require very low levels of CO<sub>2</sub> in the treated gas (≈13.5% CO<sub>2</sub> in the feed, ≈1.8% CO<sub>2</sub> in the treated flue gas) and therefore the solvent circulation rates can be reduced. Additives such as monomethanolamine (MMEA) and DEA could also be used in addition to PZ.<sup>16</sup>

### BASF OASE<sup>®</sup> Blue Solvent

The amine-based BASF OASE<sup>®</sup> blue solvent, was developed for post-combustion CO<sub>2</sub> capture and has significantly higher stability compared to MEA, lowering operational costs. The composition of the BASF OASE<sup>®</sup> blue solvent is proprietary, and might consist of combinations of primary/secondary/tertiary/hindered amines and activators (heterocycles, primary or secondary alkanolamines, alkylenediamines or polyamines).<sup>17,18</sup> Aminocarboxylic<sup>19</sup> or aminosulfonic acids, which become significantly more acidic with temperature may also be used to increase the cycle capacity (lower lean loading), and decrease the solvent circulation rate and steam load while only slightly affecting the rich loading.<sup>20</sup> DOE/NETL is funding a 1-MW slipstream demonstration of the BASF OASE<sup>®</sup> blue solvent in a CO<sub>2</sub> capture process developed by Linde. Technoeconomic analyses conducted by Linde indicate that the BASF OASE<sup>®</sup> blue solvent resulted in significantly lower steam requirement to strip CO<sub>2</sub> compared to MEA (2.4 to 2.6 GJ/T CO<sub>2</sub>, vs. 3.55 GJ/T CO<sub>2</sub> for MEA), leading to higher net-plant efficiency, and lower fuel costs. Compared to 8 m piperazine (PZ), the BASF OASE<sup>®</sup> blue solvent has almost the same level of steam consumption (≈2.4 to 2.6 GJ/T CO<sub>2</sub> without heat integration).

- 11 Astarita, G., Savage, D. W. and Longo, J. M. Promotion of CO<sub>2</sub> mass transfer in carbonate solutions. *Chemical Engineering Science* **36**, 581–588 (1981).
- 12 The shuttle mechanism involves the fast reaction of the promoter with CO<sub>2</sub>, diffusion of the CO<sub>2</sub>-amine intermediate product to the bulk liquid, and reaction of the intermediate with a base to form the carbonate.
- 13 Puxty, G. and Rowland, R. Modeling CO<sub>2</sub> mass transfer in amine mixtures: PZ-AMP and PZ-MDEA. *Environmental Science and Technology* **45**, 2398–2405 (2011).
- 14 Polasek, J., Bullin, J.A., Process considerations in selecting amine, Proceedings GPA Regional Meeting, Sept. 1994, Tulsa, OK. <http://www.bre.com/portals/0/technicalarticles/Selecting%20Amines%20for%20Sweetening%20Units.pdf>.
- 15 Appl, M. et al. United States Patent: 4336233—Removal of CO<sub>2</sub> and/or H<sub>2</sub>S and/or COS from gases containing these constituents. (1982).
- 16 Piperazine—Why it’s used and how it works, *The Contactor*. 2(4), (2008). <http://www.ogtrt.com>.
- 17 Asprien, N., Clausen, I. and Lichtfers, U. United States Patent: 7887620—Removal of carbon dioxide from flue gases. (2011).
- 18 Asprien, N., Clausen, I., Lichtfers, U. and Wagner, R. United States Patent: 8034166—Carbon dioxide absorbent requiring less regeneration energy. (2011).
- 19 Aminocarboxylic acids exist in the zwitterionic form from pH ≈2.2–9.4, but can exist as anions at high-pH values and cations at low-pH values, accelerating CO<sub>2</sub> absorption and desorption respectively.
- 20 Asprien, N., Sieder, G., Lichtfers, U. and Andarcia, H. R. G. United States Patent: 8388738—Method for removing carbon dioxide from fluid flows, in particular combustion exhaust gases. (2013).



## KS-1™

Kansai Electric Power Company (KEPCO) and Mitsubishi Heavy Industries, Ltd. (MHI) has developed the KM-CDR® process which uses the KS-1™ solvent.

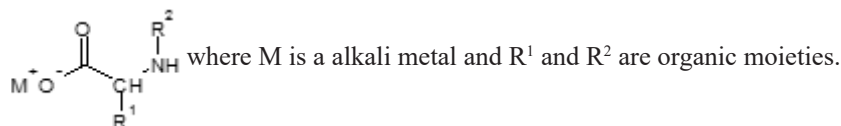
The composition of KS-1™ is proprietary, and may consist of activated hindered amines<sup>21, 22, 23</sup> (e.g., hindered amine compound selected from the group consisting of 2-amino-2-methyl-1,3-propanediol, 2-amino-2-methyl-1-propanol, 2-(ethylamino)-ethanol, 2-(methylamino) ethanol, 2-(diethylamino)-ethanol, 2-amino-2-ethyl-1,3-propanediol, t-butyl-diethanolamine and 2-amino-2-hydroxymethyl-1,3-propanediol; an activator selected from the group consisting of piperazine, piperidine, morpholine, glycine, 2-methylaminoethanol, 2-piperidineethanol, and 2-ethylaminoethanol). Additives such as CuCO<sub>3</sub> may also be used as corrosion inhibitors to permit the use of carbon steel instead of stainless steel.<sup>21</sup>

Ten CO<sub>2</sub> capture plants using the KM-CDR process, with a maximum capacity of 450 T/d have been built to date. In the majority of these plants, CO<sub>2</sub> is recovered from natural gas-fired reformer flue gas and used for urea synthesis.<sup>24</sup> A 500 T/d CO<sub>2</sub> plant capturing CO<sub>2</sub> from coal-fired flue gas started operating at Southern Company's (Alabama Power) Plant Barry in June 2011.<sup>25</sup> The capture CO<sub>2</sub> is injected into a saline formation for storage. The plant capacity is equivalent to a 25 MWe power plant with a design flue gas flow rate of 1,16,840 Nm<sup>3</sup>/h (90% capture with a design CO<sub>2</sub> concentration of 10.1 mol% [wet basis]).<sup>24</sup> The KM-CDR® process consists of a direct-contact flue gas cooler cooling the flue gas to 95–113 °F, a packed tower absorber for countercurrent flow of gas and solvent, a water-wash section for removing volatiles in treated flue gas, and a stripper/reboiler section. Saturated steam at 3 bar gauge fed to the reboiler, and the temperature at the bottom of the stripper is ≈250 °F.<sup>24</sup> In operation, the capture plant removed CO<sub>2</sub> at the design rate of 90%, and also exceeded the specific steam consumption measure of 0.98 kg steam/kg CO<sub>2</sub> (3 bar g saturated). Further reduction in energy consumption and the cost of electricity can be achieved through heat integration, e.g., using the heat content of the stripper overhead gas and flue gas to heat the boiler condensate, replacing the preheaters.<sup>26</sup>

The KS-1™ solvent was also tested for three months from January to March 2012 at the Brindisi power station in Italy capturing 60 T/d CO<sub>2</sub> (approximately equivalent to ≈2.9 MWe<sub>net</sub>) from one boiler (flue gas flow rate 12,000 Nm<sup>3</sup>/h at ≈13% CO<sub>2</sub>).<sup>27</sup> The results indicate that KS-1™ could achieve a lower thermal regeneration energy (1.2 kg-steam/kg CO<sub>2</sub>) vs. 30 w/w% MEA (1.5 kg-steam/kg CO<sub>2</sub>), with a lean-solvent flow rate 25% lower than that of MEA. Further, ammonia emissions in the treated flue gas were also significantly lower than that with MEA.

**Amino-Acid Salts (AAS)**

Amino-acid salts are a family of solvents which contain both the amine and carboxylic acid functionalities, e.g.,



The metal carboxylate (-COO<sup>-</sup>M<sup>+</sup>) group lowers the solvent vapor pressure and increases water solubility, while the amine group is active for CO<sub>2</sub> absorption. AASs exhibit low volatility, high cyclic-molar-CO<sub>2</sub> loadings, and high resistance to oxidative degradation. They are typically used in their metal salt form because of the increased solubility in aqueous solutions. The amine group reacts with CO<sub>2</sub> similar to primary/secondary amine, forming carbamates with a stoichiometry of 1:2. Amino-acid carbamates can further react to form bicarbonate and carbonate ions (especially if the amine group contains a hindered amine or a tertiary amine). The Alkazid process formerly licensed by BASF used sodium or potassium salts of amino acids (alanine, or diethyl- or dimethyl

21 Iijima, M. et al. United States Patent: 6036931—Method for removing carbon dioxide from combustion exhaust gas. (2000).

22 Yoshida, K. et al. United States Patent: 6689332—Process for removing carbon dioxide from combustion gases. (2004).

23 Yoshida, K. et al. United States Patent: 6500397—Method for removing carbon dioxide from combustion exhaust gas. (2002).

24 At a plant currently under construction in Qatar, 500 T/d CO<sub>2</sub> would be captured using the KM-CDR™ process from steam methane reformer flue gas to increase methanol production from an existing facility.

25 Ivie II, M. A. et al. Project Status and Research Plans of 500 TPD CO<sub>2</sub> capture and sequestration demonstration at Alabama Power's Plant Barry. *Energy Procedia* **37**, 6335–6347 (2013).

26 Wall, T. Development and demonstration of waste heat integration with solvent process for more efficient CO<sub>2</sub> removal from coal-fired flue gas. Presented at the 2013 CO<sub>2</sub> Capture Technology Meeting, Pittsburgh, PA. (2013).

27 Kamijo, T. et al. Result of the 60 tpd CO<sub>2</sub> capture pilot plant in European coal power plant with KS-1™ solvent. *Energy Procedia* **37**, 813–816 (2013).

glycine [KDiMGly]) to absorb CO<sub>2</sub> and H<sub>2</sub>S from gas streams.<sup>28,29</sup> The sodium alanine solution (marketed as Alkazid solution “M”) was used to separate either H<sub>2</sub>S, or CO<sub>2</sub> when present alone, or for absorbing both gases simultaneously. Alkazid solution “di-K” contained potassium diethyl- or dimethyl glycine (KDiMGly) and was used for the selective removal of H<sub>2</sub>S from gases containing CO<sub>2</sub> and also from gases containing trace quantities of CS<sub>2</sub> and HCN.<sup>27</sup> Weiland and Hatcher estimate that piperazine-promoted KDiMGly would have 20% lower regeneration energy and 20% lower solvent circulation rates compared to 30 w/w% MEA.<sup>30,31</sup> Wetted-wall column tests show that potassium taurate AAS solutions exhibit faster mass-transfer kinetics (at 323 K to 353 K) compared to 30 w/w% (5-M) MEA (at 313 K).<sup>32</sup>

One potentially beneficial property of AASs is that they can form solids (bicarbonates, or the neutral form of the amino acid) as the CO<sub>2</sub> loading is increased. This results in a higher driving force at the higher CO<sub>2</sub> loading, resulting in faster mass-transfer kinetics.<sup>33</sup> The proprietary DECAB process is based on forming slurries in the CO<sub>2</sub> absorber using amino-acid salts and thermally regenerating the amino-acid salt.<sup>34</sup> The limitations of such processes include reduced interfacial contact area, and complications arising out of handling slurries. This may be offset by increasing solvent (molar) CO<sub>2</sub> loading,<sup>35</sup> and lower solvent circulation rates, and the higher driving force for absorption. Brouwer et al. note that a heat-integrated stripper is required to fully leverage the advantages of slurry formation.<sup>32</sup> Such processes may also use a two-stage absorber containing packed column-stage and a spray absorber stage to handle the solids formed at high-CO<sub>2</sub> loadings.<sup>36</sup>

An AAS-based solvent is the basis for the Siemens POSTCAP™ CO<sub>2</sub> capture technology which was tested at the 0.1 MWe-scale at the Staudinger coal-fired power plant in Germany starting in 2009.<sup>37</sup> Results indicate that compared to amine-based technologies, the AAS-based POSTCAP™ process did not require water wash, had ≈25% lower thermal regeneration energy (2.7 GJ/T CO<sub>2</sub> vs. 3.6 GJ/T CO<sub>2</sub> for 30 w/w% MEA), low solvent makeup requirements, and very low solvent emissions.<sup>36</sup> CO<sub>2</sub> carbonate or carbamates do not precipitate under the operating conditions of the process.<sup>38</sup>

### Cansolv

Cansolv absorbents have relatively fast kinetics, very low degradation rates, high resistance against oxidation, and low thermal regeneration energy. In brief, the Cansolv process is similar to a typical amine process with the difference that it can separate both CO<sub>2</sub> and SO<sub>2</sub> from gas streams. Cansolv solvents are stable in SO<sub>2</sub>, whereas MEA forms heat-stable salts with SO<sub>2</sub>. The need for kinetic separation between CO<sub>2</sub> and SO<sub>2</sub> indicates that tertiary amines may be relevant solvent candidates for this process. For example, DC-103® solvent is reported to consist of a tertiary amine.<sup>39</sup> Activators and free-radical scavengers are also added for improving kinetics and for reducing solvent degradation.<sup>40,41</sup> It is reported that DC-103® solvent requires lower regeneration energy but higher absorber surface area compared to the faster-acting DC-103B® solvent.<sup>42</sup>

- 28 Kohl, A. L. and Nielsen, R. Alkaline salt solutions for acid gas removal, in *Gas Purification*, 330–410 (Gulf Professional Publishing, 1997).
- 29 BASF currently licenses the amine-based OASE®-family of solvents of gas processing applications instead of the amino-acid salt-based Alkazid solvents.
- 30 The selectivity of the unpromoted Alkazid “dik” or KDiMGly solution toward H<sub>2</sub>S over CO<sub>2</sub> is the result of its slow CO<sub>2</sub> mass-transfer kinetics. The addition of piperazine as a promoter increases the rate of CO<sub>2</sub> absorption but also increases the thermal regeneration energy.
- 31 Weiland, R., H. and Hatcher, N., A. Post-combustion CO<sub>2</sub> capture with amino-acid salts. *Digital Refining* (2011).
- 32 Wei, S. C.-C., Puxty, G. and Feron, P. Amino acid salts for CO<sub>2</sub> capture at flue gas temperatures. *Energy Procedia* **37**, 485–493 (2013).
- 33 Brouwer, J., Feron, P., Ten Asbroek, N. Amino-acid salts for CO<sub>2</sub> capture from flue gases, in *Proceedings of the 4<sup>th</sup> Annual Conference on Carbon Capture and Sequestration*, Pittsburgh, PA (2009).
- 34 Versteeg, G., et al. International Patent Number WO 03/095071 A1: Method for absorption of acid gases. (2003).
- 35 Lower molar CO<sub>2</sub> loading (i.e., mol CO<sub>2</sub>/mol amine or mol AAS) does not translate to lower weight-based or volumetric CO<sub>2</sub> loading. The molecular weight and density of the amine/AAS/ionic liquid are important parameters affecting these measures.
- 36 Goetheer, E. L. V., Fernandez, E. S. and Roelands, C. P. M. United States Patent Application: US20120282158 A1: Method for absorption of acid gases using amino acids. (2012).
- 37 Schneider, R., Schramm, H. Environmentally friendly and economic carbon capture from power plant flue gases: The Siemens POSTCAP™ technology. Presented at the 1<sup>st</sup> Post-Combustion Capture Conference, Abu Dhabi, Dubai. (2011). [http://www.ieaghg.org/docs/General\\_Docs/PCCC1/Presentations/1\\_11%2005%2018\\_%20Siemens%20PostcapTM\\_PCCC1\\_ext\\_2.pdf](http://www.ieaghg.org/docs/General_Docs/PCCC1/Presentations/1_11%2005%2018_%20Siemens%20PostcapTM_PCCC1_ext_2.pdf).
- 38 Winkler, J.L. Slipstream development and testing of post-combustion CO<sub>2</sub> capture and separation technology for existing coal-fired plants. Presented at the 2011 CO<sub>2</sub> Capture Technology Meeting, Pittsburgh, PA. (2011).
- 39 Figueroa, J. D., Fout, T., Plasynski, S., McIlvried, H. and Srivastava, R. D. Advances in CO<sub>2</sub> capture technology—The U.S. Department of Energy’s Carbon Sequestration Program. *International Journal of Greenhouse Gas Control* **2**, 9–20 (2008).
- 40 IEA Greenhouse Gas R&D Programme (IEAGHG). Evaluation of novel post-combustion CO<sub>2</sub> capture solvent concepts. 2009/14. (2009). <http://www.globalccsinstitute.com/publications/evaluation-novel-post-combustion-co2-capture-solvent-concepts/online/109251>.
- 41 Hakka, L. E. and Ouimet, M. A. United States Patent: 7056482—Method for recovery of CO<sub>2</sub> from gas streams. (2006).
- 42 Rameshni, M. Carbon capture overview. (2010).

The unique features of the Cansolv integrated CO<sub>2</sub>/SO<sub>2</sub> capture process are the possibilities for process integration between the CO<sub>2</sub> and SO<sub>2</sub> capture steps. For example, the SO<sub>2</sub> stripper overhead stream contains considerable water vapor, whose latent energy can be recovered using mechanical vapor recompressors (MVRs) to reduce the primary steam requirement in the CO<sub>2</sub> stripper by about 15%.<sup>43</sup> The exothermic heat of reaction in sulfuric acid synthesis from SO<sub>2</sub> can be used to raise steam for the CO<sub>2</sub> capture process, and the latent heat of the lean amine exiting the CO<sub>2</sub> stripper may also be recovered. Further, a rectangular integrated CO<sub>2</sub>/SO<sub>2</sub> absorber tower with a built-in prescrubber section is constructed with concrete and lined with ceramic/carbon tiles, reducing the construction and materials costs.<sup>44</sup>

DOE/NETL-funded tests at EERC indicate that the Cansolv next generation solvents have ≈38% lower solvent circulation rates (at 90% CO<sub>2</sub> capture) and 21% lower regeneration energy compared to 30 w/w% MEA.<sup>44</sup> In 0.5 MWe slipstream tests at the National Carbon Capture Center (NCCC), the Shell Cansolv DC-201<sup>®</sup> solvent had 50% lower solvent circulation rate compared to MEA and a thermal regeneration energy of 2.1 GJ/T CO<sub>2</sub> (35% lower than that of MEA).<sup>45</sup> It was found that the optimum solvent concentration for minimizing the thermal regeneration energy was 45 w/w% to 55 w/w%.<sup>46</sup>

Cansolv solvents will be used to capture CO<sub>2</sub> and SO<sub>2</sub> from SaskPower's 150 MWe lignite-fired Boundary Dam (Unit 3) power plant where the flue gas contains ≈12% CO<sub>2</sub> and ≈1,000 ppm SO<sub>2</sub>.<sup>44</sup> Approximately 1.2 million T/y CO<sub>2</sub> would be captured and sold for enhanced-oil recovery, while the captured SO<sub>2</sub> would be converted to H<sub>2</sub>SO<sub>4</sub> (60 T/d) and sold to the fertilizer market. Two different solvents, Cansolv DS<sup>®</sup> and Cansolv DC-103<sup>®</sup> would be used to capture SO<sub>2</sub> and CO<sub>2</sub> at the Boundary Dam project.<sup>47, 48</sup> The project construction came online late 2014.<sup>49</sup>

### Hitachi H<sub>3</sub>-1

Babcock Hitachi developed an amine-based solvent (H<sub>3</sub>-1) containing additives for reducing the regeneration energy and solvent degradation rates. It is also claimed that the H<sub>3</sub>-1 solvent has low degradation, low amine loss and low corrosivity. H<sub>3</sub>-1 was tested for 1,300 hours at NCCC, is being used at LG&E and KU Energy Service Company (LG&E-KU)'s EW Brown Generating Station as part of a DOE-funded University of Kentucky 0.7 MWe pilot-scale heat integrated absorption capture system test and is going to be used at the 20 MWth-scale at SaskPower's coal-fired Shand Power Station in Canada, starting in 2014.<sup>50</sup> Tests at EERC indicate that 2.88 GJ of thermal energy (21.3% lower than that of MEA) is required to regenerate a tonne of CO<sub>2</sub> using the H<sub>3</sub>-1 solvent.<sup>51</sup> The solvent flow rate needed for 90% CO<sub>2</sub> capture is ≈46% lower than that required for 30 w/w% MEA. Results from tests at the NCCC show that the thermal regeneration energy was reduced by 33% compared to MEA (2.4 GJ/T CO<sub>2</sub> vs. 3.6 GJ/T CO<sub>2</sub>) while capturing a higher fraction of the incoming CO<sub>2</sub> (96% capture vs. 92% capture with MEA), with 38% lower liquid flow rates.<sup>52</sup> Wetted-wall column testing at University of Kentucky showed that H<sub>3</sub>-1 has a lower overall mass-transfer coefficient compared to MEA at lean CO<sub>2</sub> loadings but higher overall mass-transfer coefficient at rich CO<sub>2</sub> loading conditions.

### KoSol Solvents

A 10-MW post-combustion CO<sub>2</sub> capture plant operating on a proprietary solvent KoSol-4 began operating in May 2013.<sup>53</sup> The process captures ≈70,000 T/y CO<sub>2</sub> from 14% CO<sub>2</sub> coal-fired flue gas, some of which would be used for precision welding products and

43 Shaw, D. Cansolv CO<sub>2</sub> capture: The value of integration. *Energy Procedia* **1**, 237–246 (2009).

44 Holmes, M.J. Fossil generation and the Clean Air Act. Presented at the 125<sup>th</sup> Annual Meeting of NARUC, Bonnet Creek, FL (2013). <http://www.narucmeetings.org/Presentations/MJHolmes-NARUC%20Nov2013.pdf>.

45 Just, P.-E. Shell Cansolv deploying CCS worldwide. Presented at the 2<sup>nd</sup> Post-Combustion Capture Conference, Bergen, Norway. (2013).

46 Southern Company Services Inc. 2012. The National Carbon Capture Center at the Power Systems Development Facility. Topical Report: Budget Period 4. [http://www.nationalcarboncapturecenter.com/pdf/PSDF\\_NCCC%20%20Budget%20Period%20Four%20Topical%20Report.pdf](http://www.nationalcarboncapturecenter.com/pdf/PSDF_NCCC%20%20Budget%20Period%20Four%20Topical%20Report.pdf).

47 Sarlis, J. Providing the capture process. Presented at the SaskPower CCS Information and Planning Symposium, Regina, Canada. (May 21–23, 2013). [http://www.saskpowerccsconsortium.com/symposium/presentations/SK%20CCS%20Symposium%20John%20Sarlis%20CX%20Cansolv%20\(REVISED\).pdf](http://www.saskpowerccsconsortium.com/symposium/presentations/SK%20CCS%20Symposium%20John%20Sarlis%20CX%20Cansolv%20(REVISED).pdf).

48 Global CCS Institute. CO<sub>2</sub> capture technologies. Post-combustion capture (PCC). <http://cdn.globalccsinstitute.com/sites/default/files/publications/29721/co2-capture-technologies-pcc.pdf>.

49 <http://saskpowerccs.com/ccs-projects/boundary-dam-carbon-capture-project/>

50 Honoki, M. et al. Hitachi's Carbon dioxide scrubbing technology with H<sub>3</sub>-1 absorbent for coal-fired power plants. *Energy Procedia* **37**, 2188–2195 (2013).

51 Pavlish, B. Partnership for CO<sub>2</sub> capture: Results of the pilot-scale solvent evaluations. Presented at the 2010 NETL CO<sub>2</sub> Capture Technology Meeting, Pittsburgh, PA. (September 13–17, 2010).

52 Eswaran, S. et al. Recent developments of Hitachi's advanced solvent technology for post-combustion CO<sub>2</sub> capture. [http://www.hitachipowersystems.us/sup-portingdocs/forbus/hpsa/technical\\_papers/Recent%20Developments%20of%20Hitachi's%20Advanced%20Solvent%20Technology%20for%20Post-Combustion%20CO2%20Capture.pdf](http://www.hitachipowersystems.us/sup-portingdocs/forbus/hpsa/technical_papers/Recent%20Developments%20of%20Hitachi's%20Advanced%20Solvent%20Technology%20for%20Post-Combustion%20CO2%20Capture.pdf).

53 [http://www.ieaghq.org/docs/General\\_Docs/Newsletter/March%202014%20LR.pdf](http://www.ieaghq.org/docs/General_Docs/Newsletter/March%202014%20LR.pdf)

agricultural products. The Korea Electric Power Company (KEPCO) developed the KoSol family of solvents. Thermal energy to regenerate the KoSol-4 solvent is estimated to be 30% lower than that of MEA ( $\approx 2.5$  to  $3$  GJ/T CO<sub>2</sub>).<sup>54</sup>

In summary, many of the proprietary amine blends discussed in this section have significantly better resistance against oxidative and thermal degradation, tolerance to other acid gases, lower vapor pressures, higher carrying capacities and lower energy consumption (30–40% lower) compared to 30 w/w% MEA. Higher carrying capacity also results in lower operating (fuel) costs and also lower capital costs (smaller pumps, heat exchangers, reboilers, strippers). Further, some of these proprietary amines can be regenerated at higher temperatures compared to MEA, resulting in higher CO<sub>2</sub> partial pressure in the stripper overhead and lowering the compression load. Notwithstanding such advances, considerable improvements are further required to attain the DOE capture cost goals. Novel gas-liquid contactors, new, more cost-effective routes to solvent synthesis, and solvents with considerably higher mass-transfer coefficients, and lower thermal regeneration energies represent some of the means to attain DOE goals.

### 1.3.1.5 PIPERAZINE AND OTHER NON-PROPRIETARY AMINES

Piperazine (PZ) is a diamine. Concentrated eight molal (8-m) PZ has been used in several DOE-funded capture projects as a CO<sub>2</sub> capture solvent because it has a higher cyclic capacity, faster kinetics, is thermally stable at higher temperatures (150 °C) compared to MEA, and requires less energy to strip CO<sub>2</sub>, resulting in lower regeneration energy. Benefits include lower capital costs and lower operating costs. However, PZ forms a solid phase with water (PZ·6H<sub>2</sub>O) and also with CO<sub>2</sub> (H<sup>+</sup>PZCOO·H<sub>2</sub>O), and solvent developers need further experience in operating PZ-based capture plants at low-temperature and large scale.

## 1.3.2 NON-AQUEOUS SOLVENTS (NASS)

As discussed in section 1.3.1.2, amines used commercially for gas treatment contain 70–50% w/w water. The water content negatively affects solvent working capacity, thermal regeneration energy, and solvent circulation rates. To overcome these issues, several developers are in the process of testing solvents containing low quantities of water (as-formulated). The working solution might nevertheless pick up water from the flue gas, a part of which would be stripped off in solvent regeneration. Common features of this class of solvent technologies are their comparatively higher weight-percent loading of CO<sub>2</sub>, higher solution viscosity, potentially slower mass transfer rates, and potential issues with solid solvent-CO<sub>2</sub> products precipitating in the absorber. NAS development efforts currently underway are focused on the use of hydrophobic amines, CO<sub>2</sub>-binding organic liquids, aminosilicone solvents, functionalized-ionic liquids, and amine/organic solvent mixtures. These efforts are described below.

### 1.3.2.1 HYDROPHOBIC AMINES

As part of a recently-initiated, DOE/NETL-funded effort, RTI and BASF are developing hydrophobic amine solvents with significantly lower thermal regeneration energy requirements, capable of being regenerated at low temperatures (70–90 °C) compared to MEA.<sup>55</sup> The process uses a hydrophobic primary or secondary amine to form a carbamate in the non-aqueous phase. Water condensed from flue gas or otherwise present in the working solution is separated from the CO<sub>2</sub>-loaded amine solution in a decanter. The separated aqueous phase is used as water for amine wash at the top of the absorber. The hydrophobic amine phase containing the carbamate is fed to a stripper/reboiler thereby regenerating the hydrophobic amine. This process combines the relative fast kinetics of using primary or secondary amines with the lower quantity of regeneration energy made possible by the absence of water in the stripper. The technology is at the laboratory/bench scale of development, and preliminary analyses indicate a 30–50% reduction in thermal energy consumption compared to state-of-the-art solvents. The use of low regeneration temperatures permits low-pressure steam to be used for regeneration, reducing parasitic load. Preliminary analyses also suggest that the solvent circulation rates with the RTI/BASF NASSs would be higher compared with conventional amines, which might increase the capital cost for solvent pumps, heat exchangers and regenerators.<sup>55</sup>

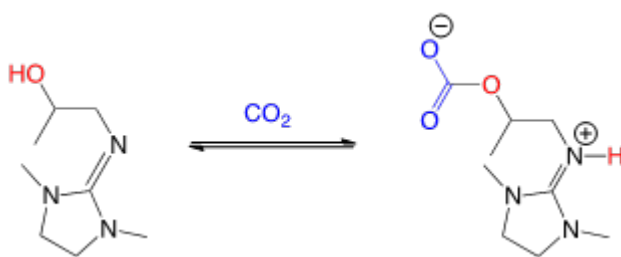
### 1.3.2.2 CO<sub>2</sub>-BINDING ORGANIC LIQUIDS

CO<sub>2</sub>BOLs are a class of switchable ionic liquids (i.e., molecular liquids which become ionic in the presence of CO<sub>2</sub>) having lower specific heat capacities and higher CO<sub>2</sub> working capacities compared to aqueous amines, resulting in potential savings in the sensible heat required to strip CO<sub>2</sub>.

54 <http://www.globalccsinstitute.com/insights/authors/dennisvanpuyvelde/2013/07/23/capture-demonstration-koreas-boryeong-thermal-power>

55 Kail, M., et al. Non-aqueous solvents for post-combustion CO<sub>2</sub> capture. Presented at the 2012 NETL CO<sub>2</sub> Capture Technology Meeting, Pittsburgh, PA. <http://www.netl.doe.gov/publications/proceedings/12/co2capture/presentations/3-Wednesday/L%20Coleman-RTI-ARPA-e-Non-aqueous%20Solvents.pdf>.





Equation 1-9

Similar to aqueous amines, CO<sub>2</sub>BOLs are basic, but the base (e.g., guanidine, amidine) does not directly react with CO<sub>2</sub>. Instead, the alcohol component, reacts with CO<sub>2</sub> forming alkyl carbonic acid, and subsequently transfers a proton to the base, forming liquid alkylcarbonate.

The current generation of CO<sub>2</sub>BOLs in DOE/NETL funded research at the Pacific Northwest National Laboratory (PNNL) combine the base and the alcohol moieties in a single molecule, lowering volatility (e.g., Equation 1-9). The addition of non-polar solvent (anti-solvent) to CO<sub>2</sub>BOLs and other switchable solvents during the solvent regeneration destabilizes bound CO<sub>2</sub>, thus potentially lowering the temperature at which the stripper can be operated (polarity-swing-assisted regeneration [PSAR]). Preliminary results indicate that PSAR could reduce the regeneration temperatures of CO<sub>2</sub>BOLs by more than 20°C. This allows novel possibilities for heat integration such as transferring heat from the absorber to the stripper using heat pumps, thereby lowering steam demand for solvent regeneration. The anti-solvent can be separated out from the CO<sub>2</sub>BOL by cooling, and liquid-liquid phase separation.

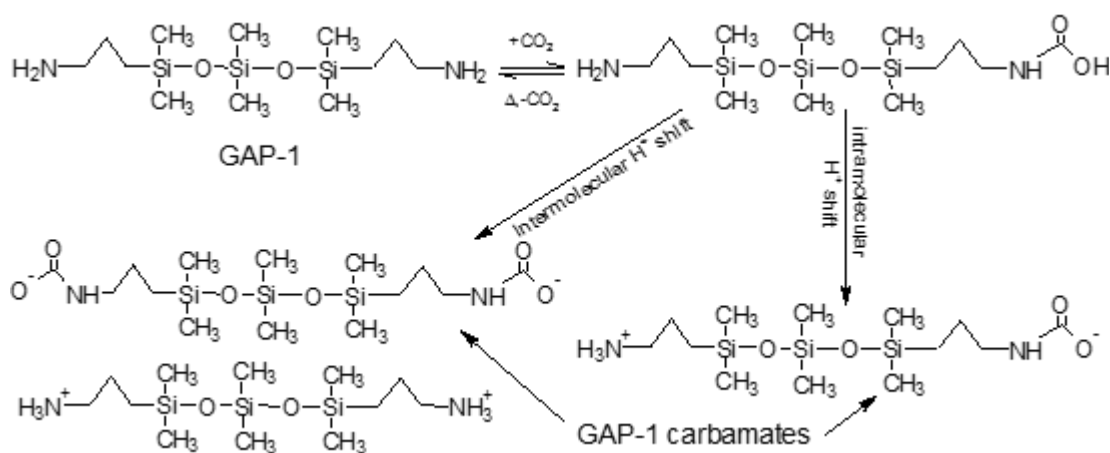
CO<sub>2</sub>BOLs offer the potential to lower the parasitic energy requirements of CO<sub>2</sub> capture by reducing the specific heat of the solvent, and lowering the amount of water present in the solvent. The lower regeneration steam requirements also result in higher power plant output. The polarity swing represents a means to lower the regeneration temperature further. One significant challenge to the CO<sub>2</sub>BOL (or other switchable ionic liquid) technology is the high viscosity of the solvent after CO<sub>2</sub> absorption. Test results indicate that the viscosity of the CO<sub>2</sub>-loaded solvent needs to be reduced by one-to-two orders of magnitude for the process to be technically feasible.<sup>56</sup>

### 1.3.2.3 AMINOSILICONE SOLVENTS

Aminosilicones are amine-functionalized siloxane compounds having a CO<sub>2</sub>-philic backbone (physisorbing CO<sub>2</sub>) and an amine group chemically reacting with CO<sub>2</sub>. They exhibit lower vapor pressure, higher thermal stability, and lower thermal energy requirement for CO<sub>2</sub> capture, leading to up to 27% lower thermal energy consumption (2,954 kJ/kg CO<sub>2</sub>) compared to MEA. In DOE/NETL-funded projects, General Electric (GE) has developed a family of aminosilicones starting with GAP-0 (bis(aminopropyl)tetramethyldisiloxane). Although GAP-0 resulted in a high CO<sub>2</sub> loading, it was found that the GAP-0 carbamate precipitated as a solid, even when triethylene glycol (TEG) was used as a solvent. Therefore, a mixture of GAP compounds (40% GAP-0, 33% GAP-1, 19% GAP-2, 8% GAP-3)<sup>57</sup> with an average molecular weight similar to GAP-1 (designated as GAP-1<sub>m</sub>) and TEG in a 60/40 w/w% mixture is being tested as a non-aqueous solvent for CO<sub>2</sub> absorption.

56 With the current alkanolguanidine CO<sub>2</sub>BOL, the viscosity of the hydrated CO<sub>2</sub>BOL increased from 22 cP at 0 w/w% CO<sub>2</sub> to 117 cP at 5 w/w% CO<sub>2</sub>. The viscosity would exceed 550 cP at 10 w/w% CO<sub>2</sub>, a typical value for rich-solvent loading.

57 The number in GAP-0, GAP-1, GAP-2, etc. refers to the number of repeating [SiO(CH<sub>3</sub>)<sub>2</sub>] units between the end siloxane members.



The GAP-1/TEG solvent reacts slower than MEA,<sup>58</sup> and may require larger reaction vessels. The solvent is regenerated in a stirred tank reactor with solvent recirculation, enabling CO<sub>2</sub> recovery at higher pressures (4.3 bar), lowering parasitic load and CO<sub>2</sub> compression costs. Bench-scale test results indicate that the solvent has a lower CO<sub>2</sub> carrying capacity compared to MEA ( $\approx 4.1$  w/w% vs. 5% to 7%), and  $\approx 40\%$  higher liquid-to-gas (L/G) ratio (kg lean solvent/Nm<sup>3</sup> flue gas) compared with MEA. However, the energy consumption is lower than that for MEA due to the low water-content of the solution and the low specific heat capacity of the solvent.

### 1.3.2.4 FUNCTIONALIZED-IONIC LIQUIDS

Researchers at the University of Notre Dame, funded by DOE/NETL, have synthesized, tested, and evaluated several candidate ionic liquids (ILs) for post-combustion CO<sub>2</sub> capture. A best-candidate solvent IL was identified, NDIL0157, and techno-economic analysis were performed. Extensive experimental studies could not be performed on this IL because of the high cost of making its anion component on a large scale. However detailed data is available on another IL (NDIL0046).<sup>59</sup> Laboratory-scale results suggest that a viscous solvent (diluted NDIL0046, 100 cP) can be operated in a column with structured packing (possibly with significant modifications). The corrosion rates of materials in contact with NDIL0046 and CO<sub>2</sub> is also very low, which has the potential to lower costs. Techno-economic calculations using NDIL0157 as a solvent to capture CO<sub>2</sub> from a supercritical coal power plant indicate an  $\approx 80\%$  increase in the cost of electricity (COE), similar to the DOE Base Case (Fluor Econamine process) using MEA. NDIL0157 has significantly lower parasitic electricity loss compared to MEA, but slightly higher CO<sub>2</sub> capture and compression equipment costs.

The Notre Dame IL technology is unique in that the viscosity does not change after CO<sub>2</sub> absorption. NDIL0046 solvent is viscous, and reacts about 2.5 times slower than MEA (liquid film mass transfer coefficient [kg'] at 5 kPa rich-solvent loading and 40 °C for NDIL0046:  $1.4e-7$  mol/s/m<sup>2</sup>-Pa vs.  $3.5e-7$  mol/s/m<sup>2</sup>-Pa for MEA). Because absorber volume is inversely proportional to the mass transfer coefficient, the size of the absorber needed for NDIL0046 or similar solvents would be larger (approximately at least twice) than that needed for MEA assuming that the driving force is the same. The IL used for techno-economic study, NDIL0157 has a lower viscosity (156 cP vs. 126 cP at 40 °C) than NDIL0046, and could potentially react faster than NDIL0046.<sup>60</sup>

The net-CO<sub>2</sub> carrying capacity of NDIL0157 was estimated to be  $\approx 0.0656$  kg CO<sub>2</sub>/kg IL, or 0.059 kg CO<sub>2</sub> for a 90:10 diluted solution. This is marginally higher than that of MEA, and is advantageous. The use of diluents such as tetraglyme to lower viscosity may also lead to increased water absorption and higher parasitic energy requirements.

58  $\approx 70\%$  lower mass-transfer coefficient, may require 42% larger surface area in absorber for the same driving force.

59 Apparently, NDIL0046 and NDIL0157 do not share any common components (cation/anion), and so it is not apparent if the trends in physical properties for NDIL0046 could be relevant for NDIL0157.

60 The Notre Dame wetted-wall column (WWC) experiments compared the height of a transfer unit (HTU) (or absorber volume needed for a single stage of separation) for a diluted 90 wt% NDIL0046+10% tetraglyme solution with 10–20 wt% MEA, whereas the commercial Fluor Econamine process uses  $\approx 30$  wt% MEA (quarterly progress report, Nov 6, 2012). It is significant that the HTUs measured with diluted NDIL0046 were comparable to that of 10–20 wt% MEA, and that a 100 cP solvent could be operated in a column. However, the HTUs for 30 wt% MEA would be lower than that of the diluted NDIL0046 due to higher amine concentration and higher reactivity (lower absorber volume or packing height needed to remove the same amount of CO<sub>2</sub>).



### 1.3.2.5 AMINE-ORGANIC SOLVENT MIXTURES

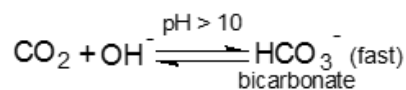
DOE/NETL and ION Engineering have been developing a solvent with relatively low heat of regeneration ( $\approx 1.6$  to  $2.5$  GJ/T  $\text{CO}_2$ ) which has low water-content and is resistant to thermal degradation with low heat-stable salt buildup on exposure to  $\text{SO}_x$  and  $\text{NO}_x$ . The solvent consists of a non-aqueous amine with ‘organic liquid’ as the solvent for the amine instead of water, resulting in low thermal regeneration energy due to the lower sensible and latent heats (see for example, Bara et al.<sup>61</sup>). The ION solvent (C) also has  $\approx 30\%$  lower solvent circulation vs. MEA for 90%  $\text{CO}_2$  capture, which may lower the capital costs of the pumps, heat exchangers, and the flash vessels. The solvent is regenerated in dual-stage flash vessels at two different temperatures ( $< 120$  °C). The use of flash vessels instead of conventional packed bed stripper columns and reboilers has the potential to lower capital costs.

### 1.3.3 CARBONATE-BASED SOLVENTS

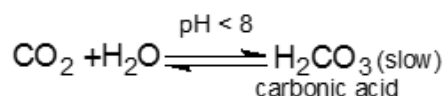
This category consists of alkali or ammonium salts with weak acids (e.g., carbonic acid) used to absorb  $\text{CO}_2$ . A key feature is the reaction of  $\text{CO}_2$  to form carbonate or bicarbonate ions in solution. The heat of desorption of  $\text{CO}_2$  from carbonate-based solvents is lower than that from amine-based solvents (e.g., 600 kJ/kg  $\text{CO}_2$ , or 26.4 kJ/g-mol  $\text{CO}_2$  vs.  $\approx 80$  kJ/g-mol  $\text{CO}_2$  for MEA), and can potentially lower the overall thermal regeneration energy. Historically, these solvents were primarily used in natural gas and synthesis gas processing. Previous and current technologies include:

- Processes based on hot potassium carbonate solutions used for  $\text{CO}_2$  (and  $\text{H}_2\text{S}$ ) removal from high-pressure gas streams (with promoters to enhance  $\text{CO}_2$  absorption,<sup>27</sup> e.g., Benfield process, Giammarco-Vetrocoke process),
- Processes based on ambient-temperature absorption of  $\text{CO}_2$  with vacuum regeneration (e.g., vacuum carbonate process,<sup>27</sup> aqueous ammonia-based processes [CSIRO,  $\text{ECO}_2$ ®]<sup>62</sup>),
- Processes based on low-temperature absorption (e.g., chilled ammonia<sup>63</sup>).

The reaction of  $\text{CO}_2$  with basic carbonate solutions takes place by two mechanisms: reaction with hydroxide ion ( $\text{OH}^-$ ) (Equation 1-11), and reaction of dissolved  $\text{CO}_2$  with water followed by dissociation of carbonic acid (Equation 1-12).<sup>10,27</sup>



Equation 1-11



Equation 1-12

The reaction shown in Equation 1-12 occurs in the absence of strong bases. It involves the reaction of  $\text{CO}_2$  with water, forming carbonic acid ( $\text{H}_2\text{CO}_3$ ), which dissociates into bicarbonate and a proton. This is a slower reaction compared to the reaction of  $\text{CO}_2$  with hydroxide ions (Equation 1-11). The latter is the dominant reaction in the pH ranges of interest for commercial solvents ( $\text{pH} > 8$ ). The reaction rate of  $\text{CO}_2$  in carbonate-bicarbonate solution is slow at room temperature, and high temperatures are required to increase the reaction rate. Rate-increasing additives, or promoters improving the rate of  $\text{CO}_2$  absorption, include formaldehyde, methanol, phenol, ethanolamines, arsenious acid, glycine, and the enzyme carbonic anhydrase.<sup>27</sup> Promoters previously used commercially include diethanolamine (DEA), hindered amines, glycine, and arsenious oxide.<sup>27</sup>

One unique feature of the carbonate-based processes is that if the stripper and absorber are operated at similar temperatures (either both hot or otherwise), there is no need for an intermediate lean-rich heat exchanger, lowering capital costs. In general, carbonate-based solvents cannot absorb  $\text{CO}_2$  faster than MEA from coal-fired power plant flue gas, resulting in higher absorber capital costs.

61 Bara, J. E. et al. W02012158609 A1: Compositions and methods for gas capture processes. (2012).

62 Yang, N. et al. Aqueous ammonia ( $\text{NH}_3$ ) based post-combustion  $\text{CO}_2$  capture: A review. *Oil & Gas Science and Technology—Revue d'IFP Energies nouvelles* (2013). doi:10.2516/ogst/2013160

63 Telikapalli, V. et al. CCS with the Alstom chilled ammonia process development program—Field pilot results. *Energy Procedia* 4, 273–281 (2011).

### 1.3.3.1 AMMONIA-BASED PROCESSES

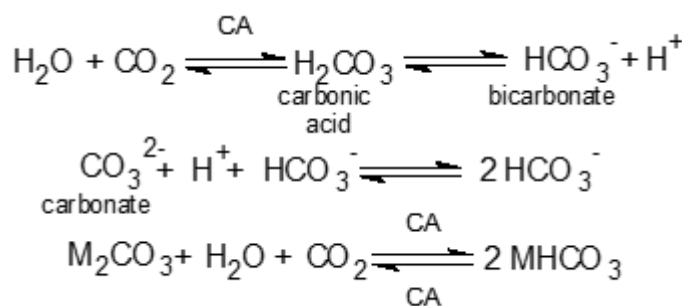
Ammonium carbonate or aqueous ammonia solvents have been used for flue gas treatment. Although ammonium carbonate solutions are good CO<sub>2</sub> solvents, the loss of ammonia to flue gas is a serious drawback. This is partly overcome by the use of low temperatures or extensive wash sections, or the use of a second salt to lower the vapor pressure of ammonia. Processes under development include the Alstom chilled-ammonia process (CAP), ambient temperature (Powerspan ECO<sub>2</sub><sup>®</sup>, CSIRO) processes, and the ammonium carbonate-potassium carbonate mixed-salt process.

#### *Alstom chilled ammonia process (CAP)*

A detailed description of the process is provided in reference 39 and Cerimele, 2011.<sup>64</sup> In brief, the use of a high concentration of aqueous ammonium carbonate in the absorber results in the formation of ammonium bicarbonate, which precipitates under the absorber operating conditions. The rich solvent consists of a slurry of ammonium bicarbonate (NH<sub>4</sub>HCO<sub>3</sub>) and ammonium carbonate ((NH<sub>4</sub>)<sub>2</sub>CO<sub>3</sub>). The formation of solid NH<sub>4</sub>HCO<sub>3</sub> phase permits higher CO<sub>2</sub> loading in solution compared to MEA, with carrying capacities up to 20 kg CO<sub>2</sub>/100 kg solution, with a lean loading of 24–28 w/w% CO<sub>2</sub> versus ≈5 kg CO<sub>2</sub>/kg solution working capacity for MEA.<sup>39</sup> The absorber operates at 0 ° to 10 °C, and requires a separate refrigeration system. The rich solution exiting the absorber can be concentrated to 30–50 w/w% solids and heated by heat exchangers and the stripper/reboiler to separate CO<sub>2</sub>. Ammonium carbonate can be regenerated at high temperatures (and pressures, ≈300 psig, or 21 bar<sup>65</sup>) without solvent degradation, unlike amines. However, the partial pressure of ammonia (and reflux to the top of the stripper) would increase with increased stripper temperatures (and pressures). It is reported that the mass transfer kinetics in the CAP are slower than those with aqueous MEA, and are primarily affected by the free ammonia content in solution.<sup>39</sup> With DOE/NETL support, the chilled-ammonia process was demonstrated at AEP's Mountaineer coal-fired power plant and was designed to capture 100,000 T CO<sub>2</sub>/y. Third-party assessments indicate that the chilled ammonia process has a parasitic load comparable to 30 wt% MEA, ≈385 kWh/T CO<sub>2</sub>.<sup>66</sup>

### 1.3.3.2 ENZYME-CATALYZED PROCESSES

In living cells, the reaction of CO<sub>2</sub> with water is accelerated by the enzyme carbonic anhydrase (CA). The in vivo reaction rate of CA is very high, with a turnover rate of 10<sup>6</sup> reactions per second. CA helps to maintain the acid-base balance in living cells (e.g., by converting produced CO<sub>2</sub> into bicarbonate for transport in the blood to the lungs where it is converted back into CO<sub>2</sub> and expelled). In CO<sub>2</sub> capture systems, the reactions involved are:



where *M* is a monovalent cation

Equation 1-13

64 Cerimele, G., L. *Mountaineer Commercial Scale Carbon Capture and Storage Project. Topical Report: Preliminary Public Design Report*. DOE Award No.: DE-FE0002673, Reporting Period: 2/01/10–9/30/11 (American Electric Power Service Corporation, Columbus, OH, 2011). [http://www.netl.doe.gov/File%20Library/Research/Coal/major%20demonstrations/ccpi/MTCCS-II---Preliminary-Public-Design-Report-Rev-12\\_14\\_2011-b.pdf](http://www.netl.doe.gov/File%20Library/Research/Coal/major%20demonstrations/ccpi/MTCCS-II---Preliminary-Public-Design-Report-Rev-12_14_2011-b.pdf).

65 Telikapalli, V. et al. CCS with the Alstom chilled ammonia process development program—Field pilot results. *Energy Procedia* **4**, 273–281 (2011).

66 Calculated from values provided in Versteeg, P. and Rubin, E. S. Technical and economic assessment of ammonia-based post-combustion CO<sub>2</sub> capture. *Energy Procedia* **4**, 1957–1964 (2011).

Normal variants of CA are unstable at the conditions involved in CO<sub>2</sub> absorption and desorption. There has been work on developing versions of CA which are more stable at absorber and desorber conditions, and immobilizing the CA so that it is not exposed to high temperatures in the CO<sub>2</sub> stripper. Technologies under development include:

- Regenerating potassium carbonate (K<sub>2</sub>CO<sub>3</sub>) solution containing carbonic anhydrase (CA) at milder conditions compared to the use of high-temperature steam (Novozymes),
- The use of sol-gel chemistry to immobilize the enzyme within micelles and coat it over commercial high-surface area packing (Akermin).

Bench-scale testing results and techno-economic analyses indicate that both absorption and regeneration of CO<sub>2</sub> need to be enzyme catalyzed to fully leverage the low-heat input advantage using K<sub>2</sub>CO<sub>3</sub>. The development of encapsulated enzymes stable at temperatures from 70 ° to 80 °C is a challenge being addressed by currently funded NETL/DOE research. Low-temperature regeneration also results in low partial pressures of CO<sub>2</sub> in the stripper overhead, requiring additional power for a compressor or vacuum blower.

### 1.3.3.3 AMINE-PROMOTED CARBONATE

The Benfield hot potassium carbonate process, developed for acid-gas removal from natural gas streams used a hot potassium carbonate solvent with diethanolamine (DEA) to promote CO<sub>2</sub> absorption. This process is not directly relevant to coal-fired power plant CO<sub>2</sub> capture because the absorber is operated at higher pressures ( $\approx 40$  psig) and temperatures ( $\approx 75$  °C) than those encountered in post-combustion CO<sub>2</sub> capture. However, certain process design elements and heat integration features might be of interest. The aggressive process conditions in the hot-potassium carbonate process require the use of corrosion inhibitors (typically based on vanadium ions). Recently, new amine promoters such as LRS-10 (London Research Station-10, a 3 w/w% solution of several formulated secondary amines<sup>67</sup>) have been used to increase the percentage of CO<sub>2</sub> captured, and to reduce the reboiler load.

NETL-funded research has also examined piperazine as an activator in K<sub>2</sub>CO<sub>3</sub> solutions.<sup>68</sup> It was found that 4-m K<sup>+</sup>/4-m PZ solution had faster absorption kinetics, higher solvent cyclic capacity, and lower parasitic load compared to 7-m MEA. One limitation encountered was that potassium sulfate (K<sub>2</sub>SO<sub>4</sub>) formed by the reaction of K<sub>2</sub>CO<sub>3</sub> with flue gas SO<sub>2</sub> could precipitate in 4-m K<sup>+</sup>/4-m PZ solvent, necessitating slurry operation of the CO<sub>2</sub> absorber.

NETL-funded research resulted in the proof-of-concept testing of an integrated vacuum carbonate absorption process (IVCAP), where CO<sub>2</sub> would be stripped under vacuum using a combination of direct and indirect steam stripping.<sup>69</sup> The low-quality steam (2 to 9 psia) would be withdrawn from the low-pressure (LP) turbine,<sup>70</sup> minimizing the derating loss due to the extraction of high-pressure (temperature) steam. A related process, but operating at higher temperature and pressure (Hot-CAP) is also being developed at the bench scale.

## 1.3.4 PHASE CHANGE SOLVENTS

The use of solvents which can undergo phase change is advantageous because:

- It increases driving force for CO<sub>2</sub> absorption by lowering the equilibrium CO<sub>2</sub> pressure in the rich solvent,
- It lowers regeneration energy by reducing the quantity of material that has to be heated to liberate CO<sub>2</sub> in the regenerator.

In spite of these thermodynamic and kinetic advantages, development of phase change solvent technologies is challenging because:

- Novel contactors for optimal gas-liquid-solid contact need to be designed and tested,
- There is limited operational experience in operating conventional packed column absorbers with slurries at power plant scales,
- Liquid-solid separation, or slurry concentration require additional equipment, which may increase capital costs and auxiliary load.

67 <http://www.summitdownloadportal.com/logos/1276600709-TGC%202010%20-%20Lee%20-%20Hyundai%20-%20ENGLISH.pdf>

68 Rochelle, G., et al. CO<sub>2</sub> capture by absorption with potassium carbonate. Final Report: DE-FC26-02NT41440. 2007.

69 Lu, Y, et al. Development and evaluation of a novel integrated vacuum carbonate absorption process. Presented at the 2011 DOE/NETL CO<sub>2</sub> Capture Technology Meeting, Pittsburgh, PA. (August 22–26, 2011).

70 Chen, S., Lu, Y. and Rostam-Abadi, M. WO2007133595 A2: Integrated vacuum absorption steam cycle gas separation. (2007).

The ammonia-based CO<sub>2</sub> absorption process described in section 1.3.3.1, and the CO<sub>2</sub>-binding organic liquids summarized in section 1.3.2.2 are two examples of phase-change solvent technologies. Another example of this category of processes is the GE phase-changing aminosilicone absorbent process. In the DOE/NETL-funded solvent project described in section 1.3.2.3, it was observed that the GAP-0 aminosiloxane reacts with CO<sub>2</sub> forming a solid carbamate. It was further observed that the GAP-0 carbamate was a chunky solid in the wet-salt form and a powder in its dry state. The proposed process, which is at the bench scale of development, consists of a spray absorber to contact the flue gas with the liquid lean GAP-0 solvent thereby forming a solid carbamate. A cyclone downstream of the absorber separates the fines from the flue gas, and an extruder is used to pressurize and heat the solid carbamate. The heated, pressurized solid carbamate is fed to stirred tank pressure vessels to dissolve the solid carbamate, liberate CO<sub>2</sub> at two pressures, and the lean liquid GAP-0 is recycled back to the spray absorber.

### 1.3.5 PROCESS INNOVATIONS AND IMPROVEMENTS

In addition to the advancements made in solvent technologies described above, significant advancements have been made in capture processes that have moved technologies toward achievement of DOE program goals. These can be generally categorized as advanced solvent regeneration (stripping) technologies, advanced gas-liquid contactors, and advanced heat integration. These are described below.

#### 1.3.5.1 ADVANCED SOLVENT REGENERATION TECHNOLOGIES

NETL/DOE is supporting the development of innovative means to regenerate CO<sub>2</sub>-rich solvents such as:

- Gas-pressurized stripping (GPS) to improve the efficiency of the stripping process and regenerate solvent at high pressure, reducing CO<sub>2</sub> compression cost (Carbon Capture Scientific [CCS] LLC). Salient features of the GPS process are:
  - The use of a stripping gas at high pressures to recover CO<sub>2</sub> from the CO<sub>2</sub>-rich solvent, with a GPS column heated throughout its height, producing high-pressure CO<sub>2</sub> along with the stripping gas.
  - Absorption of CO<sub>2</sub> from the GPS column overhead gas at high pressures using the rich solvent leaving the flue-gas CO<sub>2</sub> absorber, and subsequent recovery of CO<sub>2</sub> at high pressure by flashing (pressure reduction).
  - The GPS process has a higher heat of absorption (due to the second absorber tower), but lower thermal energy needed to heat the solvent and evaporate water compared with the conventional MEA process.
  - The energy required to compress the CO<sub>2</sub> is also reduced because CO<sub>2</sub> is stripped at pressures of 15–90 atm.
  - In addition to the conventional lean-rich solvent heat exchanger, the GPS process also requires a lean-stripping/gas-rich-stripping gas heat exchanger, which may lead to higher equipment costs. Modeling results indicate that the GPS process could lower the parasitic (steam+electric) load of CO<sub>2</sub> capture as much as 40% compared to conventional MEA CO<sub>2</sub> capture process, resulting in a load of 180 kWh/T CO<sub>2</sub>.
- Air stripping with heat integration (University of Kentucky Center for Advanced Energy Research [UKy-CAER]). The UKy-CAER process integrates three elements:
  - A secondary air stripper reduces the lean loading of the solvent subsequent to primary steam stripping, with the separated CO<sub>2</sub> being recycled to the boiler, increasing the driving force for absorption by increasing the incoming CO<sub>2</sub> concentration in the flue gas and reducing the amount of CO<sub>2</sub> in the lean solvent,
  - Utilizing the waste heat from the primary stripper overhead and the CO<sub>2</sub> compression intercooling to reduce the water content of the air provided to the cooling tower, in turn decreasing the cooling water temperature and lowering the condenser temperature, improving the turbine (and plant) efficiency,
  - Advanced H<sub>3</sub>-I solvent with lower thermal regeneration energy and comparable or faster kinetics compared to MEA.

### 1.3.5.2 ADVANCED GAS-LIQUID CONTACTORS

The capital cost of the flue-gas CO<sub>2</sub> absorber is a major (≈40%) component of overall capture plant costs. The development of equipment capable of contacting the capture solvent and the flue gas effectively has also been a focus of NETL/DOE efforts. Examples include:

- Flat-jet absorbers for high interfacial mass transfer areas: (Neumann Systems Group [NSG]): The size of absorber needed is proportional to amount of CO<sub>2</sub> absorbed/(mass transfer coefficient \* effective surface area \* log-mean driving force). NSG's novel jet-based absorber lowers absorber volume by having high effective surface area (≈930 m<sup>2</sup>/m<sup>3</sup> projected for the full-scale system, and 400 m<sup>2</sup>/m<sup>3</sup> for the 0.5 MWe pilot) and relatively high superficial gas velocity (≈4–7 m/s). The theoretical maximum gas velocity in the Neustream™-C absorber is ≈15 m/s. In typical packed bed absorbers, overall surface areas (which are higher than the 'effective' surface area) vary from 100 to 250 m<sup>2</sup>/m<sup>3</sup>. In conventional packed-bed absorbers, flue gas velocities are often limited to 1–2 m/s to avoid flooding and high pressure drops. The low gas velocities lead to larger absorber dimensions and higher costs. In contrast, the NSG flat-jet design permits the use of high gas velocities, which could decrease the size of the equipment needed to treat a given volumetric flow rate of flue gas.
- Membrane liquid contactors for high interfacial areas: Gas Technology Institute (GTI) is developing a hybrid membrane/absorption process in which a polyether ether ketone (PEEK)-based membrane contactor is used to separate CO<sub>2</sub> from flue gas. The membrane device has high interfacial gas-liquid contact area. CO<sub>2</sub> permeates through the membrane, reacting with the solvent. Relatively high mass transfer coefficients (≈1.8 s<sup>-1</sup>) and low gas-side pressure drops were demonstrated during bench-scale testing.<sup>71</sup>

### 1.3.5.3 ADVANCED HEAT INTEGRATION

The use of intermediate-to-low pressure steam from the steam cycle for CO<sub>2</sub> solvent stripping results in significant energy penalties because of the loss of electric power which would otherwise be generated by the steam. Thermal integration of the capture process with the overall power plant cycle can minimize the steam withdrawn from the power plant steam cycle, improving the efficiency. For example, CO<sub>2</sub> strippers and CO<sub>2</sub> compressors produce low-quality heat which can be used elsewhere in the power plant. Similarly, heat recovered from the flue gases before SO<sub>x</sub> removal can be used to offset part of the heat requirement for solvent regeneration. Another example is the use of mechanical vapor compression in the Cansolv process (discussed in section 1.3.1.4). It is to be noted that increased heat integration requires additional capital expenditure, and often gains in energy efficiency due to advanced heat integration may be offset by increased capital costs, with the result that the overall capture cost is not reduced proportionally.

- Heat integration of the CO<sub>2</sub> stripper overhead and the flue gas for condensate feedwater preheating: Southern Company, with NETL/DOE support, will design and operate a 25 MWe pilot using the Mitsubishi high-efficiency system (HES) waste heat recovery technology integrated with an amine (H<sub>2</sub>-1)-based CO<sub>2</sub> capture process unit. Waste heat in flue gas and CO<sub>2</sub> stripper overhead streams will be used to preheat a slipstream of boiler condensate in the power plant steam cycle. Ancillary advantages include reduction in the gaseous SO<sub>3</sub> emissions from the flue gas desulfurization (FGD) unit and savings in FGD make-up water consumption, while simplifying the boiler steam cycle.
- Use of heat recovered from flue gas for interstage heating of solvent in the CO<sub>2</sub> stripper: Linde proposed the use of a heat recovery unit, where energy recovered from flue gas exiting the power plant baghouse (375 °F) would be used to partly offset the steam requirement in the CO<sub>2</sub> stripper. Low-pressure steam (<4 bar) produced in the heat recovery unit would be used to heat solvent in the CO<sub>2</sub> stripper, akin to absorber intercooler. It is estimated that this use of low-grade heat and the use of a let-down turbine to expand the IP-LP crossover steam to <6 bar would lower the energy penalty of CO<sub>2</sub> capture from 28–25%.

### 1.3.6 KEY CHALLENGES FOR SOLVENT-BASED CO<sub>2</sub> CAPTURE

The technologies under development as part of the Carbon Capture R&D program are focused on overcoming barriers to deployment of capture technologies. Table 1-3 summarizes the barriers that the projects in the Capture Program portfolio are addressing as part of their technology development efforts.

71 Zhou, S.J. et al. Hybrid membrane/absorption process for post-combustion CO<sub>2</sub> capture. Presented at the NETL CO<sub>2</sub> Capture Technology Meeting, July 10, 2013.

Table 1-3. Key Challenges Addressed by Solvents-Based Post-Combustion CO<sub>2</sub> Capture Projects in Carbon Capture R&D Program Portfolio

PERFORMER	PROJECT FOCUS	BENEFITS	SCALEUP	CAPITAL COSTS	PARASITIC LOAD	PROCESS INTEGRATION	WATER USE
Akermin	Enzyme catalyzed	Low regeneration energy			●		
Battelle PNNL	Non-aqueous CO <sub>2</sub> -BOL	Low regeneration energy			●		
CCS, LLC	Process innovation	High-pressure regeneration			●		●
General Electric	Phase change	High-pressure regeneration			●		
General Electric	Aminosilicone	Enhanced energetics	●		●		
ION Engineering	Organic/amine mixture	Enhanced energetics	●	●	●		
Linde	Advanced amine/process innovation	Single-process train	●	●	●	●	
Neumann Systems	Process innovation	Modular; solvent agnostic	●	●	●		
Novozymes	Enzyme catalyzed	Low regeneration energy			●		
RTI	Hydrophobic amine	Enhanced energetics			●		
Southern Company	Process innovation	Thermal management	●			●	
SRI International	Carbonate-based	Capital cost reduction			●	●	
University of Kentucky	Catalyzed	VOC eliminated/high pressure			●		
University of Kentucky	Advanced amine/process innovation	High-pressure regeneration	●	●	●	●	●
URS/ University of Texas	Piperazine/process innovation	Enhanced energetics	●	●	●	●	

## 1.4 ADVANCES AND FUTURE WORK

Significant reductions in the quantity of electricity lost per unit quantity of CO<sub>2</sub> have been achieved. Currently funded solvent technologies have lower thermal regeneration energy, lower equivalent work loss due to steam withdrawal for stripping, and require smaller quantities of solvent to capture a given amount of CO<sub>2</sub>.



## 1.4.1 SUMMARY OF ADVANCES

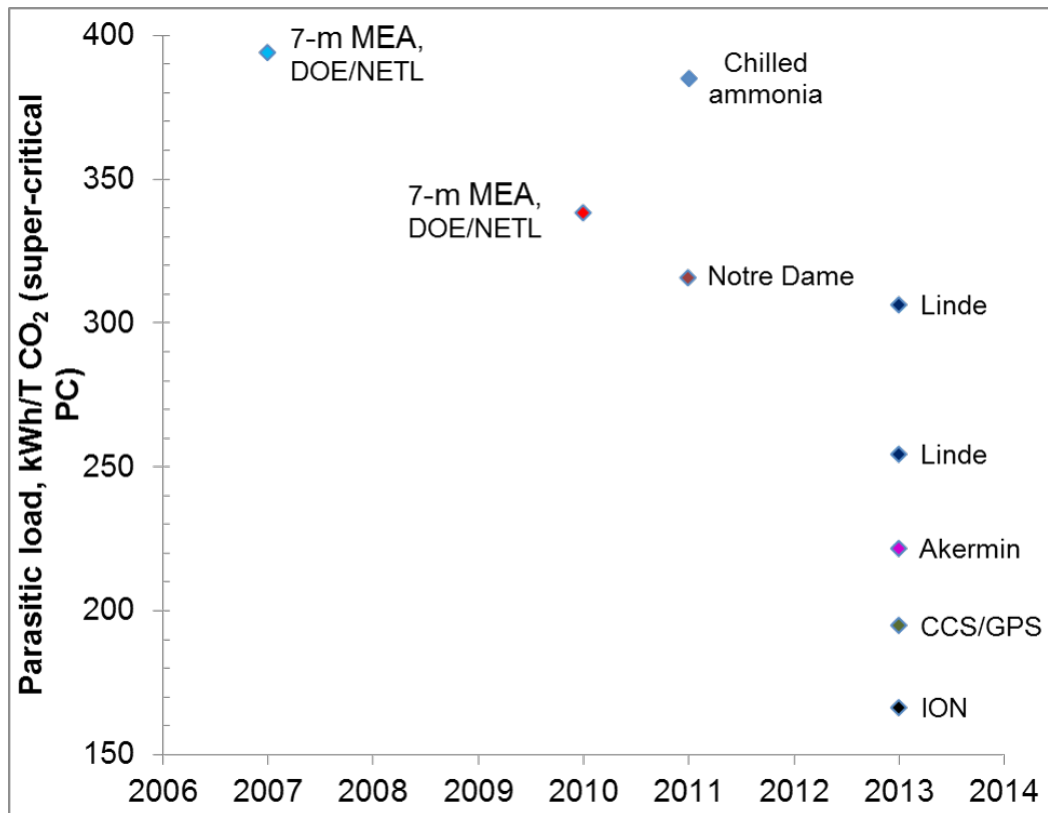


Figure 1-4. Progress in Reducing Parasitic Load for Solvent-Based Post-Combustion CO<sub>2</sub> Capture in DOE/NETL Funded Projects

Figure 1-4 and Figure 1-5 represent the progress made by the DOE/NETL post-combustion CO<sub>2</sub> capture program in reducing the parasitic load due to CO<sub>2</sub> capture (kWh lost/T CO<sub>2</sub> captured),<sup>72</sup> and the concomitant reduction in energy penalty due to CO<sub>2</sub> capture. Technologies being developed currently have parasitic loads from less than 200–250 kWh/T CO<sub>2</sub> (including CO<sub>2</sub> compression). Reduction in parasitic load is significant because it also reduces the amount of coal to be burnt to produce a given quantity of net power. In general, the reduction of parasitic load was achieved due to a combination of more thermally stable solvents with higher cyclic capacities and lower thermal regeneration energies. Regeneration at high temperatures is advantageous because it increases the partial pressure of CO<sub>2</sub>, lowering the compression load. However, this needs to be weighed against the loss of electricity due to the use of higher quality steam for regeneration. In practice, stripping steam is typically withdrawn from the intermediate pressure-low pressure (IP-LP) crossover steam and is desuperheated to reboiler conditions.

<sup>72</sup> Parasitic load is estimated as the equivalent work lost due to steam used for CCS + capture auxiliaries (e.g., pumps, blowers) + energy required for CO<sub>2</sub> compression from the stripper overhead conditions to 152.7 bara (2,214.5 psia). There are several means to account for the loss in steam cycle output due to the withdrawal of steam for the capture process. IEAGHG (Retrofitting CO<sub>2</sub> capture to existing power plants, Report 2011/02, May 2011) used a coefficient of performance for steam extraction (COP<sub>x</sub>) defined as the ratio of the heat requirement to the drop in steam cycle output. It is claimed that typical COP<sub>x</sub> values will be ≈5. Trimeric uses a derating factor depending on the quality of steam extracted for stripping. A derating factor of 0.0902 hp-h/lb steam was used in Trimeric techno-economic analyses for Case 12, and is being used here. Note that a COP<sub>x</sub> value of 5 is equivalent to a derating factor of 0.08144 hp-h/lb steam. The actual specific steam consumption estimate from the bituminous coal baseline revision 2 is 0.1120 hp-h/lb steam, which reflects a more efficient steam cycle, and higher parasitic load for steam used for CO<sub>2</sub> stripping.

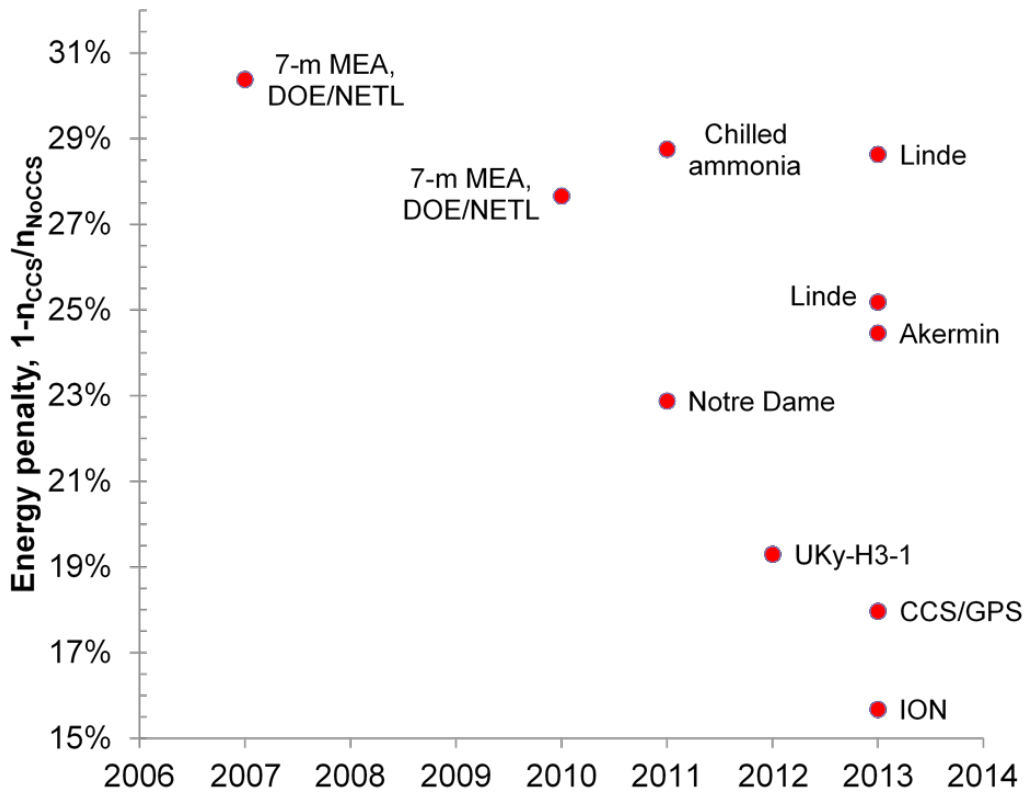


Figure 1-5. Progress in Reducing Overall Energy Penalty for Solvent-Based Post-Combustion CO<sub>2</sub> Capture in DOE/NETL Funded Projects

For a greenfield CCS project, it may be possible to match this crossover steam pressure to the pressure required for regeneration in the reboiler (e.g.,  $\approx 3$  to 4 bara pressure for amine systems<sup>73</sup>), minimizing LP turbine power losses. Other options to minimize the impact of the loss of high-grade steam include a letdown turbine which produces additional power while desuperheating the steam to match the requirements in the reboiler, which also has high capital costs. Examples of similar tradeoffs encountered in brownfield retrofits are discussed by Grol, 2012<sup>74</sup> and IEAGHG, 2007.<sup>71</sup>

## 1.4.2 KEY PARAMETERS TO BE EVALUATED MOVING FORWARD

Power plant efficiency and energy penalty have been considerably improved. However, significant reduction of capital costs and operating costs are required to achieve DOE goals. Key parameters to be evaluated in the future include:

- Solvent-CO<sub>2</sub> mass-transfer kinetics: Some of the solvent technologies with low energy penalty and parasitic load also react slowly with CO<sub>2</sub> compared with aqueous MEA solutions, resulting in higher capital costs. The absorber, intercoolers, solvent circulation pumps, heat exchangers, reboiler and stripper are some of the capital-intensive pieces of equipment in a CO<sub>2</sub> capture plant. Although solvents with improved carrying capacities can lower the capital costs of the pumps, stripper, reboiler, and cross heat exchangers, a solvent with slower kinetics adversely impacts the size of the absorber. Fundamental wetted-wall column studies, or qualitative CO<sub>2</sub> loading studies using different solvents in the same piece of equipment are required to understand the capital cost implications of selecting a solvent with slow mass transfer kinetics.
- Costs of second-generation solvents: The solvent technologies being developed in the DOE/NETL portfolio are novel and some of the solvent candidates have considerably higher cost compared to MEA, partly because they are first-of-a-kind technologies. However, significant advances in reducing the costs of solvent production are also needed to drive down the cost of solvents and thereby lower the cost of CO<sub>2</sub> capture.
- Operability concerns: These include: formation of solids in the absorber, solvent aerosol emissions, and emissions of amine degradation products.

73 IEA Greenhouse Gas R&D Programme (IEA GHG). CO<sub>2</sub> capture ready plants. 2007/4, May 2007.

74 Grol, E., Techno-economic analysis of CO<sub>2</sub> capture-ready coal-fired power plants. DOE/NETL-2012/1581. August 1, 2012.

### 1.4.3 POTENTIAL FOCUS AREAS FOR FUTURE POST-COMBUSTION SOLVENT RD&D

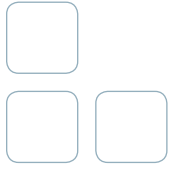
Alternate means to regenerate solvents: In conventional solvent regeneration processes, the entire solvent (with the water) has to be heated to liberate CO<sub>2</sub>. Processes which could selectively supply energy to the solvent molecules so that they would liberate CO<sub>2</sub> without energy input to the rest of the solution would reduce the parasitic energy penalty associated with CO<sub>2</sub> capture. Examples of such processes include the use of electrochemistry to capture and/or regenerate CO<sub>2</sub>.

Phase change: There has been a drive toward minimizing the energy penalty by reducing water content of solvents, and the development of novel phase-change technologies is a logical outgrowth of that approach. It is relatively easy to identify solvents which undergo phase change in the presence of CO<sub>2</sub>. However, the development of contactors and ancillary equipment to handle slurries or solids represents a potential focus area.

Hybrid approaches to CO<sub>2</sub> capture: Technologies offering potential value for the future also include those which combine multiple mass-transfer phenomena. Such processes aim to combine the advantageous feature of each mass-transfer process while attempting to limit the drawbacks of each approach. Technologies include but are not limited to:

- Approaches to immobilize viscous solvents in membranes or adsorbents to overcome viscosity limitations,
- Membrane contactors with solvents used to selectively permeate CO<sub>2</sub>,
- The use of additional mass-transfer operations (e.g., membranes, adsorbents) to reduce the water content of the rich solvent and thereby lower solvent regeneration energy.

In general, process equipment for hybrid approaches needs to be developed and tested at pilot- to slipstream-scales. Approaches combining several mass-transfer unit operations would also need additional equipment to carry out the separation processes.



## CHAPTER 2:



## SORBENT-BASED CO<sub>2</sub> CAPTURE

## 2.1 ESTABLISHED APPLICATIONS OF SORBENT-BASED CO<sub>2</sub> CAPTURE

The removal of CO<sub>2</sub> from gas streams using solid sorbents is not a new concept. In fact, lithium hydroxide (LiOH) sorbent was historically used for removal of CO<sub>2</sub> at low concentrations (<1%) from air in closed environments such as spacecraft. Demand for a practically regenerable alternative to LiOH needed for extended space missions led to development of regenerable sorbents such as the solid amine beads called HSC+, developed by Hamilton Sunstrand Space Systems International and used since the early 1990s, most notably on the space shuttle. This proprietary material consists of a liquid amine, polyethyleneimine (PEI), bonded to a high-surface-area, solid polymethyl methacrylate polymeric support. The material also consists of a second liquid phase coating, poly(ethylene glycol) (PEG), to enhance CO<sub>2</sub> adsorption and desorption rates.<sup>1</sup> For the International Space Station, CO<sub>2</sub> removal is accomplished with common, commercially available sorbents: there are four packed beds, two containing silica gel and zeolite 13X desiccant media, the other two containing zeolite 5A CO<sub>2</sub> sorbent media.<sup>2</sup>

Cryogenic air separation requires removal of trace species including water vapor and CO<sub>2</sub> from incoming feed air to avoid freezing of these in process. In large-scale commercial plants, this is typically performed in molecular sieve units containing sorbents; a very commonly used sorbent for this application is zeolite 13X<sup>3</sup> which has high selectivity for CO<sub>2</sub>, and high affinity for water common to zeolites in general.

One of the most widespread and important applications of sorbents in large-scale gas separations is for the production of hydrogen at refineries. In this case, the objective is separation of hydrogen from various gas mixtures, such as the syngas produced in a steam methane reformer consisting of H<sub>2</sub>, CO, CO<sub>2</sub>, unconverted CH<sub>4</sub>, and N<sub>2</sub>. Generally the objective is not to isolate CO<sub>2</sub>, but rather to separate relatively pure H<sub>2</sub> for refinery process use, with the leftover gas consisting of unrecovered H<sub>2</sub> and most of the rest of the other species, which is used as fuel gas in the refinery. The most commonly used hydrogen separation technology used at refineries is pressure swing adsorption (PSA) (see section 2.2.4 for further discussion). The sorbents utilized are commercially available types including molecular sieve (zeolites), activated carbon, activated alumina or silica gel.<sup>4</sup> In many refinery applications the adsorption process is not specific to CO<sub>2</sub> capture, but because CO<sub>2</sub> is a major gas species which is always targeted for capture in such PSA processes, these applications qualify in that sense as sorbent-based CO<sub>2</sub> capture.

On the other hand, in at least one instance CO<sub>2</sub> is targeted specifically for capture in a refinery process, this example being the currently operating carbon dioxide capture and storage project at Valero Energy's Port Arthur Texas refinery. In this project, 90% of the CO<sub>2</sub> from the existing steam methane reformers located within the refinery is captured in new vacuum swing adsorption (VSA) units at a rate of 1 million tonnes per year, upstream from the existing PSA process for capturing hydrogen. The process concentrates the initial gas stream from the steam methane reformers (containing 10–20% CO<sub>2</sub> prior to water gas shift, and ≈40% after WGS) to greater than 97% CO<sub>2</sub> purity. A common, commercially available sorbent is used in the VSA units. The CO<sub>2</sub> is transported to the West Hastings oil field in Brazoria County south of Houston, Texas, where it is injected for enhanced oil recovery (EOR).<sup>5</sup>

Notwithstanding certain instances of established uses of sorbents for CO<sub>2</sub> capture described above, sorbent-based CO<sub>2</sub> capture is usually not chosen over alternatives such as solvent-based and membrane-based technology for industrial-scale carbon capture applications. For example, out of the Global CCS Institute's database of 55 large-scale CCS projects in various stages of development to operation, 13 projects are classified as operating, with only one of those 13 projects using sorbent-based CO<sub>2</sub> capture (the Air Products Valero Refinery project described in preceding section). Most of the 12 remaining projects totaling 25.6 million tonnes per year CO<sub>2</sub> captured are natural gas processing, synthetic natural gas, or fertilizer production, and 11 of these plant use solvent-based processes (amine, Selexol, Rectisol) and one uses membrane separation.<sup>6</sup>

1 Satyapal, S.; Filburn, T.; Trela, J.; Strange, J., *Energy Fuels* 2001, 15 (2), 250–255.

2 Bernadette Luna, George Somi, J. Parker Winchester, Jeffrey Grose, Lila Mulloth, Jay L. Perry, "Evaluation of Commercial Off-the-Shelf Sorbents and Catalysts for Control of Ammonia and Carbon Monoxide," *American Institute of Aeronautics and Astronautics*. [ntrs.nasa.gov/archive/nasa/casi.ntrs.nasa.gov/20100039332.pdf](https://ntrs.nasa.gov/archive/nasa/casi.ntrs.nasa.gov/20100039332.pdf).

3 <http://www.sepcor.com/markets/airseparation.php>

4 Zahra Rabeie, "Hydrogen Management in Refineries," *Petroleum and Coal* 54(4) 357–368, 2012; [http://www.vurup.sk/sites/vurup.sk/files/downloads/pc\\_4\\_2012\\_rabeie\\_188.pdf](http://www.vurup.sk/sites/vurup.sk/files/downloads/pc_4_2012_rabeie_188.pdf).

5 Global CCS Institute database, information on the Air Products Steam Methane Reformer EOR Project. <http://www.globalccsinstitute.com/project/air-products-steam-methane-reformer-eor-project>. Accessed 15 Jan 2015.

6 Global CCS Institute database. <http://www.globalccsinstitute.com/projects/large-scale-ccs-projects>.

## 2.1.1 CHALLENGES ASSOCIATED WITH SORBENT-BASED CO<sub>2</sub> CAPTURE

Notwithstanding the existence of commercial CO<sub>2</sub> sorbents such as various zeolites, silica gels, activated carbons, supported amine sorbents, etc., which are suitable for utilization in CO<sub>2</sub> capture applications, the previously noted trend to opt for solvent and membrane technology alternatives to sorbents for large-scale CO<sub>2</sub> capture implies that the sorbent based technology is simply not as cost effective as the solvent or membrane separation alternatives in many or most cases. This can probably be attributed to the following challenges facing sorbents:

- Cost of many sorbents is high (i.e., particularly zeolites, some other types)
- CO<sub>2</sub> adsorption capacity limitations
- Operation at higher flue gas/exhaust gas temperatures
- Sorbent attrition
- Sorbent regeneration (energy demands)

## 2.1.2 ADVANTAGES OF SORBENT PROCESSES

A solid sorbent post-combustion CO<sub>2</sub> capture technology potentially offers several advantages over a conventional aqueous solvent-based process such as monoethanolamine (MEA):

**Energy penalty:** Solid sorbents have the potential to significantly reduce the regeneration energy penalty compared to solvents. This energy penalty reduction can be attributed to: (1) the heat capacity of solids is significantly lower than that of water (i.e., by approximately a factor of four), which dramatically reduces the sensible heat input required to accomplish the temperature swing; and (2) the moisture content during regeneration will be significantly lower for solids compared to solvents, so less evaporation will occur.

**Range of operating temperature:** Aqueous solvent-based processes are limited in their operating temperature range. In contrast, a range of solid sorbent types exist allowing operation from ambient temperatures to as high as 700 °C.

**Miscellaneous benefits:** Solid sorbents yield less waste during cycling, and spent solid sorbents have lower environmental impact than solvents easing their disposal.<sup>7</sup>

## 2.2 PRINCIPLES ASSOCIATED WITH SORBENT-BASED CAPTURE

### 2.2.1 ADSORPTION

Adsorbents being considered for carbon capture employ one of the two possible adsorption mechanisms, namely physical adsorption (physisorption) and chemical adsorption (chemisorption). In physisorption, target molecules are attracted to the surface of pore walls within a high surface-area sorbent by van der Waals forces and have a low heat of adsorption that is only slightly greater than heat of sublimation of the adsorbate. The physisorption is reversible and fast. In chemisorption, the target gas undergoes a covalent chemical reaction to bind to certain sites on the sorbent with a much greater heat of adsorption, roughly equal to the heat of reaction.

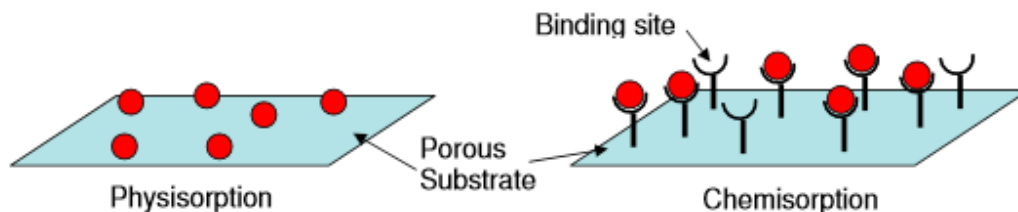


Figure 2-1. Physisorption vs. Chemisorption

*In physisorption the CO<sub>2</sub> is adsorbed weakly by the substrate itself, in chemisorption, the CO<sub>2</sub> is adsorbed more strongly by specific binding sites.<sup>8</sup>*

7 Junya Wang, Liang Huang, Ruoyan Yang, Zhang Zhang, Jingwen Wu, Yanshan Gao, Qiang Wang, Dermot O'Hareb and Ziyi Zhong, "Recent advances in solid sorbents for CO<sub>2</sub> capture and new development trends," *Energy Environ. Sci.*, 2014, 7, 3478.

8 Adam Hughmanick Berger and Abhoyjit S. Bhowm. "Comparing Physisorption and Chemisorption Solid Sorbents for use Separating CO<sub>2</sub> from Flue Gas using Temperature Swing Adsorption," *Energy Procedia* 4 (2011) 562–567.



An example of a sorbent exhibiting the physisorption mechanism is activated carbon; CO<sub>2</sub> adsorbs onto its high surface area pore walls by weak dipole interactions. The heat of adsorption of carbon dioxide on activated carbon sorbent ranges from -25 to -40 kJ/mole, which is close to the heat of sublimation. This low heat of adsorption reduces the amount of energy needed to desorb a given quantity of carbon dioxide. However, it also means that carbon dioxide is less likely to adsorb onto the porous substrate.

On the other hand, solid sorbents that capture carbon dioxide through a chemical process, such as bonding with an amine that is grafted or coated onto the surface of the sorbent, have a much higher heat of adsorption. These heats of adsorption can range between -60 and -100 kJ/mole depending on the amine used. While this increases the amount of energy needed to separate the carbon dioxide from the chemisorbent, it also increases the affinity of the amine for carbon dioxide which allows the amine-based solid sorbent to have a higher capacity at low concentrations of carbon dioxide.

While physisorbents such as activated carbon can be stable even past 200 °C, grafted amines tend to volatilize and degrade above 120 °C which restricts their regeneration temperatures. Another difference is that physisorbents tend to attract various other molecules to their surface lowering the selectivity of the sorbent, which leads to more nitrogen contamination and lower carbon dioxide purity than with chemisorption for the same process configuration. On the other hand, chemisorbents can permanently bind to species such as SO<sub>2</sub> and poison binding sites, decreasing the capacity of the sorbent.

## 2.2.2 REGENERATION

### 2.2.2.1 REGENERATION HEAT DUTY

The energy necessary to be added during the regeneration step to reverse the CO<sub>2</sub> absorption reaction is found in Equation 2-1. The energy balance assumes that state 1 is the system after CO<sub>2</sub> absorption, and state 2 is the system after CO<sub>2</sub> regeneration. The energy balance also assumes a change in temperature occurs between states 1 and 2 (i.e., thermal regeneration is employed). The subscripts represent the equipment (e), the sorbent (s), and the CO<sub>2</sub> (c), and with the indices 1 and 2 added to reference the states. The variable m is the mass, C is the specific heat, C<sub>p</sub> is the constant pressure specific heat for the gaseous CO<sub>2</sub>. Q is the heat input, and Q<sub>r</sub> is the heat of reaction (represented as a positive number) for breaking the chemical bond between the active species and the CO<sub>2</sub>. B is a constant of proportionality for dimensional units, and L is the CO<sub>2</sub> loading capacity expressed in gmole CO<sub>2</sub>/kg.

$$\frac{Q}{m_c} = \underbrace{\frac{m_e}{m_c} \cdot C_e \cdot \Delta T}_{\text{Sensible heating of the "equipment" that supports the process}} + \underbrace{\frac{B}{L} \cdot C_s \cdot \Delta T}_{\text{Heating the active species and sorbent}} + \underbrace{C_{p,c} \cdot T_2 - C_s \cdot T_1}_{\text{Delta enthalpy between gaseous CO}_2 \text{ and base sorbent}} + \underbrace{\frac{Q_r}{m_c}}_{\text{Heat of reaction}}$$

Equation 2-1

The equation shows that for fixed swing in temperature, regeneration energy can be reduced by increased loading L or decreased specific heat C. The energy balance also assumes that the only gas adsorption reaction occurring is CO<sub>2</sub>. If there are additional reactions taking place, such as adsorption/desorption of H<sub>2</sub>O, then additional analogous terms would need to be included in Equation 2-1.

The energy balance equation highlights the need for several sorbent parameters to be determined in value. They include the heat of adsorption of the gas (CO<sub>2</sub> reaction), the specific heat (heat capacity) of the sorbent, and the CO<sub>2</sub> loading capacity of the sorbent. A fourth but very important consideration is the role of moisture, whether as a participant (reactant) in the CO<sub>2</sub> reaction or as a competitor in adsorption/desorption.<sup>9</sup>

9 "Factors in Reactor Design for Carbon Dioxide Capture with Solid, Regenerable Sorbents," James S. Hoffman, George A. Richards, Henry W. Pennline, Daniel Fischer, and George Keller.

## 2.2.3 TEMPERATURE SWING ADSORPTION

### Description

The temperature swing adsorption (TSA) process is based on the tendency of sorbents such as activated alumina, silica gel, and zeolites to have higher adsorption capacities for gases at lower temperatures than at elevated temperatures. The sorbent adsorbs relatively large quantities of the target gas such as CO<sub>2</sub> at the lower temperatures of flue gas ( $\approx 100$  °F or  $\approx 40$  °C). The sorbent loaded with CO<sub>2</sub> can then be regenerated simply by increasing its temperature to  $\approx 100$  °C or greater (typically with heated purge gas) in a regeneration step which drives off the CO<sub>2</sub>, after which the regenerated sorbent can be cooled back down to operating temperature and returned to CO<sub>2</sub> capture. The simplest configuration possible is a two-bed system, with one bed undergoing adsorption of CO<sub>2</sub> from the feed (flue gas), while the other bed undergoes regeneration by heated purge gas (often steam). When breakthrough is about to occur in the bed capturing CO<sub>2</sub> from flue gas, the beds are switched. Also, gases exiting the adsorption bed may be recycled through it if necessary to increase uptake of CO<sub>2</sub>. See Figure 2-2 below which depicts the basic idea of TSA. TSA takes its name from the essential process of modulating or “swinging” temperature to drive off the adsorbed gas, in direct contrast to pressure swing adsorption (PSA) which uses changes in pressure, not temperature, to release adsorbed gas. TSA technology began commercially in the 1960s, and has current application in drying compressed air and natural gas, as well as other purification applications such as carbon dioxide removal from air. Large-scale use to capture CO<sub>2</sub> from flue gas is contemplated.

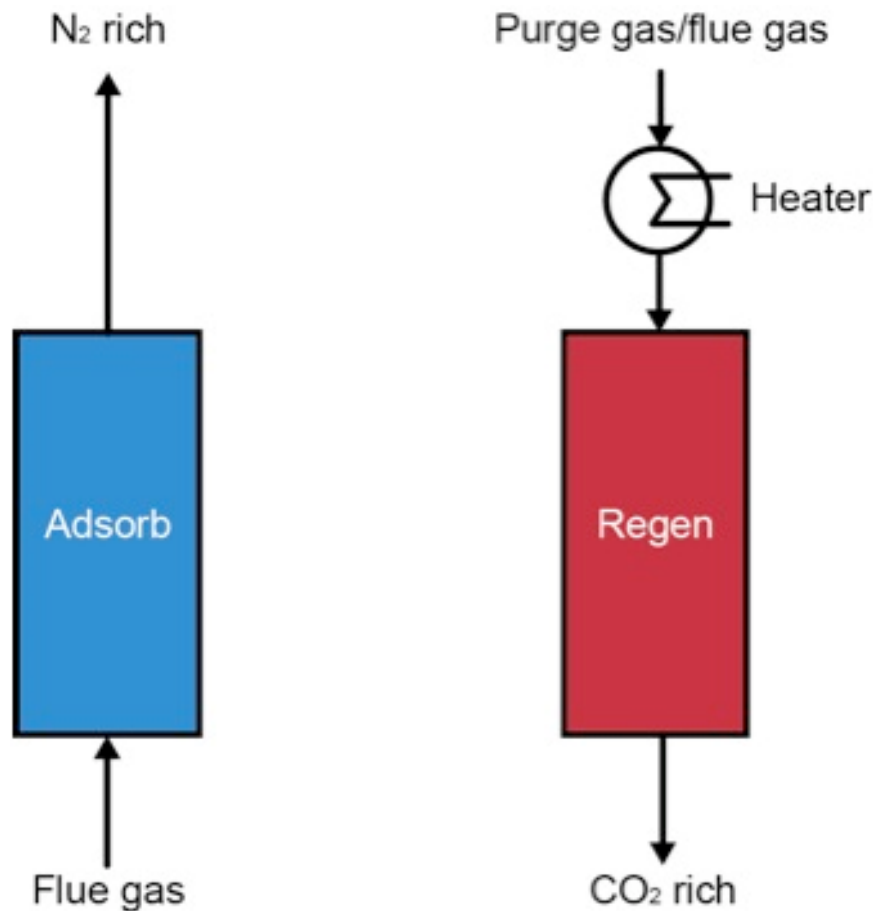


Figure 2-2. Two-Bed Temperature Swing Adsorption Process for Post-Combustion CO<sub>2</sub> Capture<sup>10</sup>

10 <http://jclfss.weebly.com/design-and-cost.html>

### Advantages

- Suitable for operation on low pressure feed streams (<60 psig) where PSA or VSA may be less practicable.
- Typically less expensive to operate than PSA.

### Challenges

- A practical problem in TSA processes is the reduction in the capacity or life of the adsorbent when it is subjected to repeated thermal cycling.
- Because beds of adsorbent cannot normally be heated and cooled quickly, the cycle time of a typical TSA process may range from several hours to several days. Long cycle times inevitably mean large bed lengths resulting in high adsorbent inventories, and high capital cost.

### Effects of Sorbent Heat of Adsorption in TSA<sup>11</sup>

Increasing the heat of adsorption also increases the temperature dependence of the isotherms (which describe sorption capacity as a function of pressure for fixed temperatures). Sorbents with small heats of adsorption will require a much larger change in temperature to affect the same change in adsorbed capacity as a sorbent with a large heat of adsorption would experience from a small temperature swing. Figure 2-3 shows this difference in the isotherms for two sorbents that are identical except for the heat of adsorption. Because the TSA cycle involves both adsorption at low temperatures with a low partial pressure of carbon dioxide and desorption at a high temperature with a high partial pressure, the difference between the low temperature low purity and high temperature high purity determines the working capacity or quantity of carbon dioxide that is produced per cycle. Therefore, having a high absolute capacity on its own is not enough to ensure a high working capacity.

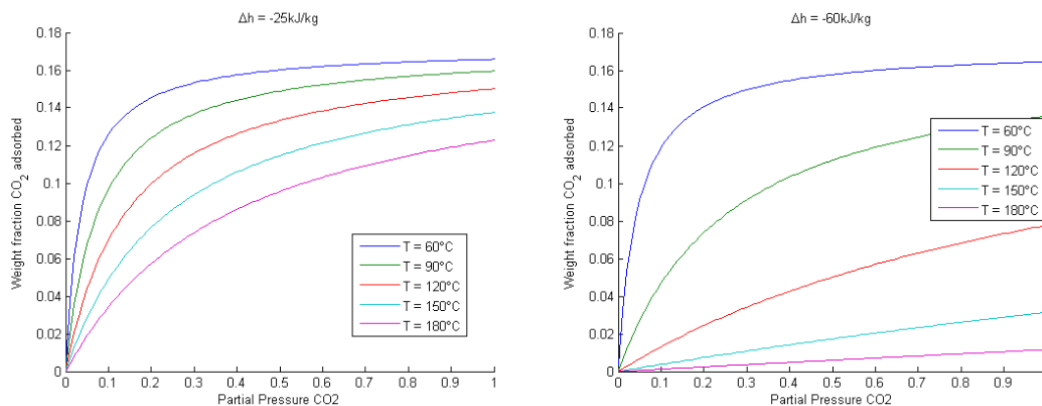


Figure 2-3. Isotherm for CO<sub>2</sub> Sorbents with Heat of Adsorption of -25kJ/kg and -60 kJ/kg

The Langmuir isotherm

$$q/q_s = \frac{b_{CO_2} P_{CO_2}}{1 + b_{CO_2} P_{CO_2}}$$

Equation 2-2

with

$$b_{CO_2} = b_0 \exp(-\Delta h/RT)$$

Equation 2-3

assumes that there are a fixed number of sites  $q_s$  to adsorb onto, with each site having the same heat of adsorption  $\Delta h$ . The number

11 Adam Hughmanick Berger and Abhoyjit S. Bhowan. "Comparing Physisorption and Chemisorption Solid Sorbents for use Separating CO<sub>2</sub> from Flue Gas using Temperature Swing Adsorption," *Energy Procedia* 4 (2011) 562–567.

of sites that are occupied,  $q$ , is determined by the partial pressure of the adsorbed species  $P_{\text{CO}_2}$  and the Langmuir parameter  $b_{\text{CO}_2}$ . In this equation  $R$  is the universal gas constant and  $b_0$  is a constant that is fit to the adsorption data. The Langmuir model is a reasonable assumption for both chemisorption and physisorption. In chemisorption, there are a fixed number of amine sites, each of which will bind to the carbon dioxide with roughly the same energy. In physisorption, the fixed number of sites is equivalent to the monolayer coating of carbon dioxide that would correspond to a saturated sorbent.<sup>12</sup> Further, from Equation 2-2, the higher the Langmuir value  $b_{\text{CO}_2}$  is, the faster the isotherm approaches saturation as  $P_{\text{CO}_2}$  increases. In Equation 2-3,  $b_{\text{CO}_2}$  depends exponentially on temperature and heat of adsorption, changes in temperature impact the isotherm more for higher heat of adsorption.

### DOE Research

DOE NETL funded research in sorbent capture using TSA in the Georgia Institute of Technology project addresses some of the key issues noted above. The project is developing a supported amine sorbent-based CO<sub>2</sub> capture module at bench scale. The sorbent incorporates supported amines in composite polymer/silica hollow fibers, with high loadings of the sorbent to facilitate large CO<sub>2</sub> adsorption capacities but without the high pressure drops normally associated with traditional packed and fluidized beds. Also the inclusion of an impermeable layer lining the fiber's interior bore allows for rapid cooling during adsorption and heating during desorption by passing water through the bore of the fibers, essentially turning the fiber module into a shell and tube heat exchanger. This will allow rapid temperature swing adsorption with the cycles running on the time scale of seconds/minutes instead of hours/days. High capital costs typical of TSA would be significantly reduced by the fast cycling; also, operating costs and parasitic loads will be reduced through heat integration of the adsorption step with preheating the boiler feed water. See Figure 2-4 for illustration of these concepts.

The project is also addressing issues of oxidation, SO<sub>x</sub> exposure, and NO<sub>x</sub> exposure in deactivation of the sorbent fibers, and developing techniques for effective field regeneration.

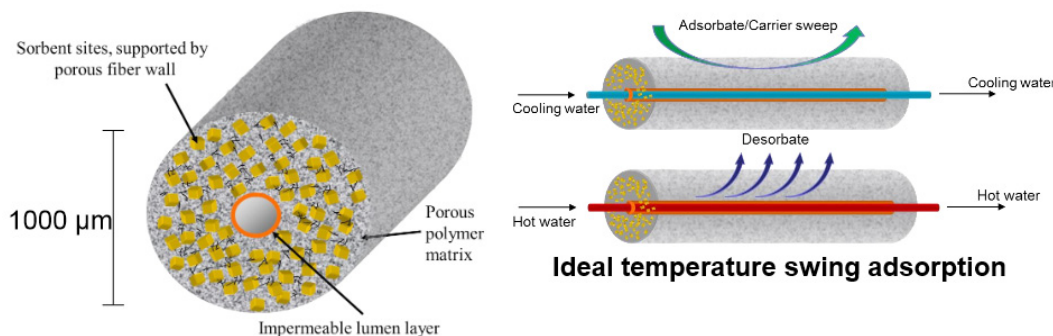


Figure 2-4. Sorption (top) and Desorption (bottom) Modes in Hollow Fiber Sorbents

Many of the other sorbent-based CO<sub>2</sub> capture projects in the DOE NETL portfolio assume conventional TSA process operation (adsorption at 40 °C, regeneration at 100 °C).

## 2.2.4 PRESSURE SWING ADSORPTION AND VACUUM SWING ADSORPTION

### Description

In PSA a pressurized gas mixture containing CO<sub>2</sub> flows through a bed of adsorbent, ideally with high selectivity and capacity for CO<sub>2</sub> adsorption, until the adsorption of the CO<sub>2</sub> approaches equilibrium with the solid (after which significant breakthrough of CO<sub>2</sub> would occur). The bed is then regenerated by stopping the feed mixture and reducing the pressure, which releases the CO<sub>2</sub> gas which can be removed. Figure 2-5 depicts the general steps of PSA, on the left with adsorption occurring and on the right with regeneration occurring and capture of the CO<sub>2</sub>-rich gas stream.

12 Figueroa J.D., Fout T., Plasynski S., McIlvried H., Srivastava R.D. "Advances in CO<sub>2</sub> capture technology—The U.S. Department of Energy's Carbon Sequestration Program," *Intl. J. of Green House Gas Control* 2008; 2:9-20.

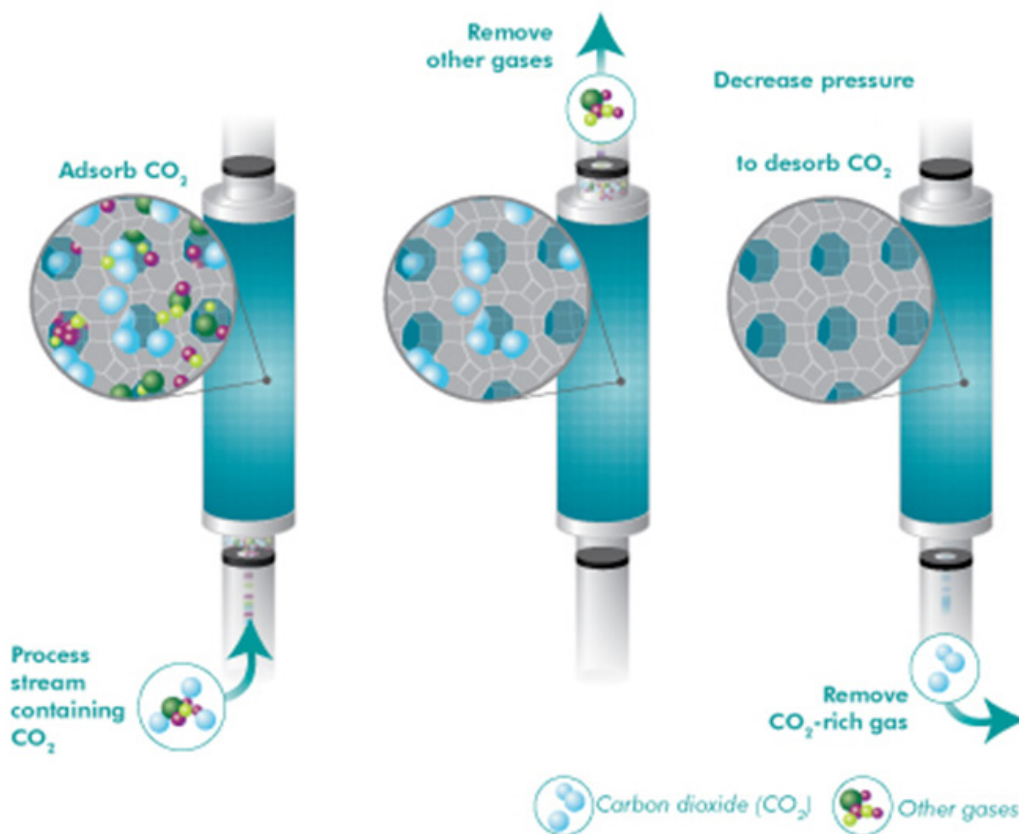


Figure 2-5. Pressure Swing or Vacuum Swing Adsorption Process for CO<sub>2</sub> Capture<sup>13</sup>

A variation of PSA is Vacuum Swing Adsorption (VSA) in which the process stream containing CO<sub>2</sub> is not pressurized. CO<sub>2</sub> is removed from the sorbent by establishing a vacuum on the regenerating sorbent bed which draws off the CO<sub>2</sub>. The mechanism is the same in either case: CO<sub>2</sub> adsorbs at higher pressure and desorbs at lower pressure, and the pressure differential can range above or below ambient pressure.

#### Advantages

- Well-established process technology, used on very large scale for certain applications
- Needs no steam or water; only electricity required to operate compressors/pumps; energy intensity generally better than conventional solvent-based CO<sub>2</sub> removal technology (amines)
- Tolerant to trace contaminants; possibly with use of guard or layered beds
- Wide range of sorbent materials are commercial and widely available
- Increase in COE potentially lower than that of other capture technologies
- Sorbent beds require limited hands-on maintenance, translating into flexibility in locating them

#### Challenges

- Energy intensity still too high to meet goals: improved sorbent and novel process designs needed to overcome
- Large sorbent beds required for high-throughput applications such as flue gas treatment
  - High capital cost for sorbent and associated process equipment
  - Implies large pressure drop and associated power penalty: could possibly be overcome by structured adsorbents and faster cycling
  - Large plant footprint for beds: possibly overcome by underground installation and faster cycling or smaller beds

<sup>13</sup> [http://www.co2crc.com.au/publications/all\\_factsheets.html](http://www.co2crc.com.au/publications/all_factsheets.html)

## 2.3 SORBENT-BASED CO<sub>2</sub> CAPTURE APPROACHES

The Carbon Capture Program has supported research and development in a diverse set of solid sorbent-based CO<sub>2</sub> capture approaches to address the technical challenges described above. A major part of the R&D sorbents portfolio consists of post-combustion capture technology projects, in which the process context is capture of CO<sub>2</sub> from relatively low-temperature exhaust and flue gases. The remainder of the portfolio consists of pre-combustion capture technology, in which the CO<sub>2</sub> would be captured from higher-temperature syngas. Recent projects are referenced in Table 2-1.

### Sorbent Types

Types of sorbents for CO<sub>2</sub> capture are highly varied, and as a rule the types are distinctly suited to the temperature regimes in which they are intended to operate for adsorption and regeneration. In their extensive surveys of the literature for sorbent-based CO<sub>2</sub> capture, Wang and fellow researchers<sup>14</sup> have adopted a general classification of adsorbents based on three sorption and desorption temperature ranges at which they operate, which are as follows:

- Low temperature (<200 °C)
- Intermediate temperature (200–400 °C)
- High temperature (>400 °C)

Applicable sorbent types fall into these categories as follows:

#### Low Temperature Sorbents

- Solid amine-based adsorbents (with variations in supports for these sorbents including silica; carbon in various forms including activated carbon, carbon nanotubes, graphite/graphene; polymers; low-cost materials such as clays, etc.)
- Carbon-based adsorbents
- Zeolite-based adsorbents
- Metal-organic framework (MOF)-based adsorbents
- Alkali metal carbonate-based adsorbents
- Others such as immobilized ionic liquid-based sorbents, etc.

#### Intermediate Temperature Sorbents

- Layered double hydroxide (LDH)-based sorbents

#### High Temperature Sorbents

- CaO-based sorbents
- Alkali ceramic-based sorbents

This classification of sorbent types is useful, because it captures essentially all of the types currently being investigated in the field of sorbent-based carbon capture, differentiates among the types according to the major temperature regimes characteristic of their application for either pre- or post-combustion capture, and provides a framework for showing how the DOE/NETL Carbon Capture Programs' R&D projects cover areas of this field of R&D.

In addition, process innovations and improvements have contributed to overcoming the technical issues that serve as barriers to deployment of carbon capture technologies. All of these are described below.

14 Junya Wang, Liang Huang, Ruoyan Yang, Zhang Zhang, Jingwen Wu, Yanshan Gao, Qiang Wang, Dermot O'Hare and Ziyi Zhong, "Recent advances in solid sorbents for CO<sub>2</sub> capture and new development trends," *Energy Environ. Sci.*, 2014, 7, 3478. Qiang Wang, Jizhong Luo, Ziyi Zhong and Armando Borgna, "CO<sub>2</sub> capture by solid adsorbents and their applications: current status and new trends," *Energy Environ. Sci.*, 2011, 4, 42.



Table 2-1. DOE/NETL Sorbent-Based CO<sub>2</sub> Capture Projects Portfolio

SORBENT PROJECTS	PERFORMER	TEMPERATURE	SORBENT TYPE	IMPLEMENTATION
Energy and Capital-Efficient Sorbent-Based CO <sub>2</sub> Capture; Bench-Scale Development and Testing of a Novel Adsorption Process	InnoSeptra LLC	Low	Zeolite-based adsorbents	Zeolite 5A, in monoliths of ¾" diameter made by Novolair
Membrane-Integrated Sorbent Adsorption Process for Carbon Capture	TDA Research Inc.	Low	Carbon-based adsorbents	Mesoporous carbon (integrated in 2-stage membrane separation process)
High Capacity Sorbent and Process for CO <sub>2</sub> Capture; Evaluation of CO <sub>2</sub> Capture from Existing Coal-Fired Plants by Hybrid Sorption Using Solid Sorbents (CACHYS™)	Envergenx LLC; University of North Dakota	Low	Alkali metal carbonate-based adsorbents	Alkali metal carbonate with additive to increase capacity and reaction rate, lower regeneration energy
Sorbent Based Post-Combustion CO <sub>2</sub> Slipstream Testing (pilot scale); Low-Cost Sorbent for Capturing CO <sub>2</sub> Emissions Generated by Existing Coal-Fired Power Plants	TDA Research Inc.	Low (near isothermal operation at 40–160 °C)	Alkali metal carbonate-based adsorbents	Alkalized alumina pellets
Pilot-Scale Evaluation of an Advanced Carbon Sorbent-Based Process for Post-Combustion Carbon Capture; Development of Novel Carbon Sorbents for CO <sub>2</sub> Capture	SRI International	Low	Carbon-based adsorbents	ATMI BrightBlack® microbeads (0.2mm diameter) carbon beads, falling in single column adsorber/ stripper
Optimizing the Costs of Solid Sorbent-Based CO <sub>2</sub> Capture Process Through Heat Integration; Evaluation of Solid Sorbents as a Retrofit Technology for CO <sub>2</sub> Capture (pilot scale)	ADA-ES, Inc.	Low	Solid amine-based adsorbents	ADAorb™ CO <sub>2</sub> sorbent: amine on polystyrene resin substrate (project focus is moving and fluid bed cross heat exchangers)
Bench Scale Development and Testing of Aerogel Sorbents for CO <sub>2</sub> Capture	Aspen Aerogels, Inc.	Low	Solid amine-based adsorbents	Amine-functionalized aerogel pellets or beads (0.30–0.35mm)
Bench-Scale Development and Testing of Rapid PSA for CO <sub>2</sub> Capture	W.R. Grace	Low (focus is rapid PSA to decrease column size)	Zeolite-based adsorbents	Commercial 13X zeolite pellets
Novel Solid Sorbents for Post-combustion CO <sub>2</sub> Capture; CO <sub>2</sub> Capture from Flue Gas Using Solid Molecular Basket Sorbents	RTI International; Pennsylvania State University	Low	Solid amine-based sorbents	Polyethyleneimine supported on commercial silica
A Low-Cost, High-Capacity Regenerable Sorbent for CO <sub>2</sub> Capture From Existing Coal-Fired Power Plants	TDA Research, Inc.	Low	Carbon-based adsorbents	Mesoporous carbon (pellets) modified with surface functional groups
Rapid Temperature Swing Adsorption Using Polymer/Supported Amine Composite Hollow Fibers	Georgia Tech Research Corporation	Low	Solid amine-based adsorbents	Amines loaded into composite polymer/silica hollow fibers, fibers built into modules (avoiding pressure drop of fixed or fluid bed)
Pilot Testing of a Highly Effective Pre-Combustion Sorbent-Based Carbon Capture System; A Low-Cost, High-Capacity Regenerable Sorbent for Pre-combustion CO <sub>2</sub> Capture	TDA Research	Low-intermediate (240–250 °C) PSA	Carbon-based adsorbents	Mesoporous carbon grafted with surface functional groups that remove CO <sub>2</sub> via an acid-base interaction

Table 2-1. DOE/NETL Sorbent-Based CO<sub>2</sub> Capture Projects Portfolio

SORBENT PROJECTS	PERFORMER	TEMPERATURE	SORBENT TYPE	IMPLEMENTATION
SO <sub>2</sub> -Resistant Immobilized Amine Sorbents for CO <sub>2</sub> Capture	The University of Akron	Low	Solid amine-based adsorbents	Porous carbon and silica support structures with immobilized aliphatic amines distributed inside the material's pores and immobilized aromatic amines placed on the external surface and pore mouth of the material
CO <sub>2</sub> Removal from Flue Gas Using Microporous Metal Organic Frameworks; Carbon Dioxide Separation with Novel Microporous Metal Organic Frameworks	UOP, LLC	Low	MOF-based adsorbents	Novel microporous metal organic frameworks (MOFs) and an associated vacuum-pressure swing adsorption (vPSA) process; Mg/dioxybenzenedicarboxylate best performing structure type <sup>15</sup>
CO <sub>2</sub> Recovery from Flue Gas using Carbon-Supported Amine Sorbents	Advanced Fuel Research, Inc.	Low	Solid amine-based adsorbents	Amines supported on low-cost activated carbon; carbon produced from scrap tires
Evaluation of Dry Sorbent Technology for Pre-Combustion CO <sub>2</sub> Capture	URS Group	High	CaO-based sorbents	FSP25, 44:56 wt% CaZrO <sub>3</sub> :CaO USP199, 25:75wt% Meyenite:CaO FSP32, 1:4 Al:Ca at% MA63, 23:77wt% MgO:CaO

**Sorbent Tradeoffs**

Table 2-2. Comparison of Sorbent Types for CO<sub>2</sub> Capture

TYPE	ADSORPTION MECHANISM	REGENERATION PARASITIC ENERGY	ADSORPTION CAPACITY	MASS TRANSFER AND HEAT CONDUCTIVITY	SELECTIVITY (CO <sub>2</sub> /N <sub>2</sub> )*	CO <sub>2</sub> UPTAKE AT LOW PRESSURE	STABILITY	COST
Ideal		Low	High	High	High	High	High (chemical and mechanical)	Low
Amine-functionalized adsorbents	Chemisorption	High	High	Variable	Variable	High	Moderate	Moderate
Zeolites	Physisorption	Low	Low	Low	Low	High	Low	Moderate
Carbon-based	Physisorption	Low	Higher (compared to zeolites)	Moderate	Low	Low	Moderate	Low
MOFs	Physisorption	Low	High	Low	Low <sup>†</sup>	Low	Moderate <sup>‡</sup>	High
CaO-based	Chemisorption	Moderate	High	Low	High	N/A	Low	Low

\* Also minimal adsorption of O<sub>2</sub> and water vapor.  
 † Major focus of development; functionalization improves selectivity.  
 ‡ Better than zeolites.

15 UOP's work is not continued in current portfolio; UOP has not pursued funding in recent FOAs.

## 2.3.1 LOW TEMPERATURE SORBENTS

### 2.3.1.1 SOLID AMINE-BASED ADSORBENTS

Aqueous amine-based solvent processes are often chosen for current, commercial applications of CO<sub>2</sub> capture. However, given the drawbacks of such processes, including the high regeneration energy, fouling of process equipment, solvent foaming problems, emissions from volatile solvents, and corrosion caused by amine solutions, effort has been made to prepare amine-based solid adsorbents for CO<sub>2</sub> capture by immobilizing organic amines on certain solid support materials. Solid amine adsorbents promise lower capital cost, lower pressure for gas recovery, and lower energy consumption for regeneration compared to baseline amine solvent processes.<sup>16</sup>

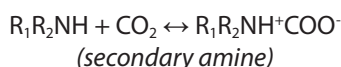
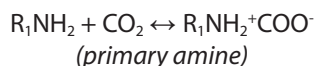
Generally the solid supports should have a good affinity for the amine molecules, high surface area, proper porosity, good mechanical strength and hydrothermal stability. Non-porous and microporous materials are generally avoided, while mesoporous silica, carbon, and certain polymers and resins are preferred due to their proper combination of high surface areas and large pore size and volume.<sup>17</sup>

#### Mechanism of Capture

Amine-base sorbents undergo the same types of reactions with CO<sub>2</sub> which are known to occur with amines in aqueous solutions. In the case of amine-based solid adsorbents, the reactions of airborne CO<sub>2</sub> and water vapor occur with amine functional groups chemically bonded to and located on the sorbent surface, or with liquid amines immobilized within a porous support. The reactions involving primary, secondary and tertiary amines are as follows:

#### Intermediate zwitterion formation

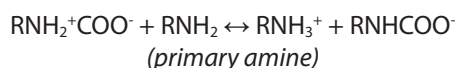
CO<sub>2</sub> forms intermediate zwitterions by reaction with primary or secondary amines:



**Equation 2-4**

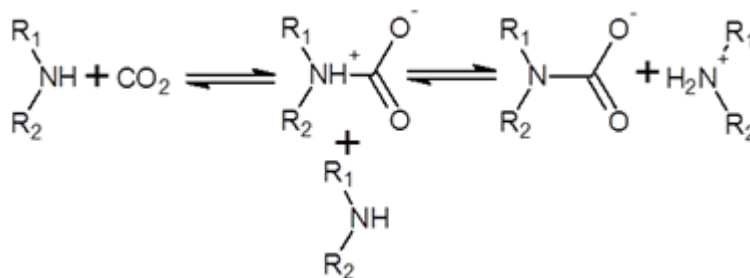
#### Carbamate formation

Intermediate zwitterions further react with more amine to form stable carbamates:



**Equation 2-5**

The zwitterion from reaction of a secondary amine with CO<sub>2</sub> is further deprotonated by a base (amine) to form carbamate (R<sub>1</sub>R<sub>2</sub>N-COO<sup>-</sup>) and a cation (R<sub>1</sub>R<sub>2</sub>NH<sub>2</sub><sup>+</sup>) as shown here:



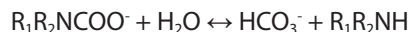
16 R. A. Khatri, S. S. C. Chuang, Y. Soong and M. Gray, *Energy Fuels*, 2006, **20**, 1514.

17 Qiang Wang, Jizhong Luo, Ziyi Zhong and Armando Borgna, "CO<sub>2</sub> capture by solid adsorbents and their applications: current status and new trends," *Energy Environ. Sci.*, 2011, **4**, 42.

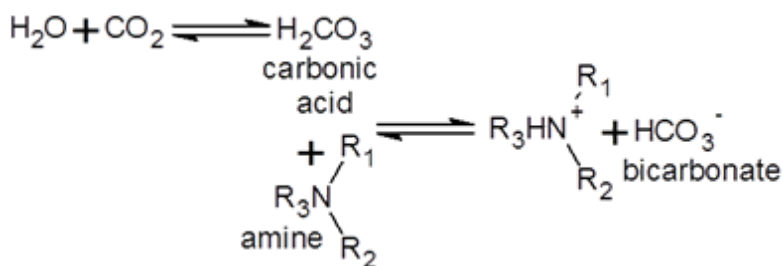
(secondary amine)

**Equation 2-6**

Without water vapor present, carbamate formation is the mechanism for CO<sub>2</sub> removal. Stoichiometrically, this allows capture of 1 mole of CO<sub>2</sub> for every 2 moles of amine (CO<sub>2</sub> loading of 0.5). However, in practice water is usually present in capture of CO<sub>2</sub> from flue or exhaust gases, which allows subsequent reaction of the carbamate to form carbonate, regenerating the amine, and increasing the CO<sub>2</sub> loading to values above 0.5 and approaching a theoretical loading of 1:

**Equation 2-7***Protonation of tertiary amine*

Tertiary amines can react with carbonic acid, formed from slow hydration of CO<sub>2</sub>. Bicarbonate ion and an alkylammonium cation result:

**Equation 2-8****Recent Developments and DOE Contribution**

An emphasis of current work in solid amine-based sorbents development has been in trying to improve the CO<sub>2</sub> sorption capacity by:

- Improved approaches for supporting amines on porous materials. Different synthesis methods include (1) impregnating amines into supports (generally resulting in high capture capacity but issues of transport limitations of CO<sub>2</sub> to active sites and the leaching of amines over multiple regeneration cycles which tend to limit their performance and long-term viability), (2) post synthesis grafting (covalently attaching amines onto solid surfaces, e.g., hyperbranched amines covalently attached to silica, amine groups functionalized onto silica or alumina supports, etc.), and (3) direct condensation (an example which did away with the amine support altogether is polyamine porous particles prepared by a precipitation-polymerization method).<sup>18</sup>
- Selecting appropriate amines. Tradeoffs exist among the choices of primary amines, secondary amines, tertiary amines, and polyamines. Primary amines can form stable complexes with CO<sub>2</sub>, capture CO<sub>2</sub> efficiently but are difficult to regenerate. Tertiary amines do not capture CO<sub>2</sub> as efficiently as primary amines, but can be regenerated readily at relatively low temperatures. Secondary amines may offer a compromise between primary and tertiary amines.
- Enhancing CO<sub>2</sub> diffusion. For example, surfactant-promoted adsorbents in which a CO<sub>2</sub>-neutral surfactant is introduced in the support might create extra CO<sub>2</sub> transfer pathways to facilitate CO<sub>2</sub> diffusion into the deeper films.

For a survey of recent work in the field, the reader is referred to Wang et al. 2014 pp. 3479–3480<sup>19</sup> for much more detailed description than can be included here.

The DOE NETL-funded research portfolio includes a number of projects investigating solid amine-based adsorbents:

- The sorbent selected for the ADA-ES project is a commercial sorbent consisting of an ion exchange resin (polystyrene) with a primary benzyl amine that removes CO<sub>2</sub> in a TSA process cycle (40 °C adsorption, 120 °C regeneration).
- Aspen Aerogels, Inc. is conducting research on amine-functionalized aerogel pellet sorbents, which have high surface

18 H. B. Wang, P. G. Jessop and G. Liu, *ACS Macro Lett.*, 2012, **1**, 944.

19 Junya Wang, Liang Huang, Ruoyan Yang, Zhang Zhang, Jingwen Wu, Yanshan Gao, Qiang Wang, Dermot O'Hare and Ziyi Zhong, "Recent advances in solid sorbents for CO<sub>2</sub> capture and new development trends," *Energy Environ. Sci.*, 2014, **7**, 3478.

area and porosity, tailored pore size distribution, highly-stable functionality, and excellent hydrophobicity for resisting degradation from flue gas and its contaminants over long-term use. Amines are grafted onto hydrophobic aerogel.

- RTI is working on polyethyleneimine (PEI) supported on commercial silica, based on Pennsylvania State University's work in "molecular basket sorbents" which had looked to replace expensive mesoporous molecular sieve supports with more cost-effective alternatives. They investigated mesocellular silica foam, hexagonal mesoporous silica, silica gel, fumed silica, activated carbon, and carbon black as supports.
- Georgia Tech Research Corporation is investigating amines loaded into composite polymer/silica hollow fibers in innovative module configurations. Both impregnated PEI and class 2 (grafted 3-aminopropylsilane) fiber sorbents utilizing composite commercial mesoporous silica and low-cost commercial polymers (e.g., cellulose acetate) were investigated.
- University of Akron is investigating sorbents based on porous carbon and silica support structures with immobilized aliphatic amines distributed inside the material's pores and immobilized aromatic amines placed on the external surface and pore mouth of the material. The idea is that the aromatic amines, while having negligible CO<sub>2</sub> capture capacity, are capable of adsorbing and desorbing SO<sub>2</sub> in the same temperature range as aliphatic amines do for CO<sub>2</sub>. The expectation is that the aromatic amines on the pore mouths and particle surface will prevent sorbent deactivation by selectively capturing SO<sub>2</sub>, thus allowing the aliphatic amines within the pores to capture CO<sub>2</sub> instead of irreversibly adsorbing residual SO<sub>2</sub> from the flue gas desulfurization-treated flue gas.
- Advanced Fuel Research was investigating amines supported on low-cost activated carbon, with the carbon produced from scrap tires. This directly addressed the issue of sometimes high capital costs of sorbent based on expensive support materials such as molecular sieves, etc.

### 2.3.1.2 CARBON-BASED ADSORBENTS

#### *General*

Carbon-based materials have advantages of low cost, high surface area, high amenability to pore structure modification and surface functionalization, and relative ease of regeneration. However, the CO<sub>2</sub> adsorption mechanism on carbon materials is physisorption and therefore weak, resulting in relatively poor CO<sub>2</sub> selectivity, and significant drop in CO<sub>2</sub> sorption capacity at temperatures associated with power plant flue gas (50–120 °C). Accordingly, research has been focused mainly on methods to increase CO<sub>2</sub> capacity by increasing surface area and tuning the pore structure of carbon sorbents, increasing alkalinity by surface modifications (such as nitrogen doping, amine modification, oxidation, fluorination, modification with metal oxides), and synthesis of carbon-based hybrid composites. The reader is referred to the reviews of R&D work in this field prepared by Wang et al.<sup>20, 21</sup> for much more detailed discussion.

#### *DOE Research*

The current research portfolio's coverage of carbon-based CO<sub>2</sub> sorbents is dominated by TDA's projects in which mesoporous carbon modified by functional groups for improved CO<sub>2</sub> capture capacity and performance is being evaluated for both pre-combustion and post-combustion applications. Further detail on the makeup of the mesoporous carbon sorbent is regarded as proprietary. However, it is noted that the functional modification allows relatively strong adsorption but without the CO<sub>2</sub> forming a true covalent bond with the surface sites. Therefore, regeneration can be carried out with only a small energy input of 4.9 kcal per mol of CO<sub>2</sub>, which is much lower than that for chemical absorbents or amine based solvents.

The process implementation of the work is innovative; in recent work the approach is to integrate a membrane module and a sorbent capture system in a two-step CO<sub>2</sub> separation process.

### 2.3.1.3 ZEOLITE-BASED ADSORBENTS

#### *Description*

- 20 Junya Wang, Liang Huang, Ruoyan Yang, Zhang Zhang, Jingwen Wu, Yanshan Gao, Qiang Wang, Dermot O'Hare and Ziyi Zhong, "Recent advances in solid sorbents for CO<sub>2</sub> capture and new development trends," *Energy Environ. Sci.*, 2014, **7**, 3478.
- 21 Qiang Wang, Jizhong Luo, Ziyi Zhong and Armando Borgna, "CO<sub>2</sub> capture by solid adsorbents and their applications: current status and new trends," *Energy Environ. Sci.*, 2011, **4**, 42.

Zeolites are porous crystalline aluminosilicates, whose structure consists of interlocking tetrahedrons of SiO<sub>4</sub> and AlO<sub>4</sub> joined together in various regular arrangements through shared oxygen atoms. They have open crystal lattices containing pores with molecular dimensions, into which molecules can penetrate. The negative charge created by the substitution of an AlO<sub>4</sub> tetrahedron for a SiO<sub>4</sub> tetrahedron is balanced by exchangeable positively charged cations (e.g., Na<sup>+</sup>, K<sup>+</sup>, Ca<sup>2+</sup>, Mg<sup>2+</sup>), which are located in the channels and cavities throughout the structure.<sup>22</sup> Such zeolites have ion-exchange, catalytic and adsorptive properties, which are highly dependent upon the size, charge density, and distribution of these cations in the porous structure. The structure is depicted in Figure 2-6 for a synthetic faujasite X zeolite (faujasite zeolites are divided into two types X and Y; for X zeolites the silica to alumina ratio is between 2 and 3, while in Y zeolites it is 3 or higher).

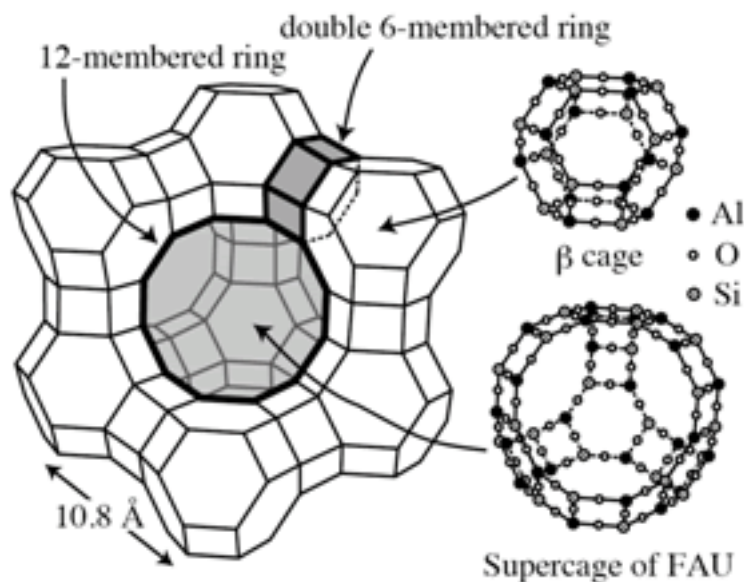


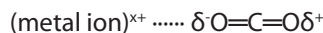
Figure 2-6. Framework Structure of Low-Silica X Zeolite (cations not shown)<sup>23</sup>

### Mechanism of Capture

Zeolites' defined crystalline structures result in uniform pore sizes in the interval of 3 to 10 Å, a property that allows them to separate molecules by means of the molecular sieve effect. Separation of gases in zeolites can also take place through the mechanism of selective adsorption of those molecules that have relatively large energetic non-saturations ( $\pi$  bonds, dipoles and quadrupoles). Generally speaking, separation of gases by these adsorbents then depends on three factors: structure and composition of the framework, cationic form, and zeolitic purity (both natural zeolites and synthetic zeolites are utilized, the former often contaminated with other minerals which drives the issue of purity).

Different cationic forms of a given zeolite may lead to significant differences in the selective adsorption of a given gas such as CO<sub>2</sub>, due to both the location and size of the interchangeable cations which affect the local electrostatic field, and the polarization of the adsorbates.<sup>24</sup>

Specifically, the CO<sub>2</sub> adsorption mechanism on zeolites includes physisorption of CO<sub>2</sub> via an ion-dipole interaction, with the CO<sub>2</sub> in a linear orientation:



22 Qiang Wang, Jizhong Luo, Ziyi Zhong and Armando Borgna, "CO<sub>2</sub> capture by solid adsorbents and their applications: current status and new trends," *Energy Environ. Sci.*, 2011, 4, 42.

23 Yasuo Nozue, "Novel Properties of Correlated Electrons in Alkali-Metal Clusters Incorporated in Regular Nanospace of Zeolite Crystals," Croatian-Japanese Workshop on Materials Science, Zagreb, 29–30 June 2009. <http://cro-jap-workshop.ifs.hr/Page.aspx?id=7>.

24 Rosario Hernández-Huesca, Lourdes Díaz, Gelacio Aguilar-Armenta, "Adsorption equilibria and kinetics of CO<sub>2</sub>, CH<sub>4</sub> and N<sub>2</sub> in natural zeolites," *Separation and Purification Technology*, Volume 15, Issue 2, 8 March 1999, pp. 163–173.



In addition to physical adsorption, more strongly bound carbonate species are also observed. These adsorbed CO<sub>2</sub> sites are bent and associated with bi-coordination, as shown in the following two types of carbonate species, as shown in this case involving sodium cations:



Equation 2-9

### Suitability for CO<sub>2</sub> capture

In recent years extensive studies have examined zeolites for their suitability as CO<sub>2</sub> capture sorbents. For example, one study examined a number of common zeolites for CO<sub>2</sub> capture from nitrogen in flue gas: 5A, 13X, NaY, NaY-10, H-Y-5, H-Y-30, H-Y-80, HiSiv 1,000, H-ZSM-5-30, H-ZSM-5-50, H-ZSM-5-80, H-ZSM-5-280, and HiSiv 3,000. The CO<sub>2</sub> pure component adsorption isotherms and expected working capacity curves for an assumed pressure swing adsorption (PSA) application were determined for a selected promising subgroup of these adsorbents (these included 13X, NaY, H-Y-5, HiSiv 1,000, ZSM-5-30, HiSiv 3,000). The results showed that promising adsorbent characteristics are a near linear CO<sub>2</sub> isotherm and a low SiO<sub>2</sub>/Al<sub>2</sub>O<sub>3</sub> ratio with cations in the zeolite structure which exhibit strong electrostatic interactions with carbon dioxide.<sup>25</sup>

The CO<sub>2</sub> capacity of zeolites is affected by temperature, with capacities strongly decreasing with increasing temperature. Zeolites 13X and UOP WEG-592 were studied in the context of CO<sub>2</sub> removal from flue gas utilizing a combination of PSA and TSA (PTSA) in an NETL systems study.<sup>26</sup> Both of the zeolites were found to have good CO<sub>2</sub> adsorption capacity at 120 °C. However, the capacities at 120 °C were considerably lower than that at ambient temperature; and in fact zeolites cannot be used above 200 °C for CO<sub>2</sub> capture since their capture capacities are extremely low at these temperatures. The marked temperature sensitivity of zeolites must be considered in process context in terms of column design: since the adsorption process is exothermic, the heat released during adsorption will tend to increase the column temperature as the heat transient moves through the column, driving down capacities. Therefore, the importance of the heat effects and operating temperature on the adsorption capacities cannot be overlooked.

So, although adsorbent capacity is an important parameter for zeolite performance in CO<sub>2</sub> capture, the optimal design of a PSA separation unit is a complex task as the separation and recovery effectiveness are highly sensitive to the chosen operating conditions as well as adsorbent type. By way of illustration, Harlick and Tezel concluded that if a low-pressure CO<sub>2</sub> feed and very low regeneration pressure are used then the NaY and 13X adsorbents would be preferable, but that as CO<sub>2</sub> feed and regeneration pressure increases, adsorbent with a linear isotherm would be in order.<sup>27</sup>

Zeolites' affinity for water represents a particular challenge in CO<sub>2</sub> capture from water vapor-containing gas streams, since water molecules directly compete with CO<sub>2</sub> molecules for the adsorption sites on zeolites, particularly X zeolites favored for CO<sub>2</sub> capture. Although CO<sub>2</sub> adsorption capacity can be regained by increasing the temperature during regeneration, the loss of adsorption capacity during the adsorption cycle has negative impacts on overall cost-effectiveness of zeolite sorbent-based processes. Also, water may have a detrimental effect on the stability of zeolite frameworks; the combination of CO<sub>2</sub> and water forming weakly acidic conditions may cause dealumination of zeolite structures, leading to a partial or total destruction of the framework.<sup>28</sup>

25 Peter J.E. Harlick, F. Handan Tezel, "An experimental adsorbent screening study for CO<sub>2</sub> removal from N<sub>2</sub>," *Microporous and Mesoporous Materials*, Volume 76, Issues 1–3, 1 December 2004, pp 71–79.

26 "CO<sub>2</sub> Capture Utilizing Solid Sorbents," Ranjani Siriwardane, Ming Shen, Edward Fisher, and James Losch. U.S. Department of Energy, National Energy Technology Laboratory. <http://www.netl.doe.gov/publications/proceedings/04/carbon-seq/039.pdf>.

27 Harlick and Tezel 2004.

28 Wang et al. 2011.

## Research

### Current Trends

Current research in improving zeolites for CO<sub>2</sub> capture is mainly focused on:

- Changing the composition and structure of the zeolitic framework.
- Cationic exchange (the cations influence the electric field inside the pores as well as the available pore volume, and provide a convenient mean for tuning the adsorptive properties of these porous materials). For example, for certain zeolites, Li<sup>+</sup> provides the highest CO<sub>2</sub> capture capacity among all the univalent cations; in other situations certain exchanged cations such as Ca<sup>2+</sup>, Mg<sup>2+</sup>, and Sr<sup>2+</sup> result in much higher capacities in given zeolites.
- Modifying the existing zeolites with various amine groups (by co-condensation, impregnation or grafting) to further increase the CO<sub>2</sub> capture capacity. Initial work tended toward simpler approaches of impregnation; however, adsorbents impregnated with amines experience low thermal stability. To overcome this problem, recent proposals have included grafting of aminosilanes through silylation onto the intrachannel surface of mesoporous silica. In general, amine-grafted adsorbents have exhibited a comparatively higher adsorption rate and higher stability in cyclic runs than the amine-impregnated adsorbents.
- Preparing zeolite-based hybrid materials. For example, zeolite-based hybrid materials such as SBA-3/cotton fiber composites have also been studied for enhanced CO<sub>2</sub> capture.

The reader is referred to Wang et al.<sup>29</sup> for a thorough review of recent work in the field.

### DOE

Recent NETL research related to zeolite type sorbents for CO<sub>2</sub> capture has tended to emphasize the overall CO<sub>2</sub> capture cycle, and improved zeolite structuring in the sorbent beds to address process concerns. The key idea of the current W.R. Grace project is to use high sorbent packing density in the fastest possible cycling rate in a PSA cycle or rapid PSA, which would result in multiple benefits including reduced capital costs (smallest possible sorbent beds and correspondingly smaller columns, and lower footprint occupied), reduced energy consumption (mainly associated with improved pressure drop, shorter sorbent regeneration times, and improving mass transfer issues), and reduced environmental burdens (less attrition of sorbent, etc.) Work demonstrated that zeolite crystals can be coated onto a crushproof metal foil structure (Catacell core structure) which has lower density, lower pressure drop and energy penalty for the same CO<sub>2</sub> removal capacity, and better plug flow behavior (corrugated structure not subject to premature breakthrough) compared to a conventional packed bed of zeolite pellets. InnoSeptra LLC's project's key innovation is sorbent in structured monolithic form, which again has significantly lower pressure drops, faster kinetics, virtually no attrition losses, requires less parasitic power, and has a lower overall capital cost compared to conventional sorbent forms of pellets and spheres.

## 2.3.1.4 METAL-ORGANIC FRAMEWORK-BASED ADSORBENTS

### Description

Metal-organic frameworks (MOFs) are novel hybrid materials that combine bridging organic ligands and metal ions or metal-containing clusters. MOF materials have usually been created by crystallization from hot solutions; upon removal of "guest" solvent molecules from the resultant crystalline network by evaporation and pressure reduction, a large internal surface area results typically with positively charged metal sites lining the cavities or channels, providing extensive active sites for other guest molecules (such as gases like hydrogen, methane and CO<sub>2</sub>) to adsorb. MOFs' robust 3D structures are crystallographically well-defined, and many of them possess superior surface areas relative to those of traditional adsorbents such as activated carbon and zeolites.<sup>30</sup> One of the archetypical examples is MOF-5, constructed from zinc atoms as the metal centers and terephthalic acid as the organic linker depicted in Figures 2-7 and 2-8 below. In this MOF, each [Zn<sub>4</sub>O] unit is bridged by six benzene-1,4-dicarboxylates. MOF-5 forms stable crystals (extended crystalline lattice of MOF-5 is depicted in the second figure) having remarkably low density for a crystalline material (0.59 g/cm<sup>3</sup>), pore volumes of 0.61±0.54 cm<sup>3</sup>/cm<sup>3</sup> and very high estimated Langmuir surface area of 2,900m<sup>2</sup>/g,<sup>31</sup> even exceeding the values of pore volumes and surface areas typical of zeolites.

29 Junya Wang, Liang Huang, Ruoyan Yang, Zhang Zhang, Jingwen Wu, Yanshan Gao, Qiang Wang, Dermot O'Hare and Ziyi Zhong, "Recent advances in solid sorbents for CO<sub>2</sub> capture and new development trends," *Energy Environ. Sci.*, 2014, **7**, 3478.

30 Yangyang Liu, Zhiyong U. Wang and Hong-Cai Zhou, "Recent advances in carbon dioxide capture with metal-organic frameworks," *Greenhouse Gas Sci Technol.* 2:239–259 (2012).

31 Li H, Eddaoudi M, O'Keeffe M and Yaghi OM, Design and synthesis of an exceptionally stable and highly porous metal-organic framework. *Nature* 402:276–279 (1999).

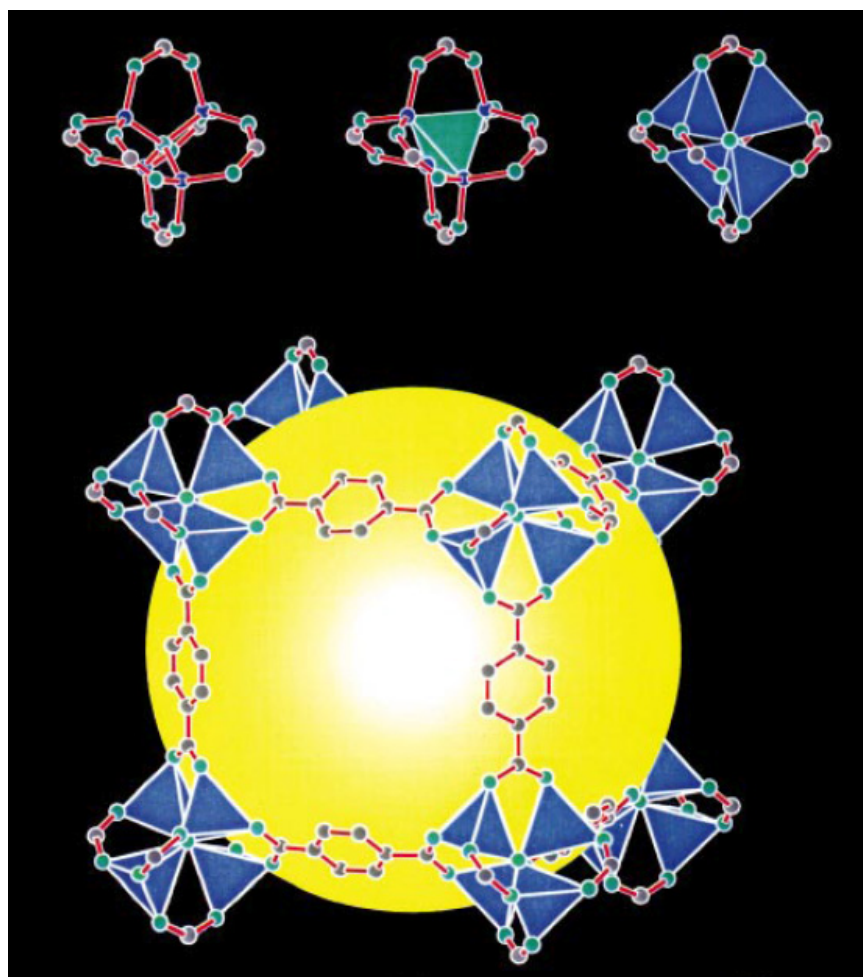


Figure 2-7. MOF-5 Framework Designed and Synthesized by Li and Co-Researchers

Top three figures show the  $Zn_4(O)_{12}C_6$  cluster, as ball and stick model (Zn, blue; O, green; C, grey) left, and with the  $Zn_4(O)$  tetrahedron indicated in green in middle and  $ZnO_4$  tetrahedra indicated in blue on right. Bottom, one of the cavities in the  $Zn_4(O)(BDC)_3$  MOF-5, framework. Eight clusters (only seven visible) constitute a unit cell and enclose a large cavity, indicated by a yellow sphere of diameter  $18.5\text{\AA}$  in contact with 72 C atoms (grey).<sup>32</sup>

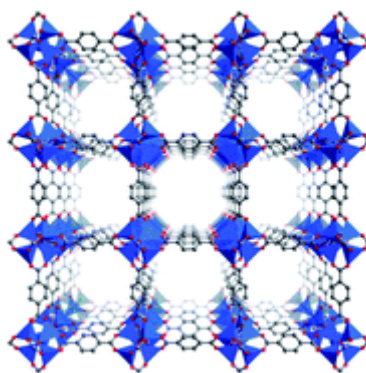


Figure 2-8. 3D Structure of Crystalline MOF-5<sup>33</sup>

- 32 Li H, Eddaoudi M, O'Keeffe M and Yaghi OM, Design and synthesis of an exceptionally stable and highly porous metal-organic framework. *Nature* 402:276–279 (1999).
- 33 Jarad A. Mason, Mike Veenstra and Jeffrey R. Long, "Evaluating metal-organic frameworks for natural gas storage," *Chem. Sci.*, 2014, **5**, 32–51.

Another well-known MOF is HKUST-1 (depicted in Figure 2-9) having the formula  $\text{Cu}_3(\text{TMA})_2(\text{H}_2\text{O})_3$  (where TMA is benzene-1,3,5-tricarboxylate); structurally, it consists of copper(II) paddlewheel dimers bridged by the TMA.<sup>34</sup>

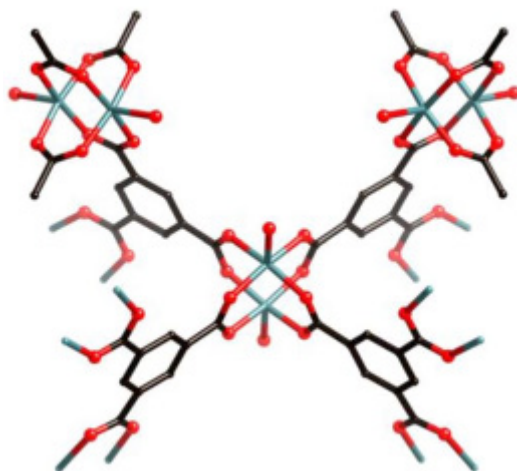


Figure 2-9. Basic Structure of HKUST-1  
Turquoise: Cu; grey: C; red: O (hydrogen atoms not depicted for clarity).<sup>35</sup>

### Tailoring MOFs for CO<sub>2</sub> Capture

Through judicious selection of metal ions and organic linkers, the structure and properties of MOFs can be systematically tuned and used for specific applications—hydrogen storage, methane storage, catalysis, and CO<sub>2</sub> capture figure prominently in the literature as applications of interest for MOFs. Beyond the tailoring of the MOF through selection of metal ions and organic bridging ligands, it is also possible to chemically modify MOFs after the crystalline materials have already been formed in a process known as post-synthetic modification (PSM) of MOFs, typically involving chemical reactions involving covalent bond formation with the framework. This is expected to open up new opportunities for functionalizing MOFs for specific applications: (1) ability to include a more diverse range of functional groups in MOFs, freed of the restrictions posed by MOF synthetic conditions; (2) easy purification and isolation of modified products because the chemical modification is performed directly on crystalline solids using reagents in non-solid phases; (3) a single given MOF structure can be modified with different reagents thereby generating a large number of topologically identical, but functionally diverse MOFs; (4) control over both the type of substituent and the degree of modification allows introduction of multiple functional units into a single framework in a combinatorial manner, enabling an effective way to systematically fine-tune and optimize MOF properties for a given intended application.<sup>36</sup>

The combined favorable properties of large surface area, permanent porosity, tunable pore size/functionality, and potential for fine tailoring possible by post-synthetic modification, have suggested great promise of MOFs as superior sorbents for CO<sub>2</sub> capture.

### DOE Research

DOE has supported research in the use of metal organic frameworks to remove CO<sub>2</sub> from flue gas. In the period of 2007–2010, a team led by UOP investigated microporous MOFs and an associated vacuum-pressure swing adsorption (vPSA) process for the removal of CO<sub>2</sub> from coal-fired power plant flue gas.<sup>37</sup> Out of an array of over 35 MOF materials evaluated for favorable CO<sub>2</sub> adsorption at more realistic flue gas conditions, they found that seven MOFs (MIL-101, MIL-53, MIL-96, Zn, Co, and Ni/DOBDC, and HKUST-1) exceeded initial performance targets. Notably, the particular MOF structure type, M/DOBDC (M designates Zn, Co, Ni, or Mg and DOBDC refers to the form of the organic linker in the resultant MOF structure, dioxybenzenedicarboxylate) performed well, and they found that one particular type, Mg/DOBDC outperformed all MOF and zeolite materials they had evaluated, with about 25 wt% CO<sub>2</sub> captured by this MOF at flue gas conditions ( $\approx 0.13$  atm CO<sub>2</sub> pressure, 311K), as opposed to Ni/DOBDC with

34 Stephen S.-Y. Chui, Samuel M.-F. Lo, Jonathan P. H. Charmant, A. Guy Orpen, Ian D. Williams, "A Chemically Functionalizable Nanoporous Material  $[\text{Cu}_3(\text{TMA})_2(\text{H}_2\text{O})_3]$ ," *Science* 19 February 1999: Vol. 283, no. 5405, pp. 1148–1150.

35 *Pure Appl. Chem.*, Vol. 85, No. 8, pp. 1715–1724, 2013.

36 Wang Z and Cohen SM, "Post-synthetic modification of metal-organic frameworks," *Chem Soc Rev* 38:1315–1329 (2009).

37 Richard Willis, "Carbon Dioxide Removal from Flue Gas Using Microporous Metal Organic Frameworks," Final Technical Report for DOE Award Number: DE-FC26-07NT43092, October 2010.



under 10 wt% CO<sub>2</sub> captured. On the other hand, they noted that MOFs fully equilibrated with water do not pick up appreciable CO<sub>2</sub>, and they ventured the conclusion that the flue gas stream would need to be dried before being passed over an adsorbent bed of Ni/DOBDC or any other MOF. Process-wise this may not be unreasonable, though flue gas drying/dehumidification would represent added process complication and cost.

Kizzie et al. examined effects of water on the same series of M/DOBDC MOFs identified by UOP as outperformers, quantifying the CO<sub>2</sub> adsorption capacities of the regenerated sorbents after exposure to 70% relative humidity. For Mg/DOBDC, Zn/DOBDC, Ni/DOBDC, and Co/DOBDC, 16%, 22%, 61% and 85% of the initial CO<sub>2</sub> capacities were recovered, respectively.<sup>38</sup> Liu et al. note that the different degree of capacity retention for these likely reflects the different stability of the MOFs toward hydrolysis. Even though Mg/DOBDC has excellent CO<sub>2</sub> adsorption in dry conditions, the results show that Co/DOBDC, having much better response and recovery from exposure to moisture, might be more suitable to CO<sub>2</sub> capture from flue gas considering the high relative humidity of flue gases in practice, and the added expense and process complication of engineering solutions such as flue gas dehumidification to accommodate moisture sensitive sorbents.<sup>39</sup>

### ***Increasing performance of MOFs for CO<sub>2</sub> capture***

Recent work in the field of improving/developing MOFs for CO<sub>2</sub> capture is reviewed by Wang et al.<sup>40</sup> In this review they note recent trends in schemes and new materials; the reader is referred to this source for a detailed description of the literature review they completed in 2014. By way of summary, the schemes/areas of investigation being pursued which they noted are as follows:

- Modification of metal sites: coordinately unsaturated metal centers are initial sites of interaction with CO<sub>2</sub> and act as physisorptive sites for CO<sub>2</sub> molecules enhanced by ion induced dipole interactions, so the metal identity within a series of MOFs will have effect on heat of adsorption and other parameters. Research in this area continues to better understand these effects.
- Selecting appropriate organic linker: choice of the appropriate organic linker, which can either increase the porosity and specific surface area or provide extra adsorbing sites, has in the last few years resulted in multiple new MOFs targeted for CO<sub>2</sub> capture.
- Novel structures: synthesis of MOFs with different microstructures and morphologies such as 1D tubular, 2D, 3D, core-shell MOFs, etc.
- Metal ion doping; for example, an ionic rho-ZMOF's CO<sub>2</sub> capture capacity was shown to be improved by doping a certain amount of Li<sup>+</sup>.
- Functionalization: CO<sub>2</sub> adsorption capacities of MOF-based adsorbents are usually not fully utilized at low pressures (<0.15 bar) characteristic of flue gas. Modifying MOFs with amines, carboxyl groups, or some other polar groups has been tried to solve this problem; various basic amine groups including EDA, 4-picolylamine, 3-picolylamine, dimethylacetamide, acylamide, PEI, etc. have been investigated with varying results.
- Hybrid MOFs: In order to utilize the MOF pore space effectively and improve the gas adsorption capacity, incorporation of some other materials such as graphite oxide or carbon has also been recently explored.

### ***Challenges of MOF-based sorbents for CO<sub>2</sub> capture***

MOFs have potential to significantly outperform traditional zeolites and other sorbents. Some examples have already been shown to have high CO<sub>2</sub> capacities and adsorption selectivity, and MOF performance may be further improved by tailoring the pore structures and the chemical compositions of MOFs, taking advantage of the unique opportunities afforded by synthesis and post-synthesis techniques discussed above.

However, MOF synthesis cost and material stability in the presence of water vapor remain as significant challenges to be overcome.<sup>41</sup> The latter issue has already been mentioned in the context of discussion of previous DOE work in this area.

38 Kizzie AC, Wong-Foy AG and Matzger AJ, Effect of humidity on the performance of microporous coordination polymers as adsorbents for CO<sub>2</sub> capture. *Langmuir* 27:6368–6373 (2011).

39 Yangyang Liu, Zhiyong U. Wang and Hong-Cai Zhou, 'Recent advances in carbon dioxide capture with metal-organic frameworks,' *Greenhouse Gas Sci Technol.* 2:239–259 (2012).

40 Junya Wang, Liang Huang, Ruoyan Yang, Zhang Zhang, Jingwen Wu, Yanshan Gao, Qiang Wang, Dermot O'Hare and Ziyi Zhong, "Recent advances in solid sorbents for CO<sub>2</sub> capture and new development trends," *Energy Environ. Sci.*, 2014, 7, 3478.

41 Jian Liu, Praveen K. Thallapally, B. Peter McGrail, Daryl R. Brown and Jun Liu, "Progress in adsorption-based CO<sub>2</sub> capture by metal-organic frameworks," *Chem. Soc. Rev.*, 2012, 41, 2308–2322.

### Hydrothermal stability

CO<sub>2</sub> capture from flue gas is distinct from other applications, because it involves capture of CO<sub>2</sub> mainly diluted by nitrogen, i.e., at partial pressures much less than atmospheric pressure (0.15 atm partial CO<sub>2</sub> pressure is common) and in humid conditions considering the saturated condition of flue gas following sulfur removal processes which results in cooled flue gas with 5–7% water vapor on a volume or molar basis.

The researchers at UOP funded by NETL for the MOF-based CO<sub>2</sub> capture study investigated hydrothermal stability (combination of thermal stability and resistance to irreversible reaction with water via hydrolysis) of MOFs in detail. This is a critical property for sorbents, because damage caused to a sorbent by moisture at process conditions or during regeneration would ultimately limit or prevent its commercial use.

The study focused on development of a model to predict energies of ligand displacement and hydrolysis and activation energies for ligand displacement for cluster models for different MOFs, tested by comparison of the modeling predictions with experimental measurements of sorbent hydrothermal stability for representative sorbent samples. The model utilized a simplified quantum mechanical approach in which interactions between metal oxide clusters and water could be manageably calculated. The calculations were made tractable by assuming that the often complex linking ligand is approximated by a simplified functional equivalent and that the flexible framework of MOFs may not impose significant restraints on metal oxide clusters during reactions. This approach was verified to be valid for estimating hydrothermal stability of MOFs, given excellent observed agreement between model predictions and experimental results. The key conclusion is that the strength of the bond between the metal oxide cluster and the bridging linker is most important in determining the hydrothermal stability of the MOF in question.

Using this method, a steam stability map was developed for a number of known MOF types, as illustrated in Figure 2-10. The method should provide a useful tool to help select and invent hydrothermally stable MOFs for desired applications such as CO<sub>2</sub> capture from flue gas.

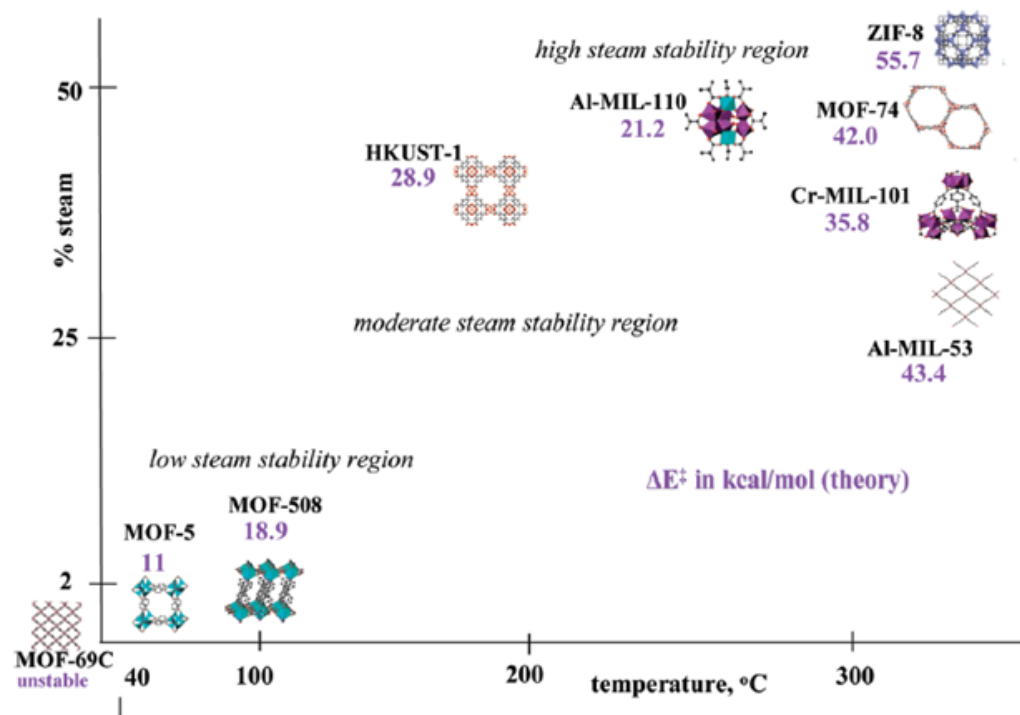


Figure 2-10. Steam Stability Map for MOFs

The position of the structure for a given MOF represents its maximum structural stability by X-ray diffraction measurement, while the energy of activation for ligand displacement by a water molecule determined by molecular modeling is represented by the magenta number (in kcal/mol).<sup>42</sup>

42 Low, J.J., Benin, A.I., Jakubczak, P., Abrahamian, J.F., Willis, R.R. J. Am. Chem. Soc. 2009, 131, 15834–15842.



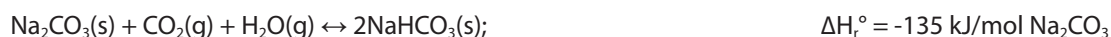
*Costs of MOFs*

Costs for synthesis of MOFs made in small quantities in laboratory settings are relatively high; ultimately, unit costs for manufacture of MOFs for large-scale CO<sub>2</sub> capture must be relatively low for them to be a cost-effective alternative to conventional CO<sub>2</sub> capture technologies. As far as manufacturing techniques are concerned, cost of reactors and utilities to manufacture MOFs can be assumed to be comparable to those for synthetic zeolites, and manufacturing methods are adaptable for conventionally available precipitation and crystallization manufacturing methods. However, cost of reagents which usually include metal source, organic linkers, solvents for reactions, and solvents for exchange processes may be high, especially the organic linkers which are specialized chemicals not available in large-scale commercial quantities. Costs would be greatly reduced if these were derived on large-scale from cheap sources such as petroleum. Assuming economies of scale in manufacturing can be realized (tonne quantities), starting costs of MOF manufacture, consisting of raw material costs, may be tractable; Liu et al. estimate these ranging from a little as \$1.19/kg to under \$10/kg for several MOFs, with only a couple of examples exceeding \$20/kg, compared to about \$1/kg for common silica gel.<sup>43</sup>

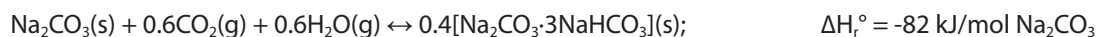
### 2.3.1.5 ALKALI METAL CARBONATE-BASED ADSORBENTS

Because of their high CO<sub>2</sub> sorption capacity and low cost, alkaline metal carbonate solids such as K<sub>2</sub>CO<sub>3</sub> and Na<sub>2</sub>CO<sub>3</sub> have received attention for CO<sub>2</sub> capture applications. Their CO<sub>2</sub> capture takes place within the temperature range of 50–100 °C, while regeneration occurs in the range of 120–200 °C, which afford a good potential match to conditions for post-combustion capture of CO<sub>2</sub> from flue gas.<sup>44</sup>

Important reactions involved in the capture of CO<sub>2</sub> using Na<sub>2</sub>CO<sub>3</sub> are as follows:<sup>45</sup>



Equation 2-10



Equation 2-11

Both reactions are reversible and highly exothermic, so energy management is an important process issue. Conversion decreases with an increase in the reaction temperature and pressure, and reaction rate increases with an increase in temperature and H<sub>2</sub>O concentration, and with a decrease in pressure, though maximum carbonation temperature is limited by the reaction thermodynamics. The resulting problem is that the overall carbonation reaction rate for Na<sub>2</sub>CO<sub>3</sub>/K<sub>2</sub>CO<sub>3</sub> is rather slow, and reactivity decreases with increases in sorption/regeneration operations due to sorbent degradation and attrition. Also, the carbonates are highly and irreversibly reactive with flue gas contaminants HCl and SO<sub>2</sub>, so stringent flue gas cleaning is required.

#### DOE Research

TDA had past projects in sodium carbonate adsorbents for DOE NETL; ultimately funding for that work was discontinued mainly because the regeneration energy demand for their sorbent was ≈1,350 BTU/lb, similar to that for amine-based systems and therefore regarded as non-competitive.

## 2.3.2 INTERMEDIATE TEMPERATURE SORBENTS

### 2.3.2.1 LAYERED DOUBLE HYDROXIDE-BASED SORBENTS

Layered double hydroxides (LDHs), also known as anionic clays or hydrotalcites, are layered basic solids. The structure consists of two types of metallic cations accommodated with the aid of a close-packed configuration of OH<sup>-</sup> groups in a positively-charged brucite-like layer, with anions and water located in the interlayer space for charge compensation.<sup>46</sup> The metal cations occupy the centers of the octahedral structures, whose vertices contain hydroxide ions, and the octahedrons are connected by edge sharing to

43 Jian Liu, Praveen K. Thallapally, B. Peter McGrail, Daryl R. Brown and Jun Liu, "Progress in adsorption-based CO<sub>2</sub> capture by metal-organic frameworks," *Chem. Soc. Rev.*, 2012, 41, 2308–2322.

44 Qiang Wang, Jizhong Luo, Ziyi Zhong and Armando Borgna, "CO<sub>2</sub> capture by solid adsorbents and their applications: current status and new trends," *Energy Environ. Sci.*, 2011, 4, 42.

45 Y. Liang, D. P. Harrison, R. P. Gupta, D. A. Green and W. J. McMichael, *Energy Fuels*, 2004, 18, 569.

46 W. Yang, Y. Kim, P. K. T. Liu, M. Sahimi and T. T. Tsotsis, *Chem. Eng. Sci.*, 2002, 57, 2945.

form an infinite sheet, as depicted in Figure 2-11.<sup>47</sup>

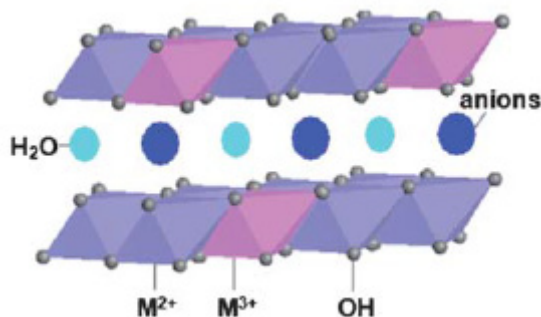
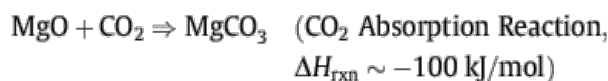


Figure 2-11. Layered Double Hydroxide Structure

In general, LDH derived mixed oxides possess high surface area, abundant basic sites, and higher temperature stability favorable for absorbing acidic CO<sub>2</sub> at 200–400 °C. Potentially, these characteristics and working temperature range should allow LDH-based CO<sub>2</sub> sorbents to be used in the sorption-enhanced water gas shift reaction and biomass reforming processes.<sup>48</sup> In terms of carbon capture, LDHs can be operated and regenerated at higher temperatures and pressures than the low temperature sorbents, potentially allowing more thermally efficient production of higher pressure CO<sub>2</sub>.

### 2.3.2.2 MGO SORBENTS

Like LDH sorbents just discussed, MgO sorbents have potential as CO<sub>2</sub> sorbents in conjunction with the water gas shift reaction. MgO has catalytic activity for the water gas shift reaction, while simultaneously taking up CO<sub>2</sub>.<sup>49</sup>



Equation 2-12

The regeneration reaction is simply the reverse of the above, with  $\Delta H_{\text{rxn}} \approx +100 \text{ kJ/mol}$ , effected by temperature swing and/or pressure swing. MgO sorbent is capable of achieving over 95% CO<sub>2</sub> capture and 40% conversion in the water gas shift (WGS) reaction. The relevant operating temperature range is 350–450 °C, which is approximately the required temperature of the first stage of the typical water gas shift reactor; it may be possible to replace the conventional two-stage water gas shift with one stage using the MgO sorbent, by benefit of the increased driving force for CO conversion provided by simultaneous removal of product CO<sub>2</sub>.<sup>50</sup>

## 2.3.3 HIGH TEMPERATURE SORBENTS

### 2.3.3.1 CAO-BASED SORBENTS

#### Basics

Calcium-based materials are good adsorbent candidates for capturing CO<sub>2</sub> due to their high reactivity with CO<sub>2</sub>, high capacity and low material cost. The reversible reaction between CaO and CO<sub>2</sub>,



Equation 2-13

occurs at 600–700 °C for carbonation, and the regeneration temperature is 850–950 °C at which the CO<sub>2</sub> release reaction occurs

<sup>47</sup> Wang et al. 2011.

<sup>48</sup> Wang et al. 2014.

<sup>49</sup> Emadoddin Abbasi, Armin Hassanzadeh, Shahin Zarghami, Hamid Arastoopour, Javad Abbasian, "Regenerable MgO-based sorbent for high temperature CO<sub>2</sub> removal from syngas: 3. CO<sub>2</sub> capture and sorbent enhanced water gas shift reaction," *Fuel*, Volume 137, 1 December 2014, pp. 260–268

<sup>50</sup> Ibid.

rapidly and to completion, producing a nearly pure stream of CO<sub>2</sub>. Capability of operation at elevated temperature offers great potential for reducing CO<sub>2</sub> from various clean energy systems, particularly high-temperature pre-combustion carbon capture from gasification processes.

The carbonation reaction is highly exothermic and it is possible to efficiently recover the large amount of energy released during the CO<sub>2</sub> capture.<sup>51</sup> Abundant and inexpensive limestone (CaCO<sub>3</sub>) is the raw material for the sorbent. Taken together, these factors tend to support favorable process economics.

Challenges in utilization of CaO-based sorbents arise principally from loss of reversibility for the carbonation reaction due to the sintering of the adsorbent particles in repeated use-regeneration cycles. To a lesser extent, attrition and irreversible reaction of calcium with sulfur species are also involved in CaO-based sorbent degradation. In order to combat this problem, a variety of approaches have been taken:<sup>52</sup>

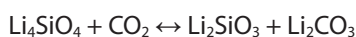
- Utilizing different sorbent synthesis methods or pretreating limestone with acids, yielding pure CaO particles with higher specific surface areas and smaller particle size, or special microstructures (e.g., hollow CaO, mesoporous CaO, etc.) that have more favorable performance.
- Preparation of CaO-based mixed oxide type CO<sub>2</sub> sorbents
- Incorporating CaO particles into inert materials that act as structural supports or matrices, in order to significantly improve sorbent durability.

#### DOE Research

DOE funded URS's "Evaluation of Dry Sorbent Technology for Pre-Combustion CO<sub>2</sub> Capture" project, which investigated engineered sorbents for a process combining CO<sub>2</sub> capture with the water gas-shift (WGS) reaction. The sorbents fall into the CaO-based mixed oxide type CO<sub>2</sub> sorbents mentioned above, and the synthesis methods used yielded more surface area and hollow structure to improve sorbent stability and performance. Ultrasonic spray pyrolysis (USP) and flame spray pyrolysis (FSP) were used to prepare the sorbents, which included zirconia (ZrO<sub>2</sub>)-doped CaCO<sub>3</sub>, yttrium oxide (Y<sub>2</sub>O<sub>3</sub>)-doped CaCO<sub>3</sub>, and MgO/CaO sorbents.<sup>53</sup> The engineered sorbents were found to perform much better than natural limestone in evaluation testing.

### 2.3.3.2 ALKALI CERAMIC-BASED SORBENTS

Alkali zirconate-based (e.g., Li<sub>2</sub>ZrO<sub>3</sub>) and alkali silicate-based sorbents (e.g., Li<sub>4</sub>SiO<sub>4</sub>) are also high-temperature sorbents, which are of interest because of their excellent CO<sub>2</sub> sorption capacities as well as small volume change during the CO<sub>2</sub> sorption/desorption cycles. In recent years the latter alkali-silicate sorbents have been most studied, given their advantages of using cheaper raw materials (as opposed to expensive zirconia) and their considerably lower regeneration temperatures (<750 °C) compared to CaO-based sorbents. The relatively low regeneration temperatures are a beneficial result of the easily reversible reaction between Li<sub>4</sub>SiO<sub>4</sub> and CO<sub>2</sub>:<sup>54</sup>



Equation 2-14

## 2.4 ADVANCES AND FUTURE WORK

Significant reductions in the quantity of electricity lost per unit quantity of CO<sub>2</sub> have been achieved. Currently funded sorbent technologies have improved performance in terms of better sorbents (higher CO<sub>2</sub> capacity, selectivity), decreasing thermal regeneration energy or regeneration at milder temperatures, better process configurations optimizing sorbents with more efficient application of pressure swing adsorption and temperature swing adsorption cycles, and utilization of increasingly cost-effective sorbents.

### 2.4.1 SUMMARY OF ADVANCES

51 Wang et al 2011.

52 Wang et al 2014.

53 "Evaluation of a Dry Sorbent Technology for Pre-Combustion CO<sub>2</sub> Capture" [PDF-1.64MB] (July 2012) Presented by Bill Steen, URS Group, 2012 NETL CO<sub>2</sub> Capture Technology Meeting, Pittsburgh, PA.

54 Wang et al 2014.

When considering sorbent-based CO<sub>2</sub> capture technologies, increasing reduction of the energy penalty incurred per ton of CO<sub>2</sub> captured is usually a useful parameter to directly gauge the advance of technological capability. This is reflected in Figure 2-12, which depicts energy penalty on this basis for a number of sorbent-based CO<sub>2</sub> capture projects in the NETL portfolio in recent years. With the exception of a stray outlier, the trend from higher to lower energy penalty is generally apparent from earlier to latter projects, showing significant progress in NETL-supported R&D sorbent-based capture technology. Projects recently underway, which have not progressed yet to calculating process performance and techno-economic parameters, cannot yet be represented in this figure.

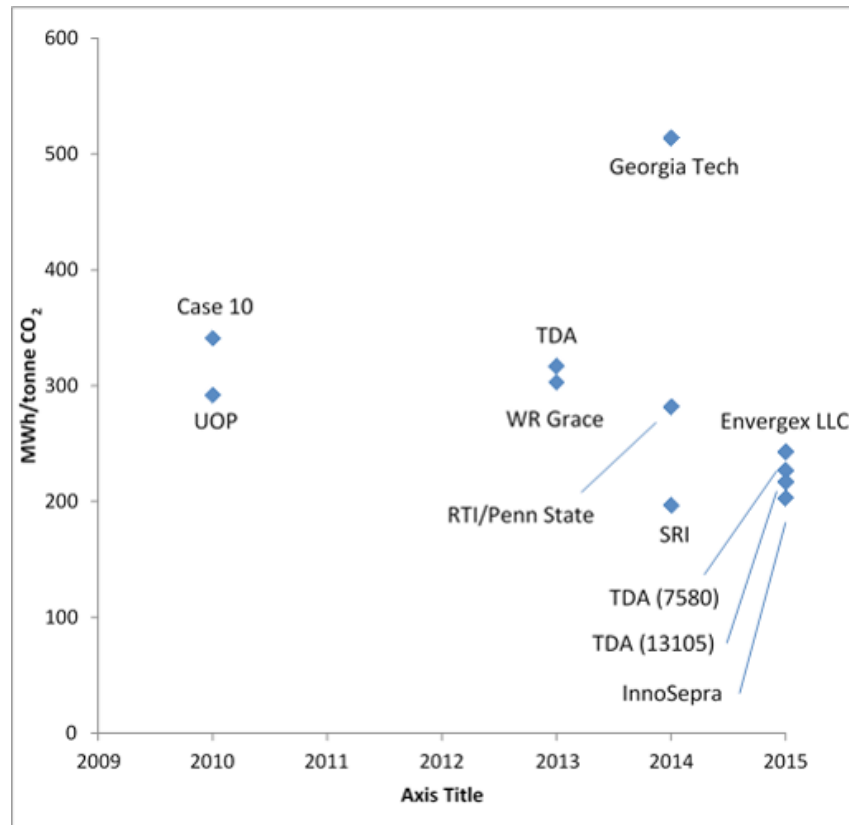


Figure 2-12. Progress in Reducing Parasitic Load of Sorbent-Based CO<sub>2</sub> Capture by DOE/NETL Funded Projects

Certain NETL sorbent-based projects of past years should not be represented in the above figure because in some cases energy penalty per ton CO<sub>2</sub> is not a meaningful basis of comparison. For example, DE-FE0000465, “Evaluation of Dry Sorbent Technology for Pre-Combustion CO<sub>2</sub> Capture” considered a dry calcium-based sorbent integrated into a water-gas shift reactor, which necessitated a radical revision of the overall plant process compared to the base case IGCC process configuration, most notably in terms of an added sorbent regenerating boiler that exceeds the gas turbine in equivalent electrical output. Techno-economic analyses showed that there was potential to better the baseline cost of electricity in such a configuration, even though the energy penalty for CO<sub>2</sub> capture is significantly higher than that of the baseline in these cases. In such instances, the recourse is to compare on basis of COE only.

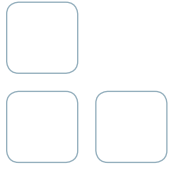
## 2.4.2 KEY PARAMETERS TO BE EVALUATED MOVING FORWARD

Power plant efficiency and energy penalty have been considerably improved. However, significant reduction of capital costs and operating costs are still required to achieve DOE goals. It is anticipated that the following issues will be increasingly emphasized as work goes forward in sorbents technology development:

- Sorbent performance under realistic conditions: Prior work has already begun to address the problems of sorbent stability in low CO<sub>2</sub> partial pressure, humid flue gas streams, but ongoing work must thoroughly lead to viable operation under realistic operating conditions. More stable sorbents may have lower capacities and reaction kinetics in both CO<sub>2</sub> uptake and regeneration, spelling higher capital costs in process equipment. Adsorption columns, compression equipment to establish pressure differentials or vacuums in PSA or VSA process schemes, heat exchangers for TSA schemes, are some of the capital-intensive pieces of equipment in a CO<sub>2</sub> capture plant; these capital costs need to be optimized in relation to sorbent costs and performance in overall process cycles.

- **Costs of advanced sorbents:** Advanced sorbents are novel and materials costs tend to be significantly higher than those associated with conventional CO<sub>2</sub> capture technologies (amine solvent-based), partly because they are first-of-a-kind technologies. Advances in reducing the costs of feedstocks are needed, along with lower production process costs through improved synthesis, economies of scale, etc.
- **Operability concerns:** These include: sorbent degradation, solids handling issues particular to sorbent based-processes which are not experienced in conventional solvent-based technologies, and understanding and managing emissions associated with novel sorbent-based processes.

this page intentionally left blank



# CHAPTER 3:



# MEMBRANE-BASED CO<sub>2</sub> CAPTURE



### 3.1 CONCEPT OF MEMBRANE-BASED GAS SEPARATIONS AND CO<sub>2</sub> CAPTURE

Membrane separation of gases such as CO<sub>2</sub> takes advantage of differences in the relative transfer rates or permeation of various gases through a membrane barrier to effect a greater or lesser degree of gas separation, which is influenced by both the relative diffusivity and surface adsorption of the various gases present. The exact mechanisms for transport and adsorption vary for different membrane materials, such as polymers, metals, and ceramics. To illustrate, the relative permeabilities<sup>1</sup> of various gas species in the polymer polydimethylsiloxane are shown in Figure 3-1.

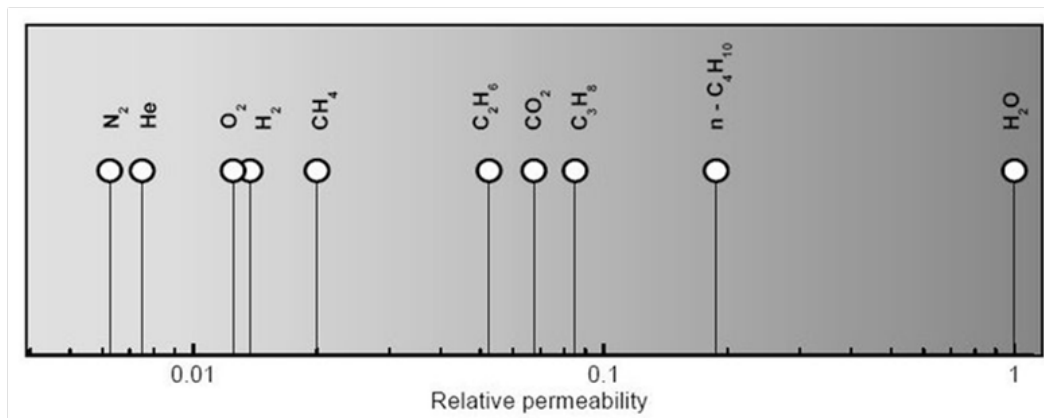


Figure 3-1. Relative Permeabilities of Gases in Polydimethylsiloxane<sup>2</sup>

Qualitatively, this distribution is typical of most polymeric membrane materials, nitrogen having the lowest permeability and carbon dioxide having higher permeability. The permeability of CO<sub>2</sub> is approximately one order of magnitude higher than that of N<sub>2</sub> in this particular polymer, meaning that the ratio of permeabilities or selectivity of CO<sub>2</sub> to N<sub>2</sub> is about 10. The latter selectivity would not be high enough for CO<sub>2</sub> separation from N<sub>2</sub> in envisioned commercial application, however. For that, selectivities would need to be higher, comparable to those typical of commercially available membranes for CO<sub>2</sub> separation from natural gas, which have selectivities of about 30.

Higher selectivity values are desirable because they result in increased purity of the captured CO<sub>2</sub>, combined with high membrane permeance to minimize required membrane area. This is a significant challenge, because permeance and selectivity tend to be inversely proportional, i.e., the higher the selectivity of membrane for any pair of gases, the lower the permeance of the more selective gas. For high permeance membranes less membrane area is needed but the desired gas in the permeate is dilute, and for high selectivity membranes the desired gas in the permeate is relatively concentrated but much more membrane area is needed. However, even a membrane with both high selectivity and high permeance may be too expensive to fabricate.

#### 3.1.1 HISTORY OF MEMBRANE-BASED GAS SEPARATIONS

The earliest experimental studies of gas separation were conducted in the 1850s by Thomas Graham, who measured permeation rates for a large number of gases through a wide assortment of materials. Based on the results of his experiments, Graham developed the solution-diffusion model for permeation and Graham's law of diffusion. The solution-diffusion model is still used today to describe permeation through dense materials such as polymers. Graham's work was first exploited in the early 1940s as part of the Manhattan project as a means of separating isotopes of uranium. Also in the 1940s and 1950s, gas permeation theory was further developed by Barrer, van Amerongen, Stern, Meares, and others leading to improvements to the solution-diffusion model. Commercial application, however, would not emerge for another twenty years.<sup>3</sup>

The development of high flux membranes and large surface area membrane modules for reverse osmosis applications in the late 1960s and early 1970s catalyzed the development of membrane-based gas separation technology. Monsanto was first to commercialize polymer-based gas separation membranes with the introduction of the PRISM™ membrane in 1980. The main application targeted was hydrogen separation from refinery waste gases, but the potential for other gas separations involving helium, CO<sub>2</sub> separation from fuel gases, and air separation were also recognized from the start. The success of PRISM resulted in the introduction

<sup>1</sup> See section on nomenclature for definition.

<sup>2</sup> Metz, D.S., 2003. "Water Vapor and Gas Transport through Polymeric Membranes," Thesis. Enschede, The Netherlands: University of Twente. <http://doc.utwente.nl/40766/>.

<sup>3</sup> Baker, R.W., *Membrane Technology and Applications*, Second Edition, Wiley, 2004.

of other gas separation membrane technologies by companies such as Cynara, Separex, Grace, Dow, Ube, and DuPont/AirLiquide.

Following the successful application of H<sub>2</sub> separation membranes for industrial processes, membranes were introduced for the removal of carbon dioxide from natural gas and for nitrogen separation from air. Since the 1980s, continuous improvements have been made in flux and selectivity through the introduction of advanced polymer materials and improved membrane fabrication technologies, and the cost of gas separation membrane systems have steadily declined. In addition to PRISM membranes currently produced by Air Products, other examples of commercial membranes are MEDAL™ membranes produced by Air Liquide and PolySep™ membranes produced by UOP.

Notwithstanding these established instances of membrane-based gas separations, commercial CO<sub>2</sub> separation/capture using membranes competes against the alternatives (dominated by solvent-based technologies) and is fairly limited to applications such as smaller-scale natural gas purification. To illustrate, baselines for large-scale pre-combustion CO<sub>2</sub> capture from syngas and post-combustion CO<sub>2</sub> capture from flue gas typically specify conventional solvent-based technologies (amine, Selexol, Rectisol, etc.) and not membrane-based capture. For example, out of the Global CCS Institute's database of 55 large-scale CCS projects in various stages of development to operation, 13 projects are classified as operating totaling 25.6 million tonnes per year CO<sub>2</sub> captured; most of these plants are for natural gas processing, synthetic natural gas, or fertilizer production. Eleven of these plants use solvent-based processes (amine, Selexol, Rectisol), one uses sorbents, and only one (the Petrobras Lula Oil Field CCS Project, 0.7 million tonnes per year) uses membrane separation.<sup>4</sup> In fact, there are no commercial membranes that can effectively separate H<sub>2</sub> from CO<sub>2</sub> (because of low selectivity).

### 3.1.2 ADVANTAGES OF MEMBRANE-BASED CO<sub>2</sub> CAPTURE PROCESSES

Notwithstanding the limited extent of membrane-based separation technology in the commercial marketplace, membrane-based CO<sub>2</sub> capture technology potentially offers several advantages over a conventional aqueous solvent-based process such as monoethanolamine (MEA) in post-combustion CO<sub>2</sub> capture:

- Simple operation; no chemical reactions, no moving parts, no heating/temperature swing required to recover CO<sub>2</sub>, no use of hazardous chemicals
- Tolerance to high levels of wet acid gases (for certain membrane types); inert to oxygen
- Compact and modular with a small footprint (at least at lower capacities); easily scalable
- Potential for inherent energy efficiency (≈20% plant energy at 90% capture)
- No additional water used (and in most configurations recovers water from flue gas)

In most configurations of membrane separation no steam use is required,<sup>5</sup> unlike solvent and sorbent based processes which typically demand steam for solvent or sorbent regeneration. Therefore, no modifications to existing boiler and steam turbine are required.

### 3.1.3 CHALLENGES ASSOCIATED WITH MEMBRANE-BASED CO<sub>2</sub> CAPTURE

The limited extent of existing capacity for commercial large-scale CO<sub>2</sub> capture by membranes suggests that competing technologies are usually more cost favorable. This is the consequence of several significant challenges facing currently membrane based CO<sub>2</sub> capture technology:

- Permeability and permselectivity (see next section for further discussion) of available membranes are lower than desirable. This translates into large membrane areas, requiring both large unwieldy footprint for membrane modules, and resulting in high capital costs (the membrane itself and module housings). High CO<sub>2</sub> permselectivity (or H<sub>2</sub> permselectivity in certain configurations of pre-combustion capture) is essential to reducing required membrane areas.
- Although utility steam is not usually needed for membrane separations, significant compression or vacuum capacity to generate the driving force for separation is often demanded. Operation of compressors or vacuum pumps requires expensive auxiliary power, decreasing the net electrical generation of the power plant. Reducing cost through more efficient process arrangements and approaches is essential.
- Potential harmful contaminants (fly ash, SO<sub>2</sub>, NO<sub>x</sub>, water, and trace metals in flue gases; H<sub>2</sub>S, ammonia, fly ash and trace metals in syngas) may reduce effectiveness and lifetime of membranes/modules in post-combustion and pre-combustion membrane-based capture configurations, respectively.

<sup>4</sup> Global CCS Institute database. <http://www.globalccsinstitute.com/projects/large-scale-ccs-projects>.

<sup>5</sup> In certain process configurations of pre-combustion membrane-based CO<sub>2</sub> capture, steam sweep might be utilized.

- The lack of experience operating membrane-based CO<sub>2</sub> capture systems, particularly at the scales associated with large coal-fueled plants, contributes to technological and financial risk that impedes deployment of these systems.

### 3.1.4 TECHNICAL PRINCIPLES OF MEMBRANE-BASED CO<sub>2</sub> CAPTURE<sup>6</sup>

#### 3.1.4.1 NOMENCLATURE AND UNITS OF MEASURE

Understanding of membrane separations demands definition of some of the more important technological parameters involved. In membrane-based gas separations, the feed gas is introduced into a membrane unit or module, and comes in contact with the membrane surface. The penetrant or permeant is the molecular species in contact with the membrane surface that passes through the membrane. The permeate is the stream containing penetrants that leaves the membrane module. The non-permeate or retentate is the stream that has been depleted of one or more penetrants that leaves the membrane module without passing through the membrane. Other important definitions include:<sup>7</sup>

**Permeability:** Transport flux per unit trans-membrane driving force per unit membrane thickness. SI units: [kmol-m/m<sup>2</sup>-s-kPa]

**Permeance:** Transport flux per unit trans-membrane driving force; permeance equals permeability divided by membrane thickness. SI units: [kmol/m<sup>2</sup>-s-kPa]

**Pressure Ratio:** Ratio of the feed pressure to the permeate pressure

**Selectivity:** Ratio of the permeability or permeance of one component to another for a given membrane material at stated conditions

**Separation Factor:** Ratio of the compositions of two components in the permeate relative to the composition ratio of these components in the retentate

**Stage Cut:** the fractional amount of the total feed entering a membrane module that passes through the membrane as permeate

It should be noted that many investigators employ the above terms haphazardly; for example, selectivity as defined above is sometimes referred to as separation factor (see discussion below). Care must be taken in interpreting reported data for permeability, permeance and selectivity.

The following units of measure are frequently employed for permeability:

$$\begin{aligned} 1 \text{ Barrer} &= 10^{-10} \text{cm}^3(\text{STP})\text{-cm/cm}^2\text{-s-cmHg} \\ &= 3.3464 \times 10^{-18} \text{g mol-cm/cm}^2\text{-s-Pa} \\ &= 3.3464 \times 10^{-16} \text{kg mol-m/m}^2\text{-s-kPa} \quad [\text{SI units}] \end{aligned}$$

and for permeance:

$$\begin{aligned} 1 \text{ GPU} &= 10^{-6} \text{cm}^3(\text{STP})/\text{cm}^2\text{-s-cmHg} \\ &= 3.3464 \times 10^{-14} \text{g mol/cm}^2\text{-s-Pa} \\ &= 3.3464 \times 10^{-10} \text{kg mol/m}^2\text{-s-kPa} \quad [\text{SI units}] \end{aligned}$$

where standard pressure and temperature (STP) are 0 °C and 1 atmosphere, and GPU stands for Gas Permeation Unit. Barrer and GPU are compound units based on the units of measure selected for quantity transported, membrane thickness, membrane surface area and partial pressure (i.e., component fugacity), respectively:

<sup>6</sup> Content of this section primarily from "Integration of H<sub>2</sub> Separation Membranes with CO<sub>2</sub> Capture and Compression," Prepared for U.S. Department of Energy, National Energy Technology Laboratory, under DOE TAMS Contract No. DE-AC26-05NT41816, John Marano, Technology and Management Services, Inc.

<sup>7</sup> IUPAC Working Party on Membrane Nomenclature.

$$1 \text{ kg mol} = 1,000 \text{ g mol} = 2.241 \times 10^7 \text{ cm}^3(\text{STP}) \\ = 2.205 \text{ lb mol} = 836.8 \text{ scf (60 }^\circ\text{F)}$$

$$1 \text{ m} = 100 \text{ cm} = 39.37 \text{ in} = 3.281 \text{ ft}$$

$$1 \text{ m}^2 = 10^4 \text{ cm}^2 = 1,550 \text{ in}^2 = 10.764 \text{ ft}^2$$

$$1 \text{ atm} = 1.013 \text{ bar} = 76.0 \text{ cmHg} = 14.696 \text{ psi} = 1.013 \times 10^5 \text{ Pa}$$

### 3.1.4.2 MEMBRANE SEPARATION FACTOR

For most perm-selective membrane materials, the flux  $J_i$  of component  $i$  through the membrane will be proportional to the difference in partial pressures on either side of the membrane barrier:

$$J_i = (P_i / l) \Delta p_i$$

Equation 3-1

where  $P_i$  is the permeability of gas component  $i$ ,  $l$  is the thickness of the membrane barrier, and  $\Delta p_i$  is the partial pressure driving force across membrane. Equation 3-1 is the basis for the definition of permeability given above. Also, the quantity  $P_i / l$  can be viewed as the pressure normalized flux; and is the basis for the definition of membrane permance:

$$P_i \equiv P_i / l$$

Equation 3-2

Permeability is a property of the membrane material; whereas, permance also depends on the thickness of the membrane. Obviously, it is desirable to minimize the membrane thickness to achieve the highest permance and flux. The minimum thickness is limited by material properties and membrane fabrication technique, and also depends on mechanical strength requirements for any gas separation application.

Separation Factor is defined as:

$$SF_{ij} \equiv (X_i/X_j)_{\text{permeate}} / (X_i/X_j)_{\text{retentate}}$$

Equation 3-3

where  $X_i$  and  $X_j$  are mole fractions of components  $i$  and  $j$  on either side of the membrane.

It can be shown for a differential membrane element that:<sup>8</sup>

$$\lim SF_{ij} = (P_i/P_j) \times (\Delta p_i/p_i \text{ permeate}) / (\Delta p_j/p_j \text{ permeate})$$

Equation 3-4

Clearly, the separation factor is a function of material properties, membrane thickness and partial pressure driving force. It is useful because it can be directly calculated from experimental data; but is not a good indicator of membrane's ability to separate gas pairs because it is a function of operating conditions (i.e.,  $\Delta p/p$ ).

<sup>8</sup> Derivation of equation A4 involves the substitution of A1 for the terms in the numerator, and the ideal gas law for the terms in the denominator. A4 is only applicable for a differential membrane. The true relationship between selectivity and separation factor is more complex and depends on actual geometry of the membrane contactor. For more details see: Koros, W.J.; Fleming, G.K., "Membrane-based gas separation," *Journal of Membrane Science*, **83**, pp.1–80, 1993.

Equation 3-4 can be used as the starting point for considering a number of different definitions for the term selectivity. The ratio ( $P_i/P_j$ ) in Equation 3-4 can be defined as the true selectivity of components  $i$  and  $j$ :

$$S_{ij} \equiv P_i/P_j = P_i/P_j$$

Equation 3-5

It is solely a property of the membrane material, and includes any effects of pressure, temperature and interactions between the molecular species present.

An ideal selectivity may be defined as:

$$S_{ij}^o \equiv P_i^o/P_j^o$$

Equation 3-6

where the superscript 'o' indicates the permeabilities are for transport of pure gas components through membrane. Unlike the true selectivity, the ideal selectivity is not a function of gas composition. Ideal selectivity is also referred to as permselectivity.

It is the true selectivity that is required for the accurate design of commercial gas separation membrane systems.  $P_i$  does not necessarily equal  $P_i^o$  nor does  $P_j$  equal  $P_j^o$ ; however, it is much easier to design experiments to measure pure gas permeabilities.

Thus, the experimental determination of permselectivity can be a reasonable, cost-effective starting point for screening membrane materials at bench scale, but must be supplemented later on in the development process with testing under realistic operating conditions using the mixed gases of interest.

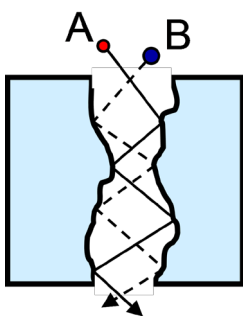
Finally, if measurements of the pure gas permeabilities,  $P_i^o$  and  $P_j^o$ , are made at the same conditions of temperature, feed and permeate pressure, then based on Equation 3-4, the ideal selectivity  $S_{ij}^o$  is equivalent to an ideal separation factor,  $SF_{ij}^o$ .

### 3.1.4.3 THEORY OF MEMBRANE-BASED GAS SEPARATION

Conceptually, the behavior of gases permeating a membrane can be considered from the viewpoint of a thin barrier containing a single large pore, which is in contact with a gas containing molecules of two components A and B.

For pore diameters 0.1  $\mu\text{m}$  or larger, flow of the gas through the pore will be by viscous Poiseuille flow and no separation will occur.

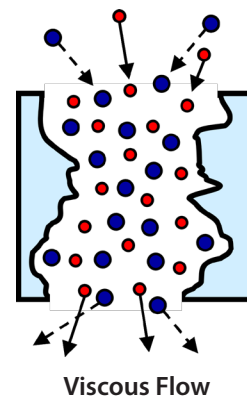
As the pore diameter is decreased, a point is reached where the radius of the pore is of the same magnitude as the mean free path of the gas molecules ( $\lambda/r \approx 1$ ).



Knudsen Diffusion

For  $\lambda/r$  less than one, a gas molecule will experience more collisions with the pore walls than with other gas molecules. Since molecule-to-molecule collisions are rare each molecule moves independently through the micropore. Therefore, for gas mixtures containing components with different average velocities, a gas separation is possible.

This pore flow regime is known as Knudsen diffusion and for an ideal cylindrical pore; the molecular flux of each component is governed by the equation:



Viscous Flow

$$J_i = \frac{4r\varepsilon}{3} \left( \frac{2RT}{\pi M_i} \right)^{1/2} \frac{(p_{Hi} - p_{Li})}{lRT}$$

Equation 3-7

where  $J_i$  is the flux of component  $i$  in units of kg-mol/m<sup>2</sup>-s,  $r$  is the pore radius in meters,  $\varepsilon$  is the porosity of the membrane,  $R$  is the ideal gas constant in kg-m<sup>2</sup>/s<sup>2</sup>-kg-mol-K,  $T$  is absolute temperature in Kelvin,  $M_i$  is the molecular weight of the gas in kg/kg-mol,  $l$  is the pore length in meters,  $p_{Hi}$  is the partial pressure at the entrance of the pore in Pascals, and  $p_{Li}$  is the partial pressure at the exit of the pore in Pascals. The subscripts H and L designate the high and low partial pressure sides of the pore, respectively.

Based on Equation 3-7, the gas permeance is defined as:

$$P_i \equiv \frac{4r\varepsilon}{3lRT} \left( \frac{2RT}{\pi M_i} \right)^{1/2}$$

Equation 3-8

Equation 3-8 illustrates that for Knudsen diffusion, the permeance is inversely proportional to the square root of the molecular weight of the gas and also to the square root of the absolute temperature. The former relationship is the basis for Graham’s law for predicting the ideal selectivity of Knudsen diffusion membranes:

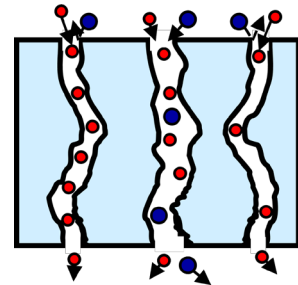
$$S_{ij} \equiv \frac{P_i}{P_j} = \sqrt{\frac{M_j}{M_i}}$$

Equation 3-9

where  $i$  and  $j$  designate different molecular species present in the gas.

When the pore diameter decreases to between 5 and 10 Å, the nanoporous membrane begins to separate gas species via a molecular sieving mechanism.

Ideally, for molecular sieving, the flux is related to the ratio of the area of the pore available for transport to the total area of the pore. This is given by:



Molecular Sieving

$$J_i \propto \frac{(d_p - d_{ki})^2}{d_{ki}^2}$$

Equation 3-10

where  $d_p$  is the diameter of the pore and  $d_{ki}$  is the kinetic diameter of the gas molecule. The ideal selectivity is then given by:



$$S_{ij} = \left( \frac{d_p - d_{k,i}}{d_p - d_{k,j}} \right)^2$$

Equation 3-11

In addition to the phenomena described above, Knudsen diffusion and molecular sieving, surface adsorption and diffusion can contribute to molecular transport through membrane pores.

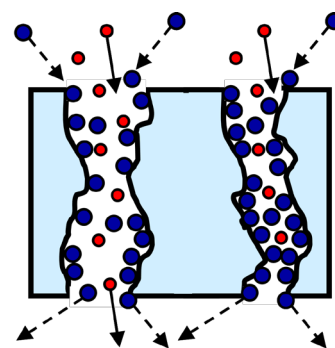
Table 3-1 lists molecular parameters for gases typically used in evaluating membrane performance. Also presented are ideal selectivities calculated from these parameters for both molecular sieving and Knudsen diffusion.

Table 3-1. Molecular Parameters of Membrane Diffusion for Various Gases<sup>9</sup>

GAS MOLECULE	KINETIC DIAMETER Å	MEAN FREE PATH (20 °C, 1 bar) Å	MOLECULAR WEIGHT	MOL. SIEVE (7 Å pore dia.) P <sub>H<sub>2</sub></sub> /P <sub>X</sub>	MOL. SIEVE (3.7 Å pore dia.) P <sub>H<sub>2</sub></sub> /P <sub>X</sub>	MOL. SIEVE (3.32 Å pore dia.) P <sub>H<sub>2</sub></sub> /P <sub>X</sub>	KNUDSEN DIFFUSION P <sub>H<sub>2</sub></sub> /P <sub>X</sub>
He	2.55	–	4.003	0.85	0.50	0.32	1.41
H <sub>2</sub> O	2.65	–	18.015	0.89	0.60	0.41	2.99
H <sub>2</sub>	2.89	1,744	2.016	1.00	1.00	1.00	1.00
CO <sub>2</sub>	3.30	615	44.010	1.23	4.10	330.00	4.67
O <sub>2</sub>	3.47	–	31.999	1.35	12.09	∞	3.98
H <sub>2</sub> S	3.52	–	34.080	1.40	20.92	∞	4.11
Ar	3.54	–	39.948	1.41	26.28	∞	4.45
N <sub>2</sub>	3.64	929	28.013	1.50	182.25	∞	3.73
CO	3.76	923	28.010	1.61	∞	∞	3.73
CH <sub>4</sub>	3.80	–	16.043	1.65	∞	∞	2.82
CF <sub>4</sub>	4.66	–	88.005	3.09	∞	∞	6.61
C <sub>3</sub> H <sub>8</sub>	5.12	–	44.097	4.77	∞	∞	4.68
SF <sub>6</sub>	5.13	–	146.054	4.82	∞	∞	8.51

As the pore diameter is decreased, selectivities can become quite large, approaching infinity when the molecule becomes larger than the pore opening. However, the rate of transport/permeance will also decrease for the smaller gas species as the pore opening decreases. It can also be seen that H<sub>2</sub> and CO<sub>2</sub> are nearly the same size, making them difficult to separate from each other based on molecular size alone. The same holds true for CO<sub>2</sub> and N<sub>2</sub> which are relatively close in size. Most porous materials other than zeolites do not possess precise pore sizes, making their use impractical with small gas molecules. Molecular weight-based separation based on Knudsen diffusion is also an inefficient means of separating H<sub>2</sub> and CO<sub>2</sub>.

Adsorption may become significant when the pore diameter drops below about 100 Å. In particular, if a gas species is condensable, the amount of gas adsorbed can be significantly greater than that occupying the free pore volume, and surface diffusion can be the dominant transport mechanism. When the diameter of the adsorbed species is of the same magnitude as the pore diameter, it is also possible for the adsorbed species to effectively block the pores, significantly decreasing or entirely preventing the transport of other gaseous species.

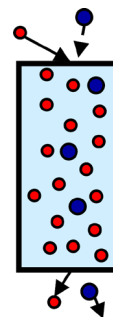


Surface Adsorption

<sup>9</sup> Compiled from: Baker, R.W., *Membrane Technology and Applications*, Second Edition, Wiley, 2004; *Handbook of Chemistry and Physics*, 56<sup>th</sup> Edition 1975–1976, CRC Press, 1975; Skelland, A.H.P., *Diffusional Mass Transfer*, Krieger Publishing Company, 1985.

Transport by surface diffusion is complex, since it is also likely to occur in parallel with either Knudsen diffusion or molecular sieving. The combined phenomena cannot be easily modeled using a single equation for predicting the total molecular flux.

At pore diameters less than about 5 Å, the membrane transport mechanism may again change from molecular sieving to one dominated by molecular diffusion. This is the mechanism for transport in most polymer membranes, where the molecular species first adsorbs onto the membrane surface, dissolves in the membrane material, and then diffuses across the membrane (i.e., solution-diffusion).



Surface Adsorption

For molecular diffusion the flux of each component is governed by the equation:

$$J_i = S_i \mathcal{D}_i \frac{(p_{Hi} - p_{Li})}{l}$$

Equation 3-12

where  $S_i$  is the surface solubility of component  $i$ , in units of  $\text{kg}\cdot\text{mol}/\text{m}^3\cdot\text{Pa}$ , and  $\mathcal{D}_i$  is the diffusivity of  $i$  in bulk membrane material, in units of  $\text{m}^2/\text{s}$ . Solubility is primarily a function of the chemical composition of the membrane and diffusion of the structure of the membrane. Gases can have high permeation rates due to high solubility, high diffusivity, or both.

Based on Equation 3-12, the gas permeance is defined as:

$$P_i \equiv \frac{S_i \mathcal{D}_i}{l}$$

Equation 3-13

The ideal selectivity for molecular diffusion in dense membranes is then given by:

$$S_{ij} = \frac{S_i \mathcal{D}_i}{S_j \mathcal{D}_j}$$

Equation 3-14

The ratio of  $\mathcal{D}_i/\mathcal{D}_j$  can be viewed as mobility selectivity, reflecting the different sizes of the molecules, and the ratio of  $S_i/S_j$  can be viewed as solubility selectivity, reflecting the relative condensabilities of the gases. In polymers, the diffusion coefficient always decreases with increasing molecular size, because big molecules interact with more segments of the polymer chain. Thus, the mobility selectivity always favors the passage of the smaller molecule. The solubility selectivity favors larger, more condensable molecules. For molecules similar in size, molecular diffusion may not provide effective gas separation; e.g., for  $\text{CO}_2$  and  $\text{N}_2$  which are relatively close in size, diffusivity selectivity in polyimide is an inefficient 2–4 (the ideal separation factor would be 15–30).<sup>10</sup>

In addition to molecular diffusion, transport may also occur in dense materials via either an atomic or ionic diffusion mechanism.

Atomic diffusion of hydrogen occurs in palladium and related transition metals and alloys. Molecular hydrogen is adsorbed on the metal surface and disassociates into atomic hydrogen, which diffuses through the metal atom matrix. The hydrogen atoms then recombine to form molecular hydrogen and desorb from the surface. When diffusion is the controlling step, the flux is given by Sievert's law:

10 Materials Science of Membranes for Gas and Vapor Separation, edited by Benny Freeman, Yuri Yampolskii, Ingo Pinnau, John Wiley and Sons, England, (2006).

$$J_i = \mathcal{K}_i \mathcal{D}_i \frac{(p_{Hi}^{1/2} - p_{Li}^{1/2})}{l}$$

Equation 3-15

Note that the partial pressure driving force is no longer linear. The partial pressure term raised to the 1/2-power results from the disassociation of diatomic hydrogen. The equilibrium constant for disassociation of H<sub>2</sub> on the membrane surface K<sub>i</sub> has units of kg-mol/m<sup>3</sup>-Pa<sup>1/2</sup>.

Based on Equation 3-15, a gas permeance can be defined as:

$$P_i \equiv \frac{\mathcal{K}_i \mathcal{D}_i}{l}$$

Equation 3-16

However, permeance as defined above for atomic diffusion is not directly comparable to that for all the other transport mechanisms previously discussed, which take the form of the general flux equation given in Equation 3-1.

The selectivity of metallic membranes for hydrogen separations is essentially infinite due to the disassociation on the membrane surface of diatomic hydrogen, with a molecular diameter of  $\approx 2.9 \text{ \AA}$ , into atomic hydrogen, with an atomic diameter of less than 1  $\text{ \AA}$ . While size loses much of its meaning on these scales as the wave nature of matter begins to noticeably manifest itself, atomic hydrogen is so small that it can easily diffuse through the dense metal phase.

Ionic diffusion can occur in high-temperature dense ceramics, such as doped rare-earth oxides. In this case, hydrogen adsorbs on the ceramic surface, disassociates, and diffuses as hydrogen ions (protons) through the membrane. The hydrogen ions then recombine to form molecular hydrogen and desorb from the surface. The flow of protons across the membrane must be balanced by an equivalent flow of negatively charged electrons in the same direction to maintain neutrality. The hydrogen flux for this transport mechanism at elevated temperature is given by the equation:

$$J_i = \frac{\sigma_{\text{amb}} RT}{4\mathcal{F}^2 l} \ln\left(\frac{p_{Hi}}{p_{Li}}\right)$$

Equation 3-17

where R is the ideal gas constant in units of J/kg-mol-K, T is the absolute temperature in Kelvin, F is the Faraday constant in Coulomb/kg-mole, and  $\sigma_{\text{amb}}$  is the ambipolar conductivity of the material in units of 1/Ohm-m, defined as:

$$\sigma_{\text{amb}} = \frac{\sigma_{\text{H}^+} \sigma_{\text{e}^-}}{\sigma_{\text{H}^+} + \sigma_{\text{e}^-}}$$

Equation 3-18

where  $\sigma_{\text{amb}}$  and  $\sigma_{\text{amb}}$  are the protonic and electronic conductivities.

Based on Equation 3-17, a gas permeance can be defined as:

$$P_i \equiv \frac{\sigma_{\text{amb}} RT}{4F^2 l}$$

Equation 3-19

Again, permeance as defined above for ionic diffusion is not directly comparable to that for all the other transport mechanisms previously discussed.

Based on Equation 3-18, the flux will be high when  $\sigma_{\text{amb}}$  is large. This requires both the protonic and electronic conductivities to be large. Conductivity can be raised by operating the membrane at high temperatures and by doping the membrane material. Ceramic materials normally do not possess high electronic conductivity. Therefore, ceramic/metallic composites, referred to as cermets, are being researched to enhance this conductivity.

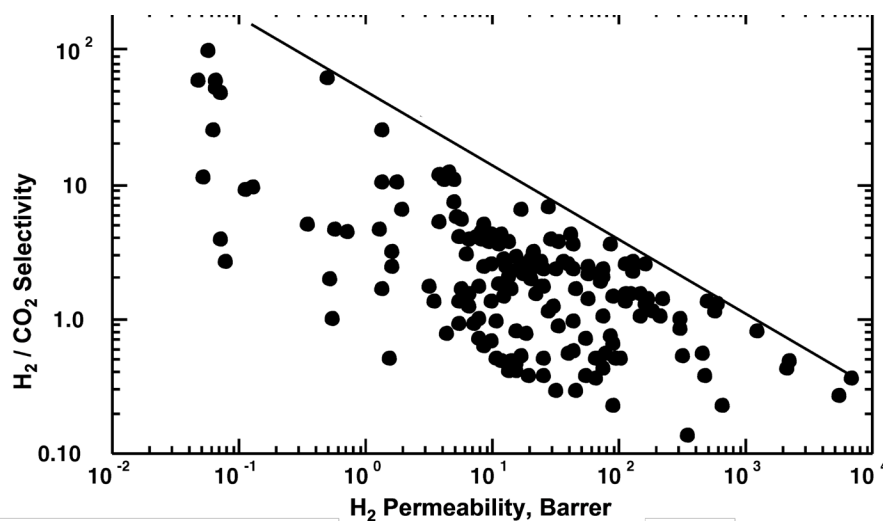
In general, permeability, and thus permeance, is a function of temperature; however, this dependence will vary based on the exact mechanism of membrane transport. Knudsen diffusion is proportional to the square root of temperature. Molecular sieving in principle does not possess a temperature dependence; but, in real systems an effect is observed due to other interacting phenomena. All mechanisms involving surface adsorption and/or diffusion will show an exponential-type temperature dependence, which can be modeled using an Arrhenius Law expression:

$$P_i(T) = K_i e^{(-E_i/RT)}$$

Equation 3-20

where  $K_i$  and  $E_i$  are constants for any given component, and  $E_i$  is the activation energy. The quantity  $R$  is the ideal gas constant expressed in energy units and the temperature  $T$  is in absolute units. In general, gas adsorption decreases with increasing temperatures; whereas, diffusion increases. These interactions can result in quite complex temperature behavior in systems involving both adsorption and diffusion. Based upon Equation 3-19, it might appear that permeance is only proportional to temperature. However, ionic conductivity also exhibits an exponential temperature dependence, increasing with increased temperatures.

For membrane systems involving molecular diffusion, most notably polymers, an inverse relationship exists between selectivity and permeability; as the selectivity is increased, the permeability decreases, and vice versa. It has also been shown experimentally that a log-log plot of the permselectivity of a binary gas pair versus the permeability of the “faster” gas molecule, results in a clearly defined upper limit on selectivity for any given value of permeability. Such a plot is referred to a Robeson plot after the membrane researcher to first describe this phenomenon in polymer-based membranes. This relationship is depicted in Figure 3-2 for H<sub>2</sub> and CO<sub>2</sub> for a wide range of polymeric membrane materials.

Figure 3-2. Robeson Plot for H<sub>2</sub>/CO<sub>2</sub> Permeability in Polymers<sup>11</sup>

11 Robeson, L.M., “Correlation of Separation Factor Versus Permeability for Polymeric Membranes,” *Journal of Membrane Science*, **62**, 1991.

No completely theoretical explanation has been identified for the Robeson limit, and many researchers have investigated modified materials with the hope of pushing this limit. However, these efforts have so far only had limited success.

Figure 3-3 shows the Robeson limits for  $H_2/CO_2$ ,  $H_2/N_2$ , and  $H_2/CH_4$ . This plot clearly demonstrate the difficulty of separating  $H_2$  from  $CO_2$  using purely a solution-diffusion mechanism, relative to  $H_2/N_2$  and  $H_2/CH_4$  membrane-based separations which have been commercialized. As discussed above, both solubility and diffusion are molecular size dependent phenomena, and as can be seen from Table 3-1,  $H_2$  and  $CO_2$  molecules have very similar sizes.

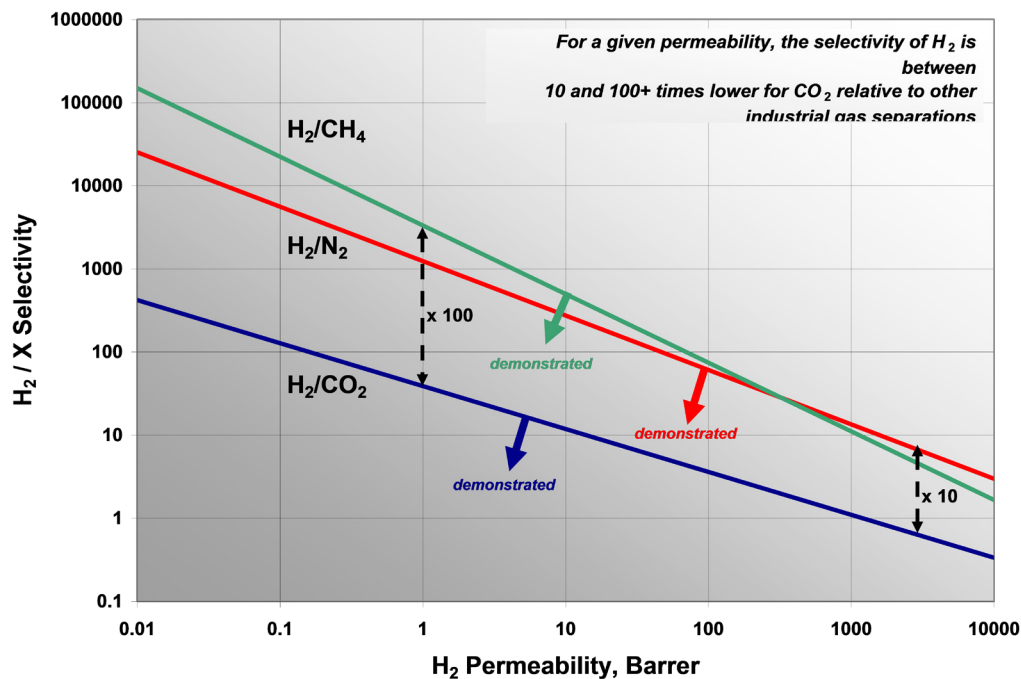
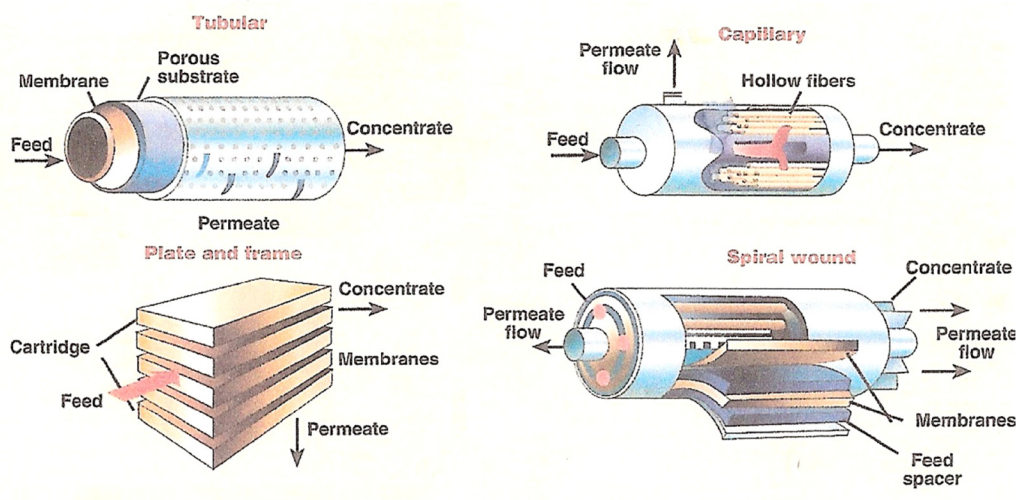


Figure 3-3. Robeson Limits for  $H_2$  Permeable Membranes<sup>12</sup>

### 3.1.4.4 MEMBRANE MODULE DESIGNS

Schematics of the four most common membrane module designs are shown in Figure 3-4. Tubular and plate-and-frame designs are common in filtration and water treatment applications. Multiple tubes are often packed into a single cylindrical vessel. This is referred to as a shell-and-tube design. Currently, all industrial, gas separation membrane applications employ polymer membrane technology based on hollow fibers or flat sheets, and these designs will be discussed in more detail below.

<sup>12</sup> Based on parameters from: Robeson, L.M., *Polymer*, 35, p. 4970, 1994.

Figure 3-4. Common Membrane Module Designs<sup>13</sup>

In hollow fiber (HF) based modules, the outside layer of the fiber is composed of a dense polymer on the order of 0.05–0.10  $\mu\text{m}$  thick. The separation occurs across this thin layer. The porous sub-layer provides structural support to the fiber so that it can withstand large pressure gradients. Individual fibers are about three times the diameter of a human hair ( $\approx 125 \mu\text{m}$ ). In a typical membrane module, thousands of fibers are bundled together in a cylindrical arrangement around a central core consisting of perforated tube known as the bore. An epoxy resin seals each end of the cylindrical fiber bundle to a tubesheet, thus separating the feed gas from the permeate. The fiber bundle and bore are enclosed in a shell similar to that used with shell-and-tube heat exchange equipment. Feed gas flows into the shell through the bundle and around the tubes. The retentate, that is the depleted feed gas, exits the membrane module through the bore. If a sweep gas is employed, it is routed through a shell head and distributed to one end of the hollow fiber bundle, exiting at the other end of the module enriched with permeate. If no sweep is used, one end of the fiber bundle may be completely sealed. Flow in this arrangement is predominantly cross flow, though co-current and counter-current arrangements are possible.

An alternative design for polymer membrane equipment uses thin sheets of polymer arranged in spiral-wound (SW) modules. The feed gas enters the module and flows between the membrane leaves. Components of the feed gas permeate the membrane and spiral inward toward a central collection pipe. The depleted feed flows across the membrane surface and exits at the other end of the module. The leaves of the membrane alternate between porous membrane sheets and non-porous spacer sheets providing passage for both the retentate and permeate. This arrangement results in cross flow. The membrane industry standard spiral-wound module is an 8-inch diameter module containing 15–30 membrane envelopes with a total membrane area of 20–50  $\text{m}^2$  per module. The spiral-wound module design is robust, fouling resistant, and very economical.<sup>14</sup> Spiral-wound modules have captured more than 90% of the reverse osmosis market, more than 70% of the ultrafiltration market, and perhaps 30% of the gas separation market.<sup>15</sup>

Membrane Technology and Research (MTR), in the context of CO<sub>2</sub> capture projects funded by DOE NETL, has devised a modification of the standard spiral-wound module that allows introduction of sweep gas on the permeate side to establish driving force without additional pressurization. It involves closing the permeate collection pipe in the middle with a plug, forming two separate compartments; also, during module fabrication, additional glue lines can be applied to direct gas flow in the permeate channel. As shown in the Figure 3-5, the modifications allow the permeate channel to be swept with a sweep gas and the module to operate in a partial countercurrent mode. The permeate gas, together with the sweep gas, flows countercurrent to the feed gas flow.<sup>16</sup>

13 Torzewski, K. (Ed.), "Facts at your Fingertips—Membrane Configuration," *Chem. Eng.*, Mar. 1, 2009

14 "Membrane Process to Sequester CO<sub>2</sub> from Power Plant Flue Gas," Final Technical Report, Tim Merkel, July 2009, DE-FC26-07NT43085. <http://www.osti.gov/scitech/servlets/purl/1015458-INdTMC/>.

15 W. Baker, *Membrane Technology and Applications*, 2<sup>nd</sup> ed., John Wiley and Sons Ltd., Chichester, England pp. 544 (2004).

16 "Membrane Process to Sequester CO<sub>2</sub> from Power Plant Flue Gas," Final Technical Report, Tim Merkel, July 2009, DE-FC26-07NT43085. <http://www.osti.gov/scitech/servlets/purl/1015458-INdTMC/>.



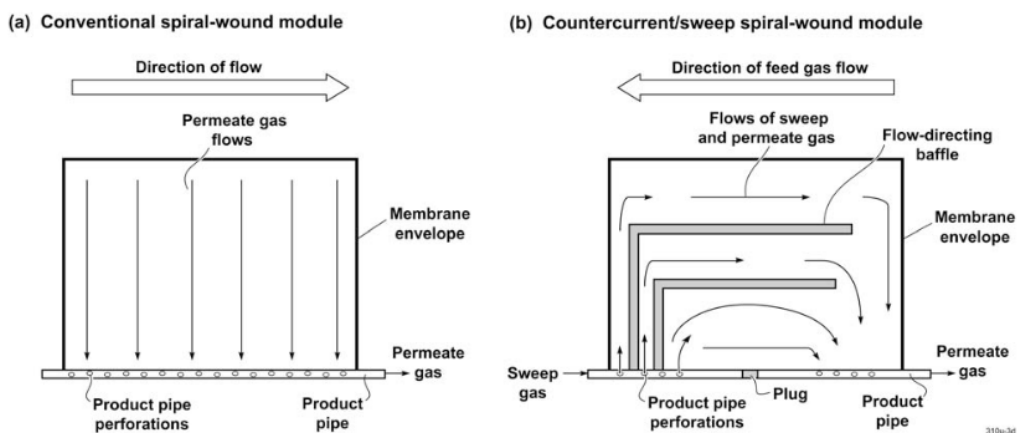


Figure 3-5. Spiral-Wound Membrane Module Flow Patterns

A less commonly used membrane module arrangement involves the use of flat sheets in a plate-and-frame (PF) design. This configuration has been explored in recent DOE-NETL work in MTR's project Low-Pressure Membrane Contactors for CO<sub>2</sub> Capture. The project focus was a compact large membrane area (>500 m<sup>2</sup>), low pressure drop plate-frame sweep module for CO<sub>2</sub> capture application. As in MTR's modified spiral-wound modules, an essential aspect of this PF module is use of sweep combustion air to establish the separation driving force (CO<sub>2</sub> partial pressure difference) instead of relying on expensive compressors or vacuum pumps (which have both high capital cost and have high energy cost to operate). Additionally, PF-type membrane module designs have the advantage of lower pressure drop compared to typical hollow fiber modules or spiral-wound modules, also saving on energy.

HF and SW membrane-based systems are typically smaller than other types of gas separation plants, such as absorption and adsorption systems, and have high surface area-to-volume ratios (packing density). Achievable packing densities are much greater for hollow fibers (HF;  $\approx 6,000 \text{ m}^2/\text{m}^3$  or  $\approx 1,800 \text{ ft}^2/\text{ft}^3$ ) versus either spiral-wound sheets (SW;  $\approx 650 \text{ m}^2/\text{m}^3$  or  $\approx 200 \text{ ft}^2/\text{ft}^3$ ) or plate-and-frame sheet arrangements (PF;  $\approx 325 \text{ m}^2/\text{m}^3$  or  $\approx 100 \text{ ft}^2/\text{ft}^3$ ). All of these are greater than what is achievable in for example an absorption column ( $\approx 260 \text{ m}^2/\text{m}^3$  or  $\approx 80 \text{ ft}^2/\text{ft}^3$ ). Since membrane units are modular, there is no limit to maximum capacity and plants consisting of over a 100 individual modules, with H<sub>2</sub> delivery rates of greater than 50 MM scfd have been built. However, modularity has the drawback that plant costs essentially scale linearly with plant capacity and the economic advantages of membranes versus other processes can be lost at high throughputs. Almost 400 hydrogen gas-separation membrane systems are operating worldwide.

The cost of H<sub>2</sub> recovery systems is proprietary, but may be estimated. Typical costs for hollow fiber and spiral wound sheet membranes are \$45–55 and \$375 per m<sup>2</sup> (\$4–5 and \$35 per ft<sup>2</sup>), respectively.<sup>17</sup> Housing can be an additional 20% of the surface area cost and final assembly an additional 1%. Installation of the system at the plant site can be assumed to be 20% of the equipment cost due to the modular nature the equipment. Installed costs of plate-and-frame or shell-and-tube modules utilizing metallic plates or tubes to support the active membrane layer would typically be expected to be higher, given higher materials and fabrication costs.<sup>18</sup>

In addition to permeance and selectivity, the useful life of the membrane and module is a critical parameter in evaluating the economic performance of a membrane-based gas separation process. A shortened lifetime results in higher maintenance and replacement costs. Membrane life for H<sub>2</sub> recovery systems with proper operation and maintenance is reported to be high, exceeding 15 years. However, operation in harsh chemical environments can shorten this lifetime to as little as 3–5 years. Reliability can also be extremely high, with on-stream factors exceeding 99%. Modularity coupled with proper valve placement allows individual modules to be taken off-line without shutting down the entire system. This feature also provides large swings in throughput. Individual module turn-down/up ratios as low as 30% and greater than 100% are possible; however, recovery will be compromised. Additional modules may be brought on-stream if additional capacity is required.

### 3.1.4.5 PROCESS CONFIGURATIONS FOR MEMBRANE SEPARATIONS

Available membranes for gas separation are usually limited in their combination of permeability characteristics and selectivity for the target gas component to be removed or purified. Accordingly, a single-stage membrane separator often cannot attain required

<sup>17</sup> Ibid.; adjusted for inflation.

<sup>18</sup> MTR has developed a concept for lowering cost of PF modules; they claim costs might be reduced to the range of \$50/m<sup>2</sup> in large area, compact PF modules. See Low-Pressure Membrane Contactors for CO<sub>2</sub> Capture. <http://www.netl.doe.gov/research/coal/carbon-capture/post-combustion/membrane-mtr>.

degrees of separation and purity of products (e.g., the DOE NETL goals of 90% CO<sub>2</sub> capture with 95%+ purity cannot practically be attained in a single-state process). This principle was documented in a series of parametric studies of CO<sub>2</sub> separation from N<sub>2</sub> at flue gas concentrations in order to quantify energy penalties compared to the conventional amine process; it was concluded that although energy cost could compare favorably, existing membrane materials did not perform well enough to meet CO<sub>2</sub> recovery/purity requirements.<sup>19</sup> Other studies have reported on both single and two-stage systems for CO<sub>2</sub> separation from N<sub>2</sub> at flue gas, including capital and operating (energy) cost considerations in their analyses.<sup>20</sup> An important observation is that energy penalty considerations alone are of limited usefulness in membrane-based capture, chiefly given the overwhelming cost penalty that a large membrane area can incur. In a recent series of studies, various arrangements of multistage membrane separators for carbon capture from flue gas were exhaustively analyzed for comparative performance, with complete cost calculations prepared.<sup>21</sup>

### Conventional Two-Stage Processes

When considering two-stage membrane separation systems, these studies have noted that two main system circuitries are possible that improve separation performance, classified as follows: (1) serial “stripper” circuits, in which retentate from the first stage becomes the feed for a second membrane separation stage, and (2) serial “enricher” circuits, in which the permeate from the first stage becomes the feed for the second stage. Figure 3-6 provides examples of the first class of stripper process arrangement, while Figure 3-7 provides examples of the second class.

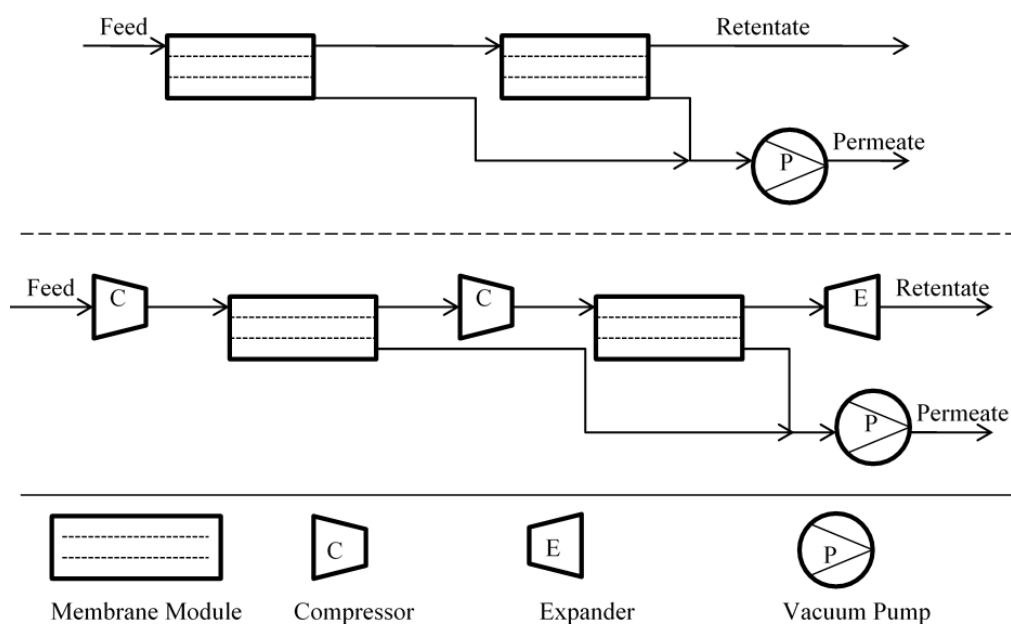


Figure 3-6. Two-Stage Membrane Circuitries: Serial Stripper Concept

- 19 Roda Bounaceur, Nancy Lape, Denis Roizard, Cecile Vallieres, Eric Favre, “Membrane processes for post-combustion carbon dioxide capture: A parametric study,” *Energy*, Volume 31, Issue 14, November 2006, pp. 2556–2570.
- 20 Dongxiao Yang, Zhi Wang, Jixiao Wang, and Shichang Wang, “Potential of Two-Stage Membrane System with Recycle Stream for CO<sub>2</sub> Capture from Post-Combustion Gas,” *Energy Fuels*, 2009, 23 (10), pp. 4755–4762; Minh T. Ho, Guy W. Allinson, Dianne E. Wiley, “Reducing the Cost of CO<sub>2</sub> Capture from Flue Gases Using Membrane Technology,” *Industrial and Engineering Chemistry Research* 2008 47 (5), pp. 1562–1568.
- 21 Li Zhao, Reinhard Menzer, Ernst Rensche, Ludger Blum, Detlef Stolten, “Concepts and investment cost analyses of multi-stage membrane systems used in post-combustion processes,” *Energy Procedia*, Volume 1, Issue 1, Greenhouse Gas Control Technologies 9, Proceedings of the 9<sup>th</sup> International Conference on Greenhouse Gas Control Technologies (GHGT-9), 16–20 November 2008, Washington DC, USA, February 2009, pp. 269–278; Li Zhao, Ernst Rensche, Reinhard Menzer, Ludger Blum, Detlef Stolten, “A parametric study of CO<sub>2</sub>/N<sub>2</sub> gas separation membrane processes for post-combustion capture,” *Journal of Membrane Science*, Volume 325, Issue 1, 15 November 2008, pp. 284–294; Li Zhao, Ernst Rensche, Ludger Blum, Detlef Stolten, “Multi-stage gas separation membrane processes used in post-combustion capture: Energetic and economic analyses,” *Journal of Membrane Science*, Volume 359, Issues 1–2, Membranes and CO<sub>2</sub> Separation, 1 September 2010, pp. 160–172.

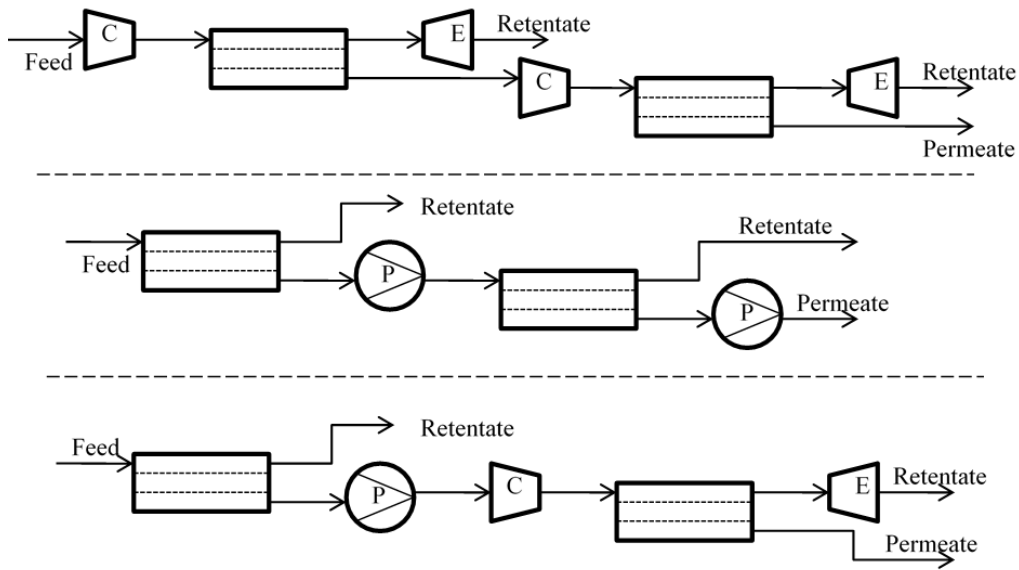


Figure 3-7. Two-Stage Membrane Circuitries: Serial Enricher Concept

In each class, three variations are depicted, which vary only in how the pressure gradient across the membrane stages is applied, whether through upstream compression by a compressor and exhaust to ambient pressure, or by downstream vacuum established by vacuum pump with the upstream at ambient pressure. Usually, the preferred method is to use vacuum pumping on the first stage, in order to avoid the necessity of compressing the whole volume of flue gas at considerable energy penalty, with compression applied to the second stage, which is economical because of the much reduced quantity of gas flow in the second stage. Obviously, a trade-off is present in that using compressors to establish the pressure gradient requires less membrane surface area to accomplish the same degree of gas recovery, and because membranes represent the majority of capital cost of a membrane separation system, higher pressures tend lead to a significant lowering of capital cost.

Calculations show that the serial enricher arrangement is more energy efficient than parallel schemes or other serial schemes. Moreover, the retentate from the second stage of the enricher system is often similar in CO<sub>2</sub> concentration to the original feed to the system, which suggests that the second-stage retentate might be recycled to the beginning of the cycle to maximize system performance and efficiency still further. This “serial enricher” with recycle circuit is depicted in Figure 3-8.

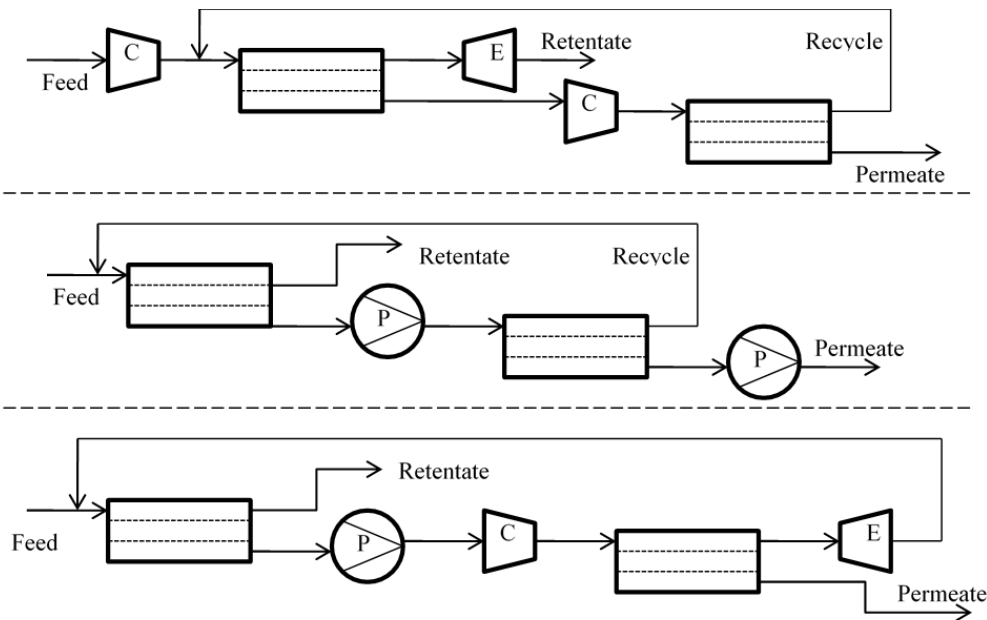


Figure 3-8. Two-Stage Membrane Circuitries: Enricher with Recycle

The latter arrangement has the best performance to cost ratio of all of the above.

### Sweep Gas Utilization

A persistent drawback of the foregoing process arrangements remains in that they all require energy-intensive compression or vacuum pumping to provide the driving force for all of the membrane separation stages. In the case of post-combustion CO<sub>2</sub> capture, MTR proposes a process solution that utilizes combustion air as the sweep gas to generate separation driving force at the sweep module, thereby reducing the overall need for energy-intensive compressors or vacuum pumps. This is depicted in Figure 3-9. Stream 4 is the combustion air sweep; the air enriched in CO<sub>2</sub> (i.e., ≈8% CO<sub>2</sub>, ≈18% O<sub>2</sub>) is utilized as combustion air at the boiler.

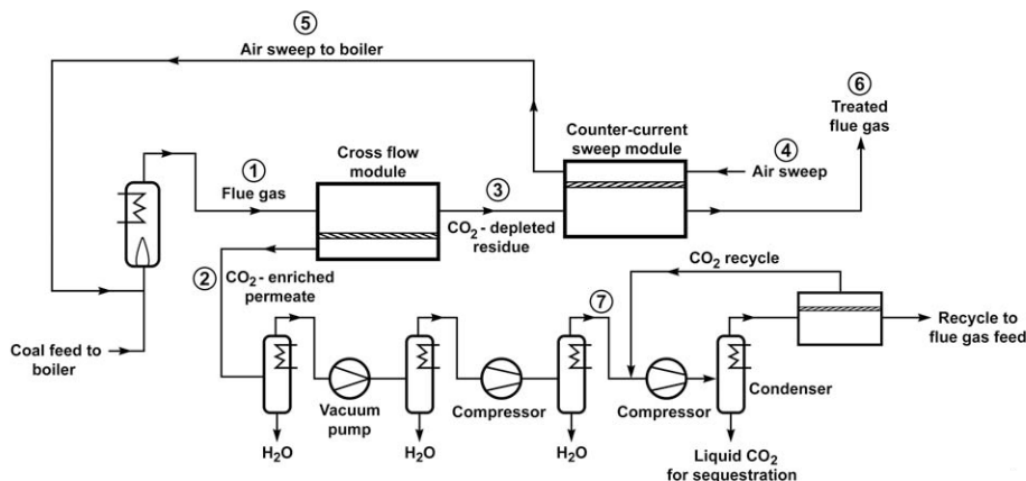


Figure 3-9. MTR Proposed Membrane Process to Capture and Sequester CO<sub>2</sub> in Flue Gas from a Coal-Fired Power Plant<sup>22</sup>

Here, the combustion air sweep generates a CO<sub>2</sub> partial pressure gradient in the second membrane stage, eliminating the need for compressors or vacuum pumps to drive this stage. In this way, the sweep module avoids the energy penalty of compression or vacuum treatment and provides an essentially “free” separation. Additionally, by recycling CO<sub>2</sub> to the boiler via the combustion air sweep loop, the CO<sub>2</sub> concentration in the flue gas exiting the boiler increases from about 13% to approximately 18%. This increases the CO<sub>2</sub> partial pressure driving force for transport in the first membrane stage. Consequently, the membrane area and system cost is reduced.<sup>23</sup> Optimization of process cycles in this way and improved membrane performance in selectivity and permeability should, in combination, result in increasingly efficient and cost-effective membrane-based gas separation technology that will be able to meet challenging DOE goals for carbon capture.

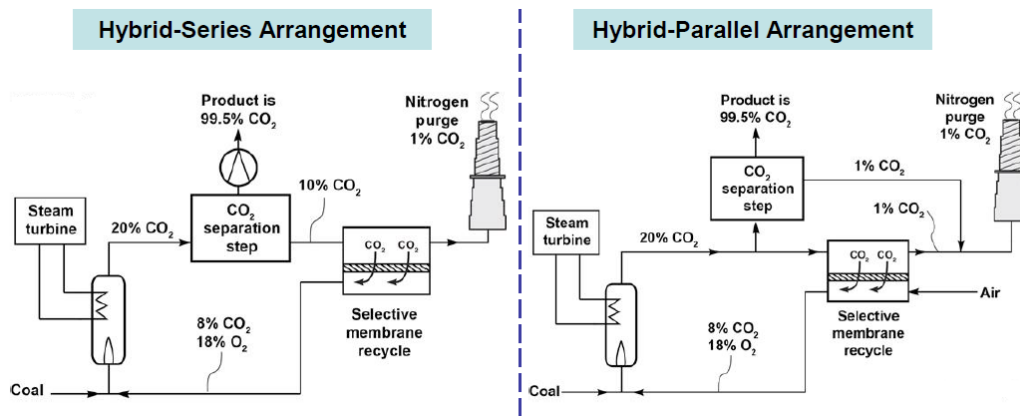
Ohio State University is assuming the same type of two stage configuration with combustion air sweep in their work on novel inorganic/polymer-supported composite membranes (see Table 3-5, fourth row).

### Hybrid Cycles

The possibility of combining solvent or sorbent-based separations with membrane-based processes to further improve energy efficiency and performance has been increasingly evident in R&D in the carbon capture field. The DOE-NETL portfolio reflects this, with a number of concepts involving hybrid process cycles emerging in recent work. For example, MTR is exploring a hybrid cycle which includes the same combustion air sweep-driven membrane stage discussed in the previous section, but with the initial CO<sub>2</sub> separation stage consisting of an absorption column utilizing 5m piperazine solvent (see Table 3-5 first row in post-combustion listings). The CO<sub>2</sub> enriched combustion air results in higher than normal CO<sub>2</sub> concentration in the flue gas, and the amine solvent stage performance can be increased/optimized for it accordingly. MRT is evaluating both hybrid-parallel and hybrid-series process arrangements to explore the opportunities of the concept, as shown in Figure 3-10.

22 “Membrane Process to Sequester CO<sub>2</sub> from Power Plant Flue Gas,” Final Technical Report, Tim Merkel, July 2009, DE-FC26-07NT43085. <http://www.osti.gov/scitech/servlets/purl/1015458-INdTMC/>.

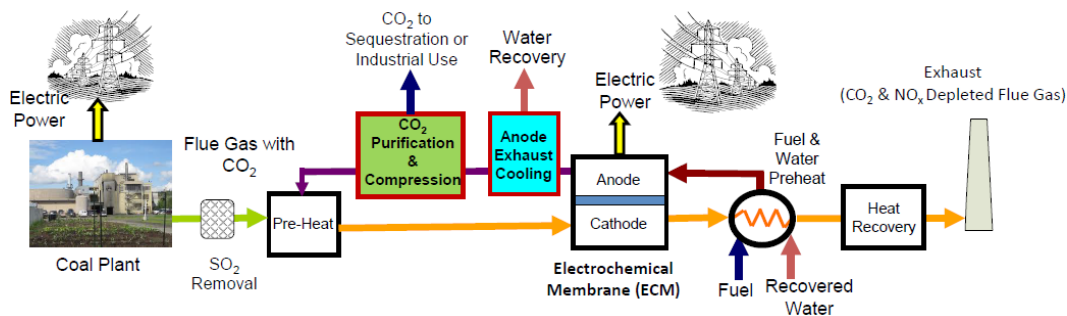
23 Ibid.

Figure 3-10. MTR Hybrid Post-Combustion CO<sub>2</sub> Capture Process Cycles

### Other

GTI is investigating a membrane contactor which utilizes polyether ether ketone (PEEK) hollow fiber membranes in a contactor having flue gas on one side and an amine solvent (MDEA) on the other side (see Table 3-5, second row of post-combustion listings). The solvent efficiently takes up the CO<sub>2</sub> permeate, lowering the CO<sub>2</sub> partial pressure on the permeate side to almost zero, thereby establishing the driving force for CO<sub>2</sub> separation without need of feed side compression or permeate side vacuum. This arrangement should be able to achieve post-combustion capture with >90% CO<sub>2</sub> removal and high CO<sub>2</sub> purity in just one stage, as opposed to most processes which demand at least two stages to attain the required removal and purity. Of course, it does require the regeneration of rich solvent as any solvent-based process (performed in this case in another PEEK contactor operated in reverse mode). This approach combines the advantages of the compactness of a membrane contactor with the high selectivity of a solvent-based absorption process, and is expected to significantly reduce the cost of CO<sub>2</sub> capture relative to the baseline amine-based process.

The considerable diversity of the DOE NETL portfolio in membrane separations is illustrated by the Fuel Cell Energy project, which is examining a concept of CO<sub>2</sub> separation from flue gas using electrochemically driven separation membranes. As shown in Figure 3-11, the process concept is markedly different from conventional membrane process arrangements, consisting of electrochemical membranes within fuel cell modules driven by supplemental fuel (presumably natural gas); the fuel cell modules generate additional electricity in addition to performing CO<sub>2</sub> capture.

Figure 3-11. Fuel Cell Energy Combined Electric Power and CO<sub>2</sub> Separation System Concept<sup>24</sup>

## 3.1.5 COMMERCIAL MEMBRANE-BASED GAS SEPARATION

Currently, gas separation membranes are used industrially for hydrogen separation within ammonia plants (H<sub>2</sub>/N<sub>2</sub> separation) and petrochemical plants (H<sub>2</sub>/hydrocarbons); and for separating nitrogen from air, removing CO<sub>2</sub> and water from natural gas, and recovering organic vapors from air or nitrogen. The most widely used membrane materials for gas separation are polymers. Polymers are attractive because they can be processed into hollow fibers or thin sheets with high surface areas per unit volume. Each membrane unit can contain thousands of fibers. As discussed above, this results in compact, modular membrane units having relatively low costs, even when permeance and selectivity are not extremely high.

24 "Electrochemical Membrane for CO<sub>2</sub> Capture and Power Generation," Hossein Ghezeli-Ayagh, NETL-DOE 2014 Transformational Carbon Capture Technology Workshop, September 23, 2014 Arlington, VA.

The three major providers of membrane technologies for gas separation applications are Air Products and Chemicals, Inc. (APCI), Air Liquide and UOP. The APCI PRISM™ membrane is based on the original Monsanto technology commercialized back in 1980. Air Liquide’s MEDAL™ membrane was developed by a joint venture between DuPont and Air Liquide. The UOP membrane technology is named PolySep™, and also has its roots in technology developed earlier. The relative permeance of these commercial membranes, based on the open literature, is:

Table 3-2. Relative Permeance of Gases in Three Commercial Membranes

	AIR LIQUIDE MEDAL™	APCI PRISM™ MEMBRANE	UOP POLYSEP™
High	H <sub>2</sub> O He H <sub>2</sub> NH <sub>3</sub> CO <sub>2</sub> H <sub>2</sub> S	H <sub>2</sub> O H <sub>2</sub> He H <sub>2</sub>	H <sub>2</sub> H <sub>2</sub> O H <sub>2</sub> S CO <sub>2</sub>
Intermediate	O <sub>2</sub> Ar CO N <sub>2</sub> CH <sub>4</sub>	H <sub>2</sub> S CO	CH <sub>4</sub> O <sub>2</sub>
Low	C <sub>2</sub> H <sub>4</sub> C <sub>3</sub> H <sub>6</sub>	O <sub>2</sub> Ar CO C <sub>2</sub> + CH <sub>4</sub> N <sub>2</sub>	C <sub>2</sub> + N <sub>2</sub>

Profiles of these three technologies are described in Table 3-3.

Table 3-3. Process Profiles for Commercial Polymer Membrane Technologies

	AIR LIQUIDE MEDAL™ (polyaramide)	APCI PRISM™ MEMBRANE (Monsanto technology)	UOP POLYSEP™	GENERIC (from literature)
Feed H <sub>2</sub> Content (wide range)	–	>25%	–	–
(optimal)	–	40–80%	75–90%	–
Feed Temperature, * °F	–	<230	Preheated 20 °F above retentate dewpoint	
LP Steam Cons., lb/M scf Feed	2.0	–	–	–
Pretreatment**	No liquids in feed or retentate; coalescing filter for particulate and entrained liquid removal; must ensure no condensation			
H <sub>2</sub> Recovery (wide range)	80–98%	80–98+%	70–95+%	>85%
(typical)	95+%	90–95%	–	90–95%
(one-stage)	–	70–90%	–	–
(two-stage)	–	<98%	–	–
H <sub>2</sub> Purity (wide range)	<99.9%	80–99+%	70–99%	>70%
(typical)	–	90–95%	90–98%	>90%
H <sub>2</sub> Contaminants (CO and CO <sub>2</sub> )	–	–	–	will be at >ppmv levels
Feed Pressure, psia (wide range)†	–	<2,500	–	–
psia (H <sub>2</sub> purge gas)	<1,741	300–1,850	1,000+	300–2,300
Pressure Drop, psi	Typically small, but may become significant at high recoveries or low permeate pressures			
Pressure Differential, psi	–	<1,650 at 105 °F	–	–
Unit Capacity, M scfd H <sub>2</sub>	–	–	unlimited (modular)	1,000–50,000+
No. of Modules	–	–	3–100+	–
Membrane Life, years	–	>15	–	3–5‡
Reliability (on-stream factor)	–	–	99.8%	99.8%
Unit Turndown/Up	–	30%	30–100+%	30%
Revamp Capacity	–	–	unlimited (modular)	–
No. of Operating Units Worldwide	>60 (c. 1998)	>270 (c. 2004)	>50 (c. 2004)	–

\* Feed heater usually required to maintain constant operating temperature and constant membrane performance.

\*\* Some resistance to water exposure and particulates, H<sub>2</sub>S or aromatics may damage membrane.

† Maximum feed pressure only limited by mechanical design pressure of ANSI flanges on pressure vessel.

‡ Under harsh chemical environment.



**Commercial experience with polymer membranes (hydrogen separation)<sup>25</sup>**

Gases with high permeabilities such as hydrogen enrich the permeate side of the membrane, and gases with lower permeabilities enrich the retentate side of the membrane because of the depletion of components with high permeability. The first fraction of the gas to permeate the membrane consists primarily of the components with the highest permeability. As a larger fraction of the feed gas is allowed to permeate, the relative amount of the components with lower permeability increases in the permeate stream.

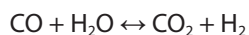
Polymer membranes can be used to process gases containing a wide variation in H<sub>2</sub> content. Feed pretreatment requirements are typically minimal, and are primarily associated with feeding a dry, clean gas to the unit. Since the water and hydrocarbon content of the feed will be increased as hydrogen is removed, it is necessary that the feed gas be heated to above the dew point of the retentate exiting the module to prevent condensation of a liquid phase within the module. Exposure to liquid water or hydrocarbons, particulates and high concentrations of H<sub>2</sub>S may permanently damage the polymer material. Polymers in commercial use are limited to temperatures not much greater than the boiling point of water.

For any given membrane, hydrogen recovery is a strong function of the feed H<sub>2</sub> content and pressure, and product requirements in regards to H<sub>2</sub> purity and delivery pressure. Feed compression or permeate re-compression requirements can add significantly to the cost of a H<sub>2</sub> recovery plant. A doubling of the feed pressure can cut H<sub>2</sub> delivery costs by as much as a fourth. Higher purity hydrogen is associated with lower recovery, with this effect much more dramatic with membrane systems versus competing PSA technology. For a membrane with a H<sub>2</sub> selectivity of 30, a 3% increase in product purity results in a 25% decrease in recovery. Higher H<sub>2</sub> recoveries also require more membrane area. For specified feed composition and system pressure levels, the amount of area required increases exponentially at high hydrogen recovery. For a specific membrane system, the recovery versus purity, is primarily dependent on the ratio of the retentate to permeate pressure and is largely independent of absolute pressure levels. However, area requirements are inversely proportional to the feed pressure. Therefore, compressing the feed gas rather than the permeate, even though the permeate flow is smaller, is often preferable when the objective is to achieve a required pressure ratio.

For properly designed and operated membrane systems, pressure drops are typically small. The pressure differential across the membrane is set by the upstream pressure and the desired H<sub>2</sub> delivery pressure, unless feed compression or permeate re-compression is included. Feed pressures as high as 2,500 psia (170 bar) have been demonstrated. More significantly, cross membrane differentials as high as 1,650 psia (112 bar) can be achieved. However, very high pressure differentials can cause compression of the membrane, detrimentally affecting performance. This effect is temperature dependent, and the maximum allowable pressure differential will be lower than 1,650 psia as the operating temperature approaches the maximum allowable operating temperature for the membrane.

**3.1.6 DEVELOPMENTAL TECHNOLOGY FOR PRE-COMBUSTION MEMBRANE-BASED SEPARATIONS****3.1.6.1 WATER GAS SHIFT MEMBRANE REACTOR**

Conventionally, a water gas shift (WGS) reactor is utilized to maximize the hydrogen content of syngas, following which CO<sub>2</sub> may be captured using standard absorption techniques. This conventional approach involves two separate stages of reaction and CO<sub>2</sub> separation. Realizing that the conventional approach has inherent drawbacks in efficiency, the DOE NETL R&D portfolio includes several projects developing WGS membrane reactors. The concept is based on increasing conversion of the equilibrium WGS reaction:

**Equation 3-21**

by withdrawing one of the products (often H<sub>2</sub>) across membranes in the reactor, causing the reaction to progress further to the right by Le Chatelier's principle. Figure 3-12 illustrates the concept of the membrane reactor. As illustrated, in this configuration syngas undergoing the WGS reaction flows into membrane modules containing hydrogen-selective membranes tubes. Hydrogen perme-

25 MacLean, D.L.; Stookey, D.J.; Metzger, T.R., "Fundamentals of gas permeation," *Hydrocarbon Processing*, pp.47–51, Aug. 1983.  
 Mazur, W.H.; Chan, M.C., "Membranes for Natural Gas Sweetening and CO<sub>2</sub> Enrichment," *Chem. Eng. Prog.*, pp.38–43, Oct. 1984.  
 Hogsett, J.E.; Mazur, W.H., "Estimate membrane system area," *Hydrocarbon Processing*, pp.52–54, Aug., 1983.  
 Whysall, M.; Picioccio, K.W., "Selection and revamp of Hydrogen Purification Processes," *1999 AIChE Spring Meeting*, Houston, TX, March 13–18, 1999.  
 Air Products Product Brochure, Advanced Prism® Membrane Systems for Cost Effective Gas Separations. [www.airproducts.com](http://www.airproducts.com).  
 Picioccio, K.; Reyes, E., "Breaking the Hydrogen Barrier with PSA Revamps—Increasing Hydrogen Production of PSA Units," UOP webpage, 2000.  
 Haggin, J., "Membrane Technology Developments Aim at Variety of Applications," *Chem. and Eng. News*, pp.25–26, April 4, 1994.

ates into the tubes and is swept away by nitrogen on the bore side. The resulting H<sub>2</sub>/N<sub>2</sub> mixture would be suitable for firing in a gas turbine for electricity generation. As hydrogen is withdrawn, the syngas increases greatly in CO<sub>2</sub> content. In this way a significant measure of carbon capture is effected within the reactor itself. (Some WGS membrane reactors might utilize CO<sub>2</sub> selective membranes in which case the separation still occurs, but with a different process flow configuration that would use steam sweep of the CO<sub>2</sub> instead of N<sub>2</sub> sweep of the hydrogen). Overall, this concept results in process intensification with its inherent reduction of energy intensity and improved separation efficiency.

The challenges of the WGS membrane reactor come from the requirement for suitable hydrogen or CO<sub>2</sub> selectivity as the case may be, permeability and durability in the reactor environment, and reasonable membrane cost. The NETL R&D work has investigated a wide range of membranes including ceramic-carbonate dual phase membranes, carbon molecular sieve membranes, Pd alloy membranes, and exfoliated hydrogen-selective zeolite membranes for the WGS reactor application.

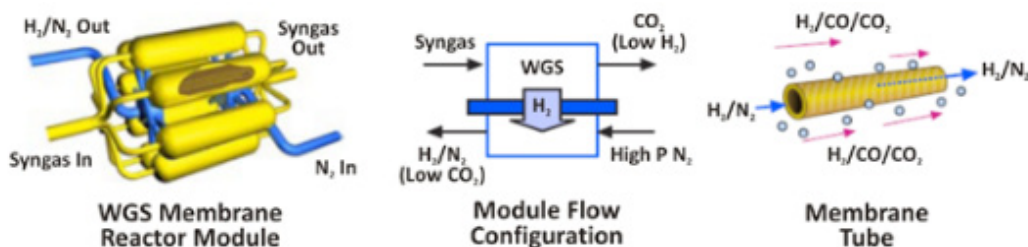


Figure 3-12. Water Gas Shift Membrane Reactor Concept<sup>26</sup>

### 3.1.6.2 TYPES OF MEMBRANES

Membranes possibly suitable for separation of CO<sub>2</sub> (or hydrogen separation from CO<sub>2</sub>-H<sub>2</sub> mixtures) fall into several categories:

- Polymeric membranes (e.g., polyethyleneoxide, polydimethylsiloxane, sulphonated polyimides)
- Ceramics (aminosilicate structures)
- Supported liquid membranes (facilitated transport)
- Metallic membranes (e.g., palladium, palladium alloys for hydrogen separation)
- Other (zeolites, etc.)

Conventional polymers have often been used for gas separations, though commercially available polymer membranes and module manufacture/sealing technologies are limited to about 150 °C operating temperatures. (Higher operating temperatures of >200 °C typical of syngas represent a challenge for this class of membranes). Many of the projects in the NETL portfolio are investigating processes and membrane configurations using polymer membranes of various types. Some are unspecified/proprietary; others are known such as polyether ether ketone (PEEK)-based hollow fiber membranes in both pre-combustion and post-combustion application.

Ceramic materials are interesting, particularly in the context of gas separation where they might conceivably be employed in high temperature regions (such as 350 °C or higher applicable to syngas or hot flue gas). For example, one recent project in the NETL portfolio is utilizing ceramic-molten carbonate dual phase membranes for CO<sub>2</sub> capture within a WGS membrane reactor.

Considerable attention to supported liquid membranes for separation of CO<sub>2</sub> can be found in the literature. Here, the chemistry of the membrane is geared toward facilitated transport of CO<sub>2</sub>, i.e., amine constituents of the membrane can induce transport of CO<sub>2</sub> at higher rates than seen in conventional polymeric materials. Some researchers are optimistic about the potential for such membranes in gas separation systems, specifically room temperature ionic liquid supported membranes,<sup>27</sup> while others believe that in general, stability problems would limit the use of supported liquid membranes in practical gas separation processes.<sup>28</sup> Certain projects in the NETL portfolio have included such membranes: in one a carbonic anhydrase enzyme-catalyzed, contained liquid membrane has

26 <http://energy.gov/sites/prod/files/2013/11/f4/water-gas-shift.pdf>.

27 Scovazzo, P., "Determination of the upper limits, benchmarks, and critical properties for gas separations using stabilized room temperature ionic liquid membranes (SILMs) for the purpose of guiding future research" *Journal of Membrane Science*, 343(1–2), **2009**, 199–211; Scovazzo, P. et al., "Long-term, continuous mixed-gas dry fed CO<sub>2</sub>/CH<sub>4</sub> and CO<sub>2</sub>/N<sub>2</sub> separation performance and selectivities for room temperature ionic liquid membranes," *Journal of Membrane Science*, 327(1–2), **2009**, 41–48.

28 Hong, S.U. et al., "Polymer-ionic liquid gels for enhanced gas transport," *Chemical Communications*, (46), **2009**, 7227–7229.

been investigated, and others involve use of amine selective layers on polymeric supports.

Metallic palladium membranes have almost infinite selectivity for hydrogen and high permeance and are suitable for operation at high temperature; they have figured in several WGS applications and syngas cleanup in the NETL portfolio.

Zeolites are microporous crystalline aluminosilicates with defined nanopore sizes, occurring naturally as minerals, and also represented by a much larger number of synthetic zeolites that have been developed for use as sorbents and catalysts. Zeolites can also be deposited as a thin layer on porous substrates, enabling their use as a selective layer in membranes. To illustrate, the zeolite sodalite exhibits pore sizes of 0.29 nm, which lies in the range of the kinetic molecule diameter of hydrogen, while CO<sub>2</sub> should be too large to pass through the small pores of the sodalite framework. Therefore sodalite membranes are candidates for molecular sieving to separate hydrogen from CO<sub>2</sub>. Zeolite membranes are cheaper than palladium or platinum membranes, while still having the latter's useful property of high specific gas selectivity. On the other hand, they are more expensive than polymeric membranes, yet can have much higher thermal and hydrothermal stability than polymeric membranes, essential for higher temperature applications such as hydrogen-CO<sub>2</sub> separations in presence of water vapor at warm syngas temperatures.<sup>29</sup>

### 3.2 DOE/NETL MEMBRANE-BASED CO<sub>2</sub> CAPTURE PORTFOLIO

The Carbon Capture Program has supported research and development in membrane-based CO<sub>2</sub> capture approaches for both pre-combustion (mainly H<sub>2</sub>-CO<sub>2</sub> separations) and post-combustion (N<sub>2</sub>-CO<sub>2</sub> separations). Pressures, temperatures, and gas composition widely vary between pre-combustion and post-combustion applications, resulting in distinct R&D portfolios for those groupings. Membranes of widely differing materials types have been suggested for development in conjunction with highly varied proposed process configurations. Earlier in the DOE/NETL program, membrane materials were unbounded, but because of excessive materials cost, work on conventional Pd-based membranes has been almost completely discontinued.

Recent pre-combustion projects are referenced in Table 3-4; post-combustion projects are listed in Table 3-5.

Table 3-4. DOE/NETL Membrane-Based Pre-Combustion CO<sub>2</sub> Capture Projects Portfolio

PRE-COMBUSTION MEMBRANE PROJECTS	PERMEANCE (H <sub>2</sub> )	SELECTIVITY (H <sub>2</sub> /CO <sub>2</sub> )	CONDITIONS	TYPE AND PROCESS IMPLEMENTATION
Techverse, Inc. Integrated Membrane Reactor for Pre-Combustion CO <sub>2</sub> Capture	Testing	Testing	300 psig, 450 °C	Ternary Pd-alloy composite membranes in a WGS membrane reactor combining WGS reaction with carbon dioxide separation; testing on real syngas from SRI gasifier; single tube study
Media and Process Technology Inc. Robust and Energy Efficient Dual-Stage Membrane-Based Process for Enhanced Carbon Dioxide Recovery	3,700	>300	20 psig, 350 °C	Hydrogen selective carbon molecular sieve membranes and novel palladium (Pd) and Pd-alloy membranes for efficient residual H <sub>2</sub> recovery, in WGS membrane reactor (tube bundle module); testing on real syngas at NCCC
SRI International Development of a Pre-Combustion Carbon Dioxide Capture Process Using High Temperature Polybenzimidazole Hollow-Fiber Membrane; Fabrication and Scale-Up of Polybenzimidazole-Based Membrane System for Pre-combustion Capture of Carbon Dioxide	80–85	30–50	450 psig, 225 °C	Polybenzimidazole (PBI) hollow-fiber membrane modules, post-WGS
Los Alamos National Laboratory Polymer-Based Carbon Dioxide Capture Membrane Systems	120	22–24	200 psia, 250 °C	Polybenzimidazole (PBI) hollow-fiber membrane modules, post-WGS (mixed gas measurement basis)

29 Christiane Günther, Hannes Richter, Ingolf Voigt, "Zeolite Membranes for Hydrogen and Water Separation under Harsh Conditions," *Chemical Engineering Transactions*, **32** (2013), pp. 1963–1968.

Table 3-4. DOE/NETL Membrane-Based Pre-Combustion CO<sub>2</sub> Capture Projects Portfolio

PRE-COMBUSTION MEMBRANE PROJECTS	PERMEANCE (H <sub>2</sub> )	SELECTIVITY (H <sub>2</sub> /CO <sub>2</sub> )	CONDITIONS	TYPE AND PROCESS IMPLEMENTATION
University of North Dakota Efficient Regeneration of Physical and Chemical Solvents for CO <sub>2</sub> Capture	Variable	Variable	80 °C	Porous membrane contactors were studied as an alternative to conventional strippers for CO <sub>2</sub> recovery from aqueous MEA solutions. Commercially available membranes were evaluated, including polytetrafluoroethylene and polypropylene membranes, and polydimethyl-siloxane and polyvinyl-alcohol based membranes.
ORD/University of Pittsburgh Novel Membranes for CO <sub>2</sub> Removal	10x greater convect. @75 °C	15	260–300 °C	Ionic liquid supported on commercial and fabricated polymer membranes; CO <sub>2</sub> selectivity increased by ionic liquid, hollow fiber assembly
Pall Corporation Designing and Validating Ternary Pd Alloys for Optimum Sulfur/Carbon Resistance	3,200–5,400	500–55,000 (H <sub>2</sub> /N <sub>2</sub> )	≈160 psig, 400–500 °C	Chemically-resistant ternary Pd alloys; combinatorial evaluation of many alloy compositions; utilization in contaminated syngas streams
Membrane Technology Research Novel Polymer Membrane Process for Pre-combustion CO <sub>2</sub> Capture from Coal-Fired Syngas	350	>20	50 psig, 135 °C	High-temperature-stable polymer membranes (Proteus) in spiral-wound modules with sweep gas
Arizona State University Pre-Combustion Carbon Dioxide Capture by a New Dual-Phase Ceramic Carbonate Membrane Reactor	150–1,500 (CO <sub>2</sub> )	Up to 3,000 (CO <sub>2</sub> /H <sub>2</sub> )	500–900 °C, 10–40 atm	Ceramic-molten carbonate dual phase membranes in CO <sub>2</sub> permeable WGS membrane reactor
University of Minnesota Hydrogen Selective Exfoliated Zeolite Membranes	≈300	30	10 bar, 350 °C	Exfoliated hydrogen-selective zeolite membranes implemented in WGS membrane reactor
Gas Technology Institute Pre-Combustion Carbon Capture by a Nanoporous, Superhydrophobic Membrane Contactor Process	Up to 2,000 (CO <sub>2</sub> )	Not specified	100 °F, 500–750 psig	Superhydrophobic polyether ether ketone (PEEK) hollow fiber membrane with optimal pore size and surface chemistry

Table 3-5. DOE/NETL Membrane-Based Post-Combustion CO<sub>2</sub> Capture Projects Portfolio

POST-COMBUSTION MEMBRANE PROJECTS	PERMEANCE (CO <sub>2</sub> )	SELECTIVITY (CO <sub>2</sub> /N <sub>2</sub> )	CONDITIONS	TYPE AND PROCESS IMPLEMENTATION
Membrane Technology and Research, Inc. Bench-Scale Development of a Hybrid Membrane-Absorption CO <sub>2</sub> Capture Process	1,500 GPU	35–40	Flue gas conditions	Hybrid process cycle: first stage solvent-based with UT Austin's piperazine (PZ) solvent and advanced, high-temperature and pressure regeneration technology, second-stage membrane sweep using MTR's Polaris™ membrane
Gas Technology Institute Pilot Test of a Nanoporous, Super-Hydrophobic Membrane Contactor Process for Post-Combustion Carbon Dioxide (CO <sub>2</sub> ) Capture; Hybrid Membrane/Absorption Process for Post-Combustion CO <sub>2</sub> Capture	>2,000 GPU	>1,000 (value dependent on solvent)	40–80 °C and 1–5 psig (adsorber); 120 °C and 1–50 psig desorber	Pilot-scale CO <sub>2</sub> capture hollow fiber contactor (HFC) system using PEEK hollow fibers in a membrane contactor; flue gas passes through one side of the PEEK HFC, while a CO <sub>2</sub> selective amine solvent is on the other side taking up/reacting with the permeate CO <sub>2</sub>
American Air Liquide, Inc. CO <sub>2</sub> Capture by Cold Membrane Operation with Actual Power Plant Flue Gas; CO <sub>2</sub> Capture by Sub-Ambient Membrane Operation	PI-1: ≈200 GPU PI-2: ≈1,000 GPU	70–90	<-10 °C	Sub-ambient temperature operation of a hollow fiber membrane separator (PI-1 and PI-2, which are proprietary polymer types) coupled with cryogenic processing technology (CO <sub>2</sub> condensed out) and limited sweep; membranes have high CO <sub>2</sub> permeance and increased CO <sub>2</sub> / N <sub>2</sub> selectivity at low temperature
Ohio State University Novel Inorganic/Polymer Composite Membranes	1,100 GPU	140	57 °C	Membranes with selective (amine) cover layer plus selective inorganic layer (zeolite), embedded on a polymer structure enabling continuous manufacturing process; incorporated in spiral-wound modules; two-stage process (vacuum first stage/second stage using combustion air sweep <sup>30</sup> )
GE Global Research Bench-Scale High-Performance Thin Film Composite Hollow Fiber Membranes for Post-combustion Carbon Dioxide Capture	<50 GPU (stable) >1,000 GPU (poor stability)	>30	Realistic flue gas conditions	Thin film phosphazene polymer on highly engineered porous support composite hollow fiber membranes
FuelCell Energy, Inc. Electrochemical Membranes for Carbon Dioxide Capture and Power Generation	>120 cc/m <sup>2</sup> /s (CO <sub>2</sub> flux)	∞	550–650 °C	Electrochemical membrane consisting of ceramic-based layers filled with carbonate salts in fuel cells; electrochemical driving force instead of pressure differential; incorporated in plant cycle including additional power generation from the fuel cells
Membrane Technology and Research, Inc. Low-Pressure Membrane Contactors for CO <sub>2</sub> Capture	1,500 GPU	35–40	Flue gas conditions	New type of membrane contactor allowing countercurrent or cross-flow sweep with minimal pressure drop and high surface area (plate and frame module, 500 m <sup>2</sup> ) compared to conventional spiral-wound modules; Polaris™ polymeric membrane
Membrane Technology and Research, Inc. Slipstream Testing of a Membrane CO <sub>2</sub> Capture Process for Existing Coal-Fired Power Plant; Membrane Process to Capture CO <sub>2</sub> from Power Plant Flue Gas	1,500 GPU	35–40	Flue gas conditions	Second-generation Polaris™ polymeric membrane (specifically developed for CO <sub>2</sub> separation from syngas); MTR's two-stage process utilizing combustion air sweep; 20 TPD unit test at NCCC
RTI International CO <sub>2</sub> Capture Membrane Process for Power Plant Flue Gas	470 GPU 380 GPU	24 40–50	60 °C 65 °C	Polycarbonate-based polymers membranes; polyvinylidene fluoride (PVDF)-based polymer membranes in hollow fiber modules



Table 3-5. DOE/NETL Membrane-Based Post-Combustion CO<sub>2</sub> Capture Projects Portfolio

POST-COMBUSTION MEMBRANE PROJECTS	PERMEANCE (CO <sub>2</sub> )	SELECTIVITY (CO <sub>2</sub> /N <sub>2</sub> )	CONDITIONS	TYPE AND PROCESS IMPLEMENTATION
University of New Mexico  Novel Dual Functional Membrane for Controlling Carbon Dioxide Emissions From Fossil-Fueled Power Plants	657 GPU	40	55 °C	Amine-modified membrane prepared by a sol-gel dip-coating process for depositing a microporous amino-silicate membrane on porous tubular Membralox-type commercial ceramic supports. Results in microporous inorganic siliceous matrix, with amine functional groups physically immobilized or covalently bonded on the membrane pore walls, enhancing surface diffusion of CO <sub>2</sub> on the pore walls and blocking other gases, enhancing selectivity.
Carbozyme, Inc.  Development of Biomimetic Membrane for Near-Zero PC Power Plant Emissions; Biomimetic Membrane for CO <sub>2</sub> Capture from Flue Gas	18.9 GPU	693	23 °C	Carbonic anhydrase enzyme-catalyzed, contained liquid membrane (CLM) permeator that selectively extracts CO <sub>2</sub> from mixed gas streams; electroalytic CO <sub>2</sub> absorber and stripper using ANL resin wafer technology, relying on a pH shift as a means of capture and of release of CO <sub>2</sub> .

### 3.3 ADVANCES AND FUTURE WORK

The cost of electricity and cost for capturing unit quantities of CO<sub>2</sub> has improved significantly under the DOE NETL Carbon Capture program. Currently DOE-funded membrane technologies have improved performance in terms of higher permeances and selectivities), increasingly compact membrane module configurations, optimized process configurations taking best advantage of pressure differentials via pressurization, vacuum, sweep, etc., and improving manufacturing techniques which result in increasingly cost-effective membranes.

#### 3.3.1 SUMMARY OF ADVANCES

When considering solvent-based CO<sub>2</sub> capture technologies, increasing reduction of the energy penalty incurred per ton of CO<sub>2</sub> captured is a meaningful parameter in gauging the advance of technological capability.<sup>31</sup> However, the same parameter is not useful in assessing membrane-based technologies because multiple factors of (1) membrane cost, (2) membrane performance in terms of separation factor and flux, (3) energy penalty to operate the membrane system, and (4) process configuration all vary significantly from one membrane system implementation to the other, often with interdependencies, and taken together determine the ultimate increase in COE for CO<sub>2</sub> capture. Indeed, in some envisioned configurations it is possible that membrane cost would dominate the economics of the CO<sub>2</sub> capture process while energy penalty is only a minor contributing factor, considering that some configurations greatly reduce energy penalty by using sweep gas. Also, excellently performing membranes may reduce required membrane areas but may be more expensive to manufacture than poorer performing membranes, so it is not inconceivable that worse-performing membranes may be less expensive overall per unit of capture. Therefore, ranking performance simply on membrane parameters such as selectivity and permeability is also not conclusive. Two parameters that do provide some useful basis of comparison are the COE (typically in units of \$/MWh) with capture compared to a baseline capture system (standard amine-based capture) and unit cost of captured CO<sub>2</sub> (typically in \$/ton captured).

Figure 3-13 depicts these parameters for post-combustion CO<sub>2</sub> capture projects in the NETL portfolio in recent years. The trends from higher to lower COE and cost per ton of CO<sub>2</sub> are readily apparent from earlier to latter projects, showing significant progress in NETL-supported R&D membrane-based capture technology.

30 Same as basic MTR scheme.

31 Often the process equipment involved in the solvent-based capture process (columns, regenerators, etc.) is the same no matter what the solvent process used, meaning that energy penalty reductions are the only significant route to increasing performance/cost effectiveness.



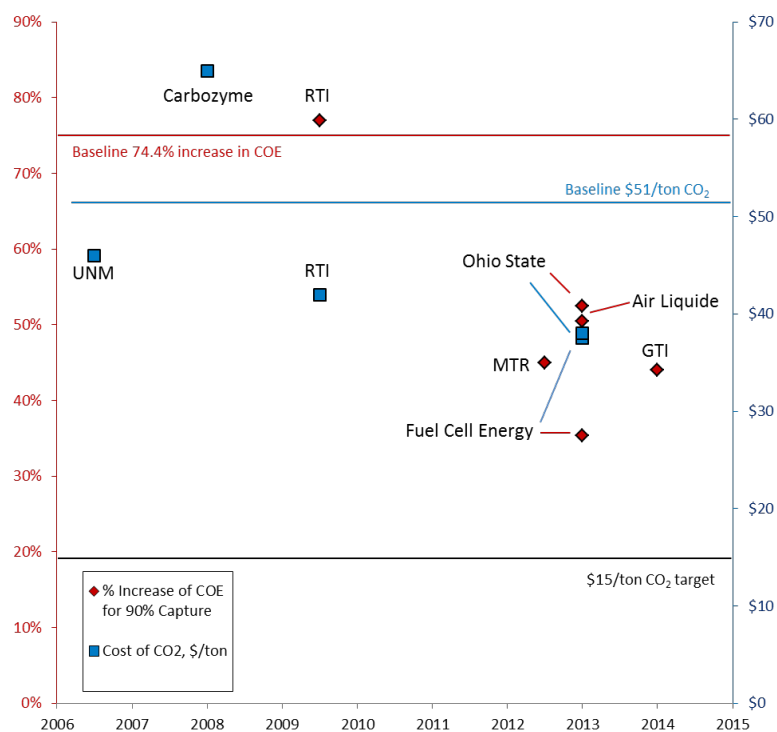
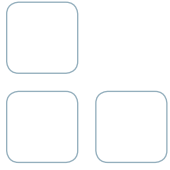


Figure 3-13. Progress in Reducing the Cost of Electricity and Cost of CO<sub>2</sub> Capture for Membrane-Based CO<sub>2</sub> Capture by DOE/NETL Funded Projects

### 3.3.2 KEY PARAMETERS TO BE EVALUATED MOVING FORWARD

Key parameters to be evaluated in the future include:

- **Membrane performance under realistic conditions:** Prior work has already begun to include evaluation of membrane stability in actual syngas streams (pre-combustion capture applications) and humid flue gas streams (post-combustion capture), but ongoing work must lead to scaled-up, viable operation under realistic operating conditions. More stable membranes may have lower capacities spelling higher capital costs for required membrane area and associated process equipment. Compression equipment to establish pressure differentials or vacuums are capital-intensive pieces of equipment in a CO<sub>2</sub> capture plant, needing to be optimized in relation to membrane costs and performance in overall process cycles.
- **Costs of advanced membranes:** Some of the advanced or developmental membranes considered in the DOE NETL portfolio are novel and materials costs tend to be significantly higher than those associated with conventional membranes, partly because they are first-of-a-kind technologies. Advances in reducing the costs of feedstocks are needed, along with lower production process costs through improved synthesis, economies of scale, etc. Prices for material for some membranes (e.g., those incorporating palladium alloys) cannot be controlled, but improved synthesis to minimize required amounts of high-value materials should be sought.
- **Operability concerns:** These are fairly limited in the case of membrane-based systems but issues such as membrane degradation remain and must be considered.



# CHAPTER 4:

# CO<sub>2</sub> COMPRESSION



## 4.1 COMPRESSION OF CAPTURED CO<sub>2</sub>

CO<sub>2</sub> captured from coal flue gas or synthesis gas must be compressed to transport it via pipeline for geologic storage, enhanced oil recovery, or CO<sub>2</sub> utilization. Compression represents a significant parasitic load in addition to the energy requirement for separating CO<sub>2</sub> from flue gas. For example, compressing CO<sub>2</sub> captured from a supercritical pulverized coal plant (capturing 90% CO<sub>2</sub> and generating 550 MW net power) consumes 45 MW.

The compression of CO<sub>2</sub> is challenging because of the high volumetric flow rate of gas (ca. 109,700 actual cubic foot/minute [acfm]) for a 550 MW supercritical pulverized coal-fired power plant,<sup>1</sup> high pressure ratio (≈100:1), large variations in the physical properties of CO<sub>2</sub> in the region of its critical temperature and pressure conditions. For example, the data in Figure 4-1 indicates that compressing CO<sub>2</sub> from a supercritical pulverized coal power plant would require two parallel multi-stage centrifugal compressor trains.

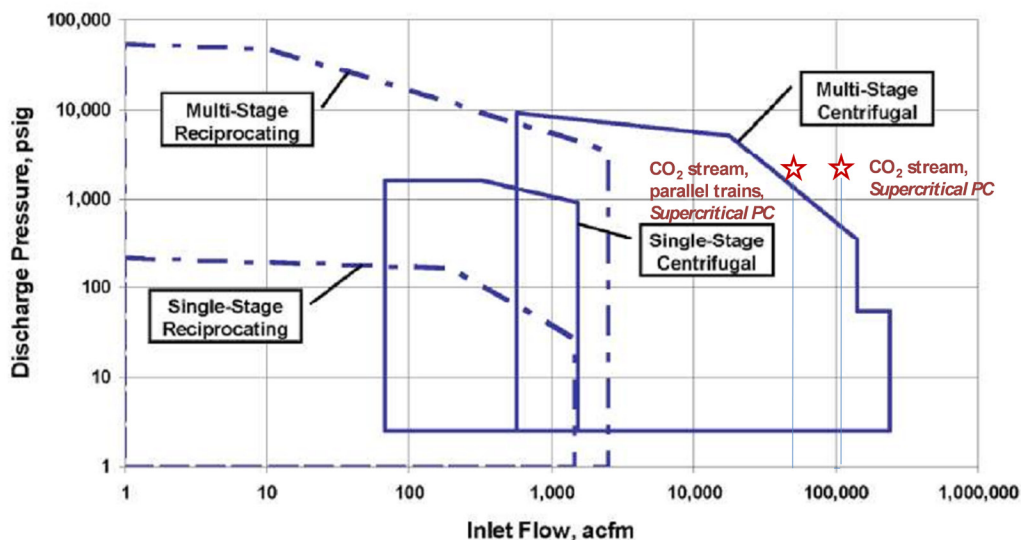


Figure 4-1. CO<sub>2</sub> Compressor Coverage Chart for a Range of Discharge Pressure and Inlet Flow

Showing the typical discharge pressure and inlet volumetric flow rate of CO<sub>2</sub> captured from supercritical pulverized coal-fired power plant. Source: Gallick et al., 2006.<sup>2</sup>

In this context, lowering the cost of capture (and the cost of electricity) requires the development of advanced compression technologies which can significantly lower the capital and operational costs.

## 4.2 COMPRESSION WORK FUNDAMENTALS

### 4.2.1 COMPRESSION WORK

The reversible work for compressing a fluid in a closed system without flow is given by  $W = \int_{V_s}^{V_d} P dV$ ,<sup>3</sup> where P is the pressure and V denotes the volume. For open systems, where fluid flows in and out of a control volume, the reversible work for compression also needs to account for the flow work, and is expressed as  $W_{reversible} = \int_{P_s}^{P_d} V dP$ .<sup>4</sup> For a compressible fluid, volume varies significantly with pressure. Adiabatic compression, where the fluid does not lose heat to its surroundings, and isothermal compression, where the fluid is in thermal equilibrium with its surroundings, represent two ends of the spectrum in gas compression. The work involved in isothermal compression is lower because the gas temperature between the inlet and the outlet of the compressor does not change, and the work being performed on the system (i.e., change in enthalpy) is not lost as the increase in the sensible heat of the gas. In a reversible adiabatic (isentropic) compression process, the entropy of the fluid being compressed does not change between

1 Black, J. Cost and performance baseline for fossil energy plants—Volume 1: Bituminous coal and natural gas to electricity. Revision 2, November 2010. DOE/NETL-2010/1397.

2 Gallick, P., Phillippi, G., Williams, B.F., What's correct for my application—A centrifugal or reciprocating compressor? In Proceedings of the Thirty-Fifth Turbomachinery Symposium, pp. 113–122, (2006). Note that the chart was developed for selecting compressors for natural gas service and is not to be used to gauge the exact boundaries of applicability for CO<sub>2</sub> service.

3 A discussion of reversible work and actual work is provided in Appendix 7.1

4 See Appendix 7.1 and Equation 13.

the inlet and the outlet. For an ideal gas undergoing an adiabatic compression,  $PV^\gamma = \text{constant}$ , where  $\gamma = C_p/C_v$  is the ratio of specific heats at constant pressure and constant volume respectively.

Multi-stage centrifugal compressors more generally employ polytropic processes, which are defined by the following relation:  $PV^n = \text{constant}$ , where  $n$  is termed the polytropic exponent. The polytropic exponent  $n$  is a function of the polytropic efficiency ( $\eta_p$ ) and gas properties. A polytropic process is a path for which the ratio of reversible work input to the enthalpy rise is constant.<sup>2</sup> A polytropic process is equivalent to a succession of an infinite number of isentropic (constant entropy) compression steps, each followed by an isobaric (constant pressure) heat addition. This reversible heat addition is such that it would generate the same temperature increase as the irreversible losses in the real process.<sup>5</sup> The polytropic efficiency is established by the manufacturer and is a function of the capacity at the inlet of the compressor.<sup>6</sup> For an ideal gas,  $\eta_p$  is related to the polytropic exponent and the ratio of specific heats ( $\gamma$ ) as:

$$\eta_p \cdot \frac{(n - 1)}{n} = \frac{(\gamma - 1)}{\gamma}$$

Equation 4-1

If  $n$  is known, the work for compressing an ideal gas in a polytropic process can be estimated by integrating  $VdP$  from  $P_s$  to  $P_d$  and is represented as:

$$\begin{aligned} W^{ideal\ gas} &= H_R^{ideal\ gas} = \frac{H_p^{ideal\ gas}}{\eta_p} \\ &= \left[ \frac{8.314}{MolWt} \right] \left[ \frac{n}{n - 1} \right] \frac{T_s}{\eta_p} \left[ \left( \frac{P_d}{P_s} \right)^{\frac{n-1}{n}} - 1 \right] [=] \frac{kJ}{kg} \end{aligned}$$

Equation 4-2

where  $H_p^{ideal\ gas}$ ,  $H_R^{ideal\ gas}$ , MolWt, and  $T_s$  refer to the polytropic head required to compress the ideal gas, actual (effective) head to compress ideal gas, gas molecular weight and temperature at the inlet of the compressor respectively. At high pressures, the ideal gas law,  $PV = RT$  (for one mole of gas) is no longer valid because molecules interact strongly with one another. To account for this deviation from ideal gas behavior, the ideal gas polytropic work can be modified using the compressibility factor.

$$\begin{aligned} W^{real\ gas} &= H_R^{real\ gas} = \frac{H_p^{real\ gas}}{\eta_p} \\ &\approx \left[ \frac{8.314}{MolWt} \right] \left[ \frac{n}{n - 1} \right] \frac{T_s Z_{avg}}{\eta_p} \left[ \left( \frac{P_d}{P_s} \right)^{\frac{n-1}{n}} - 1 \right] [=] \frac{kJ}{kg} \end{aligned}$$

Equation 4-3

In Equation 4-3,  $Z_{avg}$  ( $Z = Pv/RT$ ) represents the average of the gas compressibility at the suction and discharge conditions and requires gas discharge temperature. Note that  $v$  represents the volume occupied by a mole of gas (molar volume).  $H_p^{real\ gas}$  represents the polytropic head required to compress the gas, and  $H_R^{real\ gas}$  is the effective head required to compress the real gas.

The gas discharge temperature for a polytropic process is related to the pressure ratio as:

5 Rasumussen, P.C., Kurz, R. Centrifugal compressor applications—Upstream and downstream. In *Proceedings of the Thirty-Eighth Turbomachinery Symposium*, pp. 169–186, (2009).

6 Mohitpour, M., Golshan, H. and Murray, A. Gas compression and gas coolers. In *Pipeline design and construction: A practical approach*, pp. 129–226 (ASME, 2007).

$$\frac{Z_d T_d}{Z_s T_s} = \left(\frac{P_d}{P_s}\right)^{\frac{n-1}{n}}, \text{ if we assume that } Z_d \approx Z_s, \frac{T_d}{T_s} = \left(\frac{P_d}{P_s}\right)^{\frac{n-1}{n}}$$

Equation 4-4

In general, the polytropic exponent can be calculated from:

$$n = \frac{\ln\left(\frac{P_d}{P_s}\right)}{\ln\left(\frac{v_s}{v_d}\right)} = \frac{\ln\left(\frac{P_d}{P_s}\right)}{\ln\left(\frac{Z_s T_s P_d}{Z_d T_d P_s}\right)}$$

Equation 4-5

Because work is a path-dependent function, its value is affected by both the start- and end-points and also the compression path, which is determined by the polytropic exponent  $n$ . In a typical compression path, variations in the polytropic exponent  $n$  could change the calculated work. Schultz developed a correction factor for isentropic compression, assumed to be directly applicable to polytropic compression processes<sup>7</sup> (discussed in Appendix 7.3).

The polytropic exponent varies with the pressure and temperature of the gas and compression work calculations need to account for changes in the value of  $n$ . A study on the compression of pure CO<sub>2</sub> found that the polytropic exponent was practically unchanged for pressures less than the critical pressure ( $P_c$ , 1,069 psia) ( $P < P_c$ ).<sup>8</sup> Further, within the dense-phase region, at  $P > P_c$ ,  $T > 1.65T_c$  (critical temperature) (or  $T > 444$  °F), the exponent is relatively constant. However, at conditions where the pressure is above the critical pressure and the temperature exceeds 1.65 times the critical temperature [ $P > P_c$  and  $T < 1.65T_c$  (i.e.,  $T < 444$  °F for CO<sub>2</sub>)], the polytropic exponent varied significantly, from approximately 1.8 to 4. Because all three regions [i.e.,  $P < P_c$ ;  $P > P_c$ ,  $T < 1.65T_c$ ;  $P > P_c$ ,  $T > 1.65T_c$ ] are relevant for intercooled CO<sub>2</sub> compression (intercooler temperature at 70 °F, or  $1.15T_c$ ,  $P_s = 23.5$  psia [ $0.02P_c$ ],  $P_d = 2,215$  psia [ $2.07P_c$ ]), it is reasonable to expect that work calculations which assume a constant value of  $n$  would result in discrepancies, especially at pressures exceeding the critical pressure ( $P > P_c$ ).

## 4.2.2 CONVENTIONAL CO<sub>2</sub> COMPRESSION

Figure 4-2 represents the isentropic and isothermal compression paths on a pressure-enthalpy diagram. The initial temperature and pressure and final pressure in Figure 4-2 correspond to those for CO<sub>2</sub> compression for Case 12 of the DOE/NETL bituminous coal baseline (2010) report.<sup>1</sup>

Several methods to calculate stage outlet temperatures and head were evaluated. They included using the polytropic equation for an ideal gas, the Schultz polytropic procedure and an equation-of-state (EOS)-based approach to calculate the area under the V-P curve. Details of the calculations are provided in the Appendix. Results shown in Table 4-1 indicate that the use of an EOS-based integration approach (Prode), or Schultz polytropic procedure with a high-fidelity EOS led to more accurate outlet temperatures and compression work values compared to ideal gas equations for polytropic compression without the Schultz correction factor.<sup>9</sup>

Because the critical temperature of CO<sub>2</sub> is 87.76 °F, isothermal compression at 70 °F would result in a crossover to the vapor-liquid region before compression to the dense-phase region. Figure 4-1 also indicates that the work for isentropic compression would be higher than that for isothermal compression because the volume of the gas changes significantly in the former case. However, it is not realistic to compress a gas isothermally because real compression processes always have losses resulting in an increase of temperature (or entropy). Further, a comparison of the enthalpy after the first stage of the polytropic process and the isentropic process indicates that for the inlet pressure, temperature and discharge pressure, the work for the isentropic path is lower.

7 Schultz, J. M. The polytropic analysis of centrifugal compressors. *J. Eng. Gas Turbines Power* 84, 69–82 (1962).

8 Sandberg, M.R., Colby, G.M. Limitations of ASME PTC 10 in accurately evaluating centrifugal compressor thermodynamic performance. In *Proceedings of the Forty-Second Turbomachinery Symposium*, October 1–3, 2013, Houston, TX. <http://turbolab.tamu.edu/proc/turboproc/T42/LectureT03.pdf>.

9 The PRODE calculations used the Peng-Robinson equation of state (PR-EOS) to calculate the discharge temperature. To ensure compatibility between the Schultz polytropic procedure with the high-fidelity (Span and Wagner) EOS, the head estimated by PRODE was recalculated using the enthalpies estimated by the Span and Wagner EOS in CoolProp.

Table 4-1. Inlet and Outlet Pressures for CO<sub>2</sub> Compression Using Conventional Centrifugal Compression with Intercooling Between Stages

STAGE	1	2	3	4	5	6
$P_s/P_d$ psia	23.5/53.7	52.0/115.8	113/253	248/550	545/1,205	1,200/2,220
$T_s$ , °F	70.0	70.0	70.0	70.0	70.0	100

Note: After the sixth-stage intercooler, final CO<sub>2</sub> pressure would be 2,215 psia. For this simplified analysis, it is assumed that inlet feed stream to the compressors is 100% CO<sub>2</sub>. Case 12 stream 20 has 99.31% CO<sub>2</sub> (rest water). Triethylene glycol dehydration is not modeled in this study. Intercooler pressure drop is calculated as the lower value of  $(P_2^{0.7})/10$  psia or 5 psia.

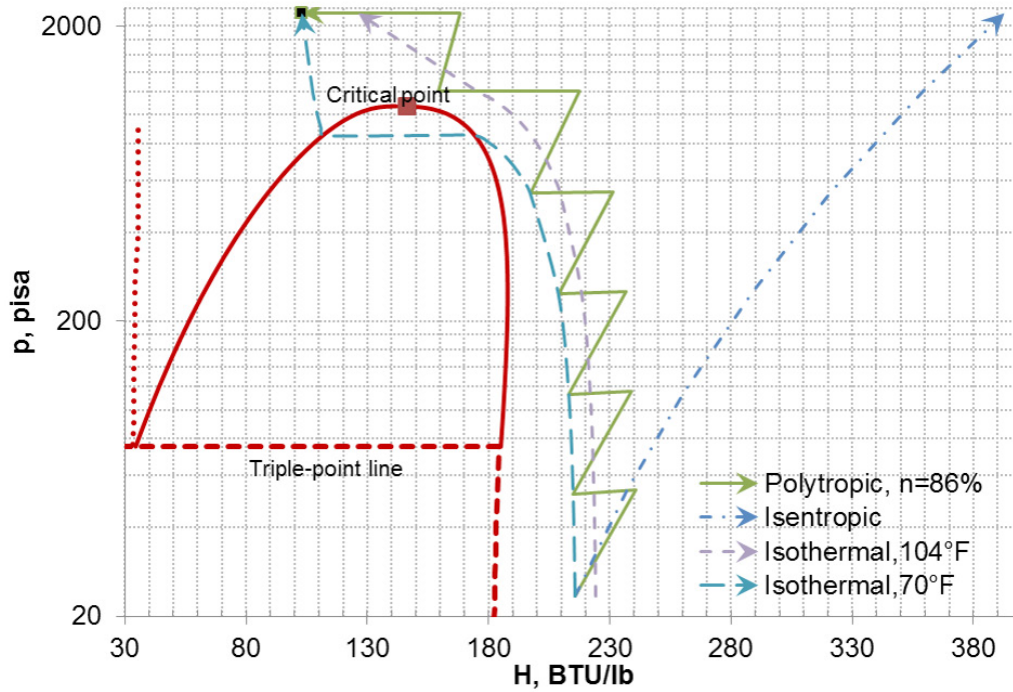


Figure 4-2. Comparison of Isentropic, Isothermal, and Intercooled Polytropic CO<sub>2</sub> Compression ( $\eta_p = 86\%$ ) Paths For compressing CO<sub>2</sub> at 23.5 psia, 70 °F to 2,215 psia.

Table 4-2. Stage Outlet Temperature, Head, and Overall Compression Work for Six-Stage Compression of CO<sub>2</sub> from 23.5–2,215 psia Using Prode, Schultz, and Ideal Gas Approximation Calculations

STAGE	1	2	3	4	5	6
$P_s$ , psia	23.5	52.0	113.0	248.0	545.0	1,200.0
$T_s$ , °F	70.0	70.0	70.0	70.0	70.0	100
Pressure ratio	2.28	2.23	2.24	2.22	2.21	1.85
$P_d$ , psia	53.7	115.8	253.0	550.0	1,205.0	2,220.0
$T_d$ , °F (Prode)	190.01	187.3	190.1	192.6	196.7	165.3
$T_d$ , °F (Schultz)	192.7	189.2	191.1	191.4	192.3	164.4
$T_d$ , °F (ideal gas, no Schultz correction factor)	192.5	189.5	192.2	194.4	198.2	167.2
Head ( $\Delta h$ ), kJ/kg (Prode)	57.6	55.3	54.9	52.3	47.1	20.5
Head ( $\Delta h$ ), kJ/kg (Schultz)	58.9	56.3	55.4	51.6	43.6	18.9
Head ( $\Delta h$ ), kJ/kg (ideal gas, no Schultz correction factor)	58.7	56.4	56.0	53.3	48.3	23.8



Table 4-2. Stage Outlet Temperature, Head, and Overall Compression Work for Six-Stage Compression of CO<sub>2</sub> from 23.5–2,215 psia Using Prode, Schultz, and Ideal Gas Approximation Calculations

STAGE	1	2	3	4	5	6
Gas power, hp/(lb <sub>m</sub> /min) (Prode)	2.92					
Power, kWe (Prode)	44,711 [vs. 44,890 for Case 12]					
Power, kWe (Schultz)	44,224 [vs. 44,890 for Case 12]					
Power, kWe (ideal gas)	46,954					
Note: Subscripts s and d denote suction and discharge respectively. All calculations assume a polytropic efficiency of 86%. The gas power [hp/(lb <sub>m</sub> /min)] does not include the mechanical efficiency of the compressor. 1 hp/(lb <sub>m</sub> /min) = 98.64 kJ/kg.						

## 4.2.3 HIGH-PRESSURE RATIO COMPRESSION

High-pressure ratio compressors are based on shock compression where a rotor operating at high (sub-sonic) speeds generates shock waves compressing the CO<sub>2</sub>. Incorporating high-pressure ratio compression in conventional compressor designs results in large forces being exerted on the compressor shaft, leading to complicated and costly designs.<sup>6</sup> Therefore, the pressure ratio in conventional compressors is limited to ≈2 to 3 for CO<sub>2</sub> compression. Ramgen has been developing a high-pressure ratio shock compression technology with DOE funding, which can increase pressure ratio per stage from 2 to approximately 10.<sup>10</sup> This lowers the number of compressor stages needed for CO<sub>2</sub> compression to 2,215 psia, and thereby decreases the physical size and lowering the capital cost.<sup>11</sup>

High-pressure ratio compressors also offer the possibility of integrating heat from the compression fluid with the Rankine cycle of the SCPC plant. A schematic of the high-pressure ratio compression is shown in Figure 4-3, where CO<sub>2</sub> is cooled from the compressor exit temperature to 70 °F.

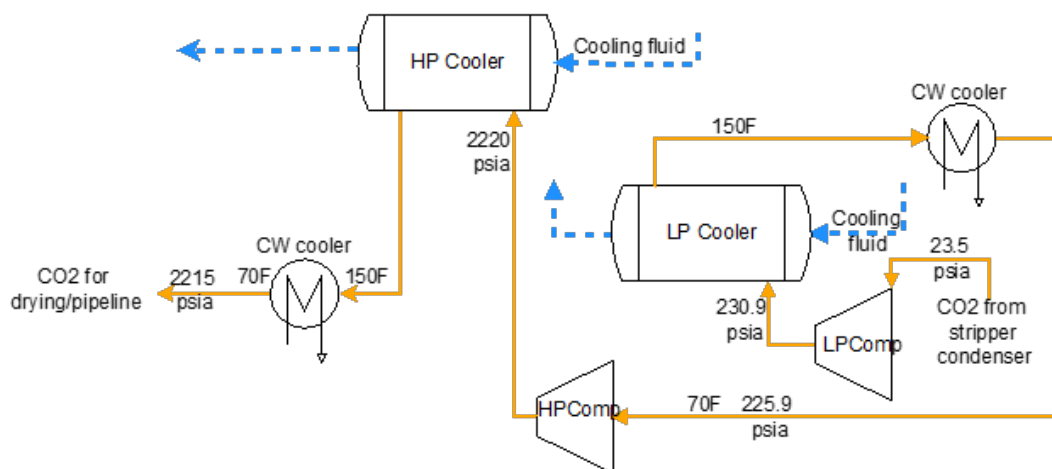


Figure 4-3. Schematic of Two-Stage Compression of CO<sub>2</sub> Using Shock Wave Compression

Note: Integration with the SCPC plant Rankine cycle is not shown in the figure.

For the purposes of power plant heat integration, the schematic shows CO<sub>2</sub> would be cooled to 150 °F using cooling fluid (e.g., boiler feedwater [BFW]) and further cooled to 70 °F using cooling water. The calculated compressor outlet temperatures, head and compression work for the two stages are presented in Figure 4-4.

Results shown in Table 4-3 are based on a 5 psia pressure drop for cooling 100% pure CO<sub>2</sub> (i.e., for both coolers per stage) and assume 86% polytropic efficiency. Both the area integration (Prode) and Schultz methods were used to calculate the exit temperature, head and compression power.

10 <http://www.netl.doe.gov/research/coal/carbon-capture/co2-compression/supersonic>

11 <https://www.netl.doe.gov/File%20Library/Research/Coal/ewr/co2/K-Lupkes-Ramgen-Shockwave-Compression.pdf>

Table 4-3. Stage Outlet Temperature, Head, and Overall Compression Load for the Two-Stage Compression of CO<sub>2</sub> from 23.5–2,215 psia Using Prode and Schultz calculations

STAGE	1	2
P <sub>sr</sub> , psia	23.5	225.9
T <sub>sr</sub> , °F	70	70
P <sub>dr</sub> , psia	230.9	2,220.0
Pressure ratio	9.83	9.83
T <sub>dr</sub> , °F (Prode)	446.8	472.4
T <sub>dr</sub> , °F (Schultz)	452.4	471.5
Head (Δh), kJ/kg (Prode)	192.2	182.1
Head (Δh), kJ/kg (Schultz)	195.5	181.5
Gas power, hp/(lb <sub>m</sub> /min) <sup>11</sup>	3.80	
Total, kWe (Prode)	58,199	
Total kWe (Schultz)	58,613	

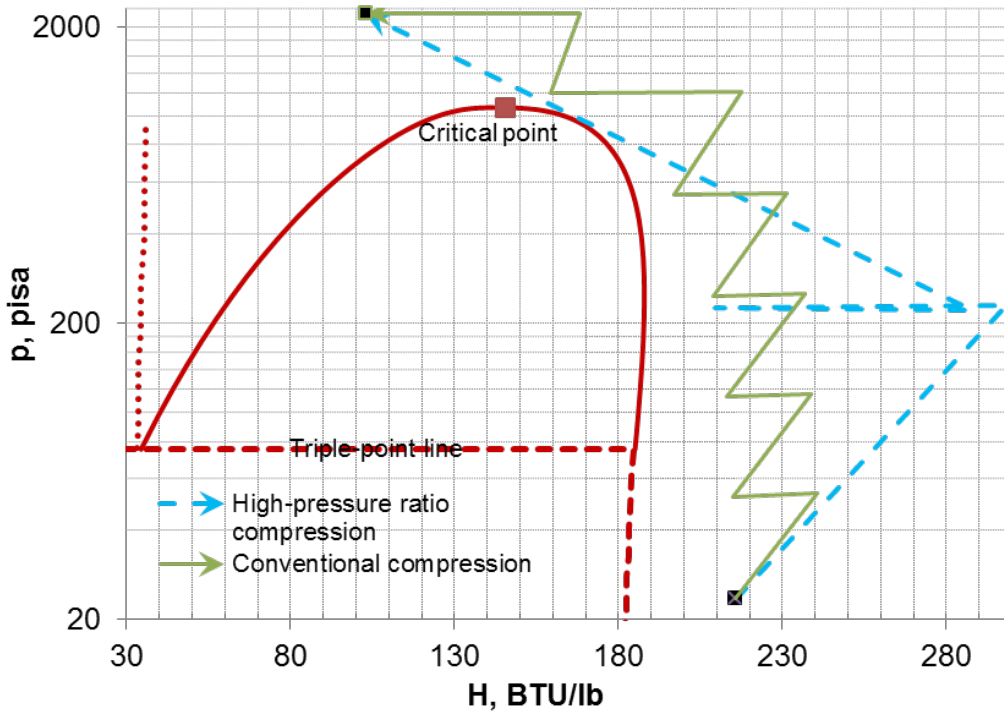


Figure 4-4. p-H Diagram for Conventional and High-Pressure Ratio CO<sub>2</sub> Compression ( $\eta_p = 86\%$ )

The results from Figure 4-4 indicate that the enthalpy at the compressor stage outlet is significantly higher for high-pressure ratio compressors compared to conventional compressors. Therefore, compressor load for high-pressure ratio compression would also be considerably (30.16%) higher because of the higher temperature (446–472 °F vs. 167–192 °F) and higher fluid volume to be compressed.

12 The gas power [hp/(lb<sub>m</sub>/min)] does not include the mechanical efficiency of the compressor. 1 hp/(lb<sub>m</sub>/min) = 98.64 kJ/kg.

## 4.2.4 ISOTHERMAL CO<sub>2</sub> COMPRESSION/COOLED-DIAPHRAGM CONCEPT

In isothermal compression, the temperature of the fluid remains constant. Isothermal compression requires that the heat produced during compression be removed as quickly as it is produced. The conventional means to lower the temperature is to cool the gas in between compression stages using external intercoolers. Multi-shaft, integral-gear centrifugal compressors can be used to achieve near-isothermal operation with external intercooling. However, their reliability is low compared to single-shaft in-line centrifugal compressors, which also offer higher operating flexibility.<sup>13</sup> The Southwest Research Institute (SwRI) is developing a technology where CO<sub>2</sub> is continually cooled in the compressor diaphragm using an internal jacket instead of using interstage cooling. Studies indicate that 6 to 12% reduction in the compression load is achievable using the cooled-diaphragm concept.<sup>14</sup> The performance of the cooled-diaphragm technology approaches that of isothermal compression. A large number (16) of semi-isothermal stages was calculated to assess the cooled-diaphragm concept.<sup>15</sup>

There are two factors of note in the compressing CO<sub>2</sub> semi-isothermally. First, it is evident from Figure 4-2 that isothermal compression at 70 °F (21.11 °C) would result in a crossover to the vapor-liquid region before compression to the dense-phase region. The physical properties of CO<sub>2</sub> fluctuate significantly in the critical region, and compression paths evaluated in this study avoid the vapor-liquid phase transition. Second, in a typical power plant (e.g., Case 12), the temperature to which CO<sub>2</sub> can be cooled using cooling water alone (i.e., without external refrigeration) depends on the temperature of the cooling water (Case 12: 60 °F). If the average CO<sub>2</sub> temperature (inlet-outlet) in each compressor stage is to remain at 70 °F, external refrigeration is required.<sup>16</sup> Two semi-isothermal compression cases were studied (Figure 4-5):

- Semi-isothermal compression using 16 stages, intercooler exit temperature: 70 °F, average temperature of ≈90 °F (between suction and discharge of each stage) [Table 4-4],
- Semi-isothermal compression using 16 stages, intercooler exit temperature: 50 °F, average temperature of ≈70 °F (between suction and discharge of each stage) [Table 4-5].

The compression path for conventional compression, isothermal compression at 70 °F, 110 °F (constant temperature lines) and semi-isothermal compression are shown in the CO<sub>2</sub> pressure-enthalpy (p-H) diagram in Figure 4-4. CO<sub>2</sub> is cooled to the same intercooler exit temperature (70 °F) for both the semi-isothermal compression path at an average temperature of 90 °F (blue line) and the conventional compression path (green). However, because only six compression stages were used in conventional compression, the temperature increase per stage is larger than that of the sixteen-stage path, leading to higher power consumption.

Table 4-4. Specific Work and Overall Compression Load for Compressing CO<sub>2</sub> from 23.5 to 2,215 psia Using Intercooler Temperature of 70 °F and 16 Compression Stages

STAGE	1	2	3	4	5	6	7	8	9	10	11	12	13	14	15	16
P <sub>s</sub> , psia	23.5	31.2	41.5	55.1	73.2	97.3	129.3	171.8	228.2	303.2	402.8	535.1	711	944.6	1254.9	1667.2
T <sub>s</sub> , °F	70	70	70	70	70	70	70	70	70	70	70	70	70	82.4	86	86
Pressure ratio	1.3286															
T <sub>avg</sub> (T <sub>s</sub> +T <sub>d</sub> )/2, °F	89.8	89.8	89.8	89.9	90	90	90.2	90.3	90.5	90.8	91.1	91.5	91.6	102.1	91.1	91
Head (Δh), kJ/kg	18.5	18.5	18.4	18.3	18.2	18.1	17.9	17.7	17.4	16.9	16.4	15.8	15.5	14.5	5.6	6.6
Gas power, hp/(lb <sub>m</sub> /min)	2.58															
Power, kWe	39,535 [vs. 44,890 for Case 12]															

13 IEAGHG. Rotating equipment for carbon dioxide capture and storage. 2011/07, September 2011.

14 Moore J. et al. Novel concepts for the compression of large volumes of carbon dioxide—Phase III. Presented at the 2013 CO<sub>2</sub> Capture Technology Meeting. <http://seca.doe.gov/publications/proceedings/13/co2capture/pdf/2-Tuesday/J%20Moore-SWI-Concepts%20for%20Compression%20of%20Large%20Volumes%20of%20CO2.pdf>.

15 This case is denoted as semi-isothermal compression because the gas temperature before and after compression (i.e., before intercooler) is almost the same, if not exactly the same. The number of intercooling stages were chosen to provide average constant temperature (T<sub>in</sub>+T<sub>out</sub>)/2. See T<sub>avg</sub> in Table 4-4 and Table 4-5.

16 Assumes a 10 °F approach temperature between the cooling water and CO<sub>2</sub> streams.

Table 4-5. Specific Work and Overall Compression Load for Compressing CO<sub>2</sub> from 23.5 to 2,215 psia Using Intercooler Temperature of 50 °F and 16 Compression Stages<sup>16</sup>

STAGE	1	2	3	4	5	6	7	8	9	10	11	12	13	14	15	16
P <sub>s</sub> , psia	23.5	31.2	41.5	55.1	73.2	97.3	129.3	171.8	228.2	303.2	402.8	535.1	711	944.6	1254.9	1667.2
T <sub>s</sub> , °F	70	50	50	50	50	50	50	50	50	50	50	50	64.4	82.4	66.2	66.2
Pressure ratio	1.3286															
T <sub>avg</sub> , (T <sub>s</sub> +T <sub>d</sub> )/2, °F	89.8	69.4	69.4	69.4	69.5	69.6	69.7	69.9	70.1	70.4	70.8	71.1	85.8	102.1	69.6	69.9
Head (Δh), kJ/kg	18.5	17.8	17.7	17.6	17.5	17.4	17.2	16.9	16.6	16.2	15.7	15.4	15.7	14.5	4.9	5.7
Gas power, hp/(lb <sub>m</sub> /min)	2.49															
Power, kWe	38,127 [vs. 44,890 for Case 12]															

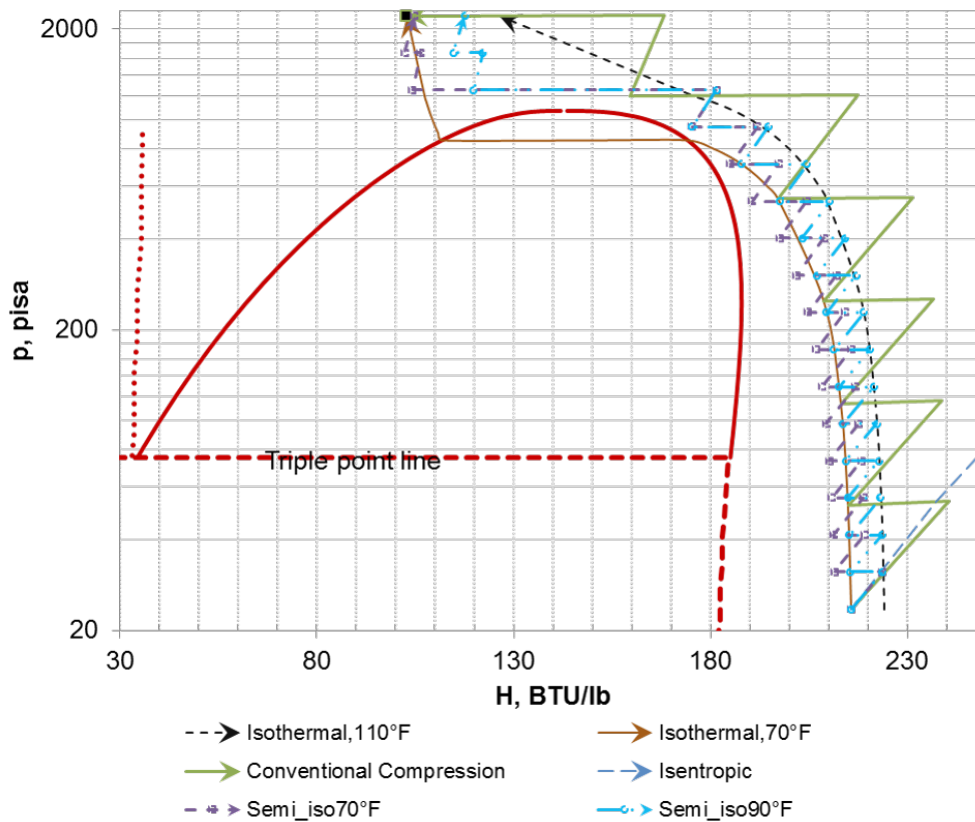


Figure 4-5. p-H Diagram for Semi-Isothermal CO<sub>2</sub> Compression Cases Compared to Conventional CO<sub>2</sub> Compression (η<sub>p</sub> = 86%)

The compression load and head (specific work) required in both cases indicate that the power consumption is reduced by 12–15% for the semi-isothermal cases compared to the load for conventional compression (Table 4-2). Note that auxiliary cooling load may be needed to cool CO<sub>2</sub> to 50 °F, increasing the total power requirement. Therefore, the power estimate for the 70 °F case represents an optimistic estimate for the power required to compress CO<sub>2</sub> at 23.5 psia to 2,215 psia. Previous analyses by SwRI suggest that a compression path with low-pressure compression using cooled diaphragm, liquefaction and pumping results in larger energy consumption than a compression path with gas cooling and therefore the liquefaction option was not evaluated.<sup>10</sup>

17 The intercooler temperature for the stages 13–14 was adjusted to keep the temperature above the phase transition boundary line.

### 4.3 OPPORTUNITIES FOR PROCESS INTEGRATION

The higher stage outlet temperature for high-pressure ratio compression offers possibilities for recovering part of the lost compression work (lost as sensible heat) for heating boiler feedwater. A previous study by Chen and Matuszewski<sup>18</sup> focused on the integration of heat recovered from high-pressure ratio CO<sub>2</sub> compression in the context of a subcritical PC plant (Conesville Unit#5). In the current study, a supercritical PC power plant with 90% CO<sub>2</sub> capture (Case 12 of the DOE/NETL bituminous coal baseline, revision 2) was chosen as the base plant for comparative analyses.

Table 4-6. Comparison of Results from the Excel Model for Case 12 to those from NETL Baseline

	CASE 12 (EXCEL MODEL)	CASE 12 (BITUMINOUS COAL BASELINE)
HP turbine output, kWe	244,627	
IP turbine output, kWe	298,727	
LP turbine output, kWe	125,705	
Gross steam turbine output, kWe	669,058	662,800
Condensate pump load, kWe	528	560
BFW pump load, kWe	24,175	
BFW pump turbine steam consumption, lb/h	368,328	375,024
Total LP condensate flow, lb/h	1,939,454	1,958,206
CO <sub>2</sub> compressor load, kWe	44,711	44,890
Gross steam turbine output-compressor load, kWe	624,347	617,910
Net power, kWe	556,440	549,970
Net efficiency HHV, %	28.76%	28.4%
Condenser duty, MMBTU/h	1,630	1,646

To facilitate heat integration studies, the Rankine cycle for Case 12 was modeled in Excel using an Excel add-in to calculate water/steam properties.<sup>19</sup> The parameters used to model the steam cycle were obtained from the bituminous coal baseline and the DOE/NETL quality guidelines for energy system modeling studies (QGESS).<sup>20</sup> These parameters are provided in Appendix 6.4. The power generated by the HP, IP and LP turbines of Case 12 is compared against baseline values, and the results indicate that the Excel model results are consistent with those from the DOE/NETL baseline. Because only the steam cycle and the CO<sub>2</sub> compressor were modeled in this study, net power calculation assumed that other loads such as miscellaneous balance-of-plant, steam turbine auxiliaries, circulating water pumps, ground water pumps, cooling fans, and transformer losses were similar to baseline values. Further, these were assumed not to vary significantly in response to heat integration.<sup>21</sup>

The compressor stage exit temperatures and the minimum CO<sub>2</sub>-BFW temperature approach determine the suitability of integrating the recovered heat within the Rankine cycle. The minimum temperature approach used in this study is 20 °F (same as that used in Chen and Matuszewski, (2009)). The feedwater heater (FWH) temperatures for Case 12 are shown in Table 4-7.

18 Chen, S., Matuszewski, M. Benefits of Ramgen shock compression technology for CO<sub>2</sub> compression. DOE/NETL-2009/0629. June 2009.

19 The International Association for Properties of Water and Steam Industrial Formulation 1997 (IAPWS IF-97) steam tables from <http://xsteam.sourceforge.net/> packaged in the 'All-in-one' add-in from the University of Alabama (<http://www.me.ua.edu/ExcelinME/thermo.htm>) were used.

20 DOE/NETL Office of Program Planning and Analysis. Quality guidelines for energy system modeling studies: Process modeling design parameters. DOE/NETL-341/081911. (January 2012).

21 The only significant load which could change upon heat integration is the circulating water pump load due to the higher condenser duty for the cases with heat integration. However, because the condenser heat duty is ≈31% of the total cooling tower duty (5,360 MMBTU/h) for case 12, and because information about the other cooling loads for the power plant is not readily available, this value is assumed to remain the same. Integrating heat from CO<sub>2</sub> compression would also lower the cooling duty for the CO<sub>2</sub> intercoolers where CO<sub>2</sub> is cooled to 70 °F, offsetting the increased condenser duty and increased cooling tower load (increased circulating pump and CT fan load), however this study does not take those into account.

Table 4-7. Boiler Feed Water Exit Temperatures for the Feedwater Heaters in Case 12

HEATER/COOLER	FWH 8	FWH 7	FWH 6	DEAERATOR	FWH 4	FWH 3	FWH 2	FWH 1	CONDENSER
Outlet BFWT, °F	545	503.3	388.7	302.9	235	190.3	151.3	124.4	101.4
Steam pressure used in FWH, psia	1,115 (HP)	711 (HP)	222 (HP)	HP, IP	29 (LP)	11.4 (LP)	4.5 (LP)	2.3 (LP)	1

A comparison of the FWH temperatures from Table 4-7 and CO<sub>2</sub> exit temperatures from Table 4-3 shows that a portion of the HP steam for FWH 7 could be potentially offset by heat integration. Decreased steam extraction to FWH 7 would result in increased IP and LP power generation, not an increase the HP turbine output. The actual amount and quality of heat that can be recovered by heat integration can be calculated by temperature-heat transferred (Q) diagrams for the two stages of CO<sub>2</sub> cooling (Figure 4-5).

The calculations shown in Figure 4-5 assume that water exiting the condenser pumps can be further pumped to BFW pressure (4,200 psia) before being fed to the CO<sub>2</sub> coolers. The temperature of the water stream exiting the HP coolers was determined by iterative calculations using Excel solver with the temperature approach of 20 °F as the minimum criterion. As discussed in Chen and Matuszewski, (2009), the specific heat capacity of CO<sub>2</sub> at 2,220 psia changes significantly with temperature, leading to a pinch in the middle of the heat exchanger. However a corresponding pinch for the low-pressure (230.9 psia) CO<sub>2</sub> cooler<sup>22</sup> was not found.

Although CO<sub>2</sub> gas temperature entering the HP cooler is higher (472 °F vs. 447 °F), the existence of the pinch for the HP cooler limits the temperature of BFW to ≈370 °F, lower than that exiting the LP cooler (≈410 °F). The effect of compression load on plant efficiency was analyzed by considering the following scenarios:

Case A: High-pressure ratio compression. Condensate pump exit BFW is pumped to 4,200 psia and is used to cool CO<sub>2</sub> for both HP and LP coolers and fed to FWH 8 (after auxiliary heating)

Case B: High-pressure ratio compression. Condensate pump exit BFW is pumped to 4,200 psia and is used to cool CO<sub>2</sub> in LP coolers and fed to FWH 8 (after auxiliary heating). HP CO<sub>2</sub> stream (2,220 psia) is cooled from 472 °F to ≈330 °F by BFW from the main BFW feed pumps (i.e., exiting the deaerator ≈306 °F<sup>23</sup>).

Case C: Heat integration similar to Case A, with 90% polytropic compression efficiency<sup>24</sup>

Case D: Heat integration similar to Case B, with 90% polytropic compression efficiency<sup>19</sup>

Case E: Semi-isothermal compression (with an average temperature of 90 °F), with 86% polytropic compression efficiency

Case F: Semi-isothermal compression with an average temperature of 70 °F, with 86% polytropic compression efficiency

Case G: Semi-isothermal compression with an average temperature of 90 °F, with 90% polytropic compression efficiency

Case H: Semi-isothermal compression with an average temperature of 70 °F, with 90% polytropic compression efficiency

## 4.4 RESULTS AND DISCUSSION

The process flow diagram for Case A is shown in Figure 4-7. The T-Q diagrams for Case A are shown in Figure 4-6. The process flow diagram for Case B is shown in Figure 4-8. The T-Q diagrams for Case B are shown in Figure 4-9. The T-Q diagrams for cases C and D are shown in Figure 4-10 and Figure 4-11. The gross steam turbine output, compressor load and efficiency for cases A-H are shown in Table 4-8, Figure 4-12 and Table 4-9.

22 One reason for the difference between the results of this analysis and that of the previous analysis (DOE/NETL-2009/0629) is that the CO<sub>2</sub> gas used in that study had ≈31.9 mol% water vapor which would be condensed during CO<sub>2</sub> cooling, increasing the specific heat (i.e., decreasing the slope of the T-Q line), leading to the pinch. Because the Case 12 feed gas did not contain an appreciable quantity of water (≈0.0069% H<sub>2</sub>O—stream 20), this 230.9 psia pinch is not likely to be prominent for the cases in this study.

23 The difference between the deaerator exit (303 °F) and BFW pump exit temperature (306 °F) is because of the pumping work lost to heat.

24 For comparison, a baseline (i.e., conventional compression) Case 12 with 90% polytropic compression efficiency was also modeled.



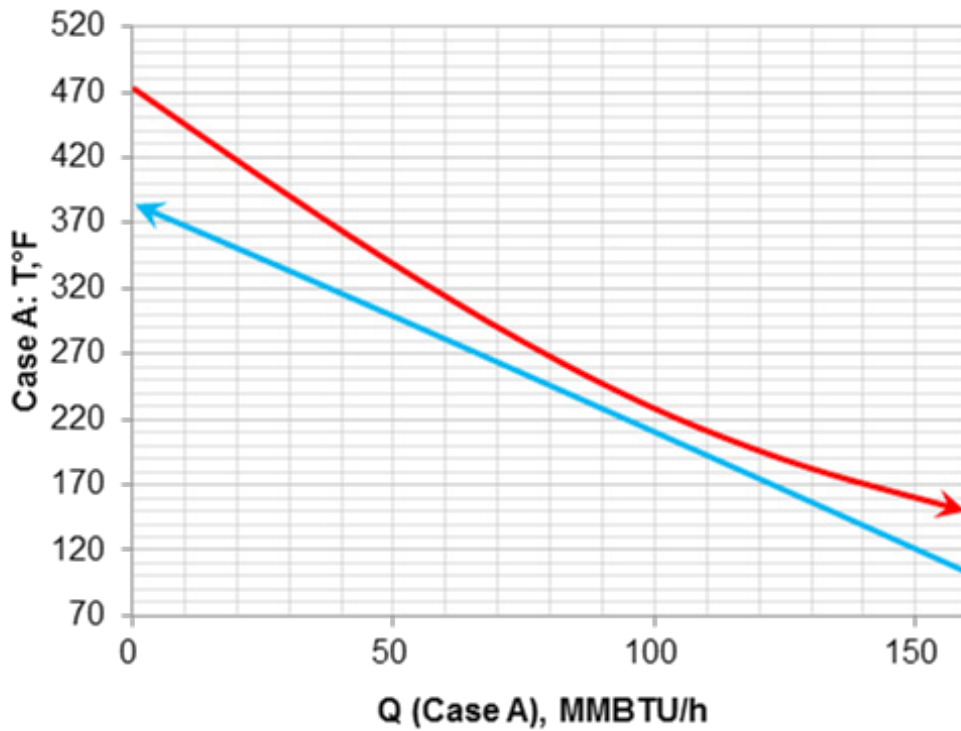
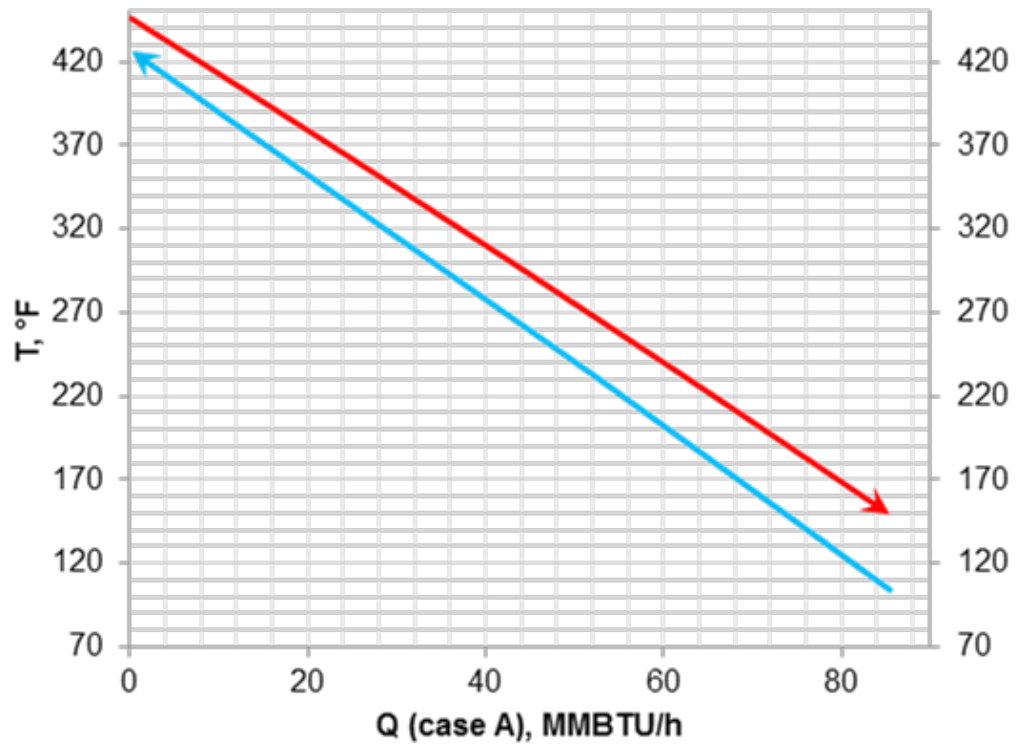


Figure 4-6. T-Q Diagrams for the 231 psia (Case A, B) and 2,220 psia CO<sub>2</sub> Coolers (Case A) ( $\eta_p = 86\%$ , high-pressure ratio compression)  
 Red: CO<sub>2</sub>, Blue: BFW,  $\Delta T_{min} = 20^\circ\text{F}$

Table 4-8. Results from CO<sub>2</sub> Compression Heat Integration Scenarios

	% CHANGE IP POWER	% CHANGE LP POWER	GROSS POWER, KWE	COMPRESSOR LOAD, KWE	MIXED HP BFW TEMP, °F	LP BFW TEMP, °F	% OF BFW HEATED BY CO <sub>2</sub>	NET EFFICIENCY, %	CONDENSER LOAD, MMBTU/H
Case 12 (baseline)	0	0	669,058	44,711	—	—	—	28.76	1,630
Case 12 90% $\eta_p$	0	0	669,058	42,611	—	—	—	28.87	1,630
Case A	0.9%	11.3%	685,958	58,199	398	—	16.5	28.95	1,878
Case B	1.6%	12.2%	689,251	58,325	440	289	12.3	29.11	1,898
Case C	0.6%	11.7%	684,372	54,989	386	—	16.5	29.03	1,871
Case D	1.5%	12.1%	688,617	55,023	425	289	13.5	29.25	1,899

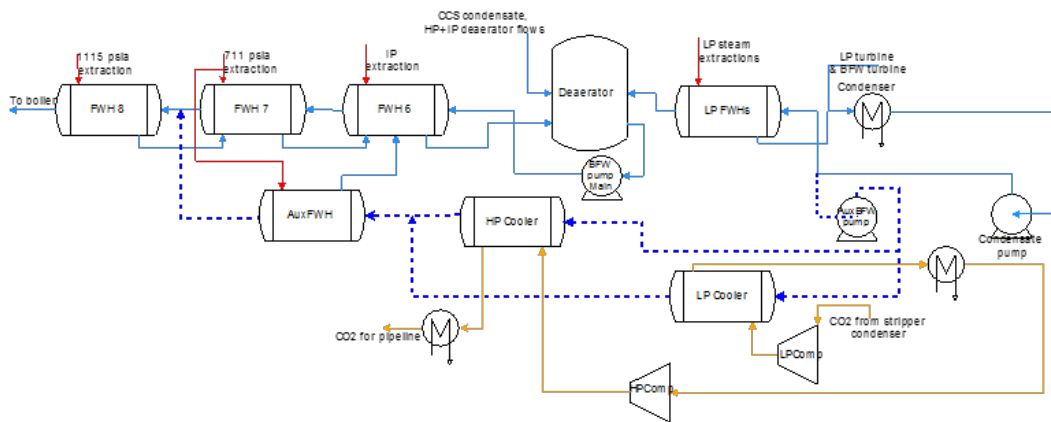


Figure 4-7. Process Flow Diagram for Case A  
Yellow: CO<sub>2</sub>, Light Blue/Violet: BFW, Red: Steam

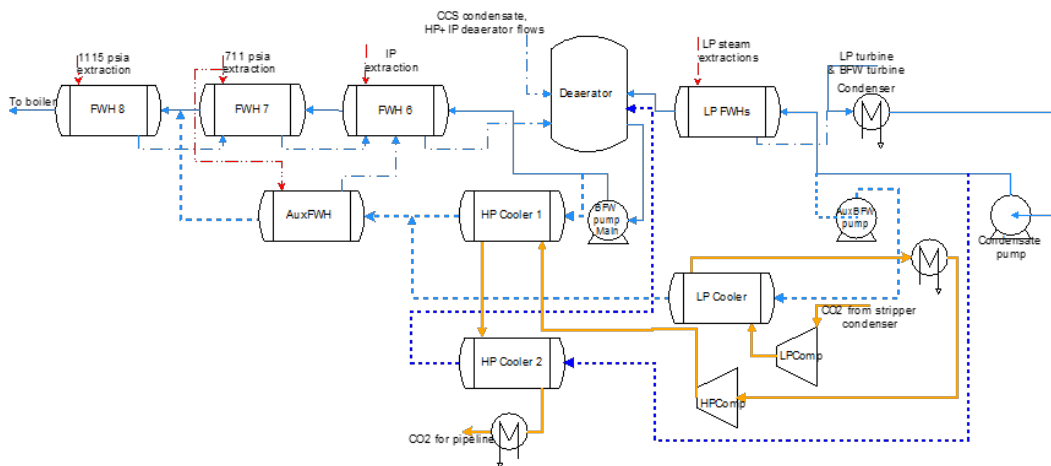


Figure 4-8. Process Flow Diagram for Case B  
Yellow: CO<sub>2</sub>, Light Blue/Violet: BFW, Red: Steam

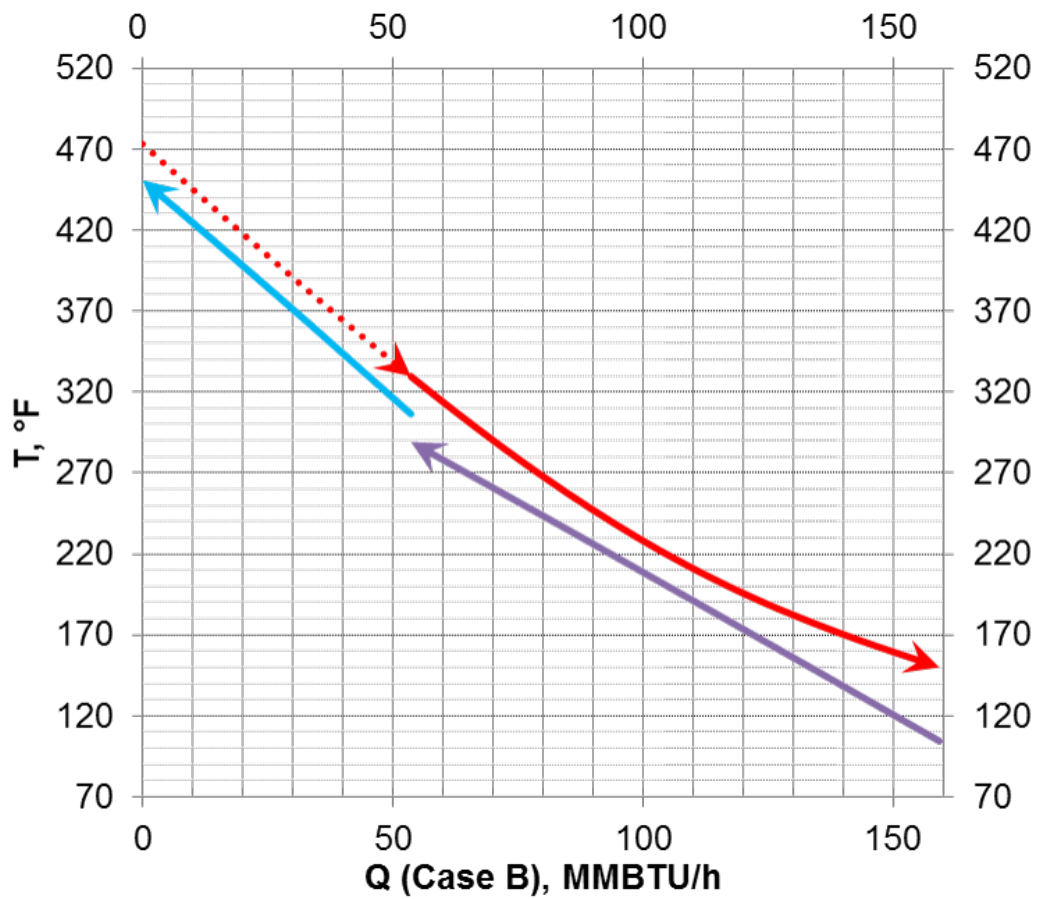


Figure 4-9. T-Q Diagrams for HP CO<sub>2</sub> Coolers in Case B  
 The LP cooler T-Q diagram is unchanged from Case A. Red: CO<sub>2</sub>, blue: HP BFW, purple: LP BFW.  $\Delta T_{min} = 20\text{ }^{\circ}\text{F}$

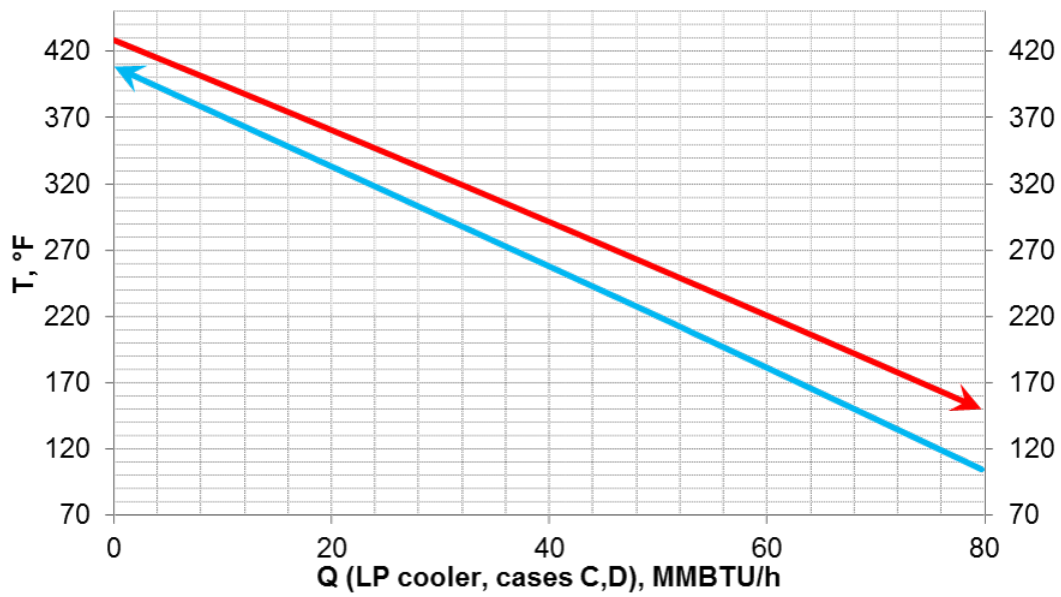


Figure 4-10. T-Q Diagrams for LP CO<sub>2</sub> Coolers in Cases C and D  
 Red: CO<sub>2</sub>, blue: HP BFW.  $\Delta T_{min} = 20\text{ }^{\circ}\text{F}$

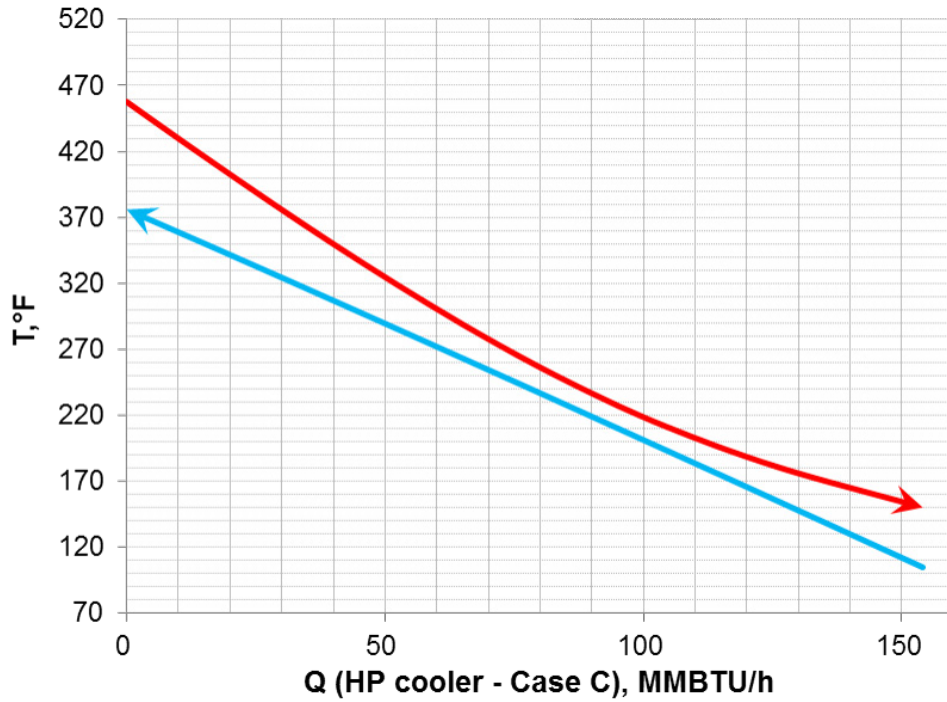
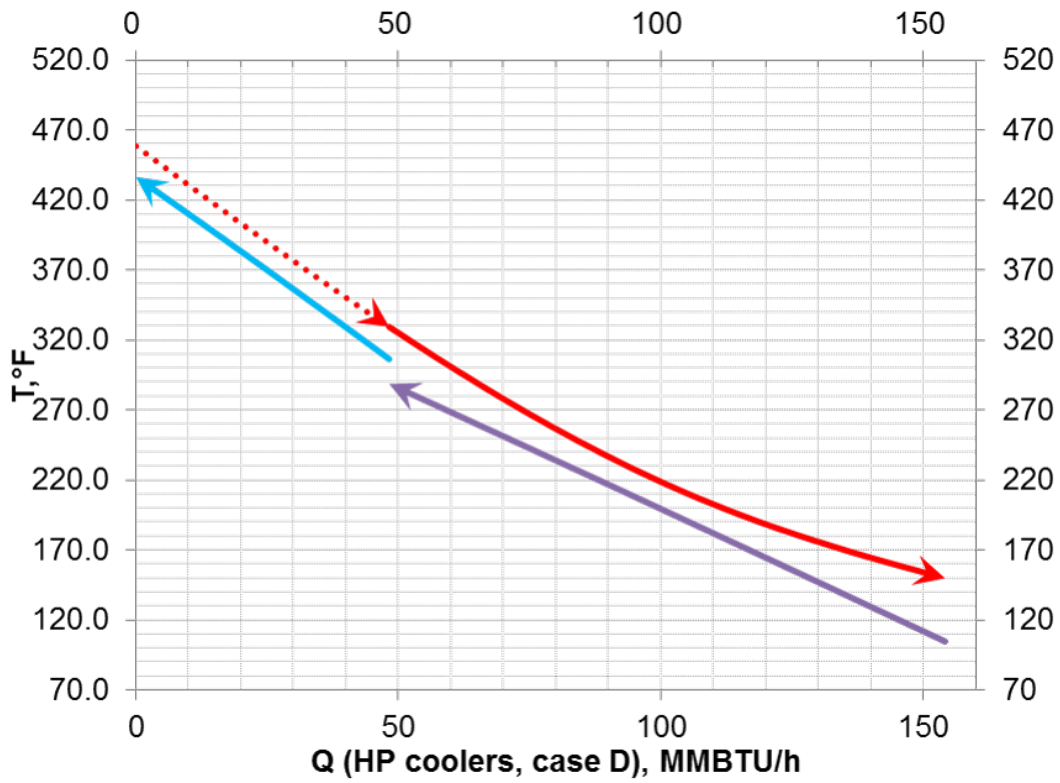


Figure 4-11. T-Q Diagrams for HP CO<sub>2</sub> Coolers (Case C and D) ( $\eta_p = 86\%$ , high-pressure ratio compression)  
 Red: CO<sub>2</sub>, blue: HP BFW, purple: LP BFW.  $\Delta T_{min} = 20^\circ F$

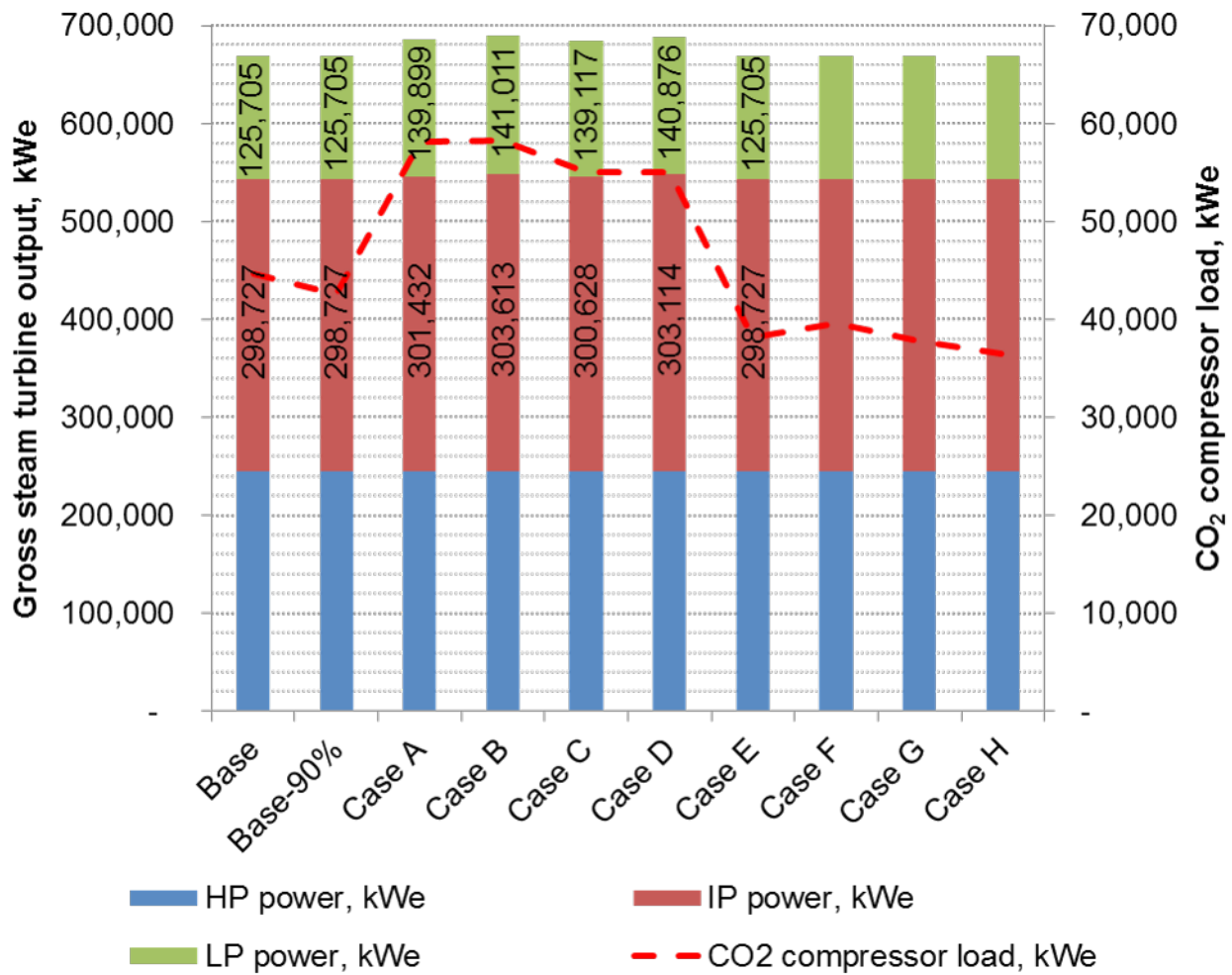


Figure 4-12. Gross Steam Turbine Output and Compressor Load for High-Pressure Ratio Cases (A, B, C, D), Baseline Case 12, and Semi-Isothermal CO<sub>2</sub> Compression Cases (E, F, G, H)

The integration of heat of CO<sub>2</sub> compression with the Rankine cycle for a SCPC power plant leads to a small (0.2% to 0.5% [percentage points]) increase in the net efficiency. Similarly, semi-isothermal compression at an average temperature of 70–90 °F would lower the compressor load by 12–15%, resulting in a comparably small increase in net efficiency (0.3%) over that for the base case (Case 12). Note that in the cases F and H, CO<sub>2</sub> is cooled to 50 °F, which may require additional parasitic energy load depending on the plant conditions, reducing the net power and efficiency produced beyond that shown in Table 4-9.

The higher compressor efficiency in Cases C and D results in a lower compressor load, lower CO<sub>2</sub> stage outlet temperature and lower BFW temperature (386 °F vs. 398 °F, 425 °F vs. 446 °F). However, the increased net efficiency for Cases C and D indicates that the reduction in compressor load outweighs the lower turbine output. Furthermore, because high-pressure ratio is inherently less efficient compared to conventional compression, the percentage reduction in compressor load when the efficiency is increased from 86% to 90% is 4.69% higher for the higher-pressure ratio compression (5.71% reduction vs. 4.6% reduction).

Table 4-9. Comparison of Net Power and Efficiency for Conventional, High-Pressure Ratio, and Semi-Isothermal CO<sub>2</sub> Compression

	$\eta_p$ : 86%		$\eta_p$ : 86%	
	NET POWER, KWE	EFFICIENCY, %HHV	NET POWER, KWE	EFFICIENCY, %HHV
Conventional	Base		Base-90%	
	556,440	28.76%	558,540	28.87%
High-Pressure Ratio-Integration 1	Case A		Case C	
	560,045	28.95%	561,672	29.05%
High-Pressure Ratio-Heat Integration 2	Case B		Case D	
	563,207	29.11%	565,880	29.25%
Semi-Isothermal-90 °F	Case E		Case G	
	563,023	29.10%	563,320	29.12%
Semi-Isothermal-70 °F	Case F		Case H	
	561,615	29.03%	564,659	29.19%

The preceding discussion noted that improvements in compression loads do not affect the net efficiency significantly. One feature of high-pressure ratio compression is that it has the potential to lower compressor capital costs significantly ( $\approx 50$ – $60\%$ ) because only two stages are needed for CO<sub>2</sub> compression. The effects of capital costs, and compressor power consumption on lowering the overall cost of CO<sub>2</sub> capture were analyzed, using the updated (capital, fixed and variable operating costs) cost estimates (2011\$) for Case 12 of the DOE/NETL baseline (Figure 4-12). A reduction in the capital cost of compressors and dryers does not contribute significantly toward lowering the CO<sub>2</sub> capture cost. The reduction in CO<sub>2</sub> capture cost (over the baseline) resulting from the several advances discussed in Cases A to H is shown in Figure 4-12. Generally, for both high-pressure ratio compression (when two levels of heat integration are considered) and semi-isothermal compression (at 70 °F and 90 °F), at compressor polytropic efficiencies of 86% and 90%, CO<sub>2</sub> capture costs were \$2 to \$3/T CO<sub>2</sub> lower than that estimated for Case 12 of the DOE/NETL bituminous coal baseline. If the compressor costs were zeroed, the potential reduction in capture costs is \$4 to \$5/T CO<sub>2</sub>.

The reduction in CO<sub>2</sub> capture costs for the high-pressure ratio compression cases does not account for the additional capital costs for the heat exchangers. Therefore the reduction in CO<sub>2</sub> capture cost represents an upper bound of the potential improvement using high-pressure ratio compression when the compression heat is integrated within the Rankine cycle.



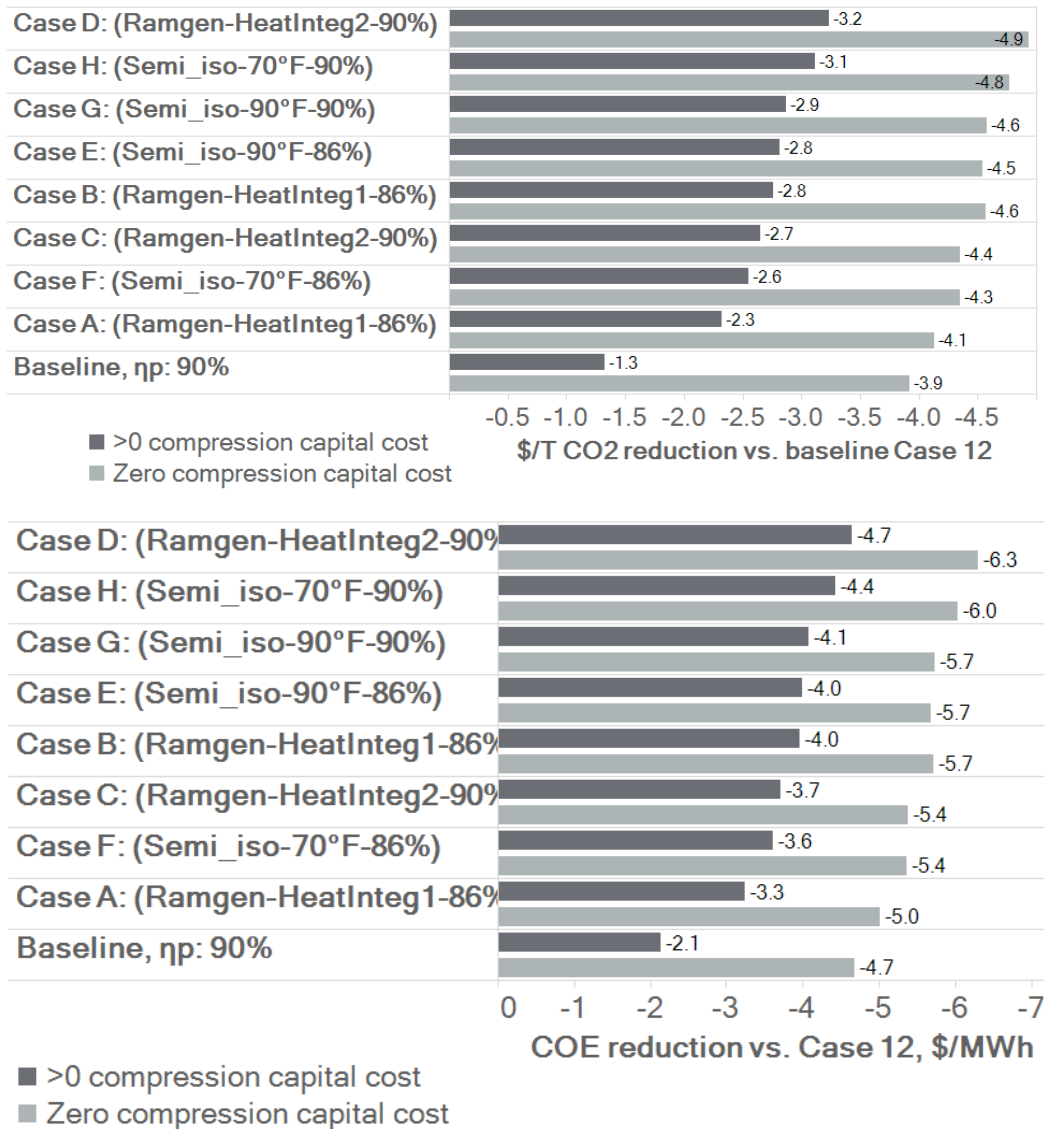


Figure 4-13. Reduction of CO<sub>2</sub> Capture Cost and Cost of Electricity Upon the Integration of Advanced CO<sub>2</sub> Compression Technologies<sup>25</sup>  
 Bars in light grey represent capture cost reduction with zero compressor capital costs.

The results from Chen and Matuszewski, (2009) indicate a slight decrease in efficiency when heat from high-pressure compression is integrated within the power plant Rankine cycle. This may arise from the higher quantity of water in the CO<sub>2</sub> stream modeled in that work, and the differences in the performance of the Rankine cycles (subcritical vs. supercritical). Nevertheless, this slight improvement in performance would also need lower compressor capital costs to lower the CO<sub>2</sub> capture costs.

### 4.5 CONCLUSIONS

The potential for improving net efficiency and reducing capture costs using advanced compression technologies, high-pressure ratio compression where compression heat is integrated with the Rankine steam cycle, and semi-isothermal compression were examined. Both technologies result in similar improvements in net plant efficiency (≈0.3 to 0.5 percentage points). Further, the CO<sub>2</sub> capture costs are reduced \$2 to \$3/T CO<sub>2</sub>. A compressor capital cost of zero would result in a reduction in the cost of capture by \$4 to \$5/T CO<sub>2</sub>. Similarly, the COE would be reduced \$2 to \$5/MWh, for the non-zero cost, and \$5 to \$6/MWh for the zero-cost scenarios. Although these results indicate that both compression technologies do not lead to significant cost reductions in capturing CO<sub>2</sub> from

<sup>25</sup> Note: The compressor capital cost (\$/hp) for semi-isothermal cases was assumed to be similar to that for Case 12. Ramgen compressor costs were escalated using the 2007\$ estimate for Ramgen and the 2007\$ and 2011\$ estimates for conventional compression and drying from Case 12. The total variable operating cost, fuel cost and total fixed operating cost were assumed be constant. Capital charge factor: 0.1243, capacity factor: 85%.

supercritical bituminous-coal fired power plants, reducing the cost of CO<sub>2</sub> compression is nevertheless important to achieve DOE CO<sub>2</sub> Capture R&D program goals. For example, reduction of the compression load, results in a smaller overall plant, reducing overall plant costs.

## 4.6 RECOMMENDATIONS

The types of technologies to be employed in the future for compressing CO<sub>2</sub> would be partly driven by the pressures at which CO<sub>2</sub> is available, either from natural sources such as the Jackson Dome, or from anthropogenic sources such as industrial or power plant gas streams. Several capture technologies being currently developed with DOE/NETL support can release CO<sub>2</sub> at pressures from 1 to 10 bar (15 psia to 150 psia), reducing compression load compared to the cases discussed in this report. The pressure at which CO<sub>2</sub> would be available may determine how much of an impact CO<sub>2</sub> compression would have on the final cost of electricity, cost of capture, or cost of the product. For example, in cases where CO<sub>2</sub> is separated at sub-atmospheric pressures, the cost impact will be relatively higher. Similarly, if a technology with low parasitic load is used to capture CO<sub>2</sub>, the quantity of CO<sub>2</sub> generated from the capture process for the same net power output would be lower, which would lower the costs of CO<sub>2</sub> compression because a comparatively lower quantity of CO<sub>2</sub> would be captured and compressed for the same net power output.

The current analysis did not consider the capital costs of heat exchange equipment for the case studies. Feed water heater costs could be considered in future techno-economic analyses to better reflect the economics of the high-pressure ratio compression steps.

The heat-integration analysis was based on a supercritical pulverized bituminous coal-fired Rankine cycle. Excess heat from the shock-wave compression is not well integrated within a steam-based Rankine cycle. On the other hand, integrating the heat energy from shock-wave compression with a supercritical CO<sub>2</sub>-based power cycle may be more effective and could be considered as an avenue for future work.

Industry demand for CO<sub>2</sub> compression would also be driven by the requirements of pipeline operators and CO<sub>2</sub> producers supplying CO<sub>2</sub> for enhanced oil recovery (EOR). CO<sub>2</sub> compression and purification is also a critical component of technologies such as oxy-fuel combustion, where the downstream CO<sub>2</sub> purification unit (CPU) is a critical component of the overall CO<sub>2</sub> capture and compression scheme. Although the analysis in the current report indicates that advanced compression technologies may not reduce CO<sub>2</sub> capture costs for supercritical power plants considerably, the development of technologies which can improve the efficiency and the capital costs of CO<sub>2</sub> compression is nevertheless of primary importance to the use and storage of CO<sub>2</sub>. For example, advancements in CO<sub>2</sub> compression which can lead to smaller, more efficient, less costly compressors are of significance to the upstream and mid-stream oil and gas industry, and are also relevant to the developers of supercritical CO<sub>2</sub> power cycles.

## 4.7 APPENDIX

### 4.7.1 COMPRESSION WORK: THERMODYNAMICS

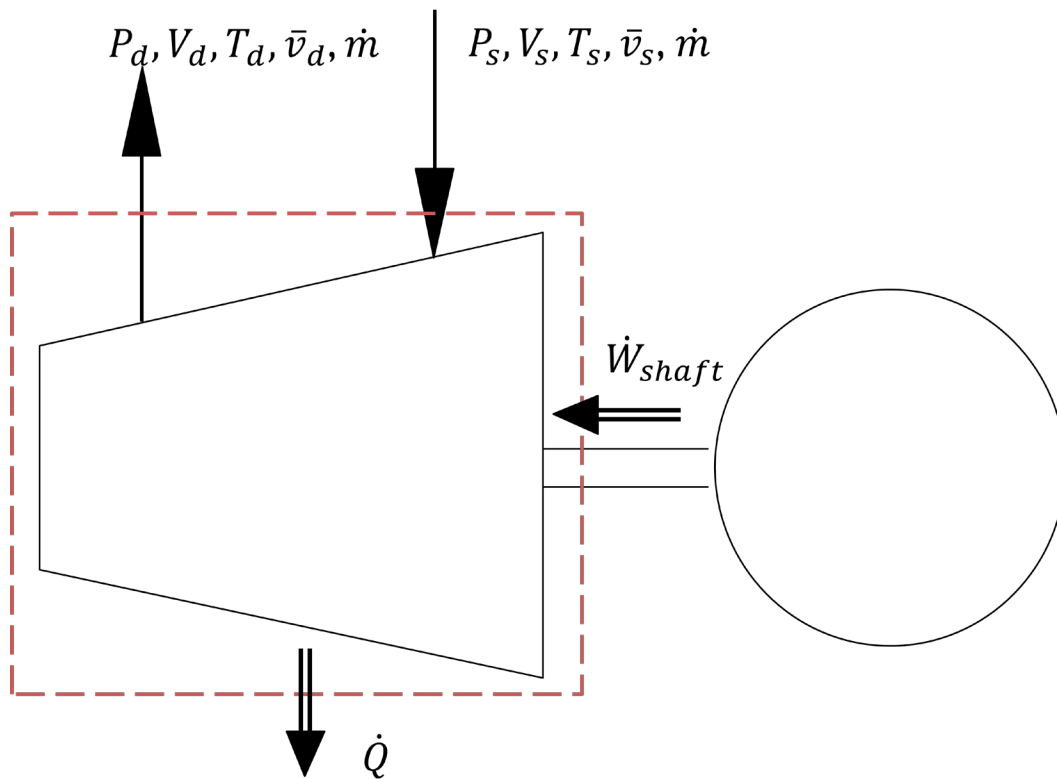
The following section describes the derivation of the equation for reversible shaft work for a control volume and the isentropic and polytropic approaches to the real compression work. The reader is referred to Boyce, 1993<sup>26</sup>; Hanlon, 2001<sup>27</sup>; Huntington, 1985<sup>28</sup>; Sandberg et al., 2013<sup>9</sup>; and Bloch, 2006<sup>29</sup> for a more detailed discussion on this topic and the aerodynamics of turbomachines.

26 Boyce, M.P. "Principles of operation and performance estimation of centrifugal compressors." In *Proceedings of the Twenty-Second Turbomachinery Symposium*, pp. 161–178, (1993).

27 Hanlon, P.C., "Compressor handbook," 754 p., McGraw-Hill, 2001.

28 Huntington, R.A., "Evaluation of polytropic calculation methods for turbomachinery performance," *Journal of Engineering for Gas Turbines and Power*, vol. 107, no. 4, pp. 872–876, Oct. 1985.

29 Bloch, H.P., "A practical guide to compressor technology," 2<sup>nd</sup> edition, 590 p., Wiley, 2006.

Figure 4-14. Schematic of a Compressor and the Control Volume<sup>30</sup>

The reversible shaft work required for compression in steady-state flow can be estimated from thermodynamics. The control volume (c.v.) for the analysis is delineated as shown in Figure 4-13. The subscripts d and s refer to discharge and suction conditions respectively.  $\dot{m}$ , P, T and  $\bar{v}$  refer to the mass flow rate, pressure, temperature and velocity of the fluid respectively. The symbol V refers to the volume occupied by a unit mass of fluid (i.e., inverse of density).

The fluid energy balance for the compressor can be written as:

(Rate of change of energy in c.v.) = (Rate of heat added to c.v.) – (Rate of work done) + (Rate of energy flow into c.v.) – (Rate of energy flow out of c.v.)

The net work done is a sum of the shaft work, shear work, piston work and flow work (i.e., work required to move the fluid through the control volume already containing fluid).

The energy balance can be written as:

$$\frac{d}{dt} \sum E_{cv} = \sum \dot{Q} + \sum \dot{W}_{shaft} + \sum \dot{W}_{flow} + \sum \dot{m} \left( u + \frac{\bar{v}^2}{2} + g \cdot z \right)$$

Equation 4-6

where u represents the internal energy of the fluid, g the acceleration due to gravity, and z represents elevation with respect to a fixed coordinate system. The symbol sigma includes the sign for energy flow: heat addition to the system or work done on the system is positive, for cases where work is done by the system, or heat extracted out of the control volume the sign is negative.

The fluid entering the compressor (suction) is pushed on and receives work from the surroundings, whereas the fluid exiting the compressor (discharge) must push back the surrounding fluid, doing work on it. The net rate of flow work is  $\dot{W}_{flow} = \dot{m} (-P_d V_d + P_s V_s)$ .

<sup>30</sup> Note that the rate of change of shaft work in the figure is the power transmitted to the gas in a compressor and does not include mechanical losses. The effective work per unit mass or effective head is the work exchanged per mass of fluid between the blading of the compressor and fluid.

At steady state and without change of elevation, the energy balance becomes:

$$\dot{m} \left( u_d + \frac{\bar{v}_d^2}{2} + P_d V_d \right) + \dot{Q} = \dot{W}_{shaft} + \dot{m} \left[ u_s + \frac{\bar{v}_s^2}{2} + P_s V_s \right]$$

Equation 4-7

where  $\dot{Q}$  is the rate of heat loss from the control volume, and  $\dot{W}_{shaft}$  is the rate of shaft work performed on the fluid in the control volume. Because the enthalpy of a substance ( $h$ ) is related to the internal energy ( $u$ ) by  $h = u + PV$ , where the energy

$$-\dot{Q} + \dot{W}_{shaft} + \dot{m} \left[ \left( h_s + \frac{\bar{v}_s^2}{2} \right) - \left( h_d + \frac{\bar{v}_d^2}{2} \right) \right] = 0$$

Equation 4-8

$$-\dot{Q} + \dot{W}_{shaft} = \dot{m}(h_d - h_s) + \dot{m} \left( \frac{\bar{v}_d^2}{2} - \frac{\bar{v}_s^2}{2} \right)$$

Equation 4-9

Equation 4-9 can also be expressed in the differential form (i.e., for a infinitesimally small control volume) as:

$$-\delta q + \delta W_{shaft} = dh + \frac{1}{2} d\bar{v}^2$$

Equation 4-10

where  $q$  and  $W_{shaft}$  refer to the rate of heat loss from the control volume per unit mass flow rate of fluid and the shaft power required for compression per unit mass flow rate of fluid. Note that both  $q$  and  $W_{shaft}$  represent energy per unit mass of fluid.

If we assume that the compression process is reversible and the kinetic energy effects are negligible,

$$-\delta q_{rev} + \delta W_{shaft,rev} = dh$$

Equation 4-11

For a completely reversible process,  $\delta q_{rev} = -Tds$  where  $ds$  is the change of entropy (it is negative because  $q$  in this scenario represents the heat loss from the control volume per unit mass of fluid<sup>31</sup>). Further, from  $Tds = dh - VdP$ , the reversible shaft compression work in an open system can be expressed as:

$$Tds + \delta W_{shaft,rev} = dh, \text{ or } \delta W_{shaft,rev} = VdP$$

Equation 4-12

31 In the thermodynamic definition  $\delta q = Tds$  refers to the heat gained by the fluid in the control volume.

The overall reversible shaft work per unit mass of fluid is therefore<sup>32</sup>

$$W_{shaft,rev} = \int_{P_s}^{P_d} V dP$$

**Equation 4-13**

From Equation 4-9, assuming that the kinetic energy effects are small, the effective shaft work per unit mass of fluid can be represented as

$$-Q + H_R = (h_d - h_s)$$

**Equation 4-14**

Where  $Q$  and  $H_R$  represent the actual heat transferred per unit mass of fluid from the control volume to its surroundings, and the specific effective work required to compress a unit mass of fluid.

Note that the specific work calculated by integrating  $VdP$  is the reversible work (i.e., the minimum work required to compress the gas). The actual compression work would be higher than this value because of the inherent irreversibilities in the compression process and mechanical losses. The work is a path function because the value of the integral depends on the path of the P-V curve. This cannot be calculated a priori because the final volume (or temperature) of the gas is unknown and the shape of the P-V curve is also unknown.

The relationship between the reversible work and actual work for compressing a gas can be expressed by assuming that the compression path follows a known reversible path where the relationship between P and V is known a priori, and by defining actual work to be the ratio of the reversible work to the efficiency.

There are two common ideal reversible compression paths assumed to measure compressor efficiencies: isentropic compression and polytropic compression.

### 4.7.1.1 ISENTROPIC COMPRESSION

An isentropic path is defined as a process which is reversible and adiabatic, with no change in entropy ( $ds = 0$ ). It is defined by  $PV^\gamma = \text{constant}$ , where  $\gamma$  is the ratio of the specific heats at constant pressure and constant volume ( $\gamma = \frac{c_p}{c_v}$ ).

The isentropic shaft work can be expressed as:

$$W_{shaft,i} = \int_{P_s}^{P_d} V dP = \int_{P_s}^{P_d} dh = (h_d^* - h_s) = \int_{P_s}^{P_d} \left( \frac{P_s V_s^\gamma}{P} \right)^{\frac{1}{\gamma}} =$$

$$\frac{\gamma}{\gamma-1} (P_s V_s) \left[ \left( \frac{P_d}{P_s} \right)^{\frac{\gamma-1}{\gamma}} - 1 \right]$$

**Equation 4-15**

Where  $h_d^*$  refers to the isentropic enthalpy measured at discharge pressure (i.e., enthalpy measured at discharge pressure and suction entropy).

<sup>32</sup> Note that  $V$  represents the volume occupied by a unit mass of fluid.

The specific isentropic work per mole of gas can be expressed as:

$$W'_{shaft,i} = \int_{P_s}^{P_d} \left( \frac{P_s v_s^\gamma}{P} \right)^{\frac{1}{\gamma}} = \frac{\gamma}{\gamma-1} (P_s v_s) \left[ \left( \frac{P_d}{P_s} \right)^{\frac{\gamma-1}{\gamma}} - 1 \right] = \frac{\gamma}{\gamma-1} (ZRT_s) \left[ \left( \frac{P_d}{P_s} \right)^{\frac{\gamma-1}{\gamma}} - 1 \right]$$

Equation 4-16

where  $v$  represents the molar volume,  $Z$  the compressibility factor ( $Z = 1$  for ideal gases), and  $R$  the universal gas constant ( $R = C_p - C_v$ ).

The specific isentropic work per unit mass of ideal gas is therefore:

$$W_{shaft,i} = H_i^{ideal\ gas} = \frac{\gamma}{\gamma-1} \left( \frac{RT_s}{Molwt} \right) \left[ \left( \frac{P_d}{P_s} \right)^{\frac{\gamma-1}{\gamma}} - 1 \right]$$

Equation 4-17

where  $H_i^{ideal\ gas}$  is the isentropic head required to compress the gas, and  $Molwt$  is the molecular weight of the gas. The actual work for an ideal gas can be obtained by dividing the isentropic work by the isentropic efficiency:

$$W^{ideal\ gas} = \frac{W_{shaft,i}}{n_i} = \frac{H_i^{ideal\ gas}}{n_i} = \frac{1}{n_i} \frac{\gamma}{\gamma-1} \left( \frac{RT_s}{Molwt} \right) \left[ \left( \frac{P_d}{P_s} \right)^{\frac{\gamma-1}{\gamma}} - 1 \right]$$

Equation 4-18

The power required for the compressor can be obtained by multiplying the actual head (work per unit mass) with the gas mass flow rate and dividing by the mechanical efficiency.

$$Compressor\ power = \frac{Brake\ power}{mechanical\ efficiency} = \frac{W^{ideal\ gas} * \dot{m}}{n_{mech}}$$

Equation 4-19

The compression cycle in positive displacement (reciprocating) compressors often approaches an isentropic compression path. If the discharge temperature is known, and kinetic effects can be neglected, the isentropic efficiency can be calculated using:

$$n_i = \frac{\left( \frac{P_{0d}}{P_{0s}} \right)^{\frac{\gamma-1}{\gamma}} - 1}{\left( \frac{T_{0d}}{T_{0s}} \right) - 1}$$

Equation 4-20

where  $P_0$  and  $T_0$  represent the total (stagnation) pressure and temperature, defined as:

$$T_0 = T + \frac{\bar{v}^2}{2c_p} \text{ and } P_0/P = \left( T_0/T \right)^{\frac{\gamma}{\gamma-1}}$$



## Equation 4-21

The isentropic efficiency of a compressor is therefore a function of the pressure ratio. Operating the compressor at a different pressure ratio would change the efficiency, which does not permit facile comparison of performance across several pressure ranges.

## 4.7.1.2 POLYTROPIC COMPRESSION

A polytropic process is a reversible, non-adiabatic compression process between the total suction pressure and temperature and the total discharge pressure and temperature.<sup>33</sup> In polytropic compression, the path between the suction and the discharge pressures (and volumes) is split into very small pressure steps, each with the same isentropic efficiency. It is represented by  $PV^n = \text{constant}$ , where  $n$ , the polytropic exponent is a real number. Polytropic head is the energy per mass of fluid accumulated in the form of increased potential energy. The term ‘head’ ( $H$ ) refers to the specific work done by a compressor, and is related to the total change in enthalpy (for each stage) during the compression process.

$$H = h_d - h_s = h(p_d, T_d) - h(p_s, T_s).$$

## Equation 4-22

The polytropic work for an ideal gas can be expressed (the subscript  $p$  denotes a polytropic process) using the polytropic efficiency  $\eta_p$  as:

$$W^{ideal\ gas} = \frac{W_{shaft,p}}{\eta_p} = \frac{H_p^{ideal\ gas}}{\eta_p} = \frac{1}{\eta_p} \frac{n}{n-1} \left( \frac{RT_s}{Molwt} \right) \left[ \left( \frac{P_d}{P_s} \right)^{\frac{n-1}{n}} - 1 \right]$$

## Equation 4-23

The polytropic head is related to the actual head by  $H_R^{ideal\ gas} = \frac{H_p^{ideal\ gas}}{\eta_p}$ . At high pressures, the ideal gas law,  $PV = RT$  (for one mole of gas) is no longer valid because molecules interact strongly with one another. To account for this deviation from ideal gas behavior, the ideal gas polytropic work can be modified using the average compressibility factor  $Z_{avg}$ .

$$W^{real\ gas} = H_R^{real\ gas} = \frac{H_p^{real\ gas}}{\eta_p} \\ \approx \left[ \frac{R}{MolWt} \right] \left[ \frac{n}{n-1} \right] \frac{T_s Z_{avg}}{\eta_p} \left[ \left( \frac{P_d}{P_s} \right)^{\frac{n-1}{n}} - 1 \right]$$

## Equation 4-24

The polytropic efficiency is defined as:  $\eta_p = \frac{\int_{P_s}^{P_d} v dP}{(h_d - h_s)}$ . For a thermally and calorifically perfect gas (i.e., an ideal gas with constant specific heats), the relation between the polytropic efficiency and the polytropic exponent  $n$  can be found by using the definition of the isentropic efficiency in Equation 4-20 (noting that the polytropic process is a succession of isentropic steps followed by heat transfer) and using the ideal gas law ( $Pv = RT$ ) as:

33 ASME Performance Test Code (PTC) 10–1997, “Performance Test Code on Compressors and Exhausters.”

$$n_p = \frac{\left(1 + \frac{dP}{P}\right)^{\frac{\gamma-1}{\gamma}} - 1}{\left(1 + \frac{dP}{P}\right)^{\frac{n-1}{n}} - 1} \approx \frac{\frac{(\gamma-1)}{\gamma}}{\frac{(n-1)}{n}}$$

Equation 4-25

## 4.7.2 EOS-BASED NUMERICAL INTEGRATION APPROACH TO CALCULATE STAGE OUTLET TEMPERATURE AND COMPRESSION WORK

Prode Properties, a property library<sup>34</sup> was used to estimate the compressor stage exit temperature and compression work. Peng-Robinson EOS was used for modeling the fluid phase. The function ‘pspf’ was used to calculate the compressor exit temperature using the inlet pressure, temperature and polytropic efficiency (86%). The compression work was estimated by the difference of the inlet and exit enthalpies<sup>35</sup> calculated using the (higher fidelity) Span and Wagner EOS from the CoolProp property database.<sup>36</sup>

## 4.7.3 SCHULTZ POLYTROPIC PROCEDURE FOR CALCULATING OUTLET TEMPERATURE AND HEAD

The Schultz procedure follows the procedure outlined in Figure 4-12.<sup>37</sup> Results for all six stages for the conventional compression are shown in Table 4-10. CoolProp property database was used to calculate thermodynamic properties. Corresponding parameters for high-pressure ratio compression are presented in Table 4-11.

## 4.7.4 IDEAL/REAL GAS POLYTROPIC COMPRESSION

Polytropic head in this case is calculated using average compressibility factor, and polytropic exponent  $n$ . Compressibility factors were estimated using CoolProp. The form of equation for the polytropic head is similar to that for the Schultz procedure, with the exception that isentropic properties and the Schultz correction factor  $f$  are not required. Given a polytropic efficiency  $n_p$ , the polytropic exponent  $n$  is calculated as:  $n_p \cdot \frac{(n-1)}{n} = \frac{(\gamma-1)}{\gamma}$  for the inlet temperature and pressure conditions.

Next, stage outlet temperature is estimated via  $T_d = T_s * \left(\frac{P_d}{P_s}\right)^{\frac{n-1}{n}}$ . Outlet compressibility factor and isentropic exponent  $\gamma$  are calculated using  $P_d$  and  $T_d$ , and thereby outlet polytropic exponent can be estimated. The polytropic head is calculated as:

$$H_p^{real\ gas} = \frac{8.314}{MolWt} T_s Z_{avg} \left(\frac{n}{n-1}\right) \left[ \left(\frac{P_d}{P_s}\right)^{\frac{n-1}{n}} - 1 \right] \text{ kJ/kg}$$

Equation 4-26

where the polytropic exponents are averaged. The polytropic head is compared against that calculated by enthalpy difference using  $P_s$ ,  $T_s$  and  $P_d$ ,  $T_d$ , and the discharge temperature is iteratively changed to match both heads. Power and effective head are calculated as:  $H_R^{real\ gas} = \frac{H_p^{real\ gas}}{n_p}$ , and  $Gas\ power = actual\ head * mass\ flow\ rate$ .

34 [www.prode.com](http://www.prode.com), release 1.2.

35 The exit temperature and enthalpy calculated by Prode account for the polytropic efficiency.

36 Bell, I. H., Wronski, J., Quoilin, S., and Lemort, V. Pure and pseudo-pure fluid thermophysical property evaluation and the open-source thermophysical property library CoolProp. *Ind. Eng. Chem. Res.* 53, 2498–2508 (2014).

37 Brun, K., Nored, M.G. Guideline for field testing of gas turbine and centrifugal compressor performance, Release 2.0. Gas Machinery Research Council, August 2006. <http://www.gmrc.org/documents/GuidelineforFieldTestingofCentrifugals.pdf>.

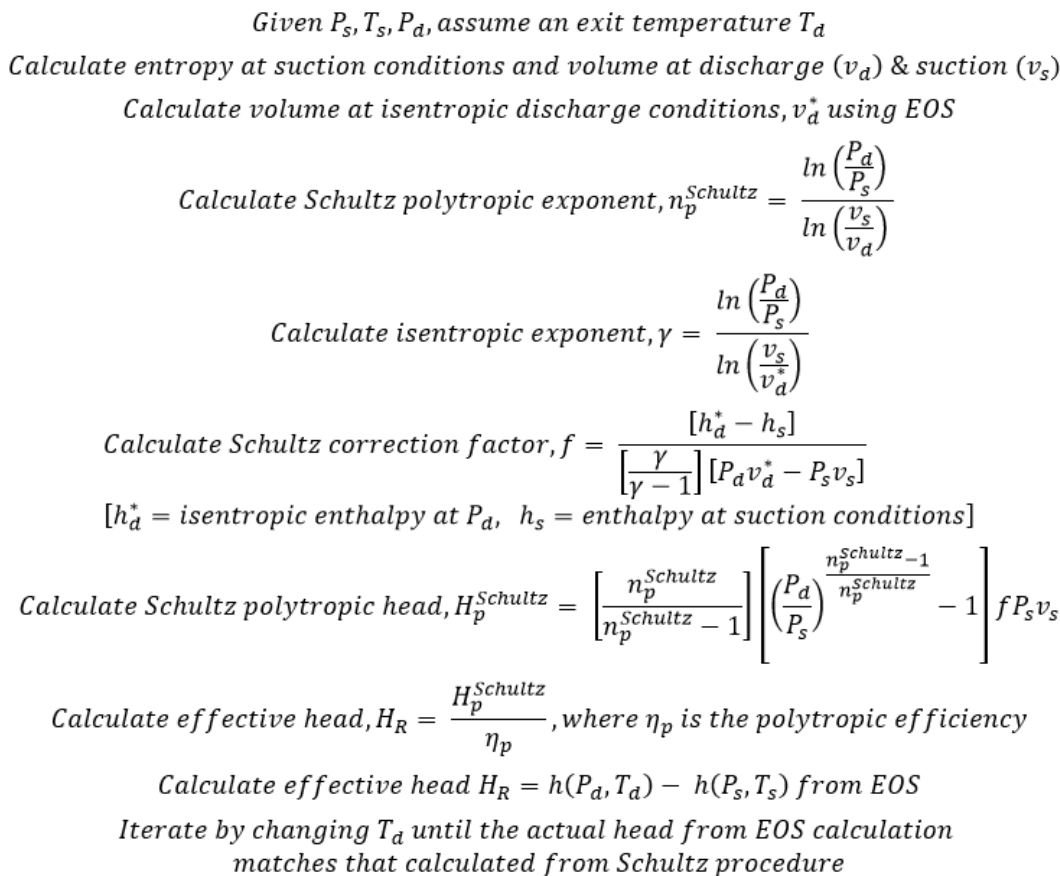


Figure 4-15. Workflow for Calculating Compressor Head and Power Requirements Using the Schultz Polytropic Analysis

Table 4-10. Stage-Wise Exit Temperature and Head From Schultz Procedure for Conventional Compression

STAGE	1	2	3	4	5	6
$n_p$	0.86	0.86	0.86	0.86	0.86	0.86
$P_s$ , kPa	162.03	358.53	779.1738	1,709.894	3,757.63	8,273.67991
$T_s$ , K	294.26	294.26	294.26	294.26	294.26	310.92
$P_d$ , kPa	369.90	798.41	1,744.368	3,792.103	8,308.154	15,306.2389
$T_d$ , K	362.4	360.5	361.5	361.7	362.2	346.7
$S_s$ , kJ/kg-K	2.636	2.481	2.324	2.151	1.933	1.553
$v_s$ , m <sup>3</sup> /kg	3.40E-01	1.52E-01	6.84E-02	2.94E-02	1.13E-02	2.72E-03
$v_d$ , m <sup>3</sup> /kg	1.83E-01	8.35E-02	3.73E-02	1.62E-02	6.31E-03	2.05E-03
$v_d^*$ , m <sup>3</sup> /kg	1.78E-01	8.12E-02	3.63E-02	1.57E-02	6.12E-03	2.02E-03
$n_{Schultz}$	1.335	1.335	1.333	1.332	1.357	2.173
$n_{Schultz}/(n_{Schultz}-1)$	3.983	3.989	4.007	4.015	3.800	1.852
K	1.277	1.275	1.272	1.268	1.289	2.067
$h_d^*$ , kJ/kg	551.83	547.76	542.74	529.49	495.48	387.08
$h_s$ , kJ/kg	501.96	500.05	495.84	485.83	458.62	370.98
F	1.000987	1.000921	1.000868	1.000478	0.997798	0.98971778
$H_p$ , kJ/kg	50.61	48.41	47.60	44.34	37.45	16.23

Table 4-10. Stage-Wise Exit Temperature and Head From Schultz Procedure for Conventional Compression

STAGE	1	2	3	4	5	6
$H_{act}$ from $H^p$ , kJ/kg	58.85	56.29	55.35	51.56	43.55	18.87
$H_{act}$ from EOS, kJ/kg	58.85	56.29	55.35	51.56	43.55	18.87
Error [ $H_{act}$ from $H^p$ - $H_{act}$ from EOS], kJ/kg	3.38E-08	-3.4E-08	-2.4E-09	1.91E-07	2.48E-07	1.4603E-07
$T_d$ , °F	192.7	189.2	191.1	191.4	192.3	164.4
Compressor power, kWe	44,224					

Table 4-11. Stage-Wise Exit Temperature and Head From Schultz Polytropic Analysis for High-Pressure Ratio Compression

STAGE	1	2
$n_p$	0.86	0.86
$P_s$ , kPa	162.03	1,558
$T_s$ , K	294.26	294.26
$P_d$ , kPa	1,592.1	15,306
$T_d$ , K	506.7	517.3
$S_s$ , kJ/kg-K	2.636	2.173
$v_s$ , m <sup>3</sup> /kg	3.40E-01	3.26E-02
$v_d$ , m <sup>3</sup> /kg	5.95E-02	5.93E-03
$v_d^*$ , m <sup>3</sup> /kg	5.54E-02	5.49E-03
$n_{Schultz}$	1.310	1.340
$n_{Schultz}/(n_{Schultz}-1)$	4.223	3.942
$k$	1.259	1.282
$h_d^*$ , kJ/kg	663.79	637.27
$h_s$ , kJ/kg	501.96	487.54
$F$	1.006148	0.992186
$H^p$ , kJ/kg	168.15	156.10
$H_{act}$ from $H^p$ , kJ/kg	195.52	181.51
$H_{act}$ from EOS, kJ/kg	195.52	181.51
Error [ $H_{act}$ from $H^p$ - $H_{act}$ from EOS], kJ/kg	1E-08	1.29E-08
$T_d$ , °F	452.4	471.5
Compressor power, kWe	58,612.86	

Table 4-12. Parameters Used to Model Case 12 Steam Cycle

Supercritical single reheat steam cycle (3,515 psia/1,100 °F/1,100 °F)	Inlet pressure, MPa (psia)	24.2	3,515
	Max steam temperature, °C (°F)	593	1,000
	Exhaust pressure, MPa (psia)	4.9	711
	HP exhaust pressure, MPa (psia)	4.9	711
	IP inlet pressure, MPa (psia)	4.5	656
	IP exhaust pressure, MPa (psia)	0.52	75
	LP inlet pressure, MPa (psia)	0.51	73.5
	Governing stage isentropic efficiency, %	80	
	HP isentropic efficiency, %	83.72	
	IP isentropic efficiency, %	88.76	
	LP isentropic efficiency, %	92.56	
	Generator efficiency, %	98.5	
Surface condenser	Operating pressure, MPa (psia)	0.0068	0.982
	Terminal temperature difference, °C (°F)	11.7	21
Condensate pumps	Discharge pressure, MPa (psia)	1.7	250
	Efficiency, %	80	
Deaerator	Operating pressure, MPa (psia)	0.12	17.4
	Operating temperature, °C (°F)	176	349
Boiler feed water pump turbine	Inlet pressure, MPa (psia)	0.5	73.5
	Exhaust pressure, MPa (psia)	0.0013	2
	Isentropic efficiency, %	80	
Boiler feed water pump, supercritical steam cycle	Discharge pressure, MPa (psia)	28.9	4,200
	Efficiency, %	80	
LP feed water heaters	Cold-side temperature approach, °C (°F)	5.56	10
	Pressure drop, MPa (psia)	0.03	5
IP feed water heaters	Cold-side temperature approach, °C (°F)	5.56	10
	Pressure drop, MPa (psia)	0.03	5
HP feed water heaters	Cold-side temperature approach, °C (°F)	5.56	10
	Pressure drop, MPa (psia)	0.03	5
CO <sub>2</sub> compression	Intercooler approach temperature, °C (°F)	5.6	10
	CO <sub>2</sub> compressor stage pressure ratio	See Ref.2	
	CO <sub>2</sub> compressor outlet pressure, MPa (psia)	15.3	2,215
	CO <sub>2</sub> compressor intercooler pressure drop, MPa (psia)	See Ref.2	
	Polytropic stage efficiency, %	86	
	Mechanical stage efficiency, %	98	
	TEG unit pressure drop, MPa (psia) [NOT modeled]	0.002	0.3
CO <sub>2</sub> stream from stripper condenser (stream 20) [inlet CO <sub>2</sub> stream]	99.61% CO <sub>2</sub> , 0.39% H <sub>2</sub> O, 12,511 kmol/h, 549,344 kg/h (1,211,096 lb/h), 21 °C (69 °F), 0.16 MPa (23.5 psia)		
Cooling water/cooling tower	11 °C (51.5 °F) wet bulb. 16 °C (60 °F) cooling water temperature		

this page intentionally left blank



## National Energy Technology Laboratory

1450 Queen Avenue SW  
Albany, OR 97321-2198  
541.967.5892

420 L Street, Suite 305  
Anchorage, AK 99501  
907.271.3618

3610 Collins Ferry Road  
P.O. Box 880  
Morgantown, WV 26507-0880  
304.285.4764

626 Cochrans Mill Road  
Pittsburgh, PA 15236-0940  
412.386.4687

13131 Dairy Ashford, Suite 225  
Sugar Land, TX 77478  
281.494.2516

Customer Service  
1.800.553.7681

Website  
[www.netl.doe.gov](http://www.netl.doe.gov)

**DOE/NETL Carbon Capture Program**  
Carbon Dioxide Capture Handbook  
August 2015



U.S. DEPARTMENT OF  
**ENERGY**

